



**HAL**  
open science

# The Higgs boson mass and cosmology

Raffaele Tito d'Agnolo

► **To cite this version:**

Raffaele Tito d'Agnolo. The Higgs boson mass and cosmology. Physics [physics]. Université Paris-Saclay, 2022. tel-04444180

**HAL Id: tel-04444180**

**<https://cea.hal.science/tel-04444180>**

Submitted on 7 Feb 2024

**HAL** is a multi-disciplinary open access archive for the deposit and dissemination of scientific research documents, whether they are published or not. The documents may come from teaching and research institutions in France or abroad, or from public or private research centers.

L'archive ouverte pluridisciplinaire **HAL**, est destinée au dépôt et à la diffusion de documents scientifiques de niveau recherche, publiés ou non, émanant des établissements d'enseignement et de recherche français ou étrangers, des laboratoires publics ou privés.

# The Higgs Boson Mass and Cosmology

**Raffaele Tito D'Agnolo**

Habilitation à Diriger des Recherches



January 28, 2022

## Abstract

This is a summary of what we think we know, thought we knew and despair of ever knowing about the Higgs boson mass  $m_h$ . Understanding its value is one of the most fascinating open problem in particle physics. It has kept many of us awake at night for the past 30 years.

The problem is reviewed in detail in the first two Chapters of this work. Its proposed solutions in the third Chapter. The last Chapter is the fruit of my sleepless nights of the last 5 years or so. There I discuss a new class of explanations for  $m_h$  that trace its origin to early times in the history of the Universe. This is a definite change of perspective compared to traditional explanations, with completely different experimental consequences.

## Acknowledgements

Without all my precious collaborators, mentors and the colleagues who are taking part in the HDR, this work would not have been possible. I would like to thank (in alphabetical order, as per honored tradition of particle physics): Nima Arkani-Hamed, Paolo Azzurri, Riccardo Barbieri, Brando Bellazzini, Asher Berlin, Kfir Blum, Marco Cirelli, Csaba Csaki, Emilian Dudas, John Ellis, Sebastian Ellis, Adam Falkowski, JiJi Fan, Michael Geller, Christophe Grojean, Gaia Grosso, Roni Harnik, Mariangela Lisanti, Yoni Kahn, Hyung Do Kim, Maurizio Pierini, Riccardo Rattazzi, Gigi Rolandi, Josh Ruderman, Ben Safdi, Géraldine Servant, Liantao Wang, Andrea Wulzer and Marco Zanetti. My parents, deserve a special thanks as my first mentors and my brother, as my first collaborator, and both in so many more ways that are impossible to list here. My girlfriend for her constant loving support, the new color palettes in my papers and her plants that, as scientifically proven, have improved my work; just to mention the tip of the iceberg.

# Contents

<b>1</b>	<b>Introduction</b>	<b>1</b>
1.1	Summary and Outline . . . . .	1
1.2	The Standard Model in a Nutshell . . . . .	2
1.3	The Standard Model from Symmetry Alone . . . . .	3
1.3.1	Spacetime dilations . . . . .	4
1.3.2	Lorentz Symmetry and Causality . . . . .	6
1.3.3	Global Symmetries . . . . .	8
1.4	The Standard Model Lagrangian . . . . .	10
1.4.1	Aside on Renormalization . . . . .	13
1.5	Beyond the Standard Model . . . . .	15
<b>2</b>	<b>The Hierarchy Problem</b>	<b>17</b>
2.1	Historical Background . . . . .	17
2.2	The Unbearable Lightness of the Higgs . . . . .	20
2.2.1	A Precise Statement in the Standard Model . . . . .	21
2.2.2	A Sharp Problem in Supersymmetry . . . . .	22
2.2.3	Common Misconceptions and an Alternative Formulation . . . . .	24
2.3	The Little Hierarchy Problem . . . . .	27
2.4	What We Learned about High Energies . . . . .	28
<b>3</b>	<b>Most Existing Solutions to the Hierarchy Problem</b>	<b>31</b>
3.1	Lowering the Scale of Gravity . . . . .	31
3.2	New Symmetries . . . . .	34
3.2.1	Scale Invariance . . . . .	34
3.2.2	Supersymmetry . . . . .	39
3.3	Scaleless Theories of Gravity . . . . .	41
3.4	The Multiverse . . . . .	42
3.4.1	Anthropic Selection . . . . .	46
3.5	Comments on UV/IR Mixing and Quantum Gravity . . . . .	50
<b>4</b>	<b>A New Class of Solutions to the Hierarchy Problem</b>	<b>55</b>
4.1	Dynamical Selection in the Multiverse and Beyond . . . . .	56
4.1.1	$N$ naturalness . . . . .	56
4.1.2	The Relaxion . . . . .	72
4.2	Weak Scale Triggers . . . . .	73
4.2.1	The SM Trigger $\text{Tr}[G\tilde{G}]$ . . . . .	75
4.2.2	The $H_1H_2$ Trigger in the Type-0 2HDM . . . . .	77
4.2.3	Vector-Like Leptons and the $\text{Tr}[F\tilde{F}]$ Trigger . . . . .	80
4.2.4	A Possible Fourth Option? . . . . .	81
4.3	Collider Phenomenology of the $H_1H_2$ Trigger: the type-0 2HDM . . . . .	82
4.3.1	Masses and Couplings . . . . .	82

4.3.2	Experimental Constraints . . . . .	85
4.4	Crunching Dilaton . . . . .	88
4.5	Sliding Naturalness . . . . .	97
4.5.1	Basic Idea . . . . .	98
4.5.2	Scalar Potential and Selection of the Weak Scale . . . . .	100
4.5.3	Cosmology . . . . .	102
4.5.4	The $H_1 H_2$ trigger . . . . .	108
4.5.5	The Standard Model Trigger . . . . .	111
4.5.6	Conclusions . . . . .	116
4.6	Triggered Landscapes . . . . .	117
4.6.1	SM Trigger of the Landscape . . . . .	118
4.6.2	Type-0 2HDM Triggering of the Landscape . . . . .	120
4.7	Statistical Selection in the Multiverse . . . . .	124
4.8	General Aspects of Cosmological Naturalness . . . . .	124
4.8.1	Cosmological Naturalness Power Counting . . . . .	127
4.8.2	Trigger Operators and Low Energy Predictions . . . . .	129

**5 Conclusion** **131**

# Chapter 1

## Introduction

Let us raise a standard to which  
the wise and honest can repair;  
the rest is in the hands of God.

---

*George Washington*

### 1.1 Summary and Outline

The Standard Model (SM) is the reference theory of particle interactions. It has been extensively tested from atomic energies to the highest energies that we can currently probe. Its continuous predictive successes have made it the unavoidable starting point of any experimental or theoretical investigation of higher energies.

The Higgs boson plays a special role in the SM. Its mass squared is the second most relevant parameter in the theory, after the cosmological constant. Therefore these two parameters are crucial to describe low energy measurements. The Higgs boson mass determines the vacuum expectation value of the Higgs field which enters the mass of most known particles and determines the scale of weak interactions. The stability of nuclei, and thus complex chemistry and ultimately life as we know it, are strongly tied to its value. The Higgs boson was discovered, and its mass measured, by the ATLAS and CMS experiments at the Large Hadron Collider (LHC) [1, 2].

A second important property of the Higgs mass  $m_h$  is that the corresponding operator in the SM Lagrangian is not protected by any symmetry, so if we try to estimate  $m_h$  we are forced to consider the highest energy scales in the theory. This high/low energy “duality” makes the problem of understanding its value quite fascinating. The pragmatist wants to compute any parameter that is so important in the description of low energy observations. The dreamer hopes to learn precious information on energies much higher than those that we can currently probe. The challenge inherent in these attempts is that we do not know how the SM is modified at high energies, in particular we do not know how to describe gravity at the Planck scale  $M_{\text{Pl}} \simeq 10^{19}$  GeV. We are trying to compute a parameter in a theory that does not yet exist.

In the SM taken in isolation  $m_h$  can not be computed at all, precisely because of this high-energy sensitivity. We can only take it as an input parameter from experiment. There is still something that we can do, however, and it is something that has never failed us once in the long history of physics: we can estimate  $m_h$  using symmetry.

The selection rules of spacetime dilations tell us that  $m_h^2$  must be proportional to the largest mass scale in the theory, so  $m_h^2 \propto M_{\text{Pl}}^2$ . The infinite symmetries that protect the free scalar Lagrangian [3], allow us to estimate the coefficient of proportionality  $m_h^2 \sim y_t^2 M_{\text{Pl}}^2 + \dots$ , where

the ellipses stand for subleading contributions from smaller mass scales.  $y_t$  is an  $\mathcal{O}(1)$  coefficient that we have measured from properties of other SM particles. The measured value of the Higgs mass is  $m_h \simeq 125$  GeV and this estimate is wrong by 34 orders of magnitude. In Sections 3.5, 3.3 and 3.1 we comment on the use of  $M_{\text{Pl}}$  as a mass scale in our estimate.

This is not yet a problem of our description of Nature, in the sense that the SM is not inconsistent. As we stated above,  $m_h$  can only be measured and never computed in the SM. However, something quite dramatic has happened. The symmetry arguments that led to our wrong estimate are used every day by thousands of people in hundreds of different disciplines, including high energy physics, and they always work. To obtain our estimate we have only used the most basic principle underlying most of our understanding of physics: the selection rules of broken symmetries.

We are forced to take the failure of these symmetry arguments seriously and ask what is happening at high energies that is making them wrong. The simplest option is that we have missed an extra symmetry that is realized in Nature well below  $M_{\text{Pl}}$  and shields  $m_h$  from higher energy corrections. Two possibilities in this sense are supersymmetry and scale invariance, both would predict  $m_h^2 \sim y_t^2 M_S^2 + \dots$ , where  $M_S$  is the scale at which the new symmetry is broken. We have been looking for these new symmetries for more than 40 years and we have not yet found a trace that they are realized in Nature. We can either accept some amount of accidental cancellations<sup>1</sup> as a fundamental aspect of Nature or look for alternatives.

In this work we advocate for a change of perspective on the problem. The apparently small value of  $m_h$  compared to other fundamental scales of Nature might be explained by an event taking place early in the history of the Universe, without any trace of new symmetries close to  $m_h$ . This general idea can be declined in a number of different ways that have been developed in the last few years. In the following we review the status of the field with special attention to experimental predictions that are common across different theoretical realizations of the idea.

This document is organized as follows, in the rest of this Chapter we introduce the Standard Model of particle physics, initially making the effort of “forgetting” quantum field theory and using only symmetry arguments. In Chapter 2 we discuss in greater detail the issues surrounding the computation of  $m_h$ , highlighting common misconceptions and giving a short historical summary of the significance of similar problems in the development of particle physics. In Chapter 3 we review the main ideas put forward to explain the value of  $m_h$ , with the exception of mechanisms that select  $m_h$  via a cosmological event, which are discussed in Chapter 4.

## 1.2 The Standard Model in a Nutshell

The SM is a relativistic quantum field theory described by a Lagrangian. It includes three interactions (strong, electromagnetic and weak) between twelve fermionic fields. The fermions can be divided into two subsets of six particles each: quarks and leptons. Quarks feel the strong force while leptons do not. Each of the two groups can be organized into three families as shown in Fig. 1.1. In particle physics jargon the different families are said to have different flavor. The upper components of all the families share the same quantum numbers and so do the lower ones, so we can further subdivide the matter fields into up-quarks, down-quarks, charged leptons and neutrinos. Ordinary matter is composed only of  $u$  and  $d$  quarks, that form protons and neutrons, and of electrons.

The three interactions mentioned above are mediated by bosonic fields. The strong force is mediated by gluons, the photon carries the electromagnetic interactions, while the  $W$  and  $Z$  bosons are responsible for the weak one, Fig. 1.1 contains a summary table. The three

---

<sup>1</sup>The quantity  $y_t^2 M_S^2$  in a realistic theory is the sum of multiple contributions of the same order that in general have different signs and might conspire to give a final result smaller than  $M_S^2$ .



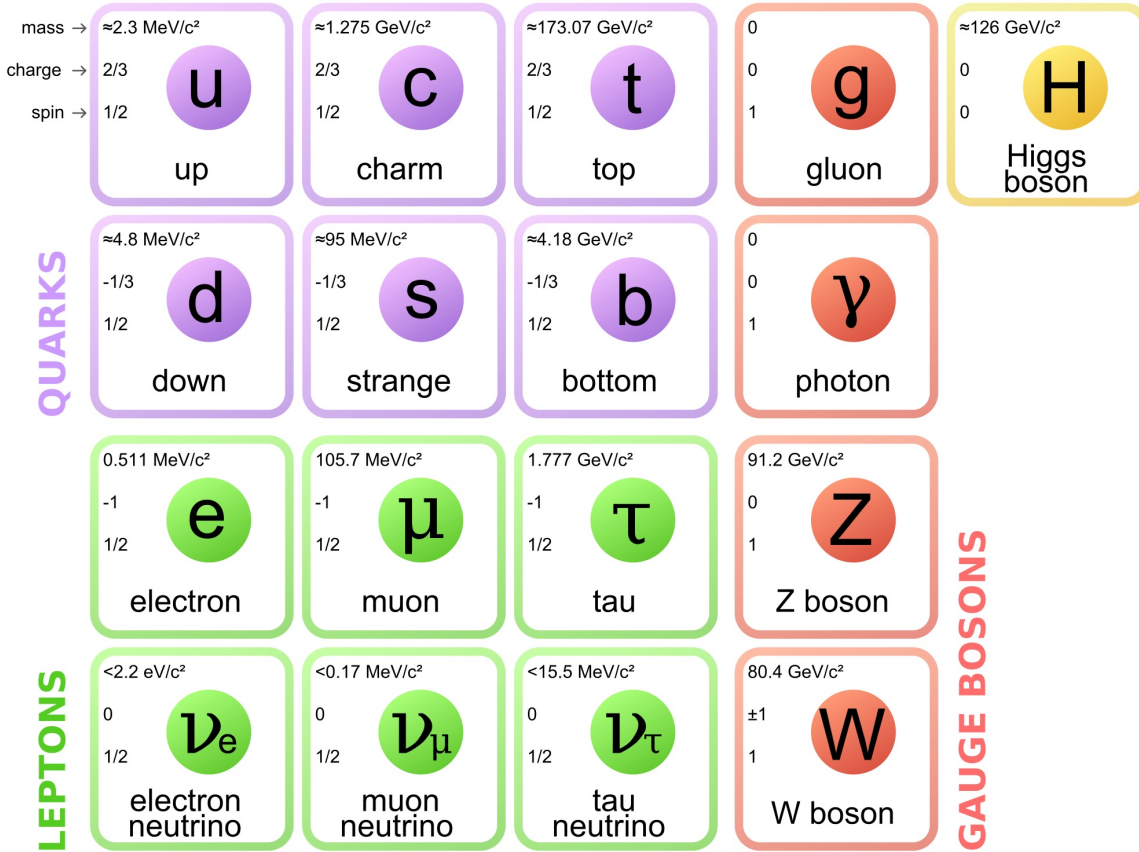


Figure 1.1: Standard Model particle content [License: CC0].

interactions do not have all the same intensity, as their names suggest. At energies close to the  $W$  mass electromagnetic and weak interactions are comparable while the intensity of the strong interaction is roughly larger by a factor of 3. The situation changes dramatically at lower energies where the strong interaction is confining and the mass of the heavy mediators of the weak force suppress its effects. For instance in the few MeV range

$$\frac{\text{strong}}{\text{electromagnetic}} \simeq 100, \quad \frac{\text{electromagnetic}}{\text{weak}} \simeq 10^9. \quad (1.1)$$

So far we have neglected gravity. The reason is that at the energies that we can currently probe its effects are not measurable.

It is useful to notice that not only forces, but also fermion masses are strongly hierarchical. This can be seen from Fig. 1.1. As we will see at the end of this Section, these masses originate from couplings to the Higgs boson, so the top quark is the particle with the largest coupling to the Higgs in the SM.

In the following Section we derive most of these statements and make them more precise using only symmetry and experimental observations, without assuming prior knowledge of quantum field theory.

### 1.3 The Standard Model from Symmetry Alone

It is instructive to see how much we can reconstruct of the SM using only symmetry, assuming for the moment that we do not know quantum field theory. The experienced reader can skip this Section. I find useful to include it for two reasons: 1) In the following I will try to argue that the hierarchy problem, in some precise sense, is a failure of symmetry and it is interesting

to see just how far one can go in understanding the laws of particle physics using symmetry alone. 2) This Section follows a lecture that I have given at SNS Pisa to explain the SM to undergraduates and it will serve as a future reference that I am hoping might be useful also to others.

Modern experiments require describing particle interactions in a regime where quantum effects are relevant and particles are relativistic. It is therefore convenient to work in natural units where the speed of light and Planck's constant are set to one,  $c = \hbar = 1$ . The existence of these fundamental constants is telling us something useful. The speed of light  $c$  in special relativity is telling us that we need to treat space and time on equal footing  $x^\mu = (t, \vec{x})$  and also energy and momentum  $p^\mu = (E, \vec{p})$ . Quantum mechanics is teaching us that spacetime coordinates in natural units have dimensions of  $E^{-1}$ . In the following we characterize quantities in natural units by their dimensions in units of energy.

After these basic preliminaries, we can identify the three main symmetries that will provide the basis to construct the SM:

1. **Spacetime dilations** are broken in the SM, but their selection rules play a central role in understanding the SM as an effective theory (EFT).
2. **Lorentz Symmetry** is respected by the SM and particles have to fall into definite representations of the Lorentz group.
3. **Global Symmetries**. In the decades leading to the establishment of the SM we have observed a host of additional symmetries that do not involve spacetime coordinates. They are related to the forces listed above.

### 1.3.1 Spacetime dilations

We start with a generic action written as the time integral of a Lagrangian

$$S = \int dt L. \quad (1.2)$$

Since we set  $\hbar = 1$ ,  $S$  in natural units is dimensionless  $S \sim E^0$ . In the following we use the shorthand notation  $[S] = 0$ .

In a Lorentz-invariant theory it is convenient to define a Lagrangian density  $\mathcal{L}$  as

$$S = \int dt L = \int dt d^3x \mathcal{L}. \quad (1.3)$$

It follows from  $[S] = 0$  that  $[\mathcal{L}] = 4$ . The volume element  $d^4x \equiv dt d^3x$  is Lorentz-invariant. Under a Lorentz transformation  $x^\mu = \Lambda^\mu_\nu x'^\nu$ , we have  $d^4x \rightarrow |\det \Lambda| d^4x'$  and  $|\det \Lambda| = 1$ . So if we construct  $\mathcal{L}$  to be Lorentz-invariant we have a Lorentz-invariant action.

Even if we did not know anything about the fundamental theory of particle interactions we could still expand the Lagrangian density as

$$\mathcal{L} = \sum_i c_i \mathcal{O}_i, \quad (1.4)$$

where  $c_i$  are numerical coefficients and  $\mathcal{O}_i$  operators describing kinetic terms and interactions. We can then use the selection rules of dilations (i.e. dimensional analysis) to conclude that if  $[\mathcal{O}_i] = \Delta_i$  then  $[c_i] = 4 - \Delta_i$ . If we take  $\Lambda$  to be the largest mass scale in the theory, we can write

$$c_i = a_i \Lambda^{4 - \Delta_i}, \quad (1.5)$$

in absence of extra symmetries (that can for instance set to zero individual  $a_i$ 's), the same selection rules of dilations suggest that the coefficients  $a_i$  should be  $\mathcal{O}(1)$ . This can be seen in the following way: we can use these selection rules to write

$$c_i = a_i^1 \Lambda^{4-\Delta_i} + a_i^2 \Lambda_2^{4-\Delta_i} + a_i^3 \Lambda_3^{4-\Delta_i} + \dots = \Lambda^{4-\Delta_i} \left[ a_i^1 + a_i^2 \left( \frac{\Lambda_2}{\Lambda} \right)^{4-\Delta_i} + a_i^3 \left( \frac{\Lambda_3}{\Lambda} \right)^{4-\Delta_i} + \dots \right] \quad (1.6)$$

where  $\Lambda > \Lambda_n > \Lambda_{n+1}$ . Barring accidental cancellations that can make  $a_i^1$  small, spacetime dilations predict  $c_i = \mathcal{O}(\Lambda^{4-\Delta_i})$ , so finally we have

$$\mathcal{L} = \sum_i a_i \Lambda^{4-\Delta_i} \mathcal{O}_i. \quad (1.7)$$

We can now ask how much each term in this sum contributes to a given observable. Imagine for instance that we are measuring the action at energies  $E < \Lambda$ . We can use again dimensional analysis to conclude that

$$S \simeq \sum_i a_i E^{-4} \Lambda^{4-\Delta_i} E_i^{\Delta_i} = \sum_i a_i \left( \frac{\Lambda}{E} \right)^4 \left( \frac{E}{\Lambda} \right)^{\Delta_i}. \quad (1.8)$$

Operators of dimension  $\Delta_i < 4$ , the so-called relevant operators, give an enhanced contribution at low energy. A finite experimental precision implies that we can neglect all the infinitely many irrelevant operators with  $\Delta_i > \Delta_*$ , where  $\Delta_*$  is determined by the accuracy of our measurement. This explains why the SM Lagrangian contains only operators up to  $\Delta_i = 4$  and as a consequence it is so compact. We have not yet reached high enough energies and resolutions to detect operators of higher dimension. This is the modern perspective on the theory of fundamental interactions. We do not think of it as something perfect and forever set in stone, but rather as the low energy limit of a more complex theory that will reveal itself in the future. We did not rely on any detailed property of quantum field theory to reach this conclusion, but just on a single, broken symmetry.

## Aside on Effective Field Theories

In what follows we extensively use the language, intuition and tools of effective field theories. Before proceeding in our construction of the SM it is useful to introduce some of these concepts. For excellent reviews, that we partially follow, we refer the reader to [4, 5].

The idea of an effective theory is implicit in the human description of reality that brings order by neglecting effects that are far removed from our perception. In this case by neglecting what is “far” in energy.

The common intuition that the dynamics at low energies does not depend on the details of the theory at high energies (small distances) can be turned into a quantitative statement. To this end we can consider the example of the Hydrogen atom. We can calculate its energy levels to a certain degree of accuracy through the Schrodinger equation, knowing just the mass and the charge of the proton and the electron. If we want to refine our analysis, including the hyperfine splitting, we need additional information, such as their spins and magnetic moments. Moving towards higher precision demands the knowledge of QCD and the underlying structure of the proton. To better quantify this progression and the level of accuracy achieved at each step, it is necessary to introduce the typical momentum scale of the problem. Through the Bohr radius  $r_0 = 1/\alpha m_e$ , it is easy to give an estimate

$$p_0 \simeq \frac{1}{r_0} = \alpha m_e. \quad (1.9)$$

Neglecting an interaction at  $p \sim \Lambda \gg p_0$  will give us an error of  $\mathcal{O}(p_0/\Lambda)^n$ ,  $n > 0$ , coming from the lowest dimensional operator among the irrelevant ones discussed in the previous Section. Since the Hydrogen atom is a non-relativistic system the typical energy is different than  $p_0$ ,  $E_0 \simeq \alpha^2 m_e$ , so we must be careful when estimating the error on different observables and technically the relativistic expansion in the previous Section does not apply directly. However the intuition that we developed on different classes of operators remains valid.

One might wonder how a large scale  $\Lambda$  can leave such a subdominant effect at much lower energies. This is of course not entirely true, but the effect of  $\Lambda$  is hidden by the fact that the low energy theory has a series of free parameter that we can measure directly.

In the previous example  $\alpha$  depends crucially on the top quark mass ( $m_t \gg \alpha m_e$ )

$$\frac{d(1/\alpha)}{d \log m_t} = -\frac{1}{3\pi} \quad (1.10)$$

and so does the proton mass

$$m_p \propto m_t^{2/27}. \quad (1.11)$$

However we can describe the Hydrogen atom without knowing that the top quark exists. The reason is that we can directly measure  $\alpha$  and  $m_p$  from low energy observations. In this sense  $m_t$  is irrelevant as far as atomic properties are concerned, but in the higher energy theory it relates two parameters that are free in the effective one.

In the language of the previous Section, all the coefficients  $c_i$  of the operators in the effective theory can be directly measured at low energy. Irrelevant operators that are sufficiently suppressed by their large scaling dimension  $\Delta_i$  can further be neglected in any calculation done with finite precision.

A more complete high-energy theory can leave also some non-trivial constraints at lower energies, a beautiful example is the spin-statistics theorem. In non-relativistic quantum mechanics the quantization of integer and non-integer spin degrees of freedom can proceed in exactly the same way without undermining the consistency of the theory. Nonetheless the full relativistic theory demands the respect of causality, which enforces the Fermi and Bose pictures also in low-energy observables.

In summary we can always find low-energy degrees of freedom that describe physics to a finite, but calculable precision. The only effect of the high-energy dynamics is to impose symmetry relations between them. In the process we do not need to know anything about the ultraviolet (UV) theory, but we loose some predictive power, in the sense that some parameters that are calculable in the complete theory might be free in our low-energy description.

### 1.3.2 Lorentz Symmetry and Causality

The existence of a limiting velocity  $c$  implies that forces can not act instantly at a distance. To respect causality we need interactions that can not propagate outside of the lightcone of an observer. The most natural way to implement this requirement is to consider local interactions. If we take electromagnetism as an example, we need to introduce a new particle  $\gamma$  that exchanges energy and momentum with other particles, for instance electrons, when they meet in the same spacetime point. This exchange is the equivalent to the classical action of the electromagnetic force.

Since we are constructing a Lorentz-invariant theory we have to assign a representation to  $\gamma$  under the Lorentz group. From classical electromagnetism we can already deduce the properties of  $\gamma$  that are needed to determine its representation:

1. We can prepare coherent electromagnetic fields in the laboratory much larger than their fundamental quantum. This means that  $\gamma$  must be a bosonic field, otherwise causality (i.e. the Pauli exclusion principle in non-relativistic quantum mechanics) would forbid the existence of these large coherent fields.
2. Electromagnetic radiation propagates at the speed of light, hence the mass of  $\gamma$  must be zero:  $m_\gamma = 0$ .
3. Electromagnetic fields have two polarizations:  $\gamma$  is in a Lorentz representation with two degrees of freedom.

In summary we have a massless bosonic field of integer spin. A scalar ( $s = 0$ ) does not have enough degrees of freedom to parametrize our two polarizations. We need to consider at least a  $s = 1$  representation that we can describe by a Lorentz vector  $A_\mu$ . However, we have too many degrees of freedom in  $A_\mu$ .

This is a difficulty that we have already encountered in classical electromagnetism. If we want to describe electromagnetic fields in terms of a vector potential, with definite transformation properties under the Lorentz group, we have a redundancy. The vector potential is defined only up to a gauge transformation

$$A_\mu \rightarrow A_\mu + \partial_\mu \alpha. \quad (1.12)$$

Configurations that differ by the derivative of an arbitrary  $C^2$  function  $\alpha$  describe the same electromagnetic fields and as a consequence the same physics. In this Section we are imagining that the reader does not know QFT. However in QFT one can prove that the only way to describe a massless spin-1 (or spin-2) field with nontrivial interactions is by introducing gauge invariance [6, 7]. This is a consequence of the definite transformation properties of  $A_\mu$  under the Lorentz group and the little group acting on massless four-momenta (so again just Lorentz symmetry!).

If we identify the  $A_\mu$  representing our new particle  $\gamma$  with the vector potential, this gauge redundancy reduces the total number of degrees of freedom to the two physical polarizations that we want to describe. This is the path that we take in the following. Causality and the Lorentz symmetry of special relativity led us to conclude that electromagnetic interactions must be described by a spin-1 particle  $A_\mu$  defined only modulo the gauge redundancy in Eq. (1.12). Using only the Lorentz symmetry we can further deduce that electromagnetic interactions must be in the form

$$\mathcal{L} = eA_\mu J^\mu, \quad (1.13)$$

with  $J^\mu$  transforming as a covariant vector and where  $e$  is a numerical coefficient. We can move forward in our understanding of Nature by noticing that the action shifted by  $A_\mu \rightarrow A_\mu + \partial_\mu \alpha$  must describe the same physics, so

$$\delta S = \int d^4x e(\partial_\mu \alpha) J^\mu = 0. \quad (1.14)$$

Without introducing quantum field theory, we can not attach a precise meaning to Eq. (1.13) or  $J^\mu$ , but we introduced  $J^\mu$  to represent particles interacting with electromagnetism and our considerations on causality and locality suggest that these particles must be localized to some extent. So if we take  $J^\mu$  to vanish sufficiently rapidly at infinity we can integrate Eq. (1.14) by parts and conclude that

$$\delta S = \int d^4x e\alpha \partial_\mu J^\mu = 0 \rightarrow \partial_\mu J^\mu = 0. \quad (1.15)$$

The last equality descends from the fact that  $\alpha$  is an arbitrary function. We can now start to appreciate the relation between forces and symmetries that we alluded to at the beginning of this Section. Noether's theorem allows us to associate each conserved current (i.e. divergenceless four-vector  $\partial_\mu J^\mu = 0$ ) to the generator of a symmetry of the action. So what are the symmetries associated to electromagnetism and the other forces of Nature?

Our straightforward application of the Lorentz symmetry and of causality has led us to ask a new question that we can still answer using symmetry, without introducing quantum field theory. To answer it, it is useful to recall another elementary property of the Lorentz group. Its algebra in terms of boosts  $K_i$  and rotations  $J_i$  ( $i = 1, \dots, 3$ ) is

$$[J_i, J_j] = i\epsilon_{ijk}J_k, \quad [K_i, K_j] = i\epsilon_{ijk}J_k, \quad [K_i, J_j] = i\epsilon_{ijk}K_k, \quad (1.16)$$

where  $i$  is the imaginary unit, when not used as an index, and  $\epsilon_{ijk}$  is the completely antisymmetric symbol. We can define a linear combination of the generators

$$A_i = \frac{J_i + iK_i}{2}, \quad B_i = \frac{J_i - iK_i}{2} \quad (1.17)$$

and notice that the algebra factorizes into two independent  $SU(2)$ 's

$$[A_i, A_j] = i\epsilon_{ijk}A_k, \quad [A_i, B_j] = 0, \quad [B_i, B_j] = i\epsilon_{ijk}B_k. \quad (1.18)$$

This means that we can have two different  $s = 1/2$  representations of the Lorentz group, depending on the  $SU(2)$  under which the particle transforms non-trivially. Particles belonging to different representations of the group can have different transformation properties under the other symmetries of the theory and hence interact differently with the SM forces. Traditionally, the two different  $s = 1/2$  representations are called left- and right-handed because parity exchanges them  $P : A \leftrightarrow B$ .

### 1.3.3 Global Symmetries

We now have all the ingredients to understand the symmetries of the SM associated to the forces of Nature. In the previous Section we have taken Lorentz invariance as a given. Here we would like to build up our knowledge of particle interactions from observations, but we still need a theoretical starting point.

In quantum mechanics a symmetry is a linear operation on the states (or more precisely the rays) of the Hilbert space  $U : |\psi\rangle \rightarrow |\psi'\rangle$  that preserves the results of our measurements

$$|\langle\psi'|\phi'\rangle|^2 = |\langle\psi|\phi\rangle|^2. \quad (1.19)$$

The above condition implies that  $U$  be unitary and linear or antiunitary and antilinear (Wigner's theorem [8]). In most cases of interest in physics the symmetry contains also the trivial element  $U = 1$ , which is of course unitary and linear and often all the other members of the symmetry group are continuously connected to the identity. Symmetries represented by antiunitary, antilinear operators are less prominent in physics. They all imply a reversal in the direction of time. This makes compact Lie groups a good place to start, since all their finite-dimensional representations are unitary (see for instance proposition 4.27 and theorem 4.28 in [9]) and the particles we know have a finite number of degrees of freedom. For this reason in the rest of this Section we will primarily consider compact Lie groups.

To move forward, first of all, we note that according to Noether's theorem each current corresponds to a generator of the symmetry group, so in general

$$\mathcal{L} = \sum_a g_a A_\mu^a J_a^\mu, \quad (1.20)$$

with  $a$  spanning the number of generators of the group. To understand if this quantity is invariant we need to know the representations that  $A_\mu^a$  and  $J_a^\mu$  are in. We already know that there are as many currents as generators and still from Noether's theorem we know that  $J_a^\mu$  is in the adjoint representation, so  $A_\mu^a$  must be as well for Eq. (1.20) to have a chance to be invariant. This means that Eq. (1.20) is invariant under the action of the group only if  $g_a = g, \forall a$ .

We know from observation that different particles interact with electromagnetism with different strength, so we need a different prefactor  $g$  for each of them. This leaves open a single possibility, the abelian group  $U(1)$ . This choice makes the adjoint representation trivial and allows us to write

$$\mathcal{L} \supset A_\mu (Q_e J_e^\mu + Q_u J_u^\mu + \dots) , \quad (1.21)$$

where, for example,  $J_e$  describes electrons,  $J_u$  up quarks and  $Q_{e,u}$  their respective charges.

We can now turn to strong interactions. Their symmetry group is  $SU(3)$ , which is traditionally called the color group. The selection of the group is unique, in view of [10]:

- (a) The group must admit complex representations to account for both quarks and anti-quarks and distinguish them. There are mesons which can be conveniently described as  $q\bar{q}$  bound states, but there is not any  $qq$  bound state.
- (b) There must be a color singlet completely antisymmetric representation made up of  $qqq$  in order to solve the statistics puzzle of the low-lying baryons of spin 1/2 and 3/2.
- (c) Given the number of quark flavors, the number of colors must be in agreement with the data on the total  $e^+e^-$  hadronic cross section and the  $\pi^0 \rightarrow \gamma\gamma$  decay rate.

Within simple groups, (a) restricts the choice to  $SU(N)$  with  $N \geq 3$ ,  $SO(4N + 2)$  with  $N > 1$  ( $SO(6)$  is homomorphic to  $SU(4)$ ) and  $E(6)$ . The remaining prescriptions lead unambiguously to  $SU(3)$  with each flavor of quarks in a fundamental representation.

We can now turn to weak interactions. It is useful to outline their history following [11]. In 1898 when Rutherford discovered that the so-called Becquerel ray consisted of two distinct types of radiation that he called  $\alpha$  and  $\beta$ . To pin down the symmetry group of weak interactions we can fast-forward to 1914, glossing over a number of important discoveries, to the observation by Chadwick of continuous (in energy)  $\beta$  emission from nuclei. Lise Meitner in 1922 pointed out the tension between this observation and quantum theory. Among competing hypothesis (for instance Bohr postulated energy non-conservation), Pauli formulated the correct one, the neutrino hypothesis. Fermi then followed with his theory of beta decay. M. Rosenbluth, C. N. Yang and T.D. Lee later found that muon decay and capture resembled beta decay. They then speculated that, in analogy with electromagnetism, the weak interaction could be carried an intermediate heavy boson and have a universal coupling.

This program was delayed by the so-called  $\theta$ - $\tau$  puzzle. In the early 50s,  $\theta$  was the name of a meson decaying into two pions, whereas  $\tau$  referred one decaying into three pions. Experiments showed that these mesons had different intrinsic parities, but had the same lifetime and the same mass. Researchers initially resisted the idea that weak interactions might violate parity. Until 1956 when Chien-Shiung Wu proved unambiguously parity non-conservation in the  $\beta$ -decay of Cobalt 60. Theorists T.D. Lee and C.N. Yang were awarded the Nobel prize for proposing the experiment. At this stage, the significance of the results at the end of the previous Section appears clear. Either only left-handed or only right-handed fermions couple to weak interactions. Further investigation along the lines of Wu's experiment led to conclude that left-handed fermions are the ones coupling to them.

In all these experiments (and many more that we had not the space to review) it was observed that: 1) electron number was conserved 2) charge was conserved. Electron number is

the sum of the number of left-handed and right-handed electrons  $E_{L,R}$  and neutrinos (taken with the opposite sign for positrons and anti-neutrinos). We know that a massless boson associated to charge conservation exists, it is the photon which mediates the  $U(1)$  interaction responsible for electromagnetism. However no equivalent particle is observed for electron number. This might be a symmetry of the theory not associated to any force at low energy. If this is the case the symmetry group of weak interactions has to commute with it. This means that electron and neutrino are in the same representation of the symmetry group of weak interactions. They form the doublet

$$L = \begin{pmatrix} \nu_e \\ e \end{pmatrix}. \quad (1.22)$$

The only Lie group with a two dimensional representation is  $SU(2)$ . This together with the observations of parity violation leaves only  $SU(2)_L$ . We can further notice that charge  $Q$  can be written as

$$Q = T_3 - E_R - \frac{E_L}{2} \equiv T_3 - Y. \quad (1.23)$$

Here  $T_3$  is one of the generators of  $SU(2)_L$ . Since  $T_3$  is part of the symmetry group of weak interactions and  $Q$  is conserved,  $Y$  must be conserved as well. This quantity is called hypercharge.

We have gone a very long way in the description of the SM. However to take the last step we need quantum field theory. In reality electromagnetic and weak interactions are unified at high energies and described by the symmetry group  $SU(2)_L \times U(1)_Y$ . The Lagrangian is invariant under this symmetry, but the vacuum is invariant only under the  $U(1)_Q$  subgroup describing electromagnetism. This is the reason why the bosons that mediate the weak force are massive, while the photon is massless and at low energy the full  $SU(2)_L \times U(1)_Y$  invariance is not manifest. We will describe these phenomena in more detail in the next Section, where we go back to assuming that the reader posses a modern knowledge of quantum field theory.

## 1.4 The Standard Model Lagrangian

We have reached the end of our symmetry-based exercise and from now on we will assume that the reader has a modern knowledge of quantum field theory. In this Section we introduce the SM Lagrangian and the role played by the Higgs boson.

We have seen in the previous Sections that strong and electroweak interactions are described by the symmetry groups  $SU(3) \times SU(2)_L \times U(1)_Y$ . The fermions representations can be summarized as follows

$$\Psi = (Q(3, 2)_{1/6}, L(1, 2)_{-1/2}, u^c(\bar{3}, 1)_{-2/3}, d^c(\bar{3}, 1)_{1/3}, e^c(1, 1)_1), \quad (1.24)$$

where the first number in parenthesis indicates the  $SU(3)$  representation, the second one the  $SU(2)_L$  one and the subscript the hypercharge. We have suppressed the flavor indexes that label different fermion families for simplicity, but we will restore them below. In most of this work we use the notation in Eq. (1.24) where the SM fermions are described by left-handed Weyl spinors. We occasionally use also a Dirac notation related to the previous one by  $Q = (u_L \ d_L)$  and  $u^c = \bar{u}_R$ .

The three forces described by the Standard Model are included in the Lagrangian as gauge interactions

$$\mathcal{L}_{\text{SMg}} = -\frac{1}{4}B_{\mu\nu}B^{\mu\nu} - \frac{1}{4}W_{\mu\nu}^i W^{\mu\nu i} - \frac{1}{4}G_{\mu\nu}^a G^{\mu\nu a} + i\bar{\Psi}\gamma^\mu D_\mu\Psi. \quad (1.25)$$



The first three operators are the kinetic terms of the gauge bosons that mediate the interaction

$$\begin{aligned} B_{\mu\nu} &= \partial_\mu B_\nu - \partial_\nu B_\mu, \\ W_{\mu\nu}^i &= \partial_\mu W_\nu^i - \partial_\nu W_\mu^i - g_W \epsilon^{ijk} W_\mu^j W_\nu^k, \\ G_{\mu\nu}^a &= \partial_\mu G_\nu^a - \partial_\nu G_\mu^a - g_s f^{abc} G_\mu^a G_\nu^b, \end{aligned} \quad (1.26)$$

where  $B_\mu, W_\mu^i, G_\mu^a$  are the quantum fields describing the gauge bosons,  $g_W$  and  $g_s$  are the weak and strong gauge couplings and  $\epsilon$  and  $f$  are the structure constants of  $SU(2)_L$  and  $SU(3)$ , respectively. The last operator in the Lagrangian contains the kinetic term of the fermions and their gauge interactions

$$i\bar{\Psi}\gamma^\mu D_\mu\Psi = i\bar{\Psi}\gamma^\mu \left( \partial_\mu + ig_s \sum_{a=1}^8 \lambda^a G_\mu^a + ig_W \sum_{i=1}^3 T^i W_\mu^i + ig_Y Y B_\mu \right) \Psi. \quad (1.27)$$

In the previous expression  $\lambda^a$  are the generators of  $SU(3)$ ,  $T^i$  those of  $SU(2)_L$  and  $Y$  is the hypercharge. They act in block-diagonal form on  $\Psi$ , which is a vector of irreducible representations.

To complete this picture we need to introduce mass terms for fermions and weak gauge bosons. The difficulty resides in the fact that a mass term for the fermions clashes with  $SU(2)_L$  invariance, since it couples left-handed fields with right-handed ones

$$m\bar{\psi}\psi = m(\bar{\psi}_L\psi_R + \bar{\psi}_R\psi_L). \quad (1.28)$$

The problem with a mass term for  $W_\mu^i$  is that it is not invariant under the gauge shift  $W \rightarrow W + \partial\alpha$  that preserves the right counting of degrees of freedom, i.e. a massive gauge boson has one extra degree of freedom compared to the massless gauge boson described by  $\mathcal{L}_{\text{SMg}}$ . The introduction of a single  $SU(2)_L$  spin zero doublet

$$H(1, 2)_{1/2} \quad (1.29)$$

solves both problems. In the following we will call this field the Higgs boson.  $H$  couples to gauge bosons

$$\mathcal{L}_H \supset |D_\mu H|^2 \quad (1.30)$$

and can have the following Yukawa couplings with SM fermions

$$\mathcal{L}_Y = -Y_u Q H u^c - Y_d Q H^\dagger d^c - Y_e L H^\dagger e^c + \text{h.c.} \quad (1.31)$$

$Y_{u,d,e}$  are matrices in flavor space, Lorentz and gauge indexes are left implied. If we further imagine a non-trivial form for its potential

$$\mathcal{L}_H = |D_\mu H|^2 + m_h^2 |H|^2 - \frac{\lambda}{2} |H|^4, \quad (1.32)$$

where  $m_h^2 > 0$ , the ground state of the theory is at a non-zero value of the field

$$\langle H \rangle = \begin{pmatrix} 0 \\ v \end{pmatrix}, \quad v = \frac{m_h}{\sqrt{\lambda}}. \quad (1.33)$$

In the following we will often use  $\langle h \rangle$  to denote the vacuum expectation value of the Higgs boson.  $h$  is the spin-0 degree of freedom that remains in the  $H$  doublet in unitary gauge. Choosing new field variables we can write  $H$  as

$$H = e^{i\frac{\sigma^i \pi^i}{2}} \begin{pmatrix} 0 \\ h \end{pmatrix}. \quad (1.34)$$

A  $SU(2)_L$  gauge transformation allows to get rid of the  $\pi^i$ 's, giving

$$H_{\text{unitary}} = \begin{pmatrix} 0 \\ h \end{pmatrix}. \quad (1.35)$$

This is the scalar that was produced at CMS and ATLAS and was observed to have  $m_h \simeq 125$  GeV. The degrees of freedom described by  $\pi^i$  of course do not disappear from the theory, they make up the extra degrees of freedom that allows three of the  $SU(2)_L \times U(1)_Y$  gauge bosons to become massive. If we expand the SM Lagrangian, including  $H$ ,

$$\mathcal{L}_{\text{SM}} = \mathcal{L}_{\text{SMg}} + \mathcal{L}_Y + \mathcal{L}_H, \quad (1.36)$$

around its true ground state, we find a mass term for the gauge bosons

$$|D_\mu H|^2 = m_W^2 W_\mu^+ W^{\mu-} + m_Z^2 Z_\mu Z^\mu + \dots, \quad (1.37)$$

where

$$W_\mu^\pm = \frac{W_\mu^1 \pm iW_\mu^2}{\sqrt{2}}, \quad m_W = \frac{g_W v}{\sqrt{2}}, \quad (1.38)$$

and

$$Z_\mu = \cos \theta_W W_\mu^3 - \sin \theta_W B_\mu, \quad m_Z = \frac{\sqrt{g_W^2 + g_Y^2} v}{\sqrt{2}}. \quad (1.39)$$

The same happens for the fermions through the Yukawa couplings to  $H$ . We can first write them using singular value decomposition

$$Y_a = U_L^a Y_a^D U_R^{a\dagger}, \quad (1.40)$$

then we can use the large flavor symmetry of the gauge Lagrangian  $SU(3)^5 \times U(1)^4$  to rotate away  $U_R^{a\dagger}$ . We can do the same for  $U_L^a$  and be left with flavor-diagonal Yukawas that give mass to the fermions

$$\begin{aligned} \mathcal{L}_Y &= -Y_u^D Q H u^c - Y_d^D Q H^\dagger d^c - Y_e^D L H^\dagger e^c + \text{h.c.} \\ &= -Y_u^D v Q u^c - Y_d^D v Q d^c - Y_e^D v L e^c + \dots \end{aligned} \quad (1.41)$$

However a single unitary matrix, known as the Cabbibo-Kobayashi-Maskawa (CKM) matrix [12, 13]

$$V \equiv U_L^u U_L^{d\dagger}, \quad (1.42)$$

remains in the Lagrangian and mixes different mass eigenstates through weak interactions

$$\mathcal{L}_{\text{SMg}} \supset g_W W_\mu^+ (\bar{u}_L V \gamma^\mu d_L) + \text{h.c.} \quad (1.43)$$

The reason being that weak interactions couple the quark doublet  $Q$  with itself, so they respect a single  $SU(3)$  flavor symmetry in the left-handed quark sector. To fully rotate away the  $U_{L,R}^a$  we need a separate  $SU(3)$  for each quark (i.e.  $u_L, d_L, u_R$  and  $d_R$ ), but the Lagrangian is symmetric only under  $SU(3)^5 = SU(3)_Q \times SU(3)_{u_R} \times SU(3)_{d_R} \times SU(3)_L \times SU(3)_{e_R}$ .

As shown in Fig. 1.1 the quark and lepton masses are strongly hierarchical. The heaviest particle is the top quark. Its Yukawa coupling is  $y_t = \mathcal{O}(1)$ . The lightest SM fermions (electron,  $u$  and  $d$  quarks) have couplings to the Higgs of  $\mathcal{O}(10^{-5})$ . At scales comparable to  $m_h$  the

particles that are most strongly coupled to the Higgs after the top quark are  $W$  and  $Z$  bosons, since their gauge couplings are  $\mathcal{O}(0.5)$ .

To conclude this Section we note that there is an operator allowed by all the symmetries introduced above that we have not yet discussed:

$$\frac{\alpha_s \theta}{8\pi} G_{\mu\nu}^a \tilde{G}^{\mu\nu a}, \quad (1.44)$$

where  $\tilde{G}^{\mu\nu a} = (1/2)\epsilon^{\mu\nu\rho\sigma} G_{\rho\sigma}^a$  and  $\epsilon^{\mu\nu\rho\sigma}$  is the completely antisymmetric symbol. This operator is a total derivative and perturbatively it does not have a measurable effect. However, at scales where QCD confines, the interference between instantons (i.e. classical solutions for the gluon field that fall off sufficiently slowly at infinity) and quark masses induces observable effects that depend on  $\theta$ . From measurements of the neutron electric dipole moment we can conclude that  $\theta \lesssim 10^{-10}$  [14]. In what follows we will return to this operator for two reasons: 1) The smallness of  $\theta$  is puzzling from the point of view of dimensional analysis (this is the so-called *strong CP problem*) 2) This is the only operator in the SM whose vacuum expectation value is sensitive to  $\langle H \rangle$  and this will play an important role in the explanations that we propose for the value of  $m_h$ .

A last aspect of the SM Lagrangian that is worth mentioning, but will not play an equally important role in what follows, are neutrino masses. The Lagrangian that we have written so far preserves a  $U(1)^4$  symmetry even after Yukawa couplings are included. We have a  $U(1)_B$ , i.e. a phase rotation of all the quarks that are therefore said to carry baryon number and a  $U(1)_{L_e} \times U(1)_{L_\mu} \times U(1)_{L_\tau}$ , i.e. the phase of each lepton family can be chosen arbitrarily. This latter symmetry is not observed in Nature, only the total lepton number (i.e. the diagonal subgroup of  $U(1)_{L_e} \times U(1)_{L_\mu} \times U(1)_{L_\tau}$ ) is conserved in current experiments. Observing the violation of individual lepton numbers has lead to experimentally establish the existence of neutrino masses [15].

We have two possibilities to include them in the SM. We can add a neutral singlet  $N(1, 1)_0$ .  $N$ , together with the neutral component of  $L$ , forms a Dirac fermion with mass given by the Yukawa interaction

$$\mathcal{L}_{Y\nu} = -y_N \bar{L} H N + \text{h.c.} \quad (1.45)$$

Alternatively we can include a small Majorana mass for the neutral component of  $L$  that would break also the total lepton number. The simplest  $SU(2)_L$  invariant operator that can generate this mass term is

$$\mathcal{L}_{M\nu} = \frac{(HL)^2}{\Lambda_N} + \text{h.c.} \quad (1.46)$$

where  $\Lambda_N$  is an unknown scale such that  $m_\nu \sim v^2/\Lambda_N$ . These two options can be distinguished experimentally, given that they preserve different symmetry groups, but we do not yet have the required sensitivity [15].

### 1.4.1 Aside on Renormalization

In this work we often use scaling arguments akin to those in Section 1.3.1 to enforce the selection rules of dilations.

It is therefore useful to recall some technical aspects of operator dimensions that make our arguments more precise. Consider first a free, shift-symmetric, real scalar field

$$S = \int d^D x \frac{(\partial_\mu \phi)^2}{2}. \quad (1.47)$$

The scaling dimensions of the field can be inferred from  $[S] = 0$  that implies  $[\phi] = \frac{D-2}{2}$ . This exercise of deducing the scaling dimension of a field from its kinetic term can be done in any theory, including strongly interacting ones. Care must be taken when there is more than one kinetic term. An example is  $2 + 1$  dimensional gauge theory where both a single derivative Chern-Simons term and a Maxwell term with two derivatives are present. A similar occurrence arises in the statistical mechanics of membranes, where there are a second derivative tension and fourth derivative rigidity. However, in general, at any given momentum a single kinetic term dominates and determines the scaling dimension.

This already shows that the scaling dimensions of the fields are not set in stone, but can depend on the energy at which we evaluate them. This is important for our arguments because we can deduce the scaling dimensions of parameters, including  $m_h$ , from that of the fields. For instance, if we consider the interacting theory

$$S = \int d^D x \left[ \frac{(\partial_\mu \phi)^2}{2} - \frac{m^2}{2} \phi^2 - \frac{\lambda}{4} \phi^4 \right]. \quad (1.48)$$

we have  $[m] = 2$ ,  $[\lambda] = 4 - D$ . From this simple example one might conclude that only rational dimensions are relevant and that, in theories with a single kinetic term, scaling dimensions are fixed. This is not true; consider the change of variables

$$x' = sx, \quad \phi(x) = s^{\frac{2-D}{2}} \phi'(x'). \quad (1.49)$$

This turns the action to

$$S = \int d^D x' \left[ \frac{(\partial_\mu \phi')^2}{2} - \frac{s^2 m^2}{2} \phi'^2 - \frac{s^{4-D} \lambda}{4} \phi'^4 \right]. \quad (1.50)$$

Since this is just a change of variables correlation functions defined as

$$G_n(x_1, \dots, x_n; m, \lambda, M) \equiv \langle \phi(x_1) \dots \phi(x_n) \rangle_M. \quad (1.51)$$

must remain unaltered. The subscript  $M$  indicates that the parameters of the theory, such as  $m$  and  $\lambda$  are measured at the scale  $M$ . From the invariance of  $G_n$  we have

$$G_n(sx; m, \lambda, M) = s^{n\gamma_\phi} G_n(x; s^2 m, s^{D-4} \lambda, sM), \quad (1.52)$$

where in a free theory  $\gamma_\phi = (2 - D)/2$ . From the previous equality we can obtain the so called renormalization group equation

$$\left[ M \frac{\partial}{\partial M} + \beta_{m^2} \frac{\partial}{\partial m^2} + \beta_\lambda \frac{\partial}{\partial \lambda} + n\gamma_\phi \right] G_n = 0, \quad (1.53)$$

where

$$M \frac{\partial}{\partial M} g(M) = \beta_g(g(M)), \quad g = m, \lambda, \gamma_\phi. \quad (1.54)$$

We have found that couplings and scaling dimensions depend on the scale  $M$  at which they are measured. In general, before using the scaling arguments anticipated at the very beginning of the chapter, we have to compute the scaling dimensions of SM fields in the full interacting theory. However in weakly coupled theories the so-called *anomalous* dimensions (i.e.  $\gamma_\phi$  minus its value in the free theory) are small, of  $\mathcal{O}(g^2/16\pi^2)$  where  $g$  is a generic coupling in the theory. In the SM, where the largest coupling is  $\mathcal{O}(1)$ , the anomalous dimensions of fields can be neglected without changing qualitatively our arguments. So we will always take  $[H] \simeq 1$  and  $[m_h] \simeq 2$ .

## 1.5 Beyond the Standard Model

The theory that we summarized in the previous Sections was built on Earth from observations of cosmic rays and particle collisions. Remarkably it can also describe most experimental observations of the Universe at early times. There are, however, some notable exceptions. The particles and forces in the SM can not account for the observed dark matter abundance and can not explain the observed asymmetry between matter and anti-matter.

Dark Matter (DM) makes up about 80% of the matter in the Universe i.e. of the energy density component that is diluted as  $a^{-3}$  as the Universe expands.  $a$  is a scale factor parametrizing the spatial size of the Universe. We can clearly distinguish it from baryons, which are the main matter component coming from the SM, mainly because it interacts very weakly with light  $\sigma(\text{DM } \gamma \rightarrow \text{DM } \gamma) \lesssim 10^{-33} \text{ cm}^2(m_{\text{DM}}/\text{GeV})$ . It was discovered through its gravitational interactions [16], and to the best of our knowledge these are the only interactions that it is guaranteed to have with SM. Given that we observe it today in our galaxy and also at redshift  $z \simeq 1100$  in the CMB power spectrum, it has a lifetime at least comparable to the age of the Universe  $\tau \simeq 14 \text{ Gy}$ . This leaves as a candidate DM particle in the SM only proton, electron and neutrinos. Proton and electrons are excluded from the stringent bounds on the DM interactions with light and from the fact that most of the DM is observed to fall into approximately spherical halos [17], while hydrogen atoms can radiate photons and at late times fall approximately onto a thin disc which defines the galactic plane. The SM neutrinos have masses around  $m_\nu \simeq \text{meV}$  and interact only through the weak force. These two properties allow to predict their abundance today and their impact on the matter power spectrum in the Universe (roughly speaking the Fourier transform of the two point function of galaxies on the celestial sphere), neither of which matches what we observe for DM. In summary, physics beyond the Standard Model is needed to explain the existence of DM. Even if we postulate the existence of primordial black holes made of SM particles, the theory needs to include new ingredients to produce them with the right abundance and in certain mass windows that are still experimentally viable. DM is not the main character in the rest of this work, but we will see how many of the ideas that we discuss here predict specific DM candidates. We elaborate on these aspect of the models and where needed we discuss experimental properties of DM that we did not include in this Section.

A second observational aspect of the Universe that the SM does not fully capture is the dominance of matter over anti-matter that we observe. In terms of particles it is a small number  $\eta \equiv (n_B - n_{\bar{B}})/n_\gamma \simeq 10^{-11}$  if compared to the number of photons, but it makes a big difference for our existence. To make this possible we clearly have to break the CP symmetry that relates particles to anti-particles. This breaking is already present in the SM, both in the CKM matrix  $V$  in Eq.s (1.42) and (1.43) and in the  $\theta$ -angle Eq. (1.44), if non-zero. We also need baryon number violation, charge conjugation violation and a departure from thermal equilibrium during the history of the Universe (together with CP-violation these are known as Sakharov's conditions [18]). The SM alone does not have all the necessary ingredients, the parameters violating C and CP are too small and baryon number is preserved.

From this brief discussion it is clear that the SM must be extended to fully describe the observable Universe. It is useful to recall that both DM and baryogenesis are not tied to a definite energy scale or type of interaction. DM could be as light at  $10^{-22} \text{ eV}$  and as heavy as  $10^{48} \text{ GeV}$ . It could be charged under  $SU(2)_L$  or coupled to us only gravitationally. It could have self-interactions as large as  $\sigma/m_{\text{DM}} \simeq \text{cm}^2/\text{g}$  or none at all. It could be produced at  $M_{\text{Pl}}$  as well as  $m_e \simeq 0.5 \text{ MeV}$  or below. Similarly, baryogenesis could take place at the electroweak phase transition, at temperatures around  $m_h$ , or close to  $M_{\text{Pl}}$ , via a variety of different mechanisms. Clearly a vast amount of experimental and theoretical work is still ahead of us if we want to pin down the precise nature of these two phenomena. There are, however, other clues on how

to extend the SM that could shed light also on these two observations.

Aside from these two unexplained observations, the SM leaves open a number of theoretical mysteries. These are not failures of the theory to describe observed phenomena, but rather peculiarities of the model that contain precious clues on what particle interactions might look like at much higher energies.

The most striking at first sight is the equality between proton and electron charge. A priori proton and electron have nothing to do with each other. They have different quantum numbers and the proton is not even an elementary particle. However their charge is the same at least in a few parts in  $10^{19}$  [19]. Stated differently, the question might be: why are all the electromagnetic charges in the SM rational multiples of a single number? The simplest and most elegant explanation is that the symmetry groups that describe SM forces are unified into a larger group at high energies. We discussed in Section 1.3.3 how this implies a single coupling constant for all fermion fields. As was often the case in particle physics in the last decades, the simplest implementation of this idea was excluded, in this case by lower bounds on the proton lifetime [20]. However this general possibility remains open and appealing.

The second peculiarity that a casual observer would notice is the structure of the fermion mass matrices. Why are the quantum numbers of the first family reproduced in two more copies with different masses? Where are the hierarchies in the Yukawa matrices coming from? While we have several answers to the second question, for instance in terms of Froggatt-Nielsen constructions [21–23], the first one remains open.

The last aspect of the SM that remains mysterious is the central theme of this work. Among the parameters in the SM Lagrangian that can not be computed there are three that keep most particle physicists awake at night: the cosmological constant  $\Lambda_{CC}$ , the Higgs boson mass  $m_h^2$  and the QCD  $\theta$ -angle.

The cosmological constant is the most relevant parameter in the Lagrangian (i.e. the one with the largest scaling dimension under spacetime dilations). It determines the maximal size of the observable universe. We can estimate it in a similar way as  $m_h^2$ , as discussed in Section 1.1. Its natural value  $\Lambda_{CC} \sim M_{\text{Pl}}^4$  is about  $10^{120}$  larger than what we observed from the expansion of the Universe  $\Lambda_{CC} \simeq (0.1 \text{ meV})^4$  [24, 25].

The Higgs mass squared is the second most relevant parameter in the Lagrangian and it determines  $\langle H \rangle$ , which, as we have seen in this Chapter, is responsible for many of the observed properties of the SM, including the masses of all massive particles. Its natural value  $m_h^2 \sim M_{\text{Pl}}^2$  is  $10^{34}$  larger than its observed one  $m_h^2 \simeq (125 \text{ GeV})^2$ .

The QCD  $\theta$ -angle parametrizes the size of the irrelevant operator in Eq. (1.44). Also in this case we expect it to be  $\sim 10^{10}$  times larger than what we observed.

These three observations are broadly called “naturalness problems” or “fine-tuning problems”. If we extend the SM into theories where we can compute these three parameters, the small values that we observe can only be explained by an accidental cancellation between unrelated contributions. Different terms in the calculation appear to be unnaturally fine-tuned to give the observed result. However it is useful to remember that purely within the SM there is no fine-tuning, these are measured parameters of the effective theory. The only potential problem from this low energy perspective is, in some sense, a failure of symmetry. To estimate the natural value of these parameters (that is so much larger than observations) we used only symmetry. This is a common procedure in every branch of science and it always gives the correct result. The fact that in these instances it did not work means that the underlying theory of Nature is quite different from what we can naively infer at low energy. In the next Chapter we return on this issue and on what it could mean in much greater detail.

# Chapter 2

## The Hierarchy Problem

And if thou gaze long into an  
abyss, the abyss will also gaze  
into thee.

---

*Friedrich Nietzsche*

The questions surrounding electroweak symmetry breaking and the Higgs boson mass have driven particle physics for decades. The efforts of thousands of researchers have led to the discovery of the Higgs boson about ten years ago at the LHC. Thanks to this research program we now have an understanding of the laws of Nature at energies never reached before with an unprecedented precision.

The most interesting consequence of this gargantuan effort is that the value of the Higgs boson mass remains mysterious. The problem is more concrete today than it ever was because we have finally discovered the Higgs boson, measured its mass and established that it is a fundamental scalar (at least up to a factor of ten in energy above its mass).

The problem is also more fascinating because its most elegant solutions can not be realized in their simplest form and it is unclear whether we should abandon them entirely and radically change our outlook on the weak scale or accept some amount of tuning as a fundamental aspect of physics. Either way we will learn something new about Nature.

In this Chapter we give a precise statement of the problem and the assumptions needed to formulate it. We then review its traditional symmetry-based solutions. Before turning to the more technical aspects of this question, we give a historical account of similar problems that we encountered in fundamental physics and their resolutions.

### 2.1 Historical Background

In Section 1.1 we have given a brief, but correct statement of what is puzzling about the value of the Higgs boson mass. An estimate based on symmetry is many orders of magnitude larger than its measured value. This does not make the SM effective theory inconsistent since the Higgs boson mass is given by the sum of multiple contributions and we can compute only some of them (which, incidentally, are of the right order). Within the SM the best that we can do is measure  $m_h$ .

However, there is a somewhat imprecise, but historically useful way to highlight a tension already in the SM EFT. If we regularize loops with a hard cutoff  $\Lambda$ , using it as a proxy for new particles or interactions at that scale, we find that  $m_h$  in the SM is given by  $m_h^2 \simeq m_{h,0}^2 + y_t^2 \Lambda^2 / 16\pi^2$ , with  $m_{h,0}$  a bare Lagrangian parameter, so a  $m_h \ll \Lambda$  can only be explained by an accidental cancellation between the two terms.

This of course is not a calculation. If we renormalize correctly the effective theory (maybe using an  $\overline{\text{MS}}$  scheme) no trace of  $\Lambda$  and of cancellations is left and we return to the conclusion that  $m_h$  is just a measured parameter of the EFT.

The previous discussion can only be made precise in a theory where  $m_h$  can be calculated. When we write  $m_h^2 \simeq m_{h,0}^2 + y_t^2 \Lambda^2 / 16\pi^2$  we are using  $\Lambda$  as a placeholder for the masses of new particles (or the threshold of a CFT) in a theory that we do not yet know. In practice we are making assumptions on high energies that we will state precisely in the next Sections.

For the moment it is useful to set aside these caveats and examine similar instances of apparent cancellations in past EFTs of Nature. This will show how this kind of tensions often signals paradigmatic changes in our understanding of physics. It will also give us an overview of their possible resolutions which often map faithfully to modern candidate explanations for the value of  $m_h$ .

Often, accidental cancellations between unrelated parameters signal that our description of Nature is incomplete. A well-known example is the rest energy of the electron in classical electrodynamics. In natural units we have

$$m_e = m_{e,0} + \frac{e^2}{4\pi r_e}. \quad (2.1)$$

The first term on the right-hand side is the bare electron mass in the Lagrangian. The second accounts for the energy stored in the electric field generated by the electron in a sphere of radius  $r_e$ , as computed in classical electrodynamics.

Experimentally we know that  $m_e \simeq 0.5$  MeV. Cheating a little for illustrative purposes we can use our modern knowledge of the electron radius  $r_e \lesssim \text{TeV}^{-1}$  to cut-off the divergence of the Coulomb self-energy. This corresponds to not having observed deviations from a point-like behavior at the LHC. Putting together these two measurements we conclude that only an accidental cancellation between the two terms on the right-hand side of Eq. (2.1) can explain the observed value of the electron mass.

This apparent fine-tuning is hiding something deep. At the length scales in our calculation classical electrodynamics breaks down and we need to include quantum effects to obtain the correct result. Restoring units, we can not ignore quantum mechanics below

$$c\Delta t \lesssim \frac{\hbar c}{\Delta E} \simeq \frac{\hbar}{m_e c}, \quad (2.2)$$

or in natural units for  $r_e \lesssim 1/m_e$ . So the result of our classical calculation is not correct. If we include the contribution of photons and positrons from vacuum fluctuations [?], the term that diverges as  $1/r_e$  is cancelled by virtue of a new symmetry. The chiral symmetry that emerges in quantum electrodynamics as  $m_e$  goes to zero. Only a term logarithmic in  $1/r_e$  and proportional to  $m_{e,0}$  survives, as dictated by the selection rules of this new symmetry,

$$m_e = m_{e,0} \left[ 1 + \frac{3\alpha}{4\pi} \log \frac{1}{m_e r_e} \right]. \quad (2.3)$$

Now we have a correction of less than 10% even for an electron that stays point-like up to the Planck scale. Incidentally, pushing classical electrodynamics beyond its limits of validity has other surprising consequences, including the emergence of an acausal behavior for the electron on time scales of  $\mathcal{O}(e^2/m_e)$  [?].

Setting violations of causality aside, we have just seen that what appeared as an accidental cancellation was pointing to a more fundamental description of our physical system in terms of quantum mechanics.

This is not the only case in which apparent coincidences is signaling the emergence of a new paradigm. A second classic example that has a completely different resolution is that



of planetary orbits in the solar system. In 1596 Johannes Kepler published the *Mysterium Cosmographicum*, where he showed that each of the five Platonic solids can be uniquely inscribed into and circumscribed by a sphere. If ordered in a specific pattern (octahedron, icosahedron, dodecahedron, tetrahedron, cube) the spheres reproduced, within the experimental accuracy of the time, the orbits of the six known planets, from Mercury to Saturn. This seems a striking coincidence that requires finely tuned values of unrelated parameters. Alternatively, as Kepler did, one could see it as an example of God’s refined aesthetic sense.

Today we know that the explanation is different, but still paradigm-shifting. Not only we are not unique in any way, but we are just a tiny speck of dust in an unimaginably vast universe. This kind of approximate accidents become likely if we think about the staggering number of other stars, planets and solar systems over which we have to integrate small probabilities.

These two examples are exemplary of two broad answers that Nature has given us when we encountered apparent fine-tunings in the past. We either have seen new symmetries, as was the case for the electron, or a landscape, i.e. multiple realizations of the observable that we thought to be unique, as in Kepler’s solar system. Each in its own way these were drastic changes in our understanding of Nature.

Importantly, these are not the only two examples. Apparent fine-tunings could have appeared also in quantum field theory, but Nature has always resolved them before they occurred. Using our modern knowledge of particle interactions we can find many of these instances. We can estimate UV-sensitive parameters in the effective theories that pre-dated the SM using the symmetries of the effective theory and find that these effective theories were completed by new symmetries before any fine-tuning occurred.

For instance, the mass difference between neutral and charged pions in the chiral Lagrangian is not protected by any symmetry. From the interaction of the charged pion with electromagnetism

$$\mathcal{L}_{\text{ChPT}} \supset \Lambda_{\text{QCD}}^2 f_\pi^2 \frac{\pi^\dagger \overleftrightarrow{\partial}_\mu \pi}{f_\pi^2 \Lambda_{\text{QCD}}^2} \frac{eA^\mu}{\Lambda_{\text{QCD}}} = eA^\mu \pi^\dagger \overleftrightarrow{\partial}_\mu \pi, \quad (2.4)$$

we can estimate

$$m_{\pi^+}^2 - m_{\pi^0}^2 \simeq \frac{3\alpha\Lambda^2}{4\pi} \approx (35.5 \text{ MeV})^2 \quad (2.5)$$

where  $\Lambda$  is the largest energy scale where this theory is valid. As we mentioned for the Higgs boson this is not a real calculation, but just an estimate based on hidden assumptions on the UV. In this effective theory  $m_{\pi^+}^2, m_{\pi^0}^2$  are two measured parameters of the chiral Lagrangian.

Our estimates and the measured mass difference  $m_{\pi^+}^2 - m_{\pi^0}^2$  point to  $\Lambda \lesssim 850 \text{ MeV}$ . Indeed, a new particle appears at  $m_\rho = 770 \text{ MeV}$  to complete this picture. In the full theory of strong interactions, given by QCD, the model that we used to obtain Eq. (2.5) is valid only up to  $\simeq m_\rho$ , at much higher energies there are no pions. The fundamental degrees of freedom are the SM quarks described in the previous Chapter, whose masses are protected by chiral symmetries.

A similar phenomenon occurs in the Fermi theory of weak interactions. Using our modern knowledge of particle physics we can write the original vertex introduced by Fermi as an effective theory of quark and lepton interactions

$$\mathcal{L}_{\text{Fermi}} \supset \frac{G_F}{\sqrt{2}} (\bar{u}_L \gamma^\mu d_L) (\bar{e}_L \gamma_\mu \nu_L) + \text{h.c.} \quad (2.6)$$

If we imagine that also neutral current interactions exist, such as

$$\mathcal{L}_{\text{Fermi}} \supset \frac{G_F}{\sqrt{2}} \cos^2 \theta_c (\bar{d}_L \gamma^\mu d_L)^2 + \frac{G_F}{\sqrt{2}} \sin^2 \theta_c (\bar{s}_L \gamma^\mu d_L) (\bar{d}_L \gamma^\mu s_L) + \dots \quad (2.7)$$

We can use this theory to compute the  $K^0$  and  $\bar{K}^0$  mesons mass mixing

$$\begin{pmatrix} \bar{K}^0 & K^0 \end{pmatrix} \begin{pmatrix} m_K^2 & \delta m_K^2 \\ \delta m_K^2 & m_K^2 \end{pmatrix} \begin{pmatrix} \bar{K}^0 \\ K^0 \end{pmatrix}, \quad (2.8)$$

and we can again estimate the splitting  $\delta m_K^2$  using a cutoff  $\Lambda$ . The two mass eigenstates  $K_L^0$  and  $K_S^0$  are split roughly by

$$\frac{m_{K_L^0} - m_{K_S^0}}{m_{K_L^0}} \simeq G_F^2 f_K^2 \cos^2 \theta_c \sin^2 \theta_c \Lambda^2, \quad f_K \approx 114 \text{ MeV}, \quad (2.9)$$

where  $f_K$  parametrizes the matrix element of the quark currents between two mesonic states and  $\Lambda$  is again the largest scale of validity of the theory. The Lagrangian  $\mathcal{L}_{\text{Fermi}}$  can be obtained from the SM,

$$\mathcal{L}_{\text{SMg}} \supset -\frac{g}{\sqrt{2}} W^\mu \left[ \bar{u} \gamma_\mu \frac{(1 - \gamma_5)}{2} (d \cos \theta_c + s \sin \theta_c) + \bar{c} \gamma_\mu \frac{(1 - \gamma_5)}{2} (-d \sin \theta_c + s \cos \theta_c) \right], \quad (2.10)$$

after integrating out up and charm quarks. The observed Kaon mass difference allows to predict the charm quark mass. From the same naturalness arguments introduced above, we conclude that  $\Lambda \lesssim 2 \text{ GeV}$  and indeed we find  $m_c = 1.2 \text{ GeV}$ .

Historically the examples that we discussed in this Section were all post-dictions of naturalness. The estimates of  $\Lambda$  and  $r_e$  were made after the new symmetries explaining them were discovered. However they still show that conceptual puzzles identical to the one that we have encountered for the Higgs boson, have hidden real paradigm changes in our description of Nature. Perhaps more importantly they also sharpen our uneasiness with accepting an accidental cancellation for the Higgs boson mass. All examples of similar issues in fundamental physics were resolved way before any fine-tuning was manifest. The only counterexample that I am aware of is that of Love numbers of rotating black holes. However also this example was recently shown to be explained by a symmetry [26, 27].

## 2.2 The Unbearable Lightness of the Higgs

In the previous Chapter we have seen that the Higgs boson mass plays a privileged role in the SM. It determines the Higgs vacuum expectation value

$$\langle H \rangle = \begin{pmatrix} 0 \\ v \end{pmatrix}, \quad v = \frac{m_h}{\sqrt{\lambda}}. \quad (2.11)$$

$\langle H \rangle$  enters the fermion masses through their Yukawa couplings  $y_i$

$$m_e = y_e v, \quad m_u = y_u, \quad \dots \quad (2.12)$$

and the  $W$  and  $Z$  masses

$$\begin{aligned} |D_\mu H|^2 &= m_W^2 W_\mu^+ W^{\mu-} + m_Z^2 Z_\mu Z^\mu + \dots, \\ m_W &= \frac{g_W v}{\sqrt{2}}, \\ m_Z &= \frac{\sqrt{g_W^2 + g_Y^2} v}{\sqrt{2}}, \end{aligned} \quad (2.13)$$

that set the range of weak interactions. These quantities determine much of the low energy phenomena that make chemistry and life possible. It is only natural to try to understand the value of this parameter.

In this Section we show why measuring  $m_h \simeq 125 \text{ GeV}$ , although expected from LEP electroweak precision constraints, is theoretically quite puzzling.

### 2.2.1 A Precise Statement in the Standard Model

There is no real problem associated to  $m_h$  in the SM, as we already recalled in the previous Sections. However, the mere fact of discovering what looks like a fundamental scalar at energies much smaller than  $M_{\text{Pl}}$  should give us pause. In this Section we make this statement more precise, following the very nice exposition in [28].

If we follow 't Hooft naturalness criterion [29]  $m_h$  is puzzling, because as  $m_h \rightarrow 0$  no new symmetry appears in the SM Lagrangian, but we observe  $m_h \ll M_{\text{Pl}}$ , at odds with the selection rules of dilations. We can be more precise on this point by starting from the Lagrangian of a free massive scalar

$$\mathcal{L} = \frac{(\partial\phi)^2}{2} - \frac{m^2\phi^2}{2}. \quad (2.14)$$

This theory respects an infinite set of symmetries, as can be readily seen in momentum space

$$\mathcal{L} = \tilde{\phi}(-k) \frac{(k^2 - m^2)}{2} \tilde{\phi}(k). \quad (2.15)$$

The phase shift

$$\tilde{\phi}(k) \rightarrow e^{i\alpha(k)} \tilde{\phi}(k), \quad (2.16)$$

is a symmetry of the action for any odd function  $\alpha$

$$\alpha(-k) = -\alpha(k). \quad (2.17)$$

The first generator of this symmetry corresponds to translations

$$\alpha(k) = a_\mu k^\mu + a_{\mu\nu\rho} k^\mu k^\nu k^\rho + \dots \quad (2.18)$$

and the conserved current is the stress-energy tensor  $T^{\mu\nu}$ . The higher order terms are generated by higher powers of derivatives and are associated with higher-spin currents. The algebra is trivial (for example  $[\partial, \partial^3] = 0$ ) and does not contain dilations or special conformal transformations. This symmetry is broken by higher-point interactions

$$\mathcal{L} = \sum_n \delta^{(n)}(k_1 + \dots + k_n) \Gamma^{(n)}(k_1, \dots, k_n) \tilde{\phi}(k_1) \dots \tilde{\phi}(k_n). \quad (2.19)$$

Under the phase shift in Eq. (2.16) we have

$$\Gamma^{(n)}(k_1, \dots, k_n) \rightarrow \Gamma^{(n)}(k_1, \dots, k_n) e^{i\sum_j \alpha(k_j)} \quad (2.20)$$

if  $n = 2$  momentum conservation gives  $k_1 = -k_2$  and the vertex is invariant. All higher point interactions break the symmetry.

The selection rules of this symmetry together with those of spacetime dilations

$$\begin{aligned} x^\mu &\rightarrow s x^\mu, \\ m_h &\rightarrow s^{-1} m_h, \end{aligned} \quad (2.21)$$

allow us to estimate the expected value of the Higgs mass. Spacetime dilations tell us that

$$m_h^2 \sim m_t^2 + \dots \quad (2.22)$$

where the ellipses represent smaller mass scales in the theory. The selection rules of the higher-spin symmetry that we just discussed further allow us to conclude that

$$m_h^2 \sim \frac{y_t^2}{16\pi^2} m_t^2 + \dots \quad (2.23)$$

So purely within the SM there is no tension at all, given that  $m_t \simeq 174$  GeV. There is, however, a much larger mass scale associated with gravity<sup>1</sup>, so naively we expect

$$m_h^2 \sim \frac{y_t^2}{16\pi^2} M_{\text{Pl}}^2 + \dots \quad (2.24)$$

So why is this expectation not realized in Nature? We give possible answers to this question in the next Section. At this stage it is perhaps more pertinent to ask: what does this estimate really mean? We have stated multiple times that there is neither a problem in the SM, nor a way to compute  $m_h$ . This estimate is actually telling us what happens in a higher energy theory where  $m_h$  can be computed. This type of theory is particularly relevant because string theory, our current best shot at describing quantum gravity, falls in this category if it requires supersymmetry. Let us see explicitly what happens in such a theory.

### 2.2.2 A Sharp Problem in Supersymmetry

We can consider the Minimal Supersymmetric Standard Model (MSSM) which extends the SM with the minimal field content needed to realize supersymmetry. The algebra of  $N = 1$  supersymmetry (i.e. the simplest version with two spinorial generators) is

$$\begin{aligned} \{Q_\alpha, Q_{\dot{\alpha}}^\dagger\} &= 2\sigma_{\alpha\dot{\alpha}}^\mu P_\mu, \\ \{Q_\alpha, Q_\beta\} &= \{Q_{\dot{\alpha}}^\dagger, Q_{\dot{\beta}}^\dagger\} = 0, \\ [Q_\alpha, P^\mu] &= [Q_{\dot{\alpha}}^\dagger, P^\mu] = 0 \\ [M^{\mu\nu}, Q_\alpha] &= \frac{(\sigma^{\mu\nu})_\alpha^\beta}{2} Q_\beta. \end{aligned} \quad (2.25)$$

with the addition of the usual Poincaré algebra that we left implicit. Supersymmetry is not the main focus of this work and we refer the reader to [30–32] for the derivation and significance of this result. For our purposes it is sufficient to notice that the existence of two spinorial generators implies that particles of different spin belong to the same supersymmetric multiplet. In practice to make the SM supersymmetric we need a new  $s = 0$  scalar for each fermion, and a new  $s = 1/2$  fermion for each boson.

Furthermore, supersymmetry does not allow us to write both up-type and down-type Yukawa couplings with a single Higgs boson. We have to introduce two new doublets  $H_{u,d}$ . The extra doublet is also needed to cancel gauge anomalies induced by the supersymmetric partner of the Higgs, the Higgsino.

The last ingredient that we need to take into account is supersymmetry breaking. We have not observed this plethora of new particles realizing the symmetry, so in Nature the symmetry must be broken at some scale. For this reason we will include also soft (i.e. dimensionful) supersymmetry breaking in what follows.

In this theory the tree-level potential of the two Higgs doublets reads

$$\begin{aligned} \mathcal{L}_{SH} &= -(m_{H_u}^2 + |\mu|^2)|H_u|^2 - (m_{H_d}^2 + |\mu|^2)|H_d|^2 - (B\mu H_u H_d + \text{h.c.}) \\ &\quad - \frac{g_W^2 + g_Y^2}{8} (|H_u|^2 - |H_d|^2)^2 - \frac{g_W^2}{2} |H_d^\dagger H_u|^2. \end{aligned} \quad (2.26)$$

In addition to the three degrees of freedom that make  $W$  and  $Z$  massive, these theory contains four mass eigenstates: a charged scalar  $H^\pm$ , a CP-odd scalar  $A$  and two CP-even scalars  $H, h$ . One of the two CP-even mass eigenstates can have properties very similar to those of a SM

---

<sup>1</sup>In Section 3.5 we comment on the use of  $M_{\text{Pl}}$  as a mass scale in our estimate.

Higgs boson. Given the results from the LHC that has observed an approximately SM-like Higgs boson, we can consider a model where  $h$  is approximately decoupled from the rest of the Higgs sector and compute its mass.

First of all we can wonder why in this theory we can compute the mass of an elementary scalar. Supersymmetry extends the Poincaré algebra and  $P_\mu P^\mu$  is one of its Casimir operators, so the masses of members of the same supersymmetric multiplet must be the same. This relates  $m_h$  to the mass of a fermion. As we have seen in the previous Chapter, fermion masses break chiral symmetries. If the mass itself is the only source of breaking, the selection rules of these symmetries tell us that the result of any calculation of the mass must be in the form

$$m = m_{\text{tree}} [\dots] . \quad (2.27)$$

There cannot be power law sensitivity to high scales as in the SM. This is of course not the whole story, because the sensitivity to high scales could still be logarithmic

$$m = m_{\text{tree}} [\log \Lambda + \dots] . \quad (2.28)$$

In addition to that, supersymmetry is broken. However the Higgs mass might still be calculable, even taking these two extra subtleties into account. If supersymmetry is only softly broken, by a dimensionful parameter  $M_S$ , we must include also contributions of the type

$$m = M_S + m_{\text{tree}} [\log \Lambda_S + \dots] . \quad (2.29)$$

The supersymmetry breaking parameters that we parameterized with  $M_S$  can in principle be measured independently of  $m$ , as we show below. The unknown high scale  $\Lambda$  in Eq. (2.28) is replaced by  $\Lambda_S$ , the scale of supersymmetry breaking, that in principle we can also measure independently of  $m$ . At higher scales there are no contributions to the Higgs mass, since it is a parameter of the superpotential which is not renormalized [33]. Summarizing, in a theory with softly broken supersymmetry the Higgs mass receives contributions only up to a finite scale  $\Lambda_S$  and we can compute it as a function of supersymmetric and supersymmetry breaking parameters that we can measure independently of  $m_h$ .

After this explanation we can turn to the actual computation. At tree-level we have for the value of the weak scale

$$m_{h,\text{tree}}^2 = \frac{1}{2} \left( m_A^2 + m_Z^2 - \sqrt{(m_A^2 + m_Z^2)^2 - 4m_A^2 m_Z^2 \frac{(v_u^2 - v_d^2)^2}{v^4}} \right) , \quad (2.30)$$

where  $m_A$  is the mass of the CP-odd Higgs, while  $v_{u,d}$  are the vacuum expectation values of the two neutral components of  $H_{u,d}$  that satisfy  $v_u^2 + v_d^2 = v^2$ .

To complete the calculation we can also include the most important loop contribution that is generated by diagrams containing the supersymmetric partner of the top quark, the stop. We indicate with  $\tilde{t}_{1,2}$  the two mass eigenstates in the stop sector that are mixtures of the partners of the left-handed and right-handed top quarks.

The result is

$$m_h^2 = m_{h,\text{tree}}^2 + \frac{3G_F}{\sqrt{2}\pi^2} \left[ m_t^4(Q_1) \log \frac{M_s^2}{m_t^2} + m_t^4(Q_2) \frac{X_t^2}{M_s^2} \left( 1 - \frac{X_t^2}{12M_s^2} \right) \right] + \dots \quad (2.31)$$

where the ellipses represent subleading contributions. Here,  $M_s^2 = m_{\tilde{t}_1} m_{\tilde{t}_2}$ ,  $Q_1 = \sqrt{m_t M_s}$ ,  $Q_2 = M_s$ ,  $X_t = A_t - \mu(v_d/v_u)$  and  $m_t(Q)$  is the running top mass.  $A_t$  is a supersymmetry-breaking parameter that enters the stop mass matrix [30].

The important point is that all the parameters in the previous expression can be measured independently of  $m_h$ . If supersymmetry breaking occurs at scales much higher than  $m_h$  the

parameters entering its calculation ( $m_A$ ,  $X_t$  and  $M_s$ ) can give the observed result only if they are precisely tuned to give an approximate cancellation in Eq. (2.31). The larger they are, the larger is the cancellation.

This is not immediately manifest from Eq.s (2.30) and (2.31), because in those equations we have already tuned! We have expressed  $m_h$  as a function of  $m_t$  and  $m_Z$  which in turn are proportional to the weak scale  $v = \sqrt{v_u^2 + v_d^2}$ . However, in the MSSM we can compute the weak scale as a function of parameters that can be measured independently of  $v$ . For instance at tree-level

$$v_{\text{tree}}^2 = \frac{2}{g_W^2 + g_Y^2} \left( \frac{|m_{H_u}^2 - m_{H_d}^2|}{\sqrt{1 - 4(v_u v_d/v^2)^2}} - m_{H_u}^2 - m_{H_d}^2 - 2|\mu|^2 \right). \quad (2.32)$$

If we found  $m_{H_{u,d}}^2, \mu^2 \gg v^2$ , we would have explain the cancellation needed to get  $v \simeq 174$  GeV. We found useful to present first Eq.s (2.30) and (2.31) because they show another tension typical of weakly coupled extensions of the SM. The tree level value for  $m_h$ , given by Eq. (2.30) is  $m_h \leq m_Z$  (or  $m_h \leq g_{\text{weak}} v$  in a different theory with a different weak coupling). If we want  $m_h \simeq 125$  GeV we need to make  $m_{\tilde{t}_{1,2}}$  large, to enhance the logarithmic contribution in Eq. (2.31). This in turns requires a tuning that grows as  $m_{\tilde{t}_{1,2}}^2$ , due to the loop corrections to  $v^2$  described in Section 3.2.2.

An intuitive measure of this fine-tuning is often taken to be [34, 35]

$$\Delta \equiv 2 \frac{\delta m_h^2}{m_{h,\text{exp}}^2}, \quad (2.33)$$

where  $m_{h,\text{exp}}^2 \simeq (125 \text{ GeV})^2$  and  $\delta m_h^2$  is any individual contribution to the calculation.

A tuning exists in every theory where the Higgs mass can be calculated. If the new symmetry that makes it calculable is realized only at scales much higher than  $m_h$  we need a fine-tuning to explain its value.

If we apply our EFT intuition, we expect the parameters entering the  $m_h$  calculation to have a roughly uniform (or power-law [36]) distribution in an  $\mathcal{O}(1)$  interval around the typical supersymmetry breaking mass. Observing a tuning is thus a real problem, in the sense that it is signalling that we are making wrong assumptions in our description of Nature. The EFT intuition that has been tremendously successful so far can be wrong in two ways: 1) either Nature accepts some amount of tuning 2) or the “natural” values for supersymmetry breaking parameters have a very different distribution compared to what we naively expect.

Both options leave us with more open questions: in the first case, why do only  $m_h$  and the CC appear to be tuned while all other parameters of Nature follow our EFT intuition? In the second one, how does a UV theory that tunes supersymmetry breaking parameters to the right value look like? The answer to the first question is unknown, but we will answer the second one in the next Chapter.

### 2.2.3 Common Misconceptions and an Alternative Formulation

We have now seen why it is interesting to think about the Higgs boson mass. In the next Section we go further by discussing what this implies about physics at high energies. Before turning to the UV, I find useful, especially as a resource for students, to review some of the most common ways to present the hierarchy problem and the confusion that they might generate.

The reader, especially if from my generation or older, will have noticed that I have never referred to quadratic divergences or loop diagrams. The reason is implicit in the previous Section. Since the hierarchy problem is really a question of why our symmetry intuition is failing, there is no reason to consider loop corrections or regularization schemes. The problem

might very well manifest itself at tree-level and has nothing to do with renormalization per se. It can be reformulated as a question about the RGE flow of a UV theory as in [37], but it does not need to be. Before discussing this RGE formulation it is useful, for pedagogical reasons, to review the traditional argument through which the problem is presented.

Take the SM and compute loop corrections to the Higgs boson mass with Pauli-Villars regulator. You will find at one loop

$$\delta m_h^2 = \frac{3\Lambda^2}{16\pi^2 v^2} (4m_t^2 - 2m_W^2 - m_Z^2 - m_h^2) + \dots \quad (2.34)$$

Now the devil is in how you interpret  $\Lambda$ . If you are imagining that at some energy above the SM a theory where  $m_h^2$  can be computed exists, then this  $\Lambda$  stands for the mass of new particles in that theory. In general the different terms are cut-off by different uncorrelated physical mass scales instead of a single scale  $\Lambda$ . In the MSSM the first term represents the loop correction to  $m_h$  in Eq. (2.31), the others were slightly subleading and we did not list them. With this in mind Eq. (2.34) makes perfect sense and can be used to roughly estimate a scale were we expect new physics to kick in

$$\Lambda_{\text{NP}} = \frac{2\pi}{3} \frac{m_t}{v} m_h \sqrt{\Delta} \simeq 400 \text{ GeV} \frac{m_h}{125 \text{ GeV}} \sqrt{\Delta}, \quad (2.35)$$

if we want to avoid an accidental cancellation of  $\mathcal{O}(\Delta^{-1})$  in the full theory (for instance the MSSM). With this UV picture in mind, it is perfectly legitimate to discuss the problem in this way.

However, we find useful to stress a few elementary aspects of this estimate that might lead to confusion. Purely within the SM the presence of a quadratic divergence cutoff by  $\Lambda$  is signalling that you are doing something dishonest. You are trying to compute a loop diagram up to energies much higher than those where you know the theory. In practice there is no quadratic divergence and no sensitivity to the cutoff if one does the calculation correctly. This should be intuitive from the discussion of EFTs in the previous Chapter.

Let us assume that the SM is valid up to a scale  $\Lambda$ . All that we are allowed to do is measure parameters at  $\Lambda$ , then measure them again at energies  $E$  lower than  $\Lambda$  and check if the SM is predicting the right relation. There is no quadratic sensitivity to infinitely high energies if we do not try to calculate quantities beyond the limits of validity of the theory. If we were to perform the calculation that we are allowed to do, we would find

$$m_h^2(E) = m_h^2(\Lambda) + \frac{3\Lambda^2}{16\pi^2 v^2} (4m_t^2 - 2m_W^2 - m_Z^2 - m_h^2) + \mathcal{O}\left(\frac{E}{\Lambda}\right)^2 + \dots \quad (2.36)$$

In this case the second term on the right-hand side is the result of integrating out momentum scales  $E < k < \Lambda$ . This calculation is just telling us how  $m_h^2$  RGE evolves between different energies. There are no divergences and no fine-tunings.

The situation would be different if, for instance, we discovered a new fermion with mass  $m_h(E) \ll M_\Psi < \Lambda$  and a Yukawa coupling to the Higgs boson

$$\mathcal{L} \supset -y_\Psi L_\Psi H \Psi - M_\Psi (L_\Psi L_\Psi^c + \Psi \Psi^c). \quad (2.37)$$

Here we have imagined the presence of a left-handed doublet  $L_\Psi$  and a singlet  $\Psi$ , both accompanied by a partner with the right quantum numbers to write a vector-like mass term. For simplicity we assume  $M_\Psi \gg y_\Psi v$ .

If we repeated the previous calculation, i.e. measure  $m_h^2$  at the scale  $\Lambda$  and then integrate out momentum shells between  $\Lambda$  and  $E$ , this time we would find, in addition to the  $\Lambda^2$  term and a term logarithmically sensitive to  $\Lambda$ , also the following contribution

$$\delta m_h^2 = c \frac{y_\Psi^2 M_\Psi^2}{16\pi^2}. \quad (2.38)$$

If  $y_{\Psi}^2 M_{\Psi}^2 \gg m_h^2(E)$  we would be left to wonder why this term is precisely cancelled by  $m_h^2(\Lambda)$ .

This example is analogous to what we already see in the SM for the cosmological constant. The parameter is still not calculable (this is true both for  $\Lambda_{\text{CC}}$  and  $m_h^2$  in the SM and this example model), but we can compute some low energy contributions that are already much larger than its measured value. In the case of the Higgs,  $\delta m_h^2$  in Eq. (2.38), in the case of the CC any contribution from SM particles,  $\Lambda_{\text{CC}} \sim m_e^4, \dots, m_t^4$ .

Some have argued that this is not the right way to compute radiative contributions to  $m_h^2$  and  $\Lambda_{\text{CC}}$ , while I disagree with them, it should be stressed that this is irrelevant to the problem. The symmetry arguments in Section 2.2.1 and the problem in the MSSM described in Section 2.2.2 make clear that a priori the questions surrounding  $m_h$  have nothing to do with loop corrections. Indeed, the problem can arise already at tree-level, as we have shown in the previous Section. Consider again the tree-level expression for the Higgs vev in the MSSM

$$v_{\text{tree}}^2 = \frac{2}{g_W^2 + g_Y^2} \left( \frac{|m_{H_u}^2 - m_{H_d}^2|}{\sqrt{1 - 4(v_u v_d / v^2)^2}} - m_{H_u}^2 - m_{H_d}^2 - 2|\mu|^2 \right). \quad (2.39)$$

If we found experimentally  $m_{H_{u,d}}^2, \mu^2 \gg v^2$ , we would have to wonder why these parameters are tuned to give a small weak scale.

To conclude this Section we give an alternative view on the problem from [37]. This formulation is equivalent to our symmetry arguments in Section 2.2.1. Consider two widely separated scales,  $\Lambda_{\text{UV}} \gg \Lambda_{\text{IR}}$ . For definiteness  $\Lambda_{\text{UV}} \simeq 10^{16}$  GeV could be the scale where a non-supersymmetric Grand Unified Theory (GUT) is realized, while  $\Lambda_{\text{IR}}$  the Fermi scale. If there are no other intermediate scales, the energy dependence of physical quantities at scales  $\Lambda_{\text{IR}} \ll E \ll \Lambda_{\text{UV}}$  is weak and we can approximate this intermediate regime with a CFT. This approximate CFT is nothing but the free SM. From the CFT viewpoint, the stability of the hierarchy between  $\Lambda_{\text{IR}}$  and  $\Lambda_{\text{UV}}$  depends on the dimensionality of the scalar operators describing the perturbations of the CFT Lagrangian around the fixed point.

If the theory contains an operator  $\mathcal{O}_{\Delta}$  with dimension  $\Delta < 4$ , we expect, from the same symmetry considerations in Section 2.2.1, that UV physics generates

$$\mathcal{L}_p = c \Lambda_{\text{UV}}^{4-\Delta} \mathcal{O}_{\Delta}, \quad (2.40)$$

with  $c = \mathcal{O}(1)$ . This gives the IR scale

$$\Lambda_{\text{IR}} = c^{\frac{1}{4-\Delta}} \Lambda_{\text{UV}}. \quad (2.41)$$

If  $4 - \Delta = \epsilon \simeq 0$ , we can have an exponential hierarchy

$$\frac{\Lambda_{\text{IR}}}{\Lambda_{\text{UV}}} = c^{\frac{1}{\epsilon}}, \quad (2.42)$$

also for  $c = \mathcal{O}(1)$ . This is the case, for instance, for the QCD scale. The corresponding deformation, the glueball field  $G_{\mu\nu}^a G^{\mu\nu a}$  is marginally relevant. Its scaling dimension deviates from 4 only from small loop corrections  $\Delta_g \simeq 4 - a g_s^2$  and becomes 4 at the gaussian fixed point.

However, if the perturbation is relevant, as is the case for the Higgs mass,  $4 - \Delta \simeq 2$ , then

$$\frac{\Lambda_{\text{IR}}}{\Lambda_{\text{UV}}} \simeq \sqrt{c}, \quad (2.43)$$

and  $\Lambda_{\text{IR}}/\Lambda_{\text{UV}} \ll 1$ , requires a tiny  $c$ , at odds with our expectations from dimensional analysis stated around Eq. (2.40).



## 2.3 The Little Hierarchy Problem

The discussion in this Chapter shows that the most natural expectation is for something (presumably a new symmetry) to appear well below  $M_{\text{Pl}}$  to explain the value of  $m_h$  that we observe. What is the scale where this symmetry should appear?

Let us call this scale  $M_S$ . If the UV completion of the SM is perturbative, we have seen that new particles give the leading contribution to the Higgs mass at one loop

$$\delta m_h^2 \simeq \frac{g_S^2}{16\pi^2} M_S^2, \quad (2.44)$$

where  $g_S$  stands for a coupling in this theory. For an effective symmetry solution to the problem, SM particles must be part of the symmetric multiplets of the new theory, otherwise we would still expect contributions of  $\mathcal{O}(g_{\text{SM}}^2 M_{\text{Pl}}^2)$  from high scales. This means that the largest  $g_S$  in our new theory is at least of the size of  $y_t = \mathcal{O}(1)$ . In principle we can further imagine that to preserve color there are three partners of the top quark in the new theory, giving  $\delta m_h^2 \simeq 3 \frac{g_S^2}{16\pi^2} M_S^2$ . In the end we arrive at the same estimate as Eq. (2.35) with  $M_S = \Lambda_{\text{NP}}$ .

Similar estimates hold also for non-perturbative completions of the SM. In this case, however, we lose the loop suppression in  $\delta m_h^2$  and we are led to predict  $M_S \simeq m_h$ . An explicit discussion of the corrections to  $m_h$  for the SM flowing into a CFT can be found in [38].

At this point it is natural to ask a second question: What is the scale where this symmetry can appear? We have probed particle physics well above scales of order  $\Lambda_{\text{NP}} \simeq 400$  GeV.

The largest scales that we have access to are related to symmetries (or approximate symmetries) of the SM Lagrangian, since these signatures make for zero background searches. If we violate baryon number via the operators

$$\mathcal{L} \supset \frac{u^c u^c d^c e^c}{M^2} + \frac{QQQL}{M^2} + \dots \quad (2.45)$$

we can induce proton decay

$$\Gamma \sim \frac{m_p^5}{M^4}. \quad (2.46)$$

Current searches at SuperKamiokande [39] and SNO [20] give

$$\frac{\tau_p}{\text{Br}(p \rightarrow e^+ \pi^0)} \gtrsim 2.4 \times 10^{34} \text{ years}, \quad \frac{\tau_p}{\text{Br}(p \rightarrow \text{invisible})} \gtrsim 2 \times 10^{29} \text{ years}, \quad (2.47)$$

corresponding to

$$M \gtrsim 3 \times 10^{16} \text{ GeV}, \quad M \gtrsim 1.5 \times 10^{15} \text{ GeV}. \quad (2.48)$$

A different form of baryon number violation can induce neutron oscillations

$$\mathcal{L} \supset \frac{(u^c d^c d^c)^2}{M^5}, \quad \tau_{n \rightarrow \bar{n}} = \delta m \sim \frac{m_n^6}{M^5} \quad (2.49)$$

Also in this case we can probe scales well above 400 GeV [40],

$$\tau_{n \rightarrow \bar{n}} > 0.86 \times 10^8 \text{ s} \quad M \gtrsim 3 \times 10^6 \text{ GeV}. \quad (2.50)$$

Similar considerations hold for tests of the approximate flavor symmetries of the SM. In the lepton sector the largest scale that we can probe is in the decay  $\mu \rightarrow e \gamma$  induced for instance by

$$\mathcal{L} \supset \frac{m_\mu}{M^2} \bar{\mu}_L \sigma_{\mu\nu} e_R F^{\mu\nu}, \quad \Gamma \sim \frac{m_\mu^5}{M^4}. \quad (2.51)$$

Current bounds from MEG [41], give

$$\text{Br}(\mu \rightarrow e\gamma) < 4 \times 10^{-13} \quad M \gtrsim 3 \times 10^6 \text{ GeV}. \quad (2.52)$$

In the quark sector the largest scales can be probed via tests of CP violation in  $K^0 - \bar{K}^0$  mixing, where we can get to scales of about  $M \gtrsim 10^8 \text{ GeV}$  [42].

Other tests along these lines include searches for CP violation in EDM searches and a host of other flavor measurements in the lepton and quark sectors.

These results are telling us that if we want to extend the SM at  $\Lambda_{\text{NP}} \simeq 400 \text{ GeV}$  the new theory better respect all the symmetries and approximate symmetries of the SM. This requires quite a bit of model building, since in general these new theories have many more free parameters with respect to the SM, which do not necessarily have to respect these symmetries. We will see an explicit example in the Section devoted to supersymmetry in the next Chapter.

A sharper tension arises from direct searches for new particles at LEP, the Tevatron and the LHC. By now we have explored a vast number of signatures that cover most options for new particles with gauge couplings to the SM. The null results at these particle colliders point to  $\Lambda_{\text{NP}} \gtrsim \text{few TeV}$ . The application of these results to the hierarchy problem is model dependent and different theories might be affected by slightly different bounds. However the general point that we have not found new physics below a few TeV remains valid. Furthermore, the LHC has explored many of the Higgs couplings to SM particles finding a good consistency with an elementary Higgs as described by the Lagrangian in the previous Chapter, leaving room for deviations of order [43–45]

$$\frac{\delta g_{h\text{SM}}}{g_{h\text{SM}}} \lesssim 5\% \div 20\% \quad (2.53)$$

This complicates embedding the Higgs in a larger symmetry structure. In light of all these null experimental searches, even if we completely forget about  $M_{\text{Pl}}$ , there is still a tension between direct and indirect searches for new physics and the simplest explanations for the value of the Higgs mass. This has been known since the times of LEP’ [46] and today we call it the ‘little hierarchy problem’.

## 2.4 What We Learned about High Energies

At this point we have discussed in great detail what is puzzling about the Higgs boson mass. In the SM we cannot point to a real problem, both because we cannot compute  $m_h$  and because it is not clear how to treat  $M_{\text{Pl}}$ , the only other scale of Nature that we know about.

If we extend the SM with new symmetries that make  $m_h$  calculable we encounter a fine-tuning if these symmetries are realized at scales much higher than  $m_h$ .

These two considerations still leave us to wonder what we learned from all the work done so far. To answer this question we are forced to think about the UV and speculate about new regimes that we do not have access to experimentally. This is the beauty and the curse of the hierarchy problem, whether we want it or not, we have to set foot in uncharted territory. Even without experimental guidance, we can still use logic alone to write down a comprehensive set of possible explanations for  $m_h$ :

1. The Higgs mass is never calculable. At every scale we have a theory similar to the SM where  $m_h$  is just an input parameter. Although seemingly harmless this possibility puts strong constraints on the UV theory realizing it and we don’t know a theory of quantum gravity that implements.

2. There is no mass scale beyond the Standard Model sufficiently strongly coupled to the Higgs to generate a fine-tuning problem. Quantum gravity either does not have a scale [47–51] or incorporates  $M_{\text{Pl}}$  non-trivially in the  $S$  matrix, leaving no power-law corrections to dimensionful parameters [52].
3. The consistency of quantum gravity leaves non-trivial imprints at low energy either in the form of UV/IR mixing or inconsistent low-energy Lagrangians that look acceptable to the low-energy observer (i.e. large  $m_h$  is in the swampland [53]).
4. A symmetry that makes  $m_h$  calculable exists below  $M_{\text{Pl}}$  and fine-tuning is a fundamental aspect of Nature.
5. A landscape of values of  $m_h$  is realized in Nature. The value that we observe is selected by an early Universe event that we can not yet observe directly.
6. The fundamental scale of quantum gravity is much smaller than  $M_{\text{Pl}}$  and close to  $m_h$ . Also in this case some amount of fine-tuning is a fundamental aspect of Nature.

In the next Chapter we review the first four possibilities. We can anticipate that we do not any consistent theory of quantum gravity that realizes the first two options. At the time of writing the third option is mostly conjectural, while possibly compatible with string theory, it is far from being implemented in a concrete model.

The only two possibilities for which we can write a complete theory and propose experimental tests are 4. and 5. These are also the simplest possibilities conceptually in the sense that they build upon our knowledge of quantum field theory. The first three options require a radical modification of particle physics at the scale of quantum gravity.

Regardless of what is your favorite option, thinking about the Higgs mass inevitably leads to learning something new (and in my opinion deep) about Nature. All the options listed above require a decisive extension of our current description of physical phenomena. The two most conservative options require adding either a new symmetry, realized by a host of new particles, or accepting the existence of a vast landscape for  $m_h$ . This landscape can be realized either by changing the history of the Universe or accepting the existence of a Multiverse of which we occupy a tiny spec.

The three most speculative possibilities require revising completely quantum field theory and our EFT intuition when it comes to quantum gravity, in case 1. and 2. well beyond what is suggested by string theory. In the next Chapter we discuss all these options in greater detail.



# Chapter 3

## Most Existing Solutions to the Hierarchy Problem

Standards are always out of date. That's what makes them standards.

---

*Alan Bennett*

In this Chapter we very briefly review classical (and not so classical) solutions to the hierarchy problem. We will not be able to do justice to all the work on supersymmetry, composite Higgs, extra-dimensions and their very clever twists (little Higgs, twin Higgs, folded supersymmetry, ...) that has appeared in the literature. Our main focus is on the core mechanisms that explains the value of  $m_h$  and we group together all the ideas that share one. We also comment on their current tension with experiment or, in the case of more adventurous options, their theoretical shortcomings. This should not be taken as a sign that the author has a negative opinion of these ideas. On the contrary, each one of them is beautiful and unique. Together they represent some of the most interesting research in particle physics of the last 30 years. My only regret is not having the space(time) to write more about them.

### 3.1 Lowering the Scale of Gravity

In the previous Sections we have taken  $M_{\text{Pl}}$  to be the dimensionful scale associated to gravity, i.e. the energy scale where we expect it to become important for particle interactions.

This general intuition can be made more precise by looking at the Einstein-Hilbert action

$$S = \int d^4x \sqrt{-g} \left( \frac{M_{\text{Pl}}^2}{16\pi} R - 2\Lambda_{\text{CC}} + \mathcal{L}_{\text{matter}} \right). \quad (3.1)$$

If we consider this as an EFT, possibly complemented by higher dimensional operators in the form

$$S = \frac{1}{16\pi G_N} \int d^4x \sqrt{-g} (R - 32\pi G_N \Lambda_{\text{CC}} + 16\pi G_N \mathcal{L}_{\text{matter}} + c_1 R^2 + c_2 R_{\mu\nu} R^{\mu\nu} + c_3 R_{\mu\nu\rho\sigma} R^{\mu\nu\rho\sigma} + \dots), \quad (3.2)$$

we can expand the metric in the regime of validity of the EFT (i.e. low energy and low curvature)

$$g_{\mu\nu} = \eta_{\mu\nu} + h_{\mu\nu}, \quad |h| \ll 1. \quad (3.3)$$

Then the action becomes schematically

$$S \sim M_{\text{Pl}}^2 \int d^4x \left[ \partial h \partial h + h \partial h \partial h + a T_{\mu\nu} h^{\mu\nu} \dots + \frac{1}{M^2} (\partial^2 h \partial^2 h + h \partial^2 h \partial^2 h + \dots) \right] \quad (3.4)$$

$$T_{\mu\nu} = \frac{-2}{\sqrt{-g}} \frac{\delta \mathcal{L}_{\text{matter}} \sqrt{-g}}{\delta g^{\mu\nu}}, \quad (3.5)$$

where in some terms we have suppressed the indexes of  $h_{\mu\nu}$  for convenience. The higher dimensional terms odd in  $h$  come from higher curvature corrections  $R \sim \text{const} + \partial^2 h$ . Canonically normalizing the kinetic term we have

$$S \sim \int d^4x \left[ \partial h \partial h + \frac{1}{M_{\text{Pl}}} h \partial h \partial h + \frac{a}{M_{\text{Pl}}} T_{\mu\nu} h^{\mu\nu} + \dots + \frac{1}{M^2} \left( \partial^2 h \partial^2 h + \frac{1}{M_{\text{Pl}}} h \partial^2 h \partial^2 h + \dots \right) \right] \quad (3.6)$$

It's hard to define a running coupling in the EFT of gravity for reasons that I'm not going to discuss here. Heuristically you can just notice from the previous action that you are starting with a dimension 6 operator. From loop diagrams you are going to get multiple dimension 8 operators with different numerical coefficients (and possibly signs)  $R^2, R_{\mu\nu} R^{\mu\nu}$ . Which one are you going to pick? Ref. [54] contains an interesting discussion on this point.

For our purposes it is sufficient to notice that at one loop scattering processes receive corrections of order  $\delta A_{2 \rightarrow 2} \sim (N G_N E^2)/(16\pi^2)$ , from the action in Eq. (3.6) (after gauge fixing) where  $N$  is the number of particles in the loop (coming from  $T_{\mu\nu}$  in (3.6)). So it is natural to expect something to happen at

$$E \sim \frac{4\pi M_{\text{Pl}}}{\sqrt{N}}, \quad (3.7)$$

where the one loop corrections becomes comparable to the tree level result. In some sense we are lowering the fundamental scale of gravity, i.e. gravity becomes important for particle interactions at  $M_{\text{Pl}}/\sqrt{N}$ . Therefore, the easiest way to solve the hierarchy problem is to imagine:

$$N \sim \frac{M_{\text{Pl}}^2}{v^2} \approx 10^{32}. \quad (3.8)$$

The idea of lowering the fundamental scale of gravity by adding new degrees of freedom was first discussed in relation to the hierarchy problem in [55–58]. An explicit way of implementing this idea is to introduce extra dimensions compactified at a scale near  $m_h$ .

Let us take  $R$  to be the typical size of the extra dimensions. If we consider  $D = 4 + n$  then Newton's law is modified to

$$F(r) \sim \begin{cases} \frac{m_1 m_2}{M^{n+2} r^{n+2}}, & r \ll R \\ \frac{m_1 m_2}{M^{n+2} R^n r^2}, & r \gg R \end{cases} \quad (3.9)$$

where  $M$  is the fundamental scale of gravity in the theory with  $D > 4$ . This result is just an application of Gauss' theorem and it shows that

$$M_{\text{Pl}}^2 = M^{n+2} R^n, \quad R = 10^{\frac{30}{n}-17} \text{ cm} \left( \frac{\text{TeV}}{M} \right)^{1+\frac{2}{n}}. \quad (3.10)$$

This means that gravity might appear weak in 4D, where it has a coupling  $G_N \sim 1/M_{\text{Pl}}^2$ , because it is diluted by multiple extra dimensions where it can propagate. In reality the fundamental scale of gravity might be  $M$  and much lower than  $M_{\text{Pl}}$ .

Particle interactions are known up to energy scales  $E \sim \text{TeV}$ , corresponding to  $R \sim 10^{-17} \text{ cm}$ , so if we want  $M \simeq \text{TeV}$ , the SM fields must be stuck on a 4D brane. On the

contrary we don't know gravity that well below a millimeter and there is no problem if gravity propagates in the extra dimension, realizing the ‘‘dilution’’ of  $M_{\text{Pl}}$  that we would like to invoke to explain the value of  $m_h$ .

If  $M \sim \text{TeV}$  we have solved the hierarchy problem, but to do so we need  $R$  to be large compared to  $M_{\text{Pl}}^{-1}$ . Before seeing this in more detail let's see where the connection with large  $N$  comes from. It is already manifest that  $N$  in the previous theories is playing the role of the volume in this case. Consider one extra dimension compactified on a circle (here I follow [59]). The metric can be split to

$$g_{MN} = \begin{pmatrix} \eta_{\mu\nu} + h_{\mu\nu} & h_{\mu 5} \\ h_{\mu 5} & h_{55} \end{pmatrix}. \quad (3.11)$$

The action of diffeomorphisms is

$$h_{MN} \rightarrow h_{MN} + \partial_M \epsilon_N + \partial_N \epsilon_M. \quad (3.12)$$

Since the extra dimension is compact  $p_5 \sim n/R$ , so  $\delta h_{55} = 2\partial_5 \epsilon_5 \propto \sum_n n \epsilon_5^{(n)}$ . We can eliminate all  $n \neq 0$  components of  $h_{55}$  and  $h_{\mu 5}$  using diff. invariance. We are left with a scalar  $\phi \equiv h_{55}^{(0)}$ , a four-vector  $A_\mu \equiv h_{5\mu}^{(0)}$  and a tower of Kaluza-Klein (KK) gravitons  $h_{\mu\nu}^{(n)}$ .

To see this explicitly we use the periodicity of the spatial coordinate in the extra dimension to write

$$h_{\mu\nu}(x, x_5) = \sum_{n=-\infty}^{n=+\infty} h_{\mu\nu}^{(n)}(x) e^{\frac{inx_5}{R}}, \quad (3.13)$$

then we integrate the Einstein-Hilbert action over  $x_5$  and we are left with

$$S = 2\pi R M^3 \int d^4x \left( h^{\mu\nu} \square h_{\mu\nu} - h_\mu^\mu \square h_\nu^\nu + 2h_{\mu\nu} \partial^\mu \partial^\nu h_\rho^\rho - 2h_{\mu\nu} \partial^\mu \partial^\rho h_\rho^\nu + \frac{n^2}{4R^2} [h_\mu^\mu h_\nu^\nu - h^{\mu\nu} h_{\mu\nu}] \right) + \dots \quad (3.14)$$

From the above action we can conclude that

$$M_{\text{Pl}}^2 = 2\pi R M^3, \quad \left( \square + \frac{n^2}{R^2} \right) h_{\mu\nu}^{(n)} = 0. \quad (3.15)$$

So how many gravitons do we have? When we hit the scale  $M$  we have to UV complete gravity also in the extra dimension therefore we can have at most

$$\frac{N^2}{R^2} \sim M^2 \quad N \sim \left( \frac{M_{\text{Pl}}}{M} \right)^{\frac{2}{n}} \quad (3.16)$$

gravitons in our EFT. For  $n = 1$  and  $M \sim \text{TeV}^1$ , we recover our large  $N$  estimate from Eq. (3.8).

How about the new hierarchy problem  $R \gg M_{\text{Pl}}^{-1}$ ? A potential for  $R$  arises from the  $(4+n)$ D cosmological constant  $\Lambda_n$  in the Einstein-Hilbert Lagrangian

$$\int d^{4+n}x \sqrt{-g} \Lambda_n \sim \int d^4x \sqrt{-\bar{g}} \Lambda_n R^n. \quad (3.17)$$

In the presence of curvature  $\kappa$  in the extra dimensions we have also

$$M^{2+n} \int d^{4+n}x \sqrt{-g} R \sim - \int d^4x \sqrt{-\bar{g}} \kappa M^{2+n} R^{n-2}. \quad (3.18)$$

---

<sup>1</sup>Phenomenologically excluded because of modifications of gravity on solar system scales.

Summing these two terms we can find a stable potential with a minimum  $R_* \sim \sqrt{M^{2+n}/\Lambda_n}$ . This means that the radius of curvature is roughly

$$L \sim \sqrt{\frac{M^{n+2}}{\Lambda_n}}. \quad (3.19)$$

If we don't want our space to split in separate inflating patches of size  $L$  or collapse into black holes we need

$$L \gtrsim R \rightarrow \Lambda_n \lesssim M^{4+n} \left( \frac{M}{M_{\text{Pl}}} \right)^{4/n} \quad (3.20)$$

Smaller than its natural value  $M^{4+n}$ . So we need to tune  $\Lambda_n$  and possibly keep it stable with supersymmetry. Furthermore, to reproduce our observed 4D universe, we need the effective (long distance) 4D CC to approximately vanish

$$\sum_i f_i^4 + R^n \Lambda_n \approx 0, \quad (3.21)$$

where  $f$  are brane tensions. They are nothing mysterious, just the equivalent of a CC on the 4D brane. Their natural value is  $f^4 \approx M^4$ . If there are  $N_w$  branes

$$\Lambda_n \lesssim N_w M^{4+n} \left( \frac{M}{M_{\text{Pl}}} \right)^{4/n}, \quad (3.22)$$

so the extra dimension can be large for the same reason that people are large (they carry large baryon number). However we are still tuning, once to get  $R$  large (Eq. (3.20)) and a second time to get the observed 4D CC (Eq. (3.21)).

The metric in the extra dimensions that we are considering here is flat. We will discuss a dynamical way of stabilizing the radius at the desired value in the context of warped extra-dimensions, where the metric is AdS-like. Not surprisingly this will correspond to introducing a symmetry in our theory that stabilizes the hierarchy between  $R$  and  $M_{\text{Pl}}^{-1}$ . The symmetry is scale invariance and we discuss this possibility in Section 3.2.1.

Before concluding this Section and turning to symmetry explanations for  $m_h$ , it is useful to point out what is currently the biggest problem with these constructions. If we want to lower the scale of gravity down to a TeV, we are predicting a plethora of new particles at that scale and we have not observed any. We can of course take  $N \lesssim 10^{32}$  or  $M \gtrsim \text{TeV}$  and accept some amount of accidental cancellation between different contributions to  $m_h$ .

## 3.2 New Symmetries

### 3.2.1 Scale Invariance

We do not worry about the stability of the QCD scale  $\Lambda_{\text{QCD}} \sim 100 \text{ MeV}$  with respect to some larger UV scale  $\Lambda_{\text{UV}}$ . The reason is that the QCD Lagrangian without quark masses is approximately scale invariant

$$S_{\text{QCD}} = \int d^x \left( -\frac{1}{4} G_{\mu\nu}^a G^{\mu\nu a} + i \bar{q} \gamma^\mu D_\mu q - \frac{\alpha_s \theta}{8\pi} G_{\mu\nu}^a \tilde{G}^{\mu\nu a} \right). \quad (3.23)$$

It does not contain operators with scaling dimension much smaller than 4. Under a scale transformation

$$x^\mu \rightarrow s x^\mu, \quad (3.24)$$



at the classical level the operators in Eq. (3.23) all get a factor of  $s^{-4}$  which compensates the  $s^4$  factor in the integration measure  $d^4x$ . Therefore a scale transformation leaves  $S$  invariant

$$S \rightarrow S. \quad (3.25)$$

If we include quantum corrections, scale invariance is broken by effects of  $\mathcal{O}(\alpha_s)$ . If we imagine that at  $\Lambda_{\text{UV}}$  we are close to a conformal fixed point, i.e. the theory is almost scale invariant also at the quantum level:  $\alpha_s(\Lambda_{\text{UV}}) \ll 1$ , then all physical quantities depend on the energy scale at most logarithmically at high energy and it takes many decades of running before QCD confines  $\alpha_s(\Lambda_{\text{QCD}}) \simeq 1$ ,

$$\log \frac{\Lambda_{\text{UV}}}{\Lambda_{\text{QCD}}} = \frac{1}{18} \frac{4\pi}{\alpha_s(\Lambda_{\text{UV}})}. \quad (3.26)$$

The running is slow because there are no relevant deformations in the theory, i.e. no operators with dimension much smaller than  $\Delta \simeq 4$ . As a consequence there are no dimensionful coefficients of dimension  $\Delta - 4$  much bigger than zero that can affect the running of physical quantities. The scale  $\Lambda_{\text{QCD}}$  is generated through running, without any dimensionful couplings in the theory. This phenomenon is known as “dimensional transmutation” in the QCD literature.

Quark masses do not change this picture. The selection rules of the chiral symmetries that they break, enforce that their running is also logarithmic

$$\frac{dm_q}{d \log E^2} \sim m_q, \quad (3.27)$$

so even if the quark mass operators

$$\mathcal{L}_q = m_q \bar{q}q, \quad (3.28)$$

have dimension  $\Delta_{\bar{q}q} = 3$  they run as marginal operators of dimension  $\Delta = 4$ .

This general idea can be applied also to explain the hierarchy  $m_h \ll \Lambda_{\text{UV}}$ . Imagine that at some scale  $m_*$  a new strongly interacting sector exists and the Higgs boson is a composite state of this sector. Above  $m_*$  there is no Higgs boson and no  $\Delta_{|H|^2} = 2$  operator associated to its mass, so we expect  $m_h^2 \sim m_*^2$ . Above this scale  $m_h^2$  does not receive any quantum correction. The scale  $m_*$  can be generated from  $\Lambda_{\text{UV}}$  from dimensional transmutation.

To make this picture compatible with current data we need a second “elementary” sector that contains all other SM particles. The elementary sector is a weakly-coupled gauge theory, essentially the SM minus the Higgs. In principle the right-handed top quark could also be composite. All other field can at most weakly mix with operators of the new strongly interacting sector (a possibility that is referred to as partial compositeness [60]).

To make this picture consistent, the composite sector must respect a symmetry group  $G$  that contains the SM gauge group, or at least the subset of the SM gauge group under which the Higgs is charged, i.e.  $G \supset SU(2)_L \times U(1)_Y$ . In analogy with QCD, the global group  $G$  is generically broken to a subgroup  $H$  at the confinement scale  $m_*$ .

$G$  is also explicitly broken by the gauging of  $SU(2)_L \times U(1)_Y$ , since the elementary SM particles do not respect  $G$  and interact with the composite ones through electroweak gauge bosons. This is analogous to QCD, where  $G = SU(3)_L \times SU(3)_R$  which is explicitly broken by gauging its subgroup  $U(1)_Q$ .

In principle extra explicit breaking terms, analogous to quark masses in QCD, are possible also for our new composite sector. However, we note that the interaction between composite and elementary sectors must not contain any strongly relevant deformation, otherwise the mechanism that stabilizes the  $m_* \ll \Lambda_{\text{UV}}$  hierarchy would be invalidated.

At the scale  $m_*$  we have massless Nambu–Goldstone Bosons (NGB) in the  $G/H$  coset. Some of them get a mass from the explicit breaking coming from the SM. At this point we have to make a choice: the Higgs boson can either be a generic state of the composite sector or one of the Goldstone bosons.

The first option was first presented in [61–64] and is known under the name of *technicolor*. The latest results from particle colliders show a strong tension with experiment. If  $m_* \simeq m_h$  we would have already observed some particles from the composite sector, the analogue of QCD hadrons, but we have not observed any of them.

The second option [65–68] is still alive if we accept some amount of tuning. The first question that we should ask if we follow this route, is why the Higgs boson observed at the LHC is consistent with the elementary  $H$  in the SM Lagrangian. If  $H$  is really part of a composite sector we would expect significant deviations in its couplings compared to the SM expectations [69].

However in these models there is a free parameter that controls how “elementary” the Higgs looks like. To see this we can split the generators of  $G$ ,  $T^A$  into unbroken generators  $T^a$  that form the algebra of  $H$  and broken generators  $\tilde{T}^{\tilde{a}}$ . The vacuum  $\vec{F}$  thus satisfies

$$T^a \vec{F} = 0, \quad \tilde{T}^{\tilde{a}} \vec{F} \neq 0. \quad (3.29)$$

A priori we can choose any embedding of  $H$  in  $G$ . If we act with the elements of  $G$  on the generators  $\{T^a, \tilde{T}^{\tilde{a}}\}$  reshuffling them between broken and unbroken the theory that we obtain is equivalent to the one that we started with, unless  $H$  can be embedded in multiple inequivalent ways in  $G$ , namely when different choices of the  $H$  algebra generators are not all related by inner automorphisms. In this case dynamics selects the right embedding. Barring this complication, we can choose the  $T^a$  to contain  $SU(2)_L \times U(1)_Y$ .

If we introduce the Goldstone bosons of  $G/H$  in the usual way

$$\vec{\Phi}(x) = e^{i\theta^{\tilde{a}}(x)\tilde{T}^{\tilde{a}}} \vec{F}, \quad (3.30)$$

it is the vev of  $\theta$ ,  $\langle \theta \rangle$ , which controls the amount of breaking of the EW gauge group

$$v = |\vec{F}| \sin \langle \theta \rangle \equiv f \sin \langle \theta \rangle. \quad (3.31)$$

Geometrically this can be understood as follows:  $\vec{F}$  is orthogonal to  $H$  ( $T^a \vec{F} = 0$ ). The Goldstone bosons are given by tilting  $\vec{F}$  by an angle  $\theta^{\tilde{a}} \tilde{T}^{\tilde{a}}$  whose sine gives the projection to the orthogonal plane where  $H$  lives.

Therefore we have a tunable parameter

$$\xi \equiv \frac{v^2}{f^2}, \quad (3.32)$$

that allows us to decouple an approximately SM-like Higgs with vev  $v$  from the rest of the Goldstone bosons that live at  $f$ . This mechanism is known as vacuum misalignment [65–68].  $\xi$  can be made small by tuning or through a clever use of symmetry as in little Higgs constructions [70–72]. The latter, however, require a large Higgs quartic at odds with Higgs mass measurements and complex model building.

Much more could be said on these models and for a more comprehensive overview we refer the reader to [73]. Since this is not the main focus of this thesis we will not further elaborate. Nonetheless, it is useful to consider two more points.

First of all, it is clear from the previous discussion that these models are in tension with current experimental observations. We have already explored scales about a factor of ten above  $v$ , without finding the new particles expected at  $f$ . This translate in about a  $\xi \simeq 1\%$  tuning.

Secondly, it is not hard to embed this construction in UV complete models [65, 66, 68] that deliver a suitable Nambu-Goldstone Higgs, with the SM gauge groups contained in  $H$ . However, not many attempts have been made to extend these constructions to the fermionic sector [74–78]. The best examples that we have, which successfully account for searches of flavor violation beyond the SM, are five-dimensional gauge theories on truncated AdS space [79–81].

Models with extra space dimensions have had a considerable impact on the field. By the AdS-CFT correspondence they can be shown to be equivalent to the 4D constructions that we just discussed. However it is instructive to spend some time discussing explicit 5D models.

## Warped Extra Dimensions

Some of the most interesting explicit realizations of scale invariance protecting the Higgs mass have been presented in the form of 5D theories, with the additional dimension described by truncated AdS space. The first examples were presented in [82, 83].

Consider adding one extra dimension with metric,

$$ds^2 = e^{-2kr_c|\phi|} dx_\mu dx^\mu + r_c^2 d\phi^2, \quad (3.33)$$

where  $\phi \sim -\phi, \phi \sim 2\pi\phi$ . The fluctuations around this classical solution are

$$r_c \rightarrow r_c + T(x) \quad \eta_{\mu\nu} \rightarrow \eta_{\mu\nu} + h_{\mu\nu}(x) \equiv \bar{g}_{\mu\nu}(x). \quad (3.34)$$

As in the case of large extra dimensions discussed in the previous Section, gravity can propagate in the bulk, but the SM is on the brane at  $\phi = \pi$

$$\int d^4x d\phi \delta(\phi - \pi) \mathcal{L}_{SM}. \quad (3.35)$$

In the 4D effective theory the Planck mass is

$$M^3 \int d^4x \int_{-\pi}^{\pi} d\phi e^{-2kr_c|\phi|} r_c \sqrt{-\bar{g}} R_4 \rightarrow M_{\text{Pl}}^2 = \frac{M^3}{k} (1 - e^{-2kr_c\pi}) \approx \frac{M^3}{k}. \quad (3.36)$$

On the SM brane we have

$$\int d^4x \sqrt{-\bar{g}} e^{-4kr_c\pi} \left[ e^{4kr_c\pi} g^{\mu\nu} (D_\mu H)^\dagger D_\nu H + m_{h,0}^2 |H|^2 + \dots \right] \quad (3.37)$$

After rescaling the kinetic term

$$m_h^2 = e^{-2kr_c\pi} m_{h,0}^2. \quad (3.38)$$

We can describe the mechanism as having a large fundamental scale for gravity, which is redshifted to  $\simeq \text{TeV}$  on the SM brane (the so-called IR brane). However a description equivalent to large extra dimensions (ED) is also possible. A covariant action satisfies

$$S(\phi, m) = S\left(\phi', \frac{m}{w}\right), \quad (3.39)$$

where  $\phi'$  is Weyl rescaled  $g \rightarrow w^{-2}g$ ,  $H \rightarrow wH$ ,  $\psi \rightarrow w^{3/2}\psi$ , ...

We can in fact see that this is the same as large ED by assuming that the fundamental mass scale of gravity is at a TeV and by rescaling everything by  $e^{-kr_c\pi}$  and getting a blue-shifted Planck mass. Here the volume of the ED is made large by the exponential factor. So, as in the previous case, now you should wonder about stabilizing  $r_c$ , this is the new hierarchy problem!

Before discussing this, note that the exponential is just a convenient artifact, but we might have chosen different coordinates

$$z = \frac{e^{-2kr_{cy}}}{k}, \quad ds^2 = \frac{1}{k^2 z^2} (dx_\mu dx^\mu + dz^2), \quad (3.40)$$

in this frame it is clear that we need a large ED in some sense.

To stabilize it we can use the symmetries of AdS, or equivalently of the boundary CFT. If we consider the metric in the previous equation, the UV brane is at  $z_{\text{UV}} = 1/k = R$  and the IR brane, whose position is parametrized by the dilaton  $\chi$  of the associated CFT, is at  $\chi = 1/z_{\text{IR}} \ll k$ . For a more comprehensive discussion of the mapping between CFT and AdS description we refer to [84].

To stabilize the dilaton (i.e. fix the position of the IR brane) we add a bulk scalar, as first proposed in [85],

$$S = \int d^4x dz \sqrt{g} (g^{MN} \partial_M \phi \partial_N \phi + \Lambda_{\text{bulk}}^5 - m_b^2 \phi^2). \quad (3.41)$$

$\phi$  is often called a Goldberger-Wise (GW) scalar. This addition to the action is equivalent to explicitly breaking conformal invariance in 4D, with an operator with dimension related to  $m_b^2$ . We imagine that some unspecified dynamics fixes the vev of  $\phi$  in the IR and in the UV and we define the dimensionless ratios  $v_{1,0}$  by dividing the vevs by their natural value

$$v_1 \equiv \frac{\langle \phi(z_{\text{IR}}) \rangle}{z_{\text{IR}}^{3/2}}, \quad v_0 \equiv \frac{\langle \phi(z_{\text{UV}}) \rangle}{z_{\text{UV}}^{3/2}}. \quad (3.42)$$

From Eq. (4.71) we can obtain the equations of motion for  $\phi$  in the bulk

$$\frac{3}{z} \partial_z \phi - \partial_z^2 \phi = -m_b^2 \frac{\phi}{k^2 z^2}, \quad (3.43)$$

whose solution is

$$\phi(z) = C_1 z^{2 + \sqrt{4 + \frac{m_b^2}{k^2}}} + C_2 z^{2 - \sqrt{4 + \frac{m_b^2}{k^2}}}. \quad (3.44)$$

Note that even if the scalar vev grows from the UV to the IR  $z_{\text{IR}} \gg z_{\text{UV}}$ , this warped ED can still solve the hierarchy problem. If we have a Higgs on the UV brane, its measured vev in the IR is suppressed by  $\sqrt{g_{\text{IR}}} = 1/(kz_{\text{IR}})^4$  which overcomes the  $z^2$  growth.

$C_{1,2}$  can be fixed using our boundary conditions Eq. (3.42). If we plug Eq. (3.44) back into the action and integrate over  $z$ , we can obtain a 4D potential for the dilaton. In the region where  $\chi \ll \chi_0$ , where  $\chi$  parametrizes the position of the IR brane, while  $\chi_0$  that of the UV brane, we have

$$V = -\epsilon v_0^2 \chi_0^4 + [(4 + 2\epsilon)\chi^4 (v_1 - v_0(\chi/\chi_0)^\epsilon)^2 - \epsilon v_1^2 \chi^4] + \mathcal{O}(\chi^8/\chi_0^4), \quad (3.45)$$

where for simplicity we took  $m_b^2 = 4\epsilon/z_{\text{UV}}^2$ . This shows explicitly that  $m_b$  breaks scale invariance, had we only included the kinetic term for  $\phi$ , we would have generated only scale-invariant  $\chi^4$  terms. The trick that allows to stabilize the hierarchy is to assume that scale invariance is broken by a small amount  $\epsilon$ . The minimum of this potential is at  $\chi = \chi_0 (v_1/v_0)^{1/\epsilon}$ . So even a mild hierarchy between fundamental parameters:  $\epsilon \simeq 1/20$  and  $v_1/v_0 \simeq 1/10$  can give  $\chi/\chi_0 \simeq m_W/M_{\text{Pl}}$ .

A small hierarchy of vevs can thus generate a big hierarchy of scales. This is equivalent to the discussion of dimensional transmutation in QCD, where the logs from quantum corrections play the role of  $\chi^{4+\epsilon}$ .

### 3.2.2 Supersymmetry

Much of the ideas presented in this Section were already discussed in the first Chapter of the thesis and in Section 2.2.2. We repeat some of those statements here to make the discussion self-contained.

Supersymmetry protects the Higgs mass by tying it to the mass of its fermionic partner, the Higgsino. The latter is protected by chiral symmetry, which can be described as follows. The two Weyl components of a Dirac fermion  $\psi_L$  and  $\psi_R$ ,

$$\bar{\Psi}i\gamma^\mu\partial_\mu\Psi - M_\Psi\bar{\Psi}\Psi = \bar{\psi}_L i\gamma^\mu\partial_\mu\psi_L + \bar{\psi}_R i\gamma^\mu\partial_\mu\psi_R - M_\Psi(\bar{\psi}_L\psi_R + h.c.) , \quad (3.46)$$

in absence of a mass term are decoupled. Their phase can be changed independently without affecting the dynamics. The selection rules of this symmetry insure that all contributions to the fermion mass are proportional to  $M_\Psi$ . This can be seen by promoting  $M_\Psi$  to a field and by assigning it transformation properties that preserve the chiral symmetry even when the mass term in (3.46) is present in the Lagrangian. This is a useful technique that allows us to keep track of the powers of  $M_\Psi$  (or any other parameter breaking a symmetry) entering our observables.

After this short description of chiral symmetry we can go back to the status of supersymmetric solutions. Adding a fermionic partner for the Higgs is not enough. For supersymmetry to be a honest symmetry we have to double the SM particle content promoting every particle to a supermultiplet with the same mass. If we failed to do it the  $\mathcal{O}(1)$  couplings of the Higgs to other SM particles (in particular the top quark and the gauge bosons) would break supersymmetry, restoring the problem. To see this we consider the effect on the Higgs mass of the supersymmetric partners of the top quark and we let their masses  $m_{\tilde{t}_1, \tilde{t}_2}$  be free parameters. Then if  $m_{\tilde{t}_1, \tilde{t}_2} \gg m_t$  we are going to introduce tuning from terms of the form  $\delta m_H^2 \propto (m_{\tilde{t}_1}^2 - m_{\tilde{t}_2}^2)$ .

In the Minimal Supersymmetric Standard Model (MSSM) we have two complex scalars (stops) with mass matrix<sup>2</sup>

$$\begin{pmatrix} m_{Q_3}^2 + m_t^2 + m_Z^2 \left(\frac{1}{2} - \frac{2}{3}s_W^2\right) \cos 2\beta & v(y_t A_t \sin \beta - \mu y_t \cos \beta) \\ v(y_t A_t \sin \beta - \mu y_t \cos \beta) & m_{u_3}^2 + m_t^2 + m_Z^2 \frac{2}{3}s_W^2 \cos 2\beta \end{pmatrix} , \quad (3.47)$$

where  $m_{Q_3}, m_{u_3}, A_t$  are parameters that softly break supersymmetry and allow the stop masses to be different from the top mass.  $s_W$  is the usual sine of the Weinberg angle, while  $\mu$  and  $\tan \beta$  characterize the Higgs sector of the theory. In the MSSM we need two Higgs doublets,  $H_u$  and  $H_d$ , in order to write Yukawa couplings in the superpotential. Their supersymmetric interactions are given by

$$\mathcal{W}_{\text{MSSM}} = \mu H_u H_d + y_u Q H_u u^c + y_d Q H_d d^c + y_e Q H_d e^c , \quad (3.48)$$

this defines  $\mu$ .  $\tan \beta = v_u/v_d$  is given by the ratio of the vacuum expectation values of the two doublets. All these definitions are just instrumental to get to the calculation of the Higgs mass. The interactions

$$\mathcal{L}_{\text{MSSM}} \supset -|y_t|^2 |H_u|^2 \left( |\tilde{Q}_t|^2 + |\tilde{t}^c|^2 \right) - \left( y_t A_t \tilde{Q}_t H_u^0 \tilde{t}^c + \mu^* y_t \tilde{Q}_t H_d^{0*} \tilde{t}^c + h.c. \right) , \quad (3.49)$$

at one-loop contribute to the supersymmetry breaking  $H_u$  mass parameter in the Lagrangian

$$\mathcal{L}_{\text{MSSM}} \supset -m_{H_u}^2 |H_u|^2 . \quad (3.50)$$

---

<sup>2</sup>For simplicity we assume all parameters to be real, their phases are in any case strongly constrained by EDM measurements [?].

For  $m_{Q_3}, m_{u_3}, A_t \gg m_t$  we have

$$\delta m_{H_u}^2 = -\frac{3y_t^2}{8\pi^2} (|m_{Q_3}|^2 + |m_{u_3}|^2 + |A_t|^2) \log \frac{\Lambda_S}{\text{TeV}}, \quad (3.51)$$

where  $\Lambda_S$  is the scale at which supersymmetry breaking effects are mediated to the MSSM. If  $m_{Q_3}, m_{u_3}$  or  $A_t$  are larger than  $m_h$  we have reintroduced a fine-tuning problem.

From this discussion the tension described in Section 2.3, called “little hierarchy problem” is already clear. We expect new particles charged under SM gauge groups near the weak scale and we do not observe them neither directly nor indirectly. Compared to the composite Higgs case, the issue is mitigated by the perturbative couplings of the new particles to the SM, but it is not completely absent. Besides, having only weak couplings introduces another problem. At tree-level in the MSSM

$$m_h < m_Z |\cos 2\beta|. \quad (3.52)$$

This means that we need one-loop corrections to raise  $m_h$  to its observed value. The leading ones come from the correction to the Higgs quartic coupling given by stop loops<sup>3</sup>. Including the leading two-loop effects we have [86]

$$\delta m_h^2 \approx \frac{3G_F}{\sqrt{2}\pi^2} \left[ m_t^4(Q_1) \log \frac{M_s^2}{m_t^2} + m_t^4(Q_2) \frac{X_t^2}{M_s^2} \left( 1 - \frac{X_t^2}{12M_s^2} \right) \right]. \quad (3.53)$$

Here,  $M_s^2 = m_{\tilde{t}_1} m_{\tilde{t}_2}$ ,  $Q_1 = \sqrt{m_t M_s}$ ,  $Q_2 = M_s$ ,  $X_t = A_t - \mu \cot \beta$  and  $m_t(Q)$  is the running top mass. In the limit  $m_{Q_3}, m_{u_3}, A_t \gg m_t, m_Z, \mu$ , the physical stop masses in terms of the parameters in (3.47) read

$$m_{\tilde{t}_{1,2}}^2 \approx \frac{1}{2} \left( m_{Q_3}^2 + m_{u_3}^2 \mp \sqrt{(m_{Q_3}^2 - m_{u_3}^2)^2 + 2|A_t|^2 v^2 (1 - \cos 2\beta)} \right). \quad (3.54)$$

As we expected from dimensional analysis the contributions of the stops to the Higgs quartic grow logarithmically with their mass. Raising this contribution is in direct tension with the desire of minimizing fine tuning from  $\delta m_{H_u}^2 \sim m_{\tilde{t}_{1,2}}^2$ . The same is true for the term proportional to  $A_t$  and  $\mu$ . The latter is the Higgsino mass and would introduce tuning already at tree-level. Of course, as you might have guessed, there are ways around this problem, but require adding more structure to the theory, for example changing the Higgs potential by the addition of a gauge-singlet scalar [87].

In summary lack of positive experimental evidence is forcing us to add extra layers to the simplest supersymmetric models and/or to accept some amount of fine-tuning. This of course does not make them experimentally excluded and the community looks forward to new LHC studies for more information. For additional details on supersymmetry phenomenology and current collider bounds we refer to [30, 88, 89].

Obviously the above discussion is quite general. We can keep pushing up the scale of new physics and still consider symmetry solutions to the hierarchy problem acceptable, if we are willing to tolerate growing amounts of fine-tuning ( $\sim E^2/m_h^2$  where  $E$  is the energy scale that we can probe without finding new physics). The question of how much tuning is reasonable to expect in a physical theory can not be answered quantitatively. However borrowing Riccardo Barbieri’s words, every honest physicist should set in their heart a tuning threshold past which they stop working on this kind of model building. The important implicit part of the statement is that this threshold should not vary with time.

---

<sup>3</sup>Recall that the physical Higgs mass is  $\propto \sqrt{\lambda}$ .

### 3.3 Scaleless Theories of Gravity

What if gravity did not have a scale? In that case, our estimate  $m_h^2 \sim y_t^2 M_{\text{Pl}}^2$  would not hold. Consider the action

$$S = \int d^4x \sqrt{-g} \left[ \frac{R^2}{6f_0^2} + \frac{\frac{1}{3}R^2 - R_{\mu\nu}^2}{f_2^2} - \xi_S |S|^2 R + \mathcal{L}_{\text{matter}} \right], \quad \xi_S \langle S \rangle^2 = \frac{M_{\text{Pl}}^2}{16\pi}. \quad (3.55)$$

Other terms of dimension greater than 4 are pure derivatives or can be redefined away. The second term is the square of the Weyl (or conformal) tensor obtained by subtracting all traces from the Riemann tensor. We have imagined that  $\mathcal{L}_{\text{matter}}$  contains a potential for  $S$  giving it the vev in the above equation.

Schematically this action gives an EOM for the graviton of the type

$$\square h + \frac{1}{M^2} \square^2 h = 0 \rightarrow \frac{1}{M^2 p^2 - p^4} = \frac{1}{M^2} \left( \frac{1}{p^2} - \frac{1}{p^2 - M^2} \right). \quad (3.56)$$

Therefore this theory contains a ghost. It is not yet clear that we can make sense of it [90–93]. However, there is at least another way to make gravity scale-less from the point of view of the Higgs boson. This second option does not pose problems of consistency of the theory, but the only known example of this behavior is in 2D where gravity is non-dynamical and very different than 4D.

In gravity local diffeomorphisms are a gauge symmetry and correlation functions are not good observables (but note that this is only a non-perturbative problem). We can only measure the  $S$  matrix or at correlation functions along a worldline  $x^\mu(\tau)$ . Although the number  $x^\mu(\tau)$  is arbitrary, it unambiguously identifies a point on the spacetime manifold and we can measure

$$\langle 0 | O(x^\mu(\tau_1)) \dots O(x^\mu(\tau_n)) | 0 \rangle. \quad (3.57)$$

The  $S$  matrix is defined at infinity where gauge symmetries are not redundancies anymore, they change states in the Hilbert space to different states, so the large gauge symmetry of gravity does not pose problems in the definition of  $S$  it only imposes honest (global) symmetry constraints on its matrix elements.

How can we see the hierarchy problem in terms of these observables? Nobody really knows, so it is possible that our estimate  $m_h^2 \sim y_t^2 M_{\text{Pl}}^2$  rooted in QFT intuition was too quick. There is one example in 2D [52], where  $M_{\text{Pl}}^2$  enters the  $S$  matrix only through a phase, not affecting the pole structure of  $S$ . The gravitational  $S$  matrix is obtained from the flat space one by multiplication by the phase factor

$$\hat{S}_n(p_i) = e^{i \frac{1}{M_{\text{Pl}}^2} \sum_{i < j} \epsilon_{\alpha\beta} p_i^\alpha p_j^\beta}. \quad (3.58)$$

The most attractive feature of these very special theories is that they implement explicit the idea that in absence of local off-shell observables the hierarchy problem might not be a problem. Its most unattractive feature is that gravity in 2D does not have a propagating massless spin-2 degree of freedom and this result looks very much like just eikonal scattering, i.e. scattering at high energies and large impact parameter  $b = J/\sqrt{s}$ . Here  $J$  is the angular momentum in a partial wave expansion of the amplitude and  $s$  the usual Mandelstam variable. By large we mean

$$b \gg \frac{E}{M_{\text{Pl}}^2}, \quad E > M_{\text{Pl}}. \quad (3.59)$$

In this regime also in 4D the effect of gravity is encoded in terms of a phase

$$e^{-i \frac{s}{4M_{\text{Pl}}^2} \log(b/R_{\text{IR}})}, \quad (3.60)$$

where  $R_{\text{IR}}$  is a IR cutoff that regulates infrared divergences. This type of scattering is indeed the only remnant of gravity in 2D.

If we ignore the problems with the previous examples (i.e. the ghost and the difficulty of extending the second idea to 4D), and power through, we still have two problems to solve. First of all, these theories still have a large scale (larger than  $M_{\text{Pl}}$ ) given by the Landau pole from the running of hypercharge in the SM. To avoid it we need new particles charged under  $U(1)_Y$ . Secondly, all BSM questions raised in Section 1.5 have to be answered without introducing new scales that are too strongly coupled to the Higgs. Rather than a problem, this is a feature of this class of ideas, which in principle can be falsified by discovering new scales coupled to  $H$ . Some of the phenomenological implications of this scenario were worked out in [94–96].

### 3.4 The Multiverse

In Section 2.1 we have seen that historical fine-tunings were resolved in two ways: 1) by the presence of a new symmetry 2) by multiple realizations of the same observable, some of which could be accidentally tuned.

We have not yet encountered anything resembling the second option for the Higgs boson mass. However proposals along these lines exist and we discuss them in this Section. The basic idea is that the observable Universe is just one patch of a vast Multiverse. Each patch has different values of fundamental parameters, in particular of  $\Lambda_{\text{CC}}$  and  $m_h^2$ . In this context, we have to explain why we live in a patch with a value of  $\Lambda_{\text{CC}}$  and  $m_h^2$  that appears unnaturally small. The traditional explanation is that only these tuned patches can support observers. These are known as anthropic arguments. We review them for  $m_h^2$  in the following subsection. First, it is instructive to see how a Multiverse can be populated.

We start with a special kind of Multiverse, first proposed by Brown and Teitelboim [97,98], that allows us to naturally build up to what is today considered the most “standard” Multiverse coming from string theory.

It is important to stress that we are still far from formulating a complete theory of the Multiverse. Such a theory would allow us to compute exactly what is the underlying distribution of metastable vacua in Nature and how they are populated. We would then be able to predict how frequent a patch is in the Multiverse, given the observed values of fundamental parameters. Nobody is currently able to do this. The most convincing examples of Multiverses come from string theory. Compactifying its extra dimensions leaves us with a multitude of moduli with  $10^{500}$  possible vacua (or more), most of them have lifetimes longer than that of the observable Universe. If the Universe is eternally inflating all these vacua can be populated by tunneling and live a long and healthy life before decaying to the true ground state.

Starting from this broad picture, concrete toy models of the landscape were proposed, showing that a Multiverse explanation of  $\Lambda_{\text{CC}}$  and  $m_h^2$  is possible. However we are not able to calculate the distribution of  $\Lambda_{\text{CC}}$  and  $m_h^2$  in the Multiverse and predict what is likely or unlikely for their observed value. Anthropic arguments allow us to bypass this difficulty, since they identify a small viable range for these parameters. If only a few values, compatible with observations, allow to have observers, we do not really need to compute how likely different patches are. We will not have a precise prediction for  $\Lambda_{\text{CC}}$  and  $m_h^2$ , but at least we have a reason to expect them to be much smaller than their natural value.

We can now turn to constructing and populating the Multiverse. Imagine having a 3-form field  $A_{\mu\nu\rho}$ , totally antisymmetric in its indexes. We can construct its kinetic term starting from the 4-form

$$F_{\mu\nu\rho\sigma} = \partial_\mu A_{\nu\rho\sigma} - \partial_\sigma A_{\mu\nu\rho} + \partial_\rho A_{\sigma\mu\nu} - \partial_\nu A_{\rho\sigma\mu}. \quad (3.61)$$



Its most general action, including also gravity, reads

$$S = -\frac{1}{48} \int d^4x \sqrt{-g} F_{\mu\nu\rho\sigma} F^{\mu\nu\rho\sigma} + S_{\text{boundary}} + S_G, \quad (3.62)$$

where the boundary action

$$S_{\text{boundary}} = \frac{1}{3!} \int d^4x \partial_\mu (\sqrt{-g} F^{\mu\nu\rho\sigma} A_{\nu\rho\sigma}) + 2M_{\text{Pl}}^2 \int_\Sigma d^3x \sqrt{-h} K \quad (3.63)$$

does not have any effect on-shell, but is needed to make the theory consistent. The second term must be included in spacetimes where the manifold is not closed (i.e. it has a boundary).  $\Sigma$  is the boundary of the manifold,  $h$  is the induced metric and  $K$  the extrinsic curvature. This is the Gibbons-Hawking-York boundary term [99].

The last term in  $S$  is the usual Einstein-Hilbert action with a cosmological constant

$$S_G = \int d^4x \sqrt{-g} \left( \frac{M_{\text{Pl}}^2}{16\pi} R - \Lambda_0 \right). \quad (3.64)$$

The equations of motion for  $A$  are

$$\partial_\mu (\sqrt{-g} F^{\mu\nu\rho\sigma}) = 0 \quad (3.65)$$

and the only solution

$$F^{\mu\nu\rho\sigma} = c \epsilon^{\mu\nu\rho\sigma}, \quad (3.66)$$

where  $c$  is a constant of dimension 2. This shows that  $A$  is non-dynamical. This is a consequence of the large gauge symmetry of the action, which is invariant under

$$A_{\mu\nu\rho} \rightarrow A_{\mu\nu\rho} + \partial_{[\mu} B_{\nu\rho]} \quad (3.67)$$

with  $B_{\mu\nu}$  any antisymmetric ( $B_{\mu\nu} = -B_{\nu\mu}$ ) tensor.

Therefore in this theory the cosmological constant is not only  $\Lambda_0$ , but also has a contribution from  $F^2$  in the action

$$\Lambda_{\text{CC}} = \Lambda_0 - \frac{c^2}{2}. \quad (3.68)$$

We do not yet have a landscape, but we are close. You might have noticed the analogy between our 3-form and the vector potential in electromagnetism (equivalently between  $F$  and the EM field). The only missing ingredient in this analogy is some form of charged matter like the electron. If such an object existed its pair production could discharge the primordial electric field  $c$  and change the cosmological constant.

To introduce this object in the theory it is useful to go deeper into the analogy with electromagnetism. Take a particle of unit charge moving along the worldline  $x_p^\mu(\tau)$ . Its current density is

$$J^\mu = e u^\mu \delta^{(3)}(\vec{x} - \vec{x}_p(\tau)), \quad u^\mu = \frac{dx_p^\mu(\tau)}{d\tau}, \quad (3.69)$$

and we can write its coupling to electromagnetism as

$$\int d^4x \sqrt{-g} J^\mu A_\mu = e \int d^4x \sqrt{-g} \delta^{(3)}(\vec{x} - \vec{x}_p(\tau)) \frac{dx_p^\mu(\tau)}{d\tau} A_\mu = e \int dx_p^\mu A_\mu, \quad (3.70)$$

where the last integral is taken along the worldline of the particle. We can now scale this example to one more dimension. A 2-form  $A_{\mu\nu} = -A_{\nu\mu}$  will couple to a one dimensional object (rather than a point particle), spanning a worldsheet  $x^\mu(\tau, \sigma) \equiv x^\mu(\vec{\xi})$ . Instead of a single four-velocity  $u^\mu$  in this case we have two possible derivatives  $\partial x^\mu/\partial\tau$ ,  $\partial x^\nu/\partial\sigma$ . Due to the antisymmetry of  $A_{\mu\nu}$  there is only one possible Lorentz-invariant coupling

$$A_{\mu\nu}\epsilon^{ab}\frac{\partial x^\mu}{\partial\xi^a}\frac{\partial x^\nu}{\partial\xi^b}. \quad (3.71)$$

To complete the analogy with electromagnetism we can integrate over the worldsheet to obtain the action

$$S_{\text{int}} = \frac{e}{2} \int d^2\xi A_{\mu\nu}\epsilon^{ab}\frac{\partial x^\mu}{\partial\xi^a}\frac{\partial x^\nu}{\partial\xi^b}. \quad (3.72)$$

It is now straightforward to apply the same reasoning to our 3-form and obtain the action of the brane coupling to it

$$S_{\text{brane}} \supset \frac{e}{3!} \int d^3\xi A_{\mu\nu\rho}\epsilon^{abc}\frac{\partial x^\mu}{\partial\xi^a}\frac{\partial x^\nu}{\partial\xi^b}\frac{\partial x^\rho}{\partial\xi^c}. \quad (3.73)$$

To complete the action we need only to generalize the free Lagrangian of a point particle to a brane

$$S_{\text{free}} = -m \int d\tau = -m \int \sqrt{g^{(1)}} dt. \quad (3.74)$$

In the last equality we have noted that  $\gamma d\tau = dt$  and introduced the one dimensional metric induced on the worldline. It is now easy to generalize the previous expression to

$$S_{\text{brane}} \supset -T \int d^3\xi \sqrt{g^{(3)}}, \quad (3.75)$$

the only difference to keep in mind is that  $T$  is now a tension of dimension mass/volume. Putting together the two terms in  $S_{\text{brane}}$  with the action in Eq. (3.62) we can obtain the new equations of motion

$$\partial_\mu c(y)\epsilon^{\mu\nu\rho\sigma} = -e \int d^3\xi \delta^{(4)}(y - x(\vec{\xi}))\epsilon^{abc}\frac{\partial x^\mu}{\partial\xi^a}\frac{\partial x^\nu}{\partial\xi^b}\frac{\partial x^\rho}{\partial\xi^c}. \quad (3.76)$$

On both sides of the brane  $c$  is constant and it jumps through it by a unit of brane charge  $e$

$$\Delta c = e. \quad (3.77)$$

If we have initially a large electric field  $c^2 > e^2$ , membranes of opposite charge can be spontaneously nucleated. The electric field inside the bubble formed by the brane and the anti-brane is now smaller than that outside. This configuration has lower energy than the outside vacuum, so the bubble walls will expand.

This is the same process as Schwinger pair production in QED. It is a tunneling process akin to a phase transition, governed by the same equations as that of a scalar jumping from a metastable minimum to a deeper minimum.

If we add to the mix eternal inflation we have created a Multiverse where each patch has a different CC. The bubble walls will expand at most at the speed of light, but the volume of the universe grows faster, so configurations with different values of  $c$  can coexist.

The smallest splitting between CCs in this Multiverse is

$$\Delta\Lambda = e^2. \quad (3.78)$$

Eternal inflation is useful for two reasons. Since it gives an exponentially expanding volume, bubble walls, even if they move at the speed of light, never manage to meet, so instead of having a single universe in the ground state, we have multiple bubbles constantly expanding under the effect of inflation. Secondly, but maybe less critically, eternal inflation provides a large volume and a long time for the bubbles to form. The tunneling process is slow

$$t_{\text{nucleation}} \simeq e^{S_E} \simeq e^{\frac{M_{\text{Pl}}^4}{e^2}}, \quad (3.79)$$

even extremely slow if we want  $\Delta\Lambda \simeq \Lambda_{\text{CC}} \simeq (0.1\text{meV})^4$ , so we need a long enough period of inflation to populate all the values of the CC. This discussion can be straightforwardly generalized to scanning the Higgs mass if we add a coupling to the 4-form, for instance

$$S \supset \int d^4x \sqrt{-g} \frac{F_{\mu\nu\rho\sigma} F^{\mu\nu\rho\sigma}}{48} |H|^2. \quad (3.80)$$

This gives at least a proof-of-principle that a Multiverse for  $\Lambda_{\text{CC}}$  and  $m_h^2$  can exist in Nature. What makes this construction more interesting is that string theory possess the ingredients that we have described in our toy model. It is very likely that if it is the right theory of quantum gravity a landscape actually exists. For instance in M-theory there is a 7-form  $F_7$  in 11D that upon compactification gives rise to several lower-order forms, including two  $F_4$  of the type that we have described [100].

The only extra subtlety to take into account is that  $c$  in string theory is quantized [101],  $c = en$  with  $n \in \mathbb{Z}$ , because both electric and magnetic sources are present for all gauge fields.

In this picture, if we have  $J$  4-forms from compactifying higher form fields, the cosmological constant is

$$\Lambda_{\text{CC}} = \Lambda_0 - \frac{1}{2} \sum_{i=1}^J e_i^2 n_i^2. \quad (3.81)$$

If we now imagine that bubbles with different  $c_i$ 's are nucleated and expand during eternal inflation we can ask what it takes to get at least one patch where  $\Lambda_{\text{CC}} = \Lambda_{\text{obs}} \simeq (0.1 \text{ meV})^4$ . If we had a single 4-form we would need

$$e^2 \simeq \Lambda_{\text{obs}} \ll M_{\text{Pl}}^4, \quad (3.82)$$

to scan the CC finely enough, as in the previous example. This is technically natural, since if we send  $e \rightarrow 0$  the 3-form and the brane decouple and we have two free theories with extra symmetries. However it is nice to notice that if we have  $J$  fields then we can get away with much smaller couplings [101]

$$\frac{2\pi^{J/2}}{\Gamma(J/2)} \Lambda_0^{J/2} \frac{\Lambda_{\text{obs}}}{\Lambda_0} \gtrsim \prod_{i=1}^J e_i. \quad (3.83)$$

For instance  $\Lambda_0 \simeq M_{\text{Pl}}^4$  and  $J = 100$  gives  $e_i \simeq 0.01 M_{\text{Pl}}$  and indeed string theory predicts a large number of such fields.

One can get Eq. (3.83) by noticing that the possible CCs given by the 4-forms are in a multidimensional grid. To find our universe in this grid, we have to cancel  $\Lambda_0$  against the 4-forms contributions with a precision  $\Lambda_{\text{obs}}$ , so we are asking if there is any point in this grid

contained within the surfaces of two spheres, one of radius  $\Lambda_0 - \Lambda_{\text{obs}}$  and another of radius  $\Lambda_0 + \Lambda_{\text{obs}}$ . Calculating the volume of this region gives us Eq. (3.83). What we have just summarized is the celebrated Bousso-Polchinski explanation [101] for the value of the CC. The only missing ingredient is the argument that explains why we are in a patch with such a tiny CC. This argument is due to Weinberg [102] and even if this work is mainly about the Higgs boson we find useful to review it here.

If we reduce it to its most basic ingredients the argument runs as follows [103]. If the energy density from the CC,  $\rho_\Lambda$ , dominates, the Universe can have one of two fates: 1) If the CC is negative it takes the Universe a time  $\sim \Lambda^{1/2}/M_{\text{Pl}}^2$  to collapse into an object of size  $\sim \Lambda^{1/2}/M_{\text{Pl}}^2$  and comparable curvature radius 2) If it is positive the Universe expands exponentially with a scale factor  $e^{(\Lambda^{1/2}/M_{\text{Pl}}^2)t}$ . All other forms of energy are diluted, leaving an empty Universe.

Therefore if we want to form galaxies we need the matter energy density  $\rho_m$  to dominated over  $\rho_\Lambda$  for a long enough time. More precisely, density perturbations grow linearly with the scale factor

$$\frac{\delta\rho}{\rho} \sim a \quad (3.84)$$

if  $\rho_m > \rho_\Lambda, \rho_r$ , where  $\rho_r$  is the energy density in radiation. We can roughly call a galaxy a density perturbation of order one, i.e  $\delta\rho/\rho \simeq 1$ . Therefore, to form galaxies we need

$$\rho_\Lambda \lesssim \rho_{\text{MR}} \left( \frac{\delta\rho_{\text{MR}}}{\rho_{\text{MR}}} \right)^3, \quad (3.85)$$

where  $\rho_{\text{MR}}$  is the matter energy density at matter-radiation equality and  $\left( \frac{\delta\rho_{\text{MR}}}{\rho_{\text{MR}}} \right)^3$  is the amount that this energy density has redshifted before density perturbations growing linearly with  $a$  become  $\mathcal{O}(1)$ . From CMB measurements we know that  $\rho_{\text{MR}} \simeq \text{eV}^4$ ,  $\delta\rho_{\text{MR}}/\rho_{\text{MR}} \simeq 10^{-5}$ , so we get

$$\rho_\Lambda \lesssim (0.1\text{meV})^4, \quad (3.86)$$

remarkably close to the observed value. If we were more precise, we would find an upper bound about 100 to 1000 times larger than the actual measurement, but it is remarkable how close this simple argument gets to the actual value of the CC.

This argument is quite robust, in the sense that it doesn't rely on a precise definition of observers, we just don't want the universe to be empty or tiny and with a large curvature. However, it must be taken with a grain of salt. As stated above we don't know what the Multiverse really looks like and other parameters, including  $\rho_{\text{MR}}$  and  $\delta\rho_{\text{MR}}$  can vary between patches. This is nonetheless a pretty striking proof-of-principle that a Multiverse explanation for the CC might work.

### 3.4.1 Anthropic Selection

We have seen how to populate a vast landscape of values for the Higgs boson mass. However, we still need to explain why we happen to be in a patch with such an improbably small value of  $m_h$ .

Nature is full of interesting coincidences. There are a number of parameters that are just at the edge of what is needed to make a certain phenomenon possible. It was argued [104] that the Higgs boson mass might be one of these parameters. If it deviated more than a factor of a few from its observed value, complex chemistry would not be possible. This is traditionally taken as a sign that complex observers like us would not exist in most other patches of the

Multiverse. In this sense the selection of the Higgs boson mass might be “anthropic”, i.e. we don’t see a more likely universe because there we don’t exist.

The key observation is that nuclear parameters depend on  $m_h^2$ . Let us first consider universes with  $m_h^2 < 0$ . For the neutron-proton mass difference we have

$$m_n - m_p = (m_d - m_u) + \Delta m_{\text{em}} \approx 3 \text{ MeV} \frac{v}{v_{\text{us}}} + \Delta m_{\text{em}} \quad (3.87)$$

For  $v \lesssim \text{few hundred} \times v_{\text{us}}$ , then  $m_{d,u} < \Lambda_{\text{QCD}}$  and we can leave  $\Delta m_{\text{em}} = -1.7 \text{ MeV}$  fixed at the value that it has in our universe. Also the QCD scale and the mass difference between isospin 1/2 and an isospin 3/2 baryons depend on  $v$ ,

$$\Lambda_{\text{QCD}} \simeq \Lambda_{\text{QCD,us}} \frac{v^\xi}{v_{\text{us}}^\xi} \quad (3.88)$$

$$m_{3/2} - m_{1/2} \simeq 300 \text{ MeV} \frac{v^\xi}{v_{\text{us}}^\xi}, \quad (3.89)$$

$$\xi \simeq 0.3 \text{ for } 10^{-2} < \frac{v}{v_{\text{us}}} < 10^4. \quad (3.90)$$

There are main more hadronic properties that depend on  $v$ . The last one that we need to formulate our anthropic arguments is that the long range nucleon potential is well approximated by single pion exchange. The pion mass is also sensitive to  $v$ :  $m_\pi^2 \sim f_\pi(m_u + m_d)$ .  $m_\pi \sim m_{\pi,\text{us}} \sqrt{v/v_{\text{us}}}$ .

If  $v$  decreases, at some point Hydrogen becomes unstable, but other nuclei still exist since  $m_p - m_n$  never gets above 1.7 MeV. So this kind of universes might support life. On the contrary if  $v$  becomes too big, the nuclear binding energy decreases (from  $m_\pi$  increasing). Besides  $m_n - m_p$  increases indefinitely. At some point ( $v/v_{\text{us}} \gtrsim 5$ ) no complex elements, beyond hydrogen, form. The reason is the following: in our universe the nuclear binding energy is negative, i.e. the mass of a nucleus is less than the mass of its constituents by an amount given by the nuclear force minus the EM repulsion, so it is energetically convenient for baryons to form nuclei.

When  $m_n - m_p$  exceeds the binding energy, the nucleus decays rapidly (if it ever forms). Consider the decay of a nucleus  ${}^A_Z\text{X}$  of mass  $m({}^A_Z\text{X})$ ,

$${}^A_Z\text{X} \rightarrow {}^A_{Z+1}\text{X} + e^- + \bar{\nu}_e, \quad m({}^A_Z\text{X}) = m_N({}^A_Z\text{X}) + Zm_e - \sum_{i=1}^Z B_{i,e}. \quad (3.91)$$

The decay rate is given by

$$\Gamma \sim G_F^2 Q^5$$

$$Q \approx m({}^A_Z\text{X}) - m({}^A_{Z+1}\text{X}) - m_e \approx m_N({}^A_Z\text{X}) - m_N({}^A_{Z+1}\text{X}) = (m_n - m_p) - B_N. \quad (3.92)$$

The difference in electron binding energy is very small for high  $Z$  atoms and we have neglected it.  $B_N$  is the difference of the nuclear binding energies. Note that  $-B_N$  is always negative because replacing a neutron with a proton increases the electrostatic repulsion. When  $Q > 0$  the decay is allowed and the rate grows rapidly with  $Q$ . This sets an upper bound on the magnitude of  $m_h^2$  in universes where  $m_h^2 < 0$ , exactly what we need to explain the smallness of  $m_h^2$ . How about  $m_h^2 > 0$  universes?

In  $m_h^2 > 0$  universes baryons are washed-out through electroweak sphalerons that convert them to neutrinos unless an asymmetry is produced after the EW phase transition. Molecules do not form until much later times compared to our universe. We need the cosmic microwave background to cool below  $\epsilon \alpha^2 m_e \sim \epsilon \alpha^2 y_e \frac{\Lambda_{\text{QCD}}^3}{m_H^2}$ ,  $\epsilon \approx 10^{-3}$ .

This “biochemical energy” characteristic of molecules, can be estimated from the quantum mechanical model of the hydrogen atom

$$V(r) = \frac{p_e^2}{2m_e} - \frac{\alpha}{r} = \frac{1}{2m_e r^2} - \frac{\alpha}{r}. \quad (3.93)$$

The minimum of this potential is at

$$r = \frac{1}{\alpha m_e}, \quad (3.94)$$

and the typical kinetic energy of the electron  $p_e^2/2m_e \sim \alpha^2 m_e$ . We can roughly understand the  $\epsilon$  suppression factor from the fact that molecules are bigger and more loosely bound than atoms. These arguments more or less rule out also  $m_h^2 > 0$  universes as hospitable hamlets for observers relying on complex chemistry.

These arguments rely on the fact that dimensionless SM parameters, in particular Yukawa couplings, do not vary appreciably between different patches of the Multiverse. This is not an unlikely occurrence, as can be seen from the explicit construction in [105]. A perhaps less debated, but more important point to keep in mind is that  $m_h^2 = 0$  or  $\Lambda_{\text{CC}} = 0$  are not special points in theories without supersymmetry or scale invariance. Therefore a generic, non-symmetric, landscape will scan  $m_h^2$  and the cosmological constant around their natural value ( $m_h^2 \simeq M_*^2$  or  $\Lambda_{\text{CC}} \simeq M_*^4$  if  $M_*$  is the fundamental high scale of our theory) with very few vacua around zero, in general not enough to explain their value.

To illustrate this point, consider the QFT toy model of a landscape in [105]. We imagine a theory with  $N$  scalars  $\phi_i$ . Each scalar has a potential  $V_{\phi_i}$  with two minima at  $\langle \phi_i \rangle = \phi_{1,2}$  and vacuum energies  $V_{1,2}$ . We take  $V_1 \geq V_2$ . The full theory has  $2^N$  vacua described by the potential

$$V = \sum_{i=1}^N V_{\phi_i}. \quad (3.95)$$

We can label the vacua using a set of integers  $\eta_i = \pm 1$ . Every choice of  $\{\eta\} = \{\eta_1, \dots, \eta_N\}$  corresponds to a different CC

$$\begin{aligned} \Lambda_{\{\eta\}} &= N\bar{V} + \sum_{i=1}^N \eta_i \Delta V, \\ \bar{V} &= \frac{V_1 + V_2}{2}, \quad \Delta V = \frac{V_1 - V_2}{2}. \end{aligned} \quad (3.96)$$

For simplicity we have taken the same values of  $V_{1,2}$  for all the scalars, since it does not affect our conclusions.

The distribution of CCs in the landscape at large  $N$  is well approximated by a Gaussian (as expected from the central limit theorem)

$$p(\Lambda) \rightarrow \frac{2^N}{\sqrt{2\pi N \Delta V}} e^{-\frac{(\Lambda - N\bar{V})^2}{N \Delta V^2}}. \quad (3.97)$$

If we have enough minima to populate only the central region of the Gaussian, the CC is finely scanned in a region  $\Lambda = \bar{\Lambda} \pm \delta\Lambda = N\bar{V} \pm \sqrt{N} \Delta V$ . If  $\bar{V} \simeq \Delta V$ , as we expect from dimensional analysis, then

$$\frac{\delta\Lambda}{\bar{\Lambda}} \simeq \frac{1}{\sqrt{N}}. \quad (3.98)$$

In particular we are not scanning around zero in the central region of the Gaussian. In this landscape the number of vacua with nearly vanishing vacuum energy is  $\simeq 2^N e^{-N\bar{V}^2/\Delta V^2}$ . To finely scan the CC around zero we need both  $\bar{V}/\Delta V \lesssim \sqrt{\log 2}$  and sufficiently large  $N$ . A generic landscape is finely scanning the CC only around  $N\bar{V}$ .

The situation is different in supersymmetry. Take for instance the odd superpotential

$$W = \lambda\phi^3 - \mu^2\phi. \quad (3.99)$$

In this case at the two minima  $W_1 = -W_2$  so that  $\bar{W} = 0$ . Then the landscape generated by  $N$  of these superpotentials is scanning the CC in the range

$$-3\frac{|\sqrt{N}\Delta W|^2}{M_{\text{Pl}}^2} \lesssim \Lambda \lesssim 0. \quad (3.100)$$

In this case supersymmetry is keeping  $\Lambda \leq 0$  and a  $Z_4$  R-symmetry that protects the odd structure of the superpotential is ensuring that the distribution of negative CCs has a central value comparable to its standard deviation:  $|\sqrt{N}\Delta W|^2/M_{\text{Pl}}^2$  [105]. After SUSY breaking, this landscape scans the CC efficiently around zero, because of its symmetries. The situation is analogous for  $m_h^2$ .

In summary, even a landscape solution is probably relying on one of the symmetries that we presented in the previous Sections. Maybe they are realized only at very high energies, but this is still an interesting information about Nature. In the next Chapter we will see that the presence of these symmetries (in disguise) is often true also for solutions that explain  $m_h^2$  through some early Universe event. However, this is just a simple toy example and we don't know the actual measure of  $\Lambda_{\text{CC}}$  and  $m_h^2$  in the landscape, but it is generic enough that it is useful to keep it in mind.

A second (less quantitative) aspect of this story that is not always appropriately emphasized, is that the arguments on chemistry outlined above are very detailed. By ‘‘detailed’’ I mean that they rely on a very specific definition of observers. If one starts searching, there are a lot of similar coincidences without which either complex chemistry would not exist or observers similar to us would not exist. The role of the Higgs is not that unique. Personally, I interpret this as a sign that maybe we are not using a good definition of observers, in the sense that it is possible that a much larger class of observers not based on complex chemistry might exist. This would make Higgs anthropic arguments contentless. Of course, until we further progress in the study of life, this discussion will remain at the philosophical level. It is nonetheless interesting to notice that Weinberg's argument for the CC, described at the beginning of this Section, is not at all detailed in this sense. It essentially only requires some amount of entropy in a causally connected patch.

To substantiate my earlier point on Nature being riddled with these coincidences, let me give two examples. I refer the reader to [106] for more fun coincidences.

When four nucleons make  ${}^4_2\text{He}$ , 0.7% of their mass is converted to energy. If this number was smaller we would have only hydrogen otherwise there would be no hydrogen.

When a star runs out of Hydrogen it collapses until its core temperature reaches 10 keV. Then



We need the excited state of Carbon on the right hand side to be between 7.3 and 7.9 MeV to produce sufficient carbon for life to exist, and must be further ‘‘fine-tuned’’ to between 7.596

MeV and 7.716 MeV to produce the amount observed in nature. There is an excited state of oxygen which, if it were slightly higher, would provide a resonance and speed up the reaction. In that case insufficient carbon would exist in nature; it would almost all have converted to oxygen. Hoyle used these facts to predict the existence of the  $^{12}_6\text{C}$  excited state. The ground state of Carbon is at 7.3367 MeV, below the  $^4_2\text{He} + ^8_4\text{Be}$  energy.

### 3.5 Comments on UV/IR Mixing and Quantum Gravity

In addition to the attempts at formulating a scaleless theory of gravity, there are two more ways in which gravity might behave differently compared to what discussed in the previous Sections, where it was simply providing a new dimensionful scale to deal with in QFT.

The first one is quite direct and violates our EFT intuition on the Higgs mass. The Higgs boson mass squared is given by an integral over multiple energy scales

$$m_h^2(\Lambda_{\text{IR}}) = m_h^2(\Lambda_{\text{UV}}) + \int_{\Lambda_{\text{IR}}}^{\Lambda_{\text{UV}}} d\Lambda \delta m_h^2(\Lambda). \quad (3.104)$$

It is possible that high energy effects are not independent of low energy ones and what appears as an accidental cancellation, is explained by the full theory of quantum gravity.

This brief discussion might have appeared vague. This is not an accident. To the best of my knowledge there is no concrete proposal to implement the previous idea. The closest we got are examples in quantum field theory on non-commutative spacetimes [107]. In this proposal IR and UV effects are related in a precise way, but the Lorentz non-invariance inherent in the theory obstructs incorporating the mechanism in the SM, given current experimental results. Still we find interesting to review the basics of this idea here. Consider

$$[\hat{x}_\mu, \hat{x}_\nu] = i\theta_{\mu\nu}, \quad (3.105)$$

where  $\theta_{\mu\nu} = -\theta_{\nu\mu}$ . This is relating long-distance and short-distance effects

$$\Delta\hat{x}_\mu\Delta\hat{x}_\nu \geq \frac{|\theta_{\mu\nu}|}{2}, \quad (3.106)$$

but is also breaking Lorentz invariance. The tensor  $\theta_{\mu\nu}$  is breaking Lorentz invariance as a uniform magnetic field breaks rotational invariance, by defining a preferred direction in space(time).

It is possible to show that a quantum field theory on these spacetimes can be written in terms of commuting coordinates, if we additionally introduce the product [108, 109]

$$f(x) \star g(x) = \exp\left(\frac{i}{2}\theta_{\mu\nu}\partial_y^\mu\partial_z^\nu\right) f(y)g(z)\Big|_{y=z=x}. \quad (3.107)$$

This trick allows to show that noncommutative quantization does not affect the free part of the tree-level action due to momentum conservation and the antisymmetry of  $\theta_{\mu\nu}$  that make the new exponential factor = 1 for the quadratic terms in the Lagrangian.

Interactions are modified to

$$\mathcal{L}_{\text{int}}^{\text{NC}} = \frac{\lambda_n}{n!} \phi(x) \star \phi(x) \star \dots \star \phi(x). \quad (3.108)$$

The corresponding action in momentum space looks like

$$S_{\text{int}}^{\text{NC}} = \frac{\lambda_n}{n!} \int \prod_{i=1}^n d^4k_i \phi(k_1) \dots \phi(k_n) \delta^{(4)}(k_1 + \dots + k_n) \exp\left(\frac{i}{2} \sum_{j<i}^n \theta_{\mu\nu} k_i^\mu k_j^\nu\right). \quad (3.109)$$



If we expand for  $\theta \ll 1$  this looks like a perfectly normal EFT with a set of irrelevant operators. If instead we keep the full exponential, an interesting UV/IR duality emerges.

The antisymmetry of  $\theta_{\mu\nu}$  together with the momentum-conserving  $\delta$ -function in each vertex, allow to considerably simplify calculations in these theories. If the graph is planar, including any tree-level graph, all exponential factors from loops can be eliminated. The only contributions to the new phase factor containing  $\theta$  come from external lines and their ordering. In non-planar graphs, internal lines that cross can also contribute. A proof can be found in [110]. In practice at tree-level these theories are identical to commutative QFTs. At loop level, it is easy to evaluate integrands, but integrations can give surprising results.

Consider the scalar  $\phi^4$  theory studied in [111], in Euclidean signature<sup>4</sup>

$$S_4 = \int d^4x \left( \frac{\partial_\mu \phi \partial^\mu \phi}{2} + \frac{m^2}{2} \phi^2 + \frac{g^2}{24} \phi \star \phi \star \phi \star \phi \right). \quad (3.110)$$

At one loop the two-point function of a scalar with external momentum  $p^\mu$  receives two contributions

$$\begin{aligned} \Gamma_p^{(2)} &= \frac{g^2}{3(2\pi)^4} \int \frac{d^4k}{k^2 + m^2}, \\ \Gamma_{np}^{(2)} &= \frac{g^2}{3(2\pi)^4} \int \frac{d^4k}{k^2 + m^2} e^{ik^\mu \theta_{\mu\nu} p^\nu}. \end{aligned} \quad (3.111)$$

The first integral can be evaluated by standard techniques using a momentum cutoff to give

$$\Gamma_p^{(2)} = \frac{g^2}{48\pi^2} \left( \Lambda^2 - m^2 \log \frac{\Lambda^2}{m^2} + \mathcal{O}(1) \right). \quad (3.112)$$

For the second integral we introduce the Schwinger parameter  $\alpha$

$$\frac{1}{k^2 + m^2} = \int_0^\infty d\alpha e^{-\alpha(k^2 + m^2)}, \quad (3.113)$$

complete the square at the exponent and add the regulator  $e^{-1/(\Lambda^2\alpha)}$

$$\Gamma_{np}^{(2)} = \frac{g^2}{96\pi^2} \int \frac{d\alpha}{\alpha^2} e^{-\alpha m^2 + \frac{p^\mu \theta_{\mu\rho} \theta^\rho_\nu p^\nu}{4\alpha} - \frac{1}{\Lambda^2\alpha}}. \quad (3.114)$$

Evaluating the integral gives

$$\begin{aligned} \Gamma_{np}^{(2)} &= \frac{g^2}{48\pi^2} \left( \Lambda_{\text{eff}}^2 - m^2 \log \frac{\Lambda_{\text{eff}}^2}{m^2} + \mathcal{O}(1) \right), \\ \Lambda_{\text{eff}}^2 &= \frac{1}{\frac{1}{\Lambda^2} - \frac{4}{p^\mu \theta_{\mu\rho} \theta^\rho_\nu p^\nu}}. \end{aligned} \quad (3.115)$$

Intriguingly  $\Gamma_{np}^{(2)}$  is finite for  $\Lambda \rightarrow \infty$ . Have we really regulated UV divergences using the fuzziness of spacetime? Not exactly, since the UV pole has not entirely disappeared. It just does not commute with a new IR pole that did not exist in the tree-level theory. If we take  $\Lambda \rightarrow \infty$  first, we have a new pole when  $p \circ p \equiv -p^\mu \theta_{\mu\rho} \theta^\rho_\nu p^\nu \rightarrow 0$ . Similarly, taking  $p \circ p \rightarrow 0$  leaves us with a UV divergence. This remains true in different regularization schemes [107].

---

<sup>4</sup>There are subtleties related to unitarity in non-commutative Lorentzian theories that do not affect our main point. We refer the reader to [107] for a more complete discussion with relevant references.

A Wilsonian effective theorist would write a low energy Lagrangian that is finite in the  $\Lambda \rightarrow \infty$  limit. This Lagrangian must contain a new field that accounts for the IR pole that appears in this limit. This means adding to  $S_4$  the terms

$$\Delta S_4(\Lambda) = \int d^4x \left( \frac{1}{2} \partial\chi \circ \partial\chi + \frac{\Lambda^2}{8} (\partial \circ \partial\chi)^2 + \frac{i}{\sqrt{24\pi^2}} g\chi\phi \right). \quad (3.116)$$

It is not clear at all to me (or to anyone, as far as I know) that this is the right perspective. Sure, this Lagrangian respects the Wilsonian tenet that the correlations functions computed from the action converge smoothly to their  $\Lambda \rightarrow \infty$  limits<sup>5</sup>. However,  $\chi$  does not look at all like a normal low-energy field. For instance, we can't simply write an effective Lagrangian for  $\chi$  by integrating out  $\phi$ , since its non-standard kinetic term prevents diagonalization of the quadratic terms in the Lagrangian. Furthermore, the new pole breaks unitarity in this theory [112] and finally the only interaction of  $\chi$  is linear mixing, which means that its action is not renormalized (any divergences are absorbed by  $\phi$  counterterms).

The Wilsonian point of view might indeed be inadequate to understand these theories, since it is based on a ‘‘UV first’’ logic, which is the right point of view is still source of debate [107].

We can content ourselves to note an intriguing fact. Given any finite UV scale  $\Lambda$  we have generated a new stable IR scale in the form of an IR cutoff  $\sim \Lambda_\theta^2/\Lambda$  (if  $1/\Lambda_\theta^2$  is the only eigenvalue of  $\theta$ ). Even more intriguingly, for  $\Lambda \rightarrow \infty$ , the theory is finite but we have a new IR pole in a two-point function at  $p^2 \sim g^2\Lambda_\theta^4/m^2$ , which can be naturally much smaller than  $m^2$ .

This is exactly what we need to solve the hierarchy problem. However, to have a real solution we still have to deal with Lorentz violation (in the Wilsonian picture  $\chi$  propagates only in non-commuting directions) and better understand unitarity in this theory. For a more complete discussion we refer the reader to [107].

The second way in which gravity might surprise us, is possibly even more speculative, but not completely unfamiliar from an EFT perspective. It is well-known that a UV theory might leave non-trivial constraints at low energy, which the low energy physicists can only accept as facts of life. The prime example is the Spin-Statics theorem in quantum mechanics that in QFT is seen as a consequence of Lorentz invariance and causality.

String theory might offer a more dramatic realization of this idea. It is possible that many perfectly sensible, local, Lorentz-invariant EFTs are in the so-called ‘‘swampland’’, i.e. they are incompatible with quantum gravity. A number of string theory examples make this intuition precise. For example the same modulus usually controls the mass of multiple towers of new states. A classic example are KK and winding modes in string theory, whose masses scale as

$$M_{\text{KK}} \sim e^{\alpha\phi}, \quad M_{\text{winding}} \sim e^{-\alpha\phi} \quad (3.117)$$

where  $\phi$  is a modulus. The two towers are related by  $T$ -duality. Given the pervasive nature of dualities in string theory this has led to the so-called Swampland Distance Conjecture [53]

- Consider a theory, coupled to gravity, with a moduli space  $M$  which is parametrized by the expectation values of some field  $\phi_i$  which have no potential. Starting from any point  $P \in M$  there exists another point  $Q \in M$  such that the geodesic distance between  $P$  and  $Q$ , denoted  $d(P, Q)$ , is infinite.
- There exists an infinite tower of states, with an associated mass scale  $m$ , such that

$$m(Q) \sim m(P)e^{-\alpha d(P, Q)}, \quad (3.118)$$

where  $\alpha$  is some positive constant.

---

<sup>5</sup>This can be verified by integrating out  $\chi$  at tree-level, since the action is quadratic in  $\chi$ .

This means that considering large field excursion might break our EFT, even if at low energy we would not suspect that.

Another example is the Weak Gravity Conjecture. When we compactify string theory we might obtain gauge fields at low energy that arise either from the high-dimensional components of the gravitational field, or from higher form fields (for instance  $B_{\mu\nu}$ ). In both cases the low dimensional gauge coupling is a function of the moduli that determine the size and geometry of the compactified dimensions. There is therefore a relation between the mass of charged states (KK and winding modes), coming from this compactification and their charge under the gauge group. Explicit examples corroborate the following Weak Gravity Conjecture [113, 114]:

- Consider a theory, coupled to gravity, with a  $U(1)$  gauge symmetry with gauge coupling  $g$

$$S = \int d^d x \sqrt{-g} \left[ M^{d-2} \frac{R^d}{2} - \frac{1}{4g^2} F^2 \right]. \quad (3.119)$$

Then

- **Electric:** There exists a particle in the theory with mass  $m$  and charge  $q$  such that

$$m \leq \sqrt{\frac{d-2}{d-3}} g q M^{\frac{d-2}{2}}. \quad (3.120)$$

- **Magnetic:** The cutoff of this EFT is bounded from above by

$$\Lambda \lesssim g M^{\frac{d-2}{2}}. \quad (3.121)$$

A third interesting example is the Refined de Sitter Conjecture [115, 116]

- The scalar potential of a theory coupled to gravity must satisfy either

$$|\nabla V| \geq \frac{c}{M_{\text{Pl}}} V, \quad (3.122)$$

or

$$\min(\nabla_i \nabla_j V) \leq -\frac{c'}{M_{\text{Pl}}^2} V \quad (3.123)$$

For  $c, c' = \mathcal{O}(1)$ . This conjecture comes from the calculation of the de Sitter entropy plus the distance conjecture. If a scalar rolls too far down its potential, the tower of states that becomes light changes the entropy, making it incompatible with what we know about de Sitter space [115–117].

All these examples have a few features in common: 1) They describe highly non-trivial constraints on the EFT that the low energy physicist could not have imagined 2) They are (conjectures)<sup>2</sup>. They arise from string theory (which we do not know for sure to be the right theory of quantum gravity), within string theory they come from a handful of examples that correspond to limits where we have the theory under control. If we want to apply them to phenomenology they become (conjectures)<sup>3</sup> in the sense that we typically have to take an extra step. For instance, by adding to the distance conjecture the statement that all low energy scalars are moduli 3) We have no idea how something similar could apply to the Higgs boson.

Having said this, the fact that  $m_h^2 = 0$  is special from the point of view of quantum gravity is not impossible, and we can keep it in mind as an intriguing possibility for future work and speculation.



# Chapter 4

## A New Class of Solutions to the Hierarchy Problem

Every man is an abyss, one feels dizzy when one looks within.

---

*Georg Büchner*

In this Chapter we explore the possibility that an early Universe event selects the value of  $m_h$  that we observe today. We need a landscape of values for  $m_h^2$  from which to select the observed one, but not all landscapes are Multiverses (as shown in Section 4.1). We need a mechanism to select  $m_h^2$  out of the landscape. The selection mechanism has two ingredients: a trigger and a symmetry. The trigger can be any quantity sensitive to  $m_h^2$ . The symmetry is needed to naturally explain the small number  $v^2/\Lambda_H^2$ , and, as we have seen in the previous Chapter, it could also be replaced by a large discrete number  $N \sim \Lambda_H^2/v^2$ .

Symmetries or large  $N$  in this Chapter could be completely hidden from a SM observer and only manifest in a sector of the theory which is extremely weakly coupled to us. In most cases we are outsourcing the hierarchy problem to new particles that can be approximately shift-symmetric or supersymmetric or scale invariant.

Therefore, unlike in the previous Chapter, symmetries are not our best shot at discovering the naturalness of the Higgs mass. Triggers are our best shot. They generically require light physics coupled at  $\mathcal{O}(1)$  with the Higgs and we will spend a good deal of ink talking about them. One lesson that I have learned is that there is a single operator in the SM whose vev is sensitive to the Higgs vev. It is  $\text{Tr}[G\tilde{G}]$ . Its vev is also sensitive to the  $\theta$ -angle that determines the CP properties of the strong force. We will see in Section 4.2.1 that these are non-trivial facts and I am starting to think that they cannot be a coincidence.

Before diving in this new class of ideas, it is useful to stress three points. First of all, from the point of view of quantum field theory they are rather conservative. I would argue the natural next step beyond supersymmetry or dimensional transmutation. After all, they are just hiding these symmetries in a new weakly coupled sector. They do not challenge any of the principles that have guided us in building quantum field theory, unlike some more speculative options briefly reviewed in the previous Chapter. Nonetheless their experimental predictions are dramatically different from those of traditional solutions to the hierarchy problem.

The second point is that albeit conservative from a low energy QFT perspective they might not be equally conservative from the point of view of quantum gravity. Often special structures in the landscape and/or large field excursions are constructed, which might be at odds with the ultimate description of quantum gravity. Given our current ignorance on quantum gravity (and even on string theory) I take a rather humble perspective on the issue. I think that as long as

we can't exclude these ideas from the UV, it is worth to test them directly with experiment. Our vague intuition about what is beautiful or allowed in physics have already failed us many times in the past, especially with regards to this problem.

The last point to stress is that even if most of these ideas appear quite unrelated, they fall into three broad categories: anthropic selection, dynamical selection and statistical selection. The difference between the first two is often blurred. The last category instead is quite distinct and, importantly, suffers from a problem of measure in the landscape. Rather than explaining this division in detail here, we first review explicit examples and then return on it in Section 4.8. The most interesting aspect of this division is that the most conceptually solid options (dynamical and anthropic selection), i.e. those that do not suffer from a measure problem, also have the most interesting phenomenology which is dominated by trigger operators. This leads to common experimental predictions also for completely unrelated selection mechanisms for  $m_h$ . Trigger operators are discussed in Section 4.2. Note, however, that the presence of trigger operators in theories that select the Higgs mass in a non-statistical way is not a theorem. We begin this Chapter with the only exception that I know of: *N*naturalness. However triggers can be relevant to explaining  $m_h$  also beyond these ideas of cosmological selection. After all, they are just the answer to a very general question: what changes in the SM (and beyond) if we vary  $m_h^2$ ?

Finally, let me remark that in this Chapter, given the ultimate goal of this thesis, I will devote most space to my own published work.

## 4.1 Dynamical Selection in the Multiverse and Beyond

In this Section we describe two mechanisms that started the wave of renewed interest in cosmological explanations for the Higgs mass. They have almost nothing to do with each other, except for one common feature that distinguishes them from earlier and later attempts.

In both cases the landscape of Higgs masses is not in the form of a Multiverse. In the Relaxion [118] it is populated in time by a scalar with trilinear coupling  $\phi|H|^2$  that is rolling down its potential during inflation. In *N*naturalness [119] it is given by multiple copies of the SM that all exist in our Universe and in principle might be directly observed.

A second unique feature of *N*naturalness is that it completely escapes the logic of trigger operators outlined above, even if it selects the Higgs mass dynamically. The interaction selecting the Higgs mass is not protected by any symmetry. The vev, of the operators that describe it, is sensitive to the cutoff of the theory. However the selection is operated through their on-shell effects and not through their vevs. This is an important point that does not feature prominently in any description of *N*naturalness and to the best of my knowledge has not been utilized since.

### 4.1.1 *N*naturalness

In this Section we follow [119]. The first step is to introduce  $N$  sectors which are mutually non-interacting. The detailed particle content of these sectors is unimportant, with the exception that the Standard Model (SM) should not be atypical; many sectors should contain scalars, chiral fermions, unbroken gauge groups, etc. For simplicity, we imagine that they are exact copies of the SM, with the same gauge and Yukawa structure.

It is crucial that the Higgs mass parameters are allowed to take values distributed between  $-\Lambda_H^2$  and  $\Lambda_H^2$ , where  $\Lambda_H$  is the (common) scale that cuts off the quadratic divergences. Then for a wide range of distributions, the generic expectation is that some sectors are accidentally tuned at the  $1/N$  level,  $|m_H^2|_{\min} \sim \Lambda_H^2/N$ . We identify the sector with the smallest non-zero Higgs vacuum expectation value (vev),  $\langle h \rangle = v$ , as “our” SM. This picture is illustrated schematically in Fig. 4.1.

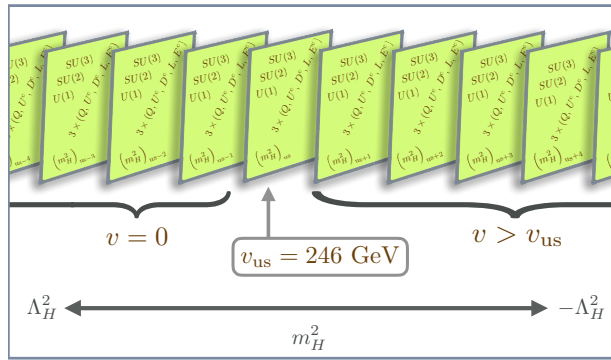


Figure 4.1: A sketch of the  $N$ naturalness setup. The sectors have been ordered so that they range from  $m_H^2 \sim \Lambda_H^2$  to  $-\Lambda_H^2$ . The sector with the smallest vacuum expectation value contains our copy of the SM.

In order for small values of  $m_H^2$  to be populated, the distribution of the mass parameters must pass through zero. For concreteness, we take a simple uniform distribution of mass squared parameters, indexed by an integer label  $i$  such that

$$(m_H^2)_i = -\frac{\Lambda_H^2}{N}(2i + r), \quad -\frac{N}{2} \leq i \leq \frac{N}{2}, \quad (4.1)$$

where  $i = 0 = \text{“us”}$  is the lightest sector with a non-zero vev:  $(m_H^2)_{\text{us}} = -r \times \Lambda_H^2/N \simeq -(88 \text{ GeV})^2$  is the Higgs mass parameter inferred from observations. The parameter  $r$  can be seen as a proxy for fine-tuning,<sup>1</sup> since it provides a way to explore how well the naive relation between the cutoff and the mass scale of our sector works in a detailed analysis. Specifically,  $r = 1$  corresponds to uniform spacing, while  $r < 1$  models to an accidentally larger splitting between our sector and the next one. A simple physical picture for this setup is that the new sectors are localized to branes which are displaced from one another in an extra dimension. In this scenario, the lack of direct coupling is clear, and the variation of the mass parameters can be explained geometrically: the  $m_H^2$  parameters may be controlled by the profile of a quasi-localized field shining into the bulk.

As a consequence of the existence of a large number of degrees of freedom, the hierarchy between  $\Lambda_H$  and the scale  $\Lambda_G$  where gravity becomes strongly coupled is reduced. The renormalization of the Newton constant implies  $\Lambda_G^2 \sim M_{\text{pl}}^2/N$ . If perturbative gauge coupling unification is to be preserved  $\Lambda_G \gtrsim M_{\text{GUT}}$ , implying that  $N \lesssim 10^4$ . This gives a cutoff no greater than  $\Lambda_H \sim 10 \text{ TeV}$ , thus predicting a little hierarchy that mirrors the GUT-Planck splitting in the UV. At the scale  $\Lambda_H$ , new dynamics (*e.g.*, SUSY) must appear to keep the Higgs from experiencing sensitivity to even higher scales. Alternatively, the full hierarchy problem can be solved with  $N \sim 10^{16}$ , so that  $\Lambda_H \sim \Lambda_G \sim 10^{10} \text{ GeV}$ . Note that this number of copies, while sufficient, is unnecessary for a complete solution. There may be two classes of new degrees of freedom: the  $N$  copies that participate directly in the  $N$ naturalness picture, and another completely sterile set of degrees of freedom that still impact the renormalization of  $\Lambda_G$ .

So far we have described a theory with a  $S_N$  permutation symmetry, broken softly by the  $m_H^2$  parameters, such that each of the sectors is SM-like. Sectors for which  $m_H^2 < 0$  are similar to our own, with the exception that particle masses scale with the Higgs vev,  $v_i \sim v \sqrt{i}$ . In addition, once  $i \gtrsim 10^8$  the quarks are all heavier than their respective QCD scales. Those sectors do not exhibit chiral symmetry breaking, nor do they contain baryons. Sectors with  $m_H^2 > 0$  are dramatically different from ours. In these sectors, electroweak symmetry is broken

<sup>1</sup>There are a variety of other ways one might choose to implement a measure of fine-tuning in this model. For example, one could assume the distribution of Higgs mass squared parameters is random with some (arbitrary) prior, and then ask statistical questions regarding how often the resulting theory is compatible with observations.

at low scales due to the QCD condensate  $\Lambda_{\text{QCD}}$ . Fermion masses are generated by the four-fermion interactions that are induced by integrating out the complete  $SU(2)$  Higgs multiplet. Thus,  $m_f \sim y_f y_t \Lambda_{\text{QCD}}^3 / (m_H^2)_i \lesssim 100$  eV, where  $y_t$  is the top Yukawa coupling. All fermionic and gauge degrees of freedom are extremely light relative to the ones in our sector.

With so many additional degrees of freedom, the naive cosmological history is dramatically excluded. In particular, if all sectors have comparable temperatures in the early Universe, then one expects  $\Delta N_{\text{eff}} \sim N$  (see Eq. (4.9)). Thus, the hierarchy problem gets transmuted into the question of how to predominantly reheat only those sectors with a tuned Higgs mass.

To accomplish this, we need to introduce a last ingredient into the story, the ‘‘reheaton’’ field, so named because it is responsible for reheating the Universe via its decays. We call this field  $S^c$  for models where the reheaton is a fermion, and  $\phi$  if the reheaton is a scalar. The cosmological history of the model begins in a post-inflationary phase where the energy density of the Universe is dominated by the reheaton. As stated multiple times we can not be unique, therefore we assume that the reheaton couples universally to all sectors. Note that the scalars must be near their true minimum when reheating occurs. This can be accomplished by having either low scale inflation, or else a coupling of the Higgses to the Ricci scalar.

In the next section, we present a set of models in which the reheaton dynamically selects and populates only the lightest sectors, despite preserving the aforementioned softly broken  $S_N$  symmetry.

## Models

We have argued that the hierarchy problem can be solved by invoking a large number of copies of the SM, along with some dynamical mechanism which dominantly populates the lightest sector with a non-zero Higgs vev. This section details some simple explicit models that realize a viable cosmological history.

As anticipated in the previous section, we imagine that at a post-inflationary stage the energy density of the Universe is dominated by a reheaton that couples universally to all the new sectors. Its decays populate the SM and its copies. The goal is to deposit as much energy as possible into the sector with the smallest Higgs vev. This may be accomplished by arranging the decays of the reheaton such that the branching fraction into the  $i^{\text{th}}$  sector scales as  $\text{BR}_i \sim (m_H)_i^{-\alpha}$  for some positive exponent  $\alpha$ . To this end, we construct models that share three features:

1. The reheaton is a gauge singlet;
2. It is parametrically lighter than the naturalness cutoff,  $m_{\text{reheaton}} \lesssim \Lambda_H / \sqrt{N}$ ;
3. Its couplings are the most relevant ones possible that involve the Higgs boson of each sector.

While the requirement of a light reheaton field may appear to require an additional coincidence, it can be easily accommodated in an extra-dimensional picture. In order to couple to all the sectors, the reheaton must be a bulk field. Then, before canonical normalization, its kinetic term carries a factor of  $N$ . If the reheaton enjoys a shift symmetry that is respected in the bulk, it will receive a  $\Lambda_H$ -sized mass from each brane on which the shift symmetry is violated. Here we assume that the dynamics above  $\Lambda_H$  respect the shift symmetry. As long as the shift symmetry is only violated on the boundaries, the reheaton mass will be parametrically the same as the weak scale after canonical normalization. In the case of a fermionic reheaton, this simple picture corresponds to the brane-localization of its Dirac partner.



The two simplest models, which we denote  $\ell$  and  $\phi$ , are

$$\mathcal{L}_\ell \supset -\lambda S^c \sum_i \ell_i H_i - m_S S S^c, \quad (4.2)$$

if the reheaton is a fermion  $S^c$ , and

$$\mathcal{L}_\phi \supset -a \phi \sum_i |H_i|^2 - \frac{1}{2} m_\phi^2 \phi^2, \quad (4.3)$$

if the reheaton is a scalar  $\phi$ . For the theory to be perturbative, we need the coupling  $\lambda$  to obey a 't Hooft-like scaling  $\lambda \sim 1/\sqrt{N}$ . Naively we would expect the same scaling for  $a$ , but we find that a stronger condition needs to be imposed ( $a \sim 1/N$ ) to insure that the loop induced mass for  $\phi$  is not much larger than  $\Lambda_H/\sqrt{N}$ . Even with this scaling, the loop-induced tadpole for  $\phi$  will be too large unless the sign of  $a$  is taken to be arbitrary for each sector. Note that  $a$  breaks a  $\mathbb{Z}_2$  symmetry on  $\phi$ , so that this choice is consistent with technical naturalness. Including the arbitrary sign, the sum over tadpole contributions only grows as  $\sqrt{N}$ , and so the natural range of  $\phi$  is restricted to  $\Lambda_H\sqrt{N}$ . The Higgses will then receive a contribution to their  $m_H^2$  parameters of order  $a\langle\phi\rangle \sim \Lambda_H^2/\sqrt{N}$ . While these contributions may be large compared to our weak scale, as long as they are smaller than  $\mathcal{O}(\Lambda_H^2)$ , they can be safely absorbed into the quadratically-divergent contributions to  $m_H^2$ . Of course, these are upper bounds on the couplings; as we will discuss later in the section, they can be consistently taken smaller, so long as the reheat temperature is sufficiently high.

Before moving on to discuss the details of reheating, we remark on the existence of cross-quartics of the form  $\kappa |H_i|^2 |H_j|^2$ . Even if these are absent in the UV theory, they will be induced radiatively. After electroweak symmetry breaking in the various sectors, these can potentially affect the spectrum, and so it is critical to the  $N$ -naturalness mechanism that they be sufficiently suppressed. Given an arbitrary,  $S_N$  symmetric cross-quartic,  $\kappa$ , the  $m_H^2$  parameters will shift by approximately  $-\kappa \Lambda_H^2 N/8 + \mathcal{O}(\kappa^2 N)$ , while the mixing effects are subdominant. Thus, the general picture of hierarchical weak scales remains intact so long as  $\kappa \lesssim 1/N$ .

At a minimum, cross-quartics of this form will be induced gravitationally, regardless of the reheaton dynamics. These quartically-divergent gravitational couplings arise at three loops, giving  $(16\pi^2)^3 \kappa_g \sim \lambda_h^2 (\Lambda_H/M_{\text{pl}})^4 \sim (\lambda_h/N)^2 (\Lambda_H/\Lambda_G)^4$ , where  $\lambda_H$  is the SM-like Higgs self quartic. Here we have taken the scale that cuts off these divergences to be  $\Lambda_H$ , as would be appropriate for a supersymmetric UV completion (for which these quartics are absent). In either case, these gravitational couplings are parametrically safe, since they scale as  $(1/N)^2$ .

In addition, potentially dangerous cross-quartics can be generated by reheaton exchange. In the  $\ell$  model, the cross-quartic is generated at one loop:  $\kappa_\ell \sim \lambda^4/16\pi^2 \lesssim 1/N^2$ , after enforcing the large- $N$  scaling of  $\lambda$ . In the  $\phi$  model, these quartics are generated at tree-level,  $\kappa_\phi \sim a^2/m_\phi^2$ . Naively this appears borderline problematic, since  $\kappa_\phi$  scales as  $1/N$ . However, the arbitrary sign of  $a$ , which was necessary to mitigate the tadpole of  $\phi$ , will once again soften the sum over sectors, so that  $\sum a_i v_i^2 \sim a \Lambda_H^2 \sqrt{N}$ . Combined with the large- $N$  scaling of  $a$ , these quartics are rendered safely negligible.

**Reheating** If the reheaton is sufficiently light, then we may analyze the leading reheaton decay operators using an effective Lagrangian computed by integrating out  $H_i$ . This immediately makes it clear why we want the reheaton to be coupled with the most relevant coupling possible, since these will suffer the fastest suppression as  $|m_H| \rightarrow \infty$ . Integrating out the Higgs and gauge bosons in the  $\ell$  model, the leading decays of  $S^c$  are given by, *e.g.*

$$\begin{aligned} \mathcal{L}_\ell^{(h)\neq 0} &\supset \mathcal{C}_1^\ell \lambda \frac{v}{m_Z^2 m_S} \nu^\dagger \bar{\sigma}^\mu S^c f^\dagger \bar{\sigma}_\mu f; \\ \mathcal{L}_\ell^{(h)=0} &\supset \mathcal{C}_2^\ell \lambda \frac{y_t}{m_H^2} S \ell Q_3^\dagger u_3^{c\dagger}, \end{aligned} \quad (4.4)$$

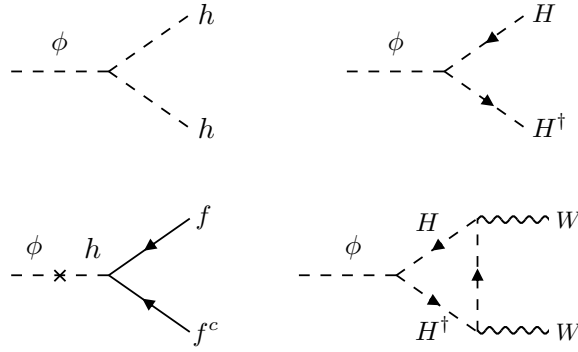


Figure 4.2: Feynman diagrams for the most important decays in the  $\phi$  model. The left (right) column is for  $\langle h \rangle \neq 0$  ( $\langle h \rangle = 0$ ). The top (bottom) row is for  $m_\phi \gg |m_H|$  ( $m_\phi \ll |m_H|$ ).

where  $m_Z$  is the relevant  $Z^0$ -boson mass and the  $\mathcal{C}_i^\ell$  are numerical coefficients. We have omitted decays through  $W$  and Higgs bosons in sectors with  $\langle h \rangle \neq 0$  as they scale in the same way. We include them in all numerical computations.

From this low energy Lagrangian we can easily infer that a light reheaton dominantly populates the lightest negative Higgs mass sector. Denoting with  $m_{h_i}$  the physical Higgs mass in sectors with  $\langle h \rangle \neq 0$ , the reheaton decay widths scale as  $\Gamma_{m_H^2 < 0} \sim 1/m_{h_i}^2$  and  $\Gamma_{m_H^2 > 0} \sim 1/m_{H_i}^4$  in sectors with and without electroweak symmetry breaking, respectively. Thus the reheaton preferentially decays into sectors with light Higgs bosons and non-zero vevs. If, instead, the reheaton were heavy enough to decay directly to on-shell Higgs or gauge bosons, the branching fractions would be democratic into those sectors, and the energy density in our sector would not come to dominate the energy budget of the Universe.

In the scalar case the decays are different, but the scaling of the decay widths is exactly the same. This can be seen once more by integrating out the Higgs and gauge bosons in all the sectors:

$$\begin{aligned} \mathcal{L}_\phi^{(h) \neq 0} &\supset \mathcal{C}_1^\phi a y_q \frac{v}{m_h^2} \phi q q^c ; \\ \mathcal{L}_\phi^{(h) = 0} &\supset \mathcal{C}_3^\phi a \frac{g^2}{16 \pi^2} \frac{1}{m_H^2} \phi W_{\mu\nu} W^{\mu\nu} , \end{aligned} \quad (4.5)$$

where again the  $\mathcal{C}_i^\phi$  are numerical coefficients, and  $W_{\mu\nu}$  is the  $SU(2)$  field strength. As in the fermionic case, this Lagrangian leads to decay widths that scale as  $\Gamma_{m_H^2 < 0} \sim 1/m_{h_i}^2$  and  $\Gamma_{m_H^2 > 0} \sim 1/m_{H_i}^4$  in sectors with and without electroweak symmetry breaking, respectively, through the diagrams shown in Fig. 4.2. We have not included the one-loop decay  $\phi \rightarrow \gamma\gamma$  in Eq. (4.5) for sectors with  $\langle h \rangle \neq 0$ . This operator scales as  $1/m_h^2$  and is important for sectors with  $N \gtrsim 10^8$ ; we find that this is never the leading decay once the bounds on  $N$  discussed in Sec. 4.1.1 are taken into account.

Before moving to a more detailed discussion of signals and constraints it is worth pointing out two important differences between the  $\phi$  and  $\ell$  models that will lead us to modify the latter. Given the scaling of the widths we can approximately neglect the contributions to cosmological observables from the  $\langle h \rangle = 0$  sectors. In the simple case that the vevs squared are equally spaced,  $v_i^2 \sim 2i \times v_{\text{us}}^2$ , as in Eq. (4.1) with  $r = 1$ , we find that the branching ratio into the other sectors is  $\sum 1/i \sim \log N$ .

In the  $\phi$  model, this logarithmic sensitivity to  $N$  is not realized. Since the reheaton decays into sectors with non-zero vevs via mixing with the Higgs, the decays become suppressed by smaller and smaller Yukawa couplings as  $h_i$  becomes heavy. After the charm threshold is crossed  $m_\phi < 2m_{c_i}$  we can neglect the contribution of the new sectors to cosmological observables (with one exception that we discuss in the next section). This behavior is displayed in the left panel of Fig. 4.3, where we show the fraction of energy density deposited in each sector.

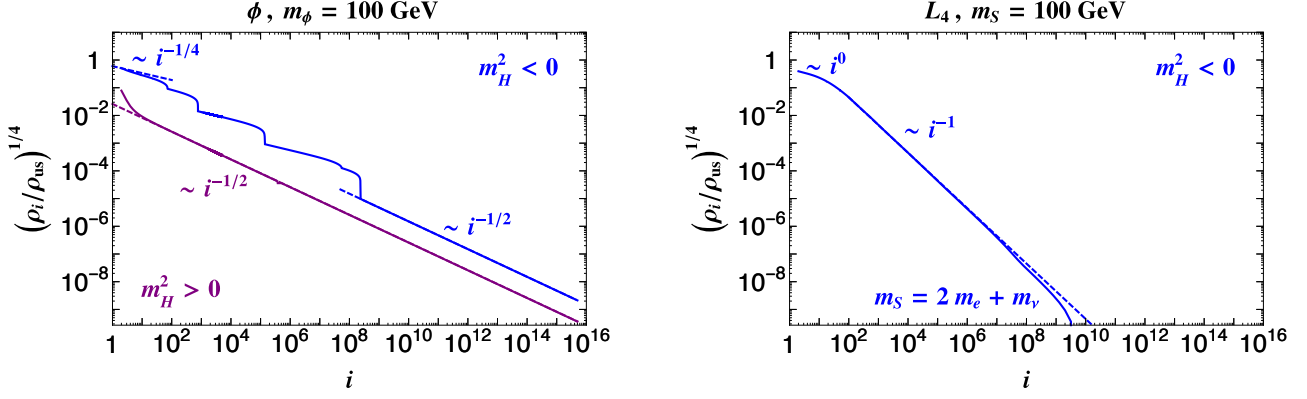


Figure 4.3: Energy density deposited in each sector as a function of sector number, normalized to the energy density in our sector. The left panel is for the  $\phi$  model with  $a = 1$  MeV. The right panel is for the  $L_4$  model with  $\lambda \times \mu_E = 1$  MeV,  $M_L = 400$  GeV,  $M_{E,N} = 500$  GeV,  $Y_E = Y_N = 0.2$ , and  $Y_E^c = Y_N^c = -0.5$ . The solid lines are the result of a full numerical calculation. The dashed lines show the expected scalings. As discussed in the text, the steps in the  $\phi$  model are proportional to Yukawa couplings due to the fact that  $\phi$  decays via mixing with the Higgs. When  $i \gtrsim 10^9$  in the  $L_4$  model, the process  $S^c \rightarrow 2e + \nu$  cannot proceed on-shell, which results in the deviation from the naive scaling as denoted by  $m_S = 2m_e + m_\nu$ . Both figures were made using the zero temperature branching ratios of the reheaton; thermal corrections are under control so long as  $T_{\text{RH}}$  is smaller than the weak scale in our sector, as discussed at the end of Sec. 4.1.1.

The second important difference is that in the  $\ell$  model the reheaton couples directly to neutrinos and, in the sectors with electroweak symmetry breaking, it mixes with them. This leads to two effects. First, the physical reheaton mass grows with  $N$ , implying that the structure of the  $\ell$  model forces the reheaton to be heavy at large  $N$ , and can be inconsistent depending on the value of  $\lambda$ . Additionally, this mixing can generate a freeze-in abundance [120] of neutrinos in the other sectors from the process  $\nu_{\text{us}} \nu_{\text{us}} \rightarrow \nu_{\text{us}} \nu_i$  via an off-shell  $Z^0$ . Tension with neutrino overclosure and overproduction of hot dark matter leads to an upper bound on the maximum number of sectors. In practice, it is hard to go beyond  $N \simeq 10^3$ .

However, there is a simple extension of the  $\ell$  model that at once mitigates its UV, *i.e.*, large  $N$ , sensitivity and solves the problems arising from a direct coupling to neutrinos. If the reheaton couples to each sector only through a massive portal (whose mass grows with  $v_i$ ), then the branching ratios will scale with a higher power of the Higgs vev after integrating out the portal states. As an example, consider introducing a 4<sup>th</sup> generation of vector-like leptons  $(L_4, L_4^c)$ ,  $(E_4, E_4^c)$ , and  $(N_4, N_4^c)$  to each sector. Then relying on softly broken  $U(1)$  symmetries, we can couple the reheaton to  $L_4$  only via the Lagrangian

$$\begin{aligned}
\mathcal{L}_{L_4} &\supset \mathcal{L}_{\text{mix}} + \mathcal{L}_Y + \mathcal{L}_M, \\
\mathcal{L}_{\text{mix}} &= -\lambda S^c \sum_i (L_4 H)_i - \mu_E \sum_i (e^c E_4)_i, \\
\mathcal{L}_Y &= -\sum_i \left[ Y_E (H^\dagger L_4 E_4^c)_i + Y_E^c (H L_4^c E_4)_i \right. \\
&\quad \left. + Y_N (H L_4 N_4^c)_i + Y_N^c (H^\dagger L_4^c N_4)_i \right], \\
\mathcal{L}_M &= -\sum_i \left[ M_E (E_4^c E_4)_i + M_L (L_4^c L_4)_i \right],
\end{aligned} \tag{4.6}$$

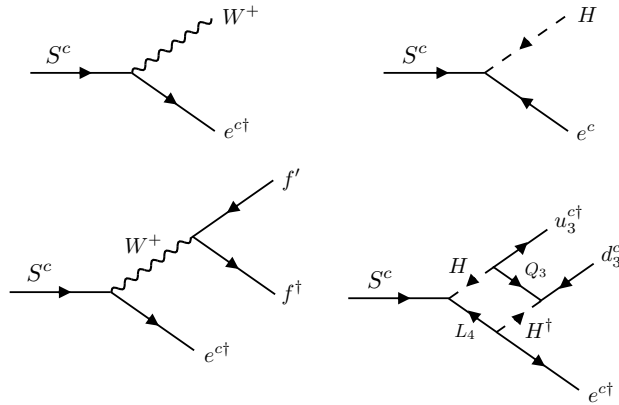


Figure 4.4: Feynman diagrams for the most important decays in the  $L_4$  model. The left (right) column is for  $\langle h \rangle \neq 0$  ( $\langle h \rangle = 0$ ). The top (bottom) row is for  $m_S \gg |m_H|$  ( $m_S \ll |m_H|$ ).

$$+ M_N (N_4^c N_4)_i \Big] - m_S S S^c ,$$

where we have assumed universal masses and couplings across all the sectors for simplicity. We again need  $\lambda \sim 1/\sqrt{N}$  for perturbativity. Note that we are assuming that the bilinear  $\mu_E e^c E$  only couples a single flavor of right handed lepton to the new 4<sup>th</sup> generation fields, in order to avoid flavor violation bounds in the charged lepton sector. The predictions relevant to cosmology (see Fig. 4.5) are insensitive to the choice of flavor; we choose couplings involving the  $\tau$  for the additional constraints discussed in Sec. 4.1.1 below since this choice yields the strongest bounds.

To explore the differences between the  $L_4$  and  $\ell$  models let us again consider the limit in which the reheaton is light. If we integrate out the Higgs and gauge bosons along with the new vector-like leptons, the leading operators for the decays of  $S^c$  are given by

$$\begin{aligned} \mathcal{L}_{L_4}^{\langle h \rangle \neq 0} &\supset \mathcal{C}_1^{L_4} \lambda' \frac{g^2}{m_W^2} \left( e^{c\dagger} \bar{\sigma}^\mu S^c \right) \left( f^\dagger \bar{\sigma}_\mu f' \right); \\ \mathcal{L}_{L_4}^{\langle h \rangle = 0} &\supset \mathcal{C}_2^{L_4} \lambda \frac{y_t y_b Y_E M_E \mu_E}{16 \pi^2 m_H^4} \left( e^{c\dagger} \bar{\sigma}^\mu S^c \right) \left( u_3^{c\dagger} \bar{\sigma}_\mu d_3^c \right), \end{aligned} \quad (4.7)$$

where once more the  $\mathcal{C}_i^{L_4}$  are numerical coefficients,  $M_4$  is used to represent the physical mass of the relevant heavy lepton, and for convenience we have defined  $\lambda'_i \equiv (\lambda v_i^2 \mu_E / M_{4i}^4) f(Y, M)$ . Here  $f$  is a function of dimension one that depends on the Yukawa couplings and vector-like masses in Eq. (4.7), but not on the Higgs vev. The  $M_{4i}$  masses receive a contribution from  $v_i$  that eventually dominates. When this happens  $S^c$  decays become suppressed by large powers of the Higgs vev. From the effective Lagrangian above, it is easy to conclude that the widths scale as  $\Gamma_{m_H^2 < 0} \sim \text{const}$  for the first few sectors, since  $M_{4i}$  is approximately independent of  $v_i$ . When the Yukawa contribution to the masses begins to dominate, such that  $M_{4i} \sim v_i$ , the scaling becomes  $\Gamma_{m_H^2 < 0} \sim 1/v_i^8$ . Contributions to observables from the sectors with positive Higgs mass squared are negligible: the decay is both three-body and loop-suppressed, and the width scales as  $1/v_i^8$  in all the sectors.

The diagrams that lead to these decays are shown in Fig. 4.4, and the energy density deposited in each sector is depicted in the right panel of Fig. 4.3. It is obvious that in this model cosmological observables are sensitive only to the few sectors for which the vector-like masses dominate over the Higgs vev, making it insensitive to the UV. This comes at the price of introducing new degrees of freedom near the weak scale. As we will discuss in the following section, the vector-like masses cannot be arbitrarily decoupled, but they must be large enough to avoid tension with direct searches and the measured properties of our Higgs.

Finally, we end this section by briefly commenting on the presence of an upper bound for the reheating temperature  $T_{\text{RH}}$  such that the mechanism is preserved. Specifically,  $T_{\text{RH}}$  should

be at most of order of the weak scale. If the temperature were larger, our Higgs mass would be dominated by thermal corrections resulting in a change in the scalings of the branching ratios. Our Higgs would obtain a large positive thermal mass and no longer be preferentially reheated over the other sectors. Noting that

$$T_{\text{RH}} \simeq 100 \text{ GeV} \sqrt{\frac{\langle h \rangle \Gamma_{\text{reheaton}T}}{10^{-14} \text{ GeV}}}, \quad (4.8)$$

where  $\langle h \rangle \Gamma_{\text{reheaton}T}$  denotes a thermal average of the reheaton width that incorporates the effect of time dilation. Then Eq. (4.8) places an upper bound on the couplings of the reheaton. In the  $\phi$  model, the  $\phi - h$  mixing angle is bounded to be  $\theta_{\phi h} \sim (a v / m_h^2)_{\text{us}} \lesssim 10^{-6} (100 \text{ GeV} / m_\phi)^{1/2}$ . In the  $L_4$  model, most of the viable region of parameter space predicts on-shell decays to our  $W$  boson (see Fig. 4.5 below). Therefore, the width of  $S^c$  is dominated by this two-body decay and the constraint on  $T_{\text{RH}}$  translates into a rough bound of  $\lambda'_{\text{us}} \lesssim 10^{-7}$  when  $m_S \simeq 100 \text{ GeV}$ . For the benchmark values used for the figures below, this in turn translates into a bound  $\lambda \times \mu_E \lesssim 10^{-2} \text{ GeV}$ .

Finally, we note that at large  $N$  there is a more stringent upper bound on the reheating temperature determined by the perturbativity of  $\lambda$ . Requiring  $\lambda \lesssim 4\pi/\sqrt{N}$  and  $m_S \sim 100 \text{ GeV}$ , we find that it is still possible to reheat to a few GeV even with  $N \sim 10^{16}$ , where this estimate has been done using the complete numerical implementation of the mixings.

In principle, we must also ensure that other sectors are not overly heated by scattering from our own plasma after reheating. However, the aforementioned constraints on the reheaton couplings sufficiently suppress this contribution to their energy density.

**Baryogenesis** A viable mechanism for baryogenesis is an even more crucial part of our mechanism for solving the hierarchy problem than in typical natural theories for new physics, where it can be treated in a modular way. One challenge is that our reheating temperature should be near or below the electroweak phase transition. Additionally, baryogenesis cannot occur in all of the copies of the SM, or there would be too much matter in the Universe.

One simple approach, which makes use of features intrinsic to the model, is to imagine that the reheaton  $S^c$  carries a lepton number asymmetry. This asymmetry is distributed to the various sectors through the decays of  $S^c$ . Only in the sectors nearest ours is this lepton asymmetry converted into a baryon asymmetry. The small number abundance of baryons results from the low reheat temperature. At temperatures just below the electroweak phase transition, the sphaleron rate is exponentially suppressed, and only a small fraction of the lepton asymmetry is converted into a baryon asymmetry. The baryon asymmetry in sectors with  $m_H^2 > 0$  is even further suppressed; since  $m_W \lesssim \Lambda_{\text{QCD}}$ , the sphalerons remain active at temperatures below the baryon masses. Any asymmetry in these sectors will eventually be redistributed back into the leptons. We have now laid out the necessary ingredients of our mechanism and we are ready to explore their phenomenology in more detail.

## Signals and Constraints

The signals and experimental constraints for  $N$ naturalness come from two sources: mixing between the sectors and energy density deposited in the new sectors by the reheaton decays. The cosmological observables sensitive to the energy density in each sector can be further divided into two categories.

First we discuss measurements that can detect new light particles. These signatures are dominated by the sectors closest to us and can not be avoided by changing the UV scalings of the model. They provide the most characteristic signatures of the theory. Then we study the impact of stable massive particles from the new sectors. This last set of constraints is

dominated by sectors with the largest Higgs masses and can be ignored in the  $L_4$  model, where the large  $i$  physics is decoupled. In the last two subsections we discuss the bounds arising from mixing between the sectors, followed by possible collider signatures.

**Massless degrees of freedom** As discussed previously, our models have a large number of massless or nearly massless degrees of freedom. For example, all additional sectors contain photons and neutrinos. There are several kinds of cosmological observations that are sensitive to new relativistic particles. For instance the measurement of the Hubble parameter during either Big Bang Nucleosynthesis or at the epoch of photon decoupling, and bounds on hot dark matter from the matter power spectrum.

The sensitivity of the expansion of the Universe to new relativistic degrees of freedom is usually phrased in terms of the number of effective neutrinos

$$\Delta N_{\text{eff}} = \frac{1}{\rho_{\nu}^{\text{us}}} \sum_{i \neq \text{us}} \rho_i. \quad (4.9)$$

Current bounds are  $\Delta N_{\text{eff}} \lesssim 1$  during BBN [121] and  $\Delta N_{\text{eff}} \lesssim 0.6$  at photon decoupling [122]. In both cases we quote an approximate 95% C.L. constraint. The CMB bound applies to free-streaming radiation [123]. However, the photons in some of the new sectors are still in equilibrium with or have just decoupled from electrons at that time and might be more similar to a perfect fluid. Until recently it was impossible to distinguish between the two types of radiation, as they affect the CMB damping tail in the same way [124]. The detection of a phase shift in the CMB anisotropies [125] has broken this degeneracy, and it is now possible to set a 95% C.L. bound:  $N_{\text{fluid}} \lesssim 1$  for  $\Delta N_{\text{eff}} = 0$  [126]. Here we have defined  $N_{\text{fluid}}$  in the same way as  $\Delta N_{\text{eff}}$ , normalizing the energy density of non-free-streaming radiation to that of a neutrino in our sector.

In the following, we do not distinguish between the two types of radiation. We use  $\Delta N_{\text{eff}}$  to denote the sum of the two components. Given the bounds discussed above and the two dimensional exclusions in [126], this is sufficient to show that the model has large areas of parameter space consistent with current data. In the future, it would be interesting to explore CMB observations in more detail, as it is a generic prediction of this type of theories to have roughly comparable amounts of free-streaming and non-free-streaming extra radiation.

Having set  $N_{\text{fluid}}$  to zero, it is straightforward to estimate the contribution to  $\Delta N_{\text{eff}}$  from our new sectors, since the ratio of energy densities  $\rho_i/\rho_{\text{us}}$  is determined by the decay widths of the reheaton:  $\rho_i/\rho_{\text{us}} \simeq \Gamma_i/\Gamma_{\text{us}}$ . For example, assume that the reheaton is lighter than the lightest Higgs across all the sectors; then we have

$$\begin{aligned} \Delta N_{\text{eff}}^{\phi} &\sim \sum_{i=1}^{N_b} \frac{1}{2i+1} + \frac{y_c^2}{y_b^2} \sum_{i=N_b+1}^{N_c} \frac{1}{2i+1} \simeq \frac{1}{2} \left( \log 2N_b + \frac{y_c^2}{y_b^2} \log \frac{N_c}{N_b} \right), \quad N_{b,c} = \left( \frac{m_{\phi}^2}{8m_{b,c}^2} - \frac{1}{2} \right), \\ \Delta N_{\text{eff}}^{L_4} &\sim \sum_{i=1}^{N_V} i^0 + \sum_{i=N_V+1}^{N/2} \frac{1}{(2i+1)^4} \simeq N_V, \quad N_V \simeq \left( \frac{M^2}{Y^2 v^2} - \frac{1}{2} \right), \end{aligned} \quad (4.10)$$

where  $M$  represents one of the vector-like masses in the  $L_4$  model and  $Y$  one of the new Yukawas. In this estimate we have neglected the contribution from  $m_H^2 > 0$  sectors and the effect of  $g_*$  in each sector, to highlight the scaling of  $\Delta N_{\text{eff}}$ . From this simple exercise we see that  $\Delta N_{\text{eff}}$  is dominated by the bottom of the spectrum. The sectors past  $i = N_{b,c}$  or  $i = N_V$  receive a negligible fraction of the total energy density and do not contribute to  $\Delta N_{\text{eff}}$ . Using Eq. (4.10) to go beyond a simple parametric estimate gives results that are in tension with current bounds. For example  $m_{\phi} \simeq 50$  GeV implies  $N_b \simeq 17$  and  $\Delta N_{\text{eff}} \simeq 2$ . However, these

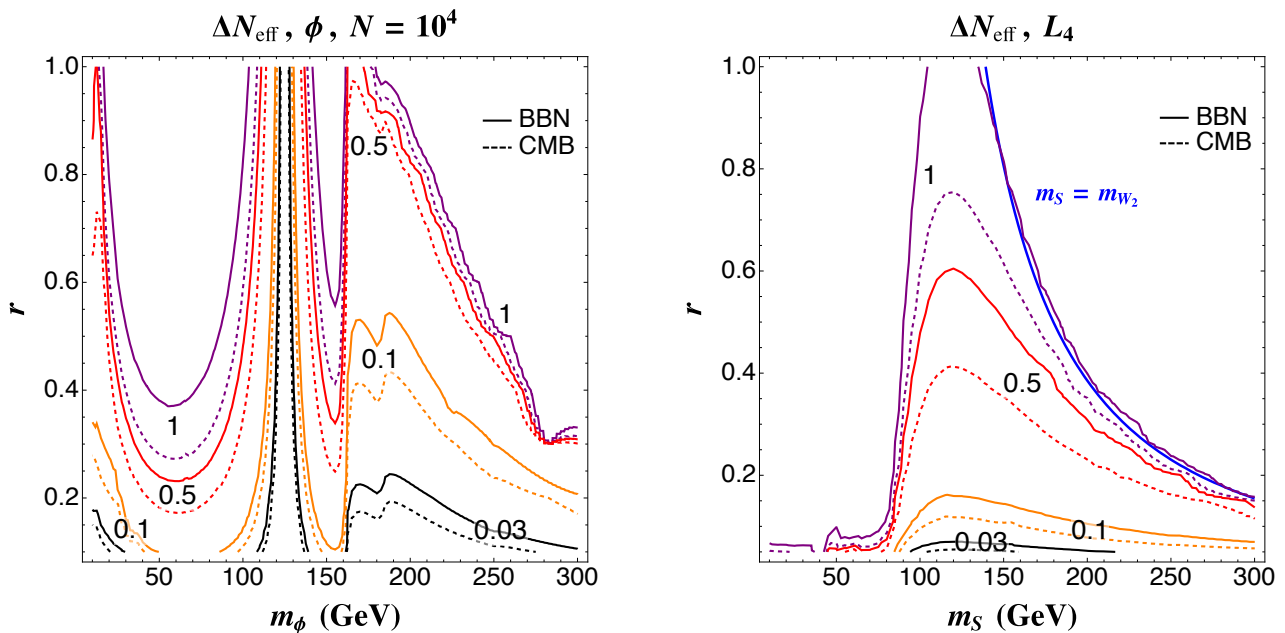


Figure 4.5:  $\Delta N_{\text{eff}}$  contours as a function of reheaton mass and the  $r$  parameter defined in Eq. (4.1).  $\Delta N_{\text{eff}} \simeq 0.03$  corresponds to the sensitivity of CMB stage 4 experiments. The current upper bound at the CMB epoch is around 0.6. The left panel is for the  $\phi$  model with  $a = 1$  MeV. The right panel is for the  $L_4$  model with  $\lambda \times \mu_E = 1$  MeV,  $M_L = 400$  GeV,  $M_{E,N} = 500$  GeV,  $Y_E = Y_N = 0.2$ , and  $Y_E^c = Y_N^c = -0.5$ . As discussed in the text, the  $L_4$  result is valid for a large range of  $N$ , namely  $30 \lesssim N \lesssim 10^9$ . Both figures were made using the zero temperature branching ratios of the reheaton; see the end of Sec. 4.1.1 for a discussion.

estimates are only qualitative, and break down in a large fraction of the parameter space of the models. The results from a full numerical computation are shown in Fig. 4.5.

There are two main messages that can be extracted from this calculation. First, we can satisfy current constraints for a range of reheaton masses up to a few hundred GeV. Second, the models predict values of  $\Delta N_{\text{eff}}$  within the range of sensitivity relevant for CMB stage 4 experiments [127]. These next generation detectors, which should start taking data within the next five years, will probe  $\Delta N_{\text{eff}} \gtrsim 0.03$ . If no beyond the SM discovery is made, then the only way to suppress this signal is to introduce “fine tuning,” which in the context of these models is the limit  $r \lesssim 0.1$ . Alternatively, we could imagine alleviating this tension by taking the vector-like masses in the  $L_4$  model far below the weak scale, in potential conflict with electroweak/Higgs measurements.

A few additional features of the  $\Delta N_{\text{eff}}$  calculation are worth discussing. In the  $L_4$  case the plot is valid for a large range of  $N$ , namely  $30 \lesssim N \lesssim 10^9$ . The upper bound is determined by requiring  $\lambda \lesssim 4\pi/\sqrt{N}$  and mixing between  $e^c$  and the vector-like leptons less than 1%. It is trivial to go beyond  $N = 10^9$ , and even possible to reach  $N = 10^{16}$ , by lowering the reheaton coupling – this comes at the expense of an overall decrease in reheating temperature, even though the result for  $\Delta N_{\text{eff}}$  would not change. For  $N < 30$ ,  $\Delta N_{\text{eff}}$  is smaller than shown in the figure. In the  $\phi$  case, the results are more sensitive to  $N$ , as shown in Eq. (4.10). We chose the largest  $N$  that is both compatible with overclosure (see the next subsection) and also interesting from a model building perspective, given the relation to the Planck/GUT hierarchy ( $N = 10^4$ ).

The shapes of the  $\Delta N_{\text{eff}}$  contours are easy to explain in terms of kinematics. In  $L_4$  the allowed region corresponds to the reheaton decaying to our sector via a two-body channel, versus a three-body decay into all the other  $m_H^2 < 0$  sectors. This is highlighted by the

$m_S = m_{W_2}$  line in the plot. In the  $\phi$  model the situation is different. The mixing with the Higgs naturally introduces a number of mass thresholds that reduce  $\Delta N_{\text{eff}}$ . At very low  $\phi$  masses, decays to a pair of  $b$ -quarks are kinematically allowed only in our sector. As the  $\phi$  mass increases, the reheaton can mix resonantly with our Higgs and subsequently decay to a pair of  $W$  or  $Z$  bosons. The last aspect of these results that is not captured by the simple estimate in Eq. (4.10) is the fact that  $(\Delta N_{\text{eff}})_{\text{CMB}} > (\Delta N_{\text{eff}})_{\text{BBN}}$ . It is easy to show that this must be the case by appealing to conservation of entropy in each of the sectors. If we compute the ratio of  $\Delta N_{\text{eff}}$  in sector  $i$  at the two different epochs, we obtain

$$\begin{aligned} \frac{(\Delta N_{\text{eff}}^i)_{\text{CMB}}}{(\Delta N_{\text{eff}}^i)_{\text{BBN}}} &= \frac{g_*^i(T_{\text{CMB}}^i)}{g_*^i(T_{\text{BBN}}^i)} \left( \frac{g_{*S}^{\text{us}}(T_{\text{BBN}}^{\text{us}})}{g_{*S}^{\text{us}}(T_{\text{CMB}}^{\text{us}})} \right)^{4/3} \left( \frac{g_{*S}^i(T_{\text{BBN}}^i)}{g_{*S}^i(T_{\text{CMB}}^i)} \frac{g_{*S}^{\text{us}}(T_{\text{CMB}}^{\text{us}})}{g_{*S}^{\text{us}}(T_{\text{BBN}}^{\text{us}})} \right)^{4/3} \\ &\simeq \left( \frac{g_{*S}^i(T_{\text{BBN}}^i)}{g_{*S}^i(T_{\text{CMB}}^i)} \right)^{1/3} \geq 1. \end{aligned} \quad (4.11)$$

The first term in the first equality counts the number of relativistic degrees of freedom in sector  $i$  at the two different temperatures. The second factor accounts for the fact that neutrinos in our sector are decoupled after BBN, so their temperature during the CMB epoch is lower than that of photons. The last term comes from entropy conservation in our sector and sector  $i$ . In the last equality we have used  $g_* \simeq g_{*S}$ .

To conclude the discussion of  $\Delta N_{\text{eff}}$ , recall that the result depends almost exclusively on the reheaton branching ratios and that it is largely insensitive to the value of its overall coupling. A single choice of  $\lambda$  and  $a$  is sufficient to understand the complete parameter space. In contrast, the precise value of the vector masses and Yukawa couplings in the  $L_4$  model can change the results considerably, as it is already clear from Eq. (4.10). When the vector-like masses are around the TeV scale or above, the models are excluded, while  $M \simeq 500$  GeV yields predictions that are consistent with current data, as shown in Fig. 4.5. We leave a more detailed exploration of the parameter space and a discussion of possible collider signatures to future work.

The second class of light particles that can impact our cosmological history are those that are non-relativistic at matter radiation equality, but might have free-streamed enough to suppress the matter power spectrum. Particles that become non-relativistic at a time  $t_{\text{NR}} < t_{\text{EQ}}$  suppress structure up to scales  $\lambda_{\text{FS}} = c \sqrt{t_{\text{EQ}} t_{\text{NR}}} (2 + \log t_{\text{EQ}}/t_{\text{NR}})/a(t_{\text{EQ}})$ . The neutrinos from many of the new sectors would have  $\lambda_{\text{FS}}$  larger than one Mpc. At these scales the matter power spectrum can be computed reliably in the linear regime and can be used to infer another upper bound on their energy density. To roughly estimate current constraints we compute the energy density in particles that can suppress structure at one Mpc or above. We find that for Dirac neutrinos the energy density is well below 1% of the total dark matter energy density in all the plane of Fig. 4.5 for both the  $\phi$  and  $L_4$  models, while for Majorana neutrinos this is true within the  $(\Delta N_{\text{eff}})_{\text{CMB}} = 0.5$  contours.

The hot dark matter population may provide another signal. The tower of sterile neutrinos results in a characteristic impact on the matter power spectrum. Furthermore, the hot dark matter signal is primarily determined by the reheaton branching ratios (and hence the spacing between the lightest sectors), so once a value of  $\Delta N_{\text{eff}} \neq 0$  is measured it is possible to make predictions for the distortion of the matter power spectrum and vice versa. In general our theories produce non-trivially related modifications in several CMB observables and we leave to future work a more detailed study. Our generic expectation is that neutrino cosmology is modified at the  $\mathcal{O}(1)$  level due to slightly heavier albeit less abundant neutrinos in the closest sectors with electroweak symmetry breaking.

**Massive stable particles** Relic neutrinos account for a fraction  $\Omega_\nu^{\text{us}} h^2 \simeq \sum m_\nu(\text{eV})/91.5 \gtrsim 10^{-3}$  of the energy density in the Universe. It is natural to ask if the heavier neutrinos in the



sectors with  $\langle h \rangle \neq 0$  can lead to overclosure problems. Furthermore, electrons and protons can be similarly problematic. This is perhaps surprising, since in the standard picture their symmetric component is completely negligible today. However, in the other sectors their masses are  $\sqrt{i}$  larger and subsequently their annihilation cross-sections decrease as  $1/i$ .<sup>2</sup>

In all cases, the relic density of the new stable particles comes from two different sources. There is a contribution that grows with  $i$  from the sectors where the stable particles reach thermal equilibrium (including a possible freeze-in abundance from our sector) and a second contribution that decreases with  $i$  from sectors where the particles never thermalize. Let us focus on this first contribution (for the moment we will neglect the freeze-in abundance from our sector):

$$\Omega h^2 = \frac{s_0}{\rho_c^0} \sum_{i=-1}^{-N_d} m_i Y_i^{\text{fo}} + \dots = a (N_d)^p + \dots \quad (4.12)$$

Here we use  $\Omega h^2$  to indicate the relic density of either neutrinos, electrons or protons;  $\rho_c^0$  is the critical energy density today;  $s_0$  is the entropy density;  $m_i$  is the mass of the stable particle;  $Y_i^{\text{fo}}$  is its yield at freeze-out;  $N_d$  is the sector after which the stable particles are not ever in thermal equilibrium with the other particles in their sector; and  $a$  and  $p$  are positive numbers. In general  $a \sim \Omega^{\text{us}} h^2$  and  $p > 1$ . The reason for  $p > 1$  is that  $m_i \sim \sqrt{i}$  (or  $\sim i$  for Majorana neutrinos) and up to a certain sector number  $Y_i^{\text{fo}}$  also grows with  $i$ , since neutrinos, electrons and protons all freeze-out earlier and earlier.

In the  $\phi$  model this thermal abundance turns out to be the only relevant one. Specifically, electrons and positrons provide the dominant constraint. Once the bound on the reheating temperature is taken into account, the freeze-in abundance from our sector is negligible. Furthermore the overclosure bound on  $N$  kicks in before including heavy enough sectors where electrons would not thermalize. Therefore the bound arises only from thermal freeze-out ( $n_e^i \sim 1/\langle \sigma_e v \rangle_i$ ) and it is straightforward to estimate:

$$\begin{aligned} \Omega_e^\phi h^2 &= \sum_{i=1}^{N_{\text{th}}} \frac{m_e^i n_e^i}{\rho_c^0} \simeq \frac{(m_e^{\text{us}} T_0^{\text{us}})^3}{\rho_c^0} \frac{N_{\text{th}}^{5/2}}{M_{\text{pl}} v_{\text{us}} \alpha^2} \\ &\lesssim 0.1 \times \Omega_{\text{DM}} h^2 \implies N_\phi \lesssim 10^5, \end{aligned} \quad (4.13)$$

where the sum runs up to the heaviest sector where the electrons have thermalized as denoted by  $N_{\text{th}}$ ,  $T_0^{\text{us}}$  is the photon temperature in our sector today,  $m_e^{\text{us}}$  is our electron mass,  $M_{\text{pl}}$  is the Planck mass, and all other quantities were defined previously. For this estimate we have assumed that our sector dominates the energy density of the Universe when electron-positron annihilations freeze-out, *i.e.*, the  $\Delta N_{\text{eff}}$  constraint is satisfied. Furthermore we have conservatively assumed freeze-out happens just after reheating (at  $T_{\text{RH}}^{\text{us}} \simeq v_{\text{us}}$ ) in all the sectors. Finally, note that we have required that electrons and positrons make up only 10% of dark matter, the rough bound for particles that behave very differently from cold, collisionless dark matter. To be more conservative we could require them to make up only 1% of dark matter, which would reduce the maximum allowed value of  $N_\phi$  by 60%, still leaving open  $N_\phi = 10^4$ .

To conclude this section we note that the rapid scaling of the energy density with sector number in  $L_4$  protects the model from overclosure. This implies that  $N$  can be taken all the way to  $10^{16}$  and still be consistent with data, at the expense of a low reheat temperature.

**Mixing Between Sectors** Upon integrating out the reheaton, the low energy theory will contain cross-couplings between the sectors. Stringent bounds from stellar and supernova cooling place limits on the size of these mixings.

---

<sup>2</sup>For protons, this scaling is only valid once the quark masses exceed  $\Lambda_{\text{QCD}}$ ; the scaling is slower for the nearer sectors.

- $\epsilon_i \mathbf{F}_{\mu\nu} \mathbf{F}_i^{\mu\nu}$

In the presence of kinetic mixing, the electrically charged particles of other sectors will have milli-charge couplings to our photon. The most stringent bound on this coupling is derived from energy loss in stars [128, 129]. In sectors with  $m_H^2 > 0$ , the charged particles are all extremely light – much lighter than stellar temperatures – so that democratic kinetic mixing leads to  $\mathcal{O}(N)$  accessible final states for plasmon decay. Thus we require  $\sqrt{\sum_i \epsilon_i^2} \lesssim 10^{-14}$ , in which  $\epsilon_i$  is the coefficient of kinetic mixing between our photon and that of sector  $i$ , and  $i$  runs over all sectors with  $m_H^2 > 0$ .

Accordingly, there must be no bi-fundamental matter in the UV, the inclusion of which would generate kinetic mixing at one loop. Even in the absence of those states, kinetic mixing may be generated in the IR through the coupling to the reheaton.<sup>3</sup> In this case the bounds may be easily avoided by the smallness of the coupling. As described in Sec. II, the portal couplings must decrease with increasing  $N$  in order to have a consistent large- $N$  limit.

For example, in the  $L_4$  model, we must have  $\lambda \sim \lambda_0/\sqrt{N}$ . The kinetic mixing parameter is generated only at three loops with four powers of the portal coupling:

$$\epsilon_i \sim \frac{\alpha}{4\pi} \left( \frac{\lambda_0}{4\pi} \right)^4 \frac{1}{N^2 i}. \quad (4.14)$$

Note that  $\epsilon_i$  decreases with  $i$  due to the scaling of  $(m_H^2)_i$ , and so kinetic mixing is dominated by the sectors nearest to our own. Then the stellar bounds may be avoided as long as  $\lambda_0/4\pi \lesssim 10^{-3}\sqrt{N}$ , and no suppression is required for  $N \gtrsim 10^6$  beyond the natural large- $N$  scaling.

- $\epsilon_i^n \nu_i^\dagger \bar{\sigma}^\mu D_\mu \nu$

At one loop in the  $L_4$  model, the reheaton mass-mixes with neutrinos. After integrating out the reheaton, this induces kinetic mixing between neutrinos of different sectors. However, because the vector-like leptons only couple to the charged leptons, the effective coupling to the neutrinos is Yukawa-suppressed:

$$\epsilon_i^n \sim (m_\ell)_{\text{us}} (m_\ell)_i \left( \frac{\lambda Y_E^c \mu_E}{16\pi^2 (M_4)_i m_S} \right)^2. \quad (4.15)$$

For sectors with  $(M_4)_i \sim M_L$ ,  $\epsilon_i \sim \sqrt{i}$ . Once  $Y_E v_i \gtrsim M_L$ , the kinetic mixing decreases as  $\epsilon_i \sim 1/\sqrt{i}$ .

Energy loss in SN1987a [130] limits the size of the kinetic mixing. The neutrino production rate from neutral-current bremsstrahlung requires  $\sqrt{\sum_i (\epsilon_i^n)^2} \lesssim 10^{-4}$ . Due to the growth of  $\epsilon_i^n$  with  $i$  for small values of  $i$ , the sum is dominated by those sectors for which the vector-like lepton masses are larger than their chiral masses. For typical parameters, such as those shown in Fig. 4.5, this is the case for only  $\mathcal{O}(10)$  sectors. Taking into account the bound on  $T_{\text{RH}}$  from Sec. 4.1.1, this gives  $\sqrt{\sum_i (\epsilon_i^n)^2} \lesssim 10^{-13} (M_L/4\pi v)^4$ , so that there is no constraint as long as the vector-like masses are taken to be sufficiently close to the weak scale.

- $\epsilon_i^c \mathbf{G}_F (\nu_i^\dagger \bar{\sigma}^\mu e^c) (p^\dagger \bar{\sigma}_\mu n)$

---

<sup>3</sup>Kinetic mixing is not generated at any order if the coupling between sectors is mediated by a single, real scalar field, since there can be no effective coupling of such a field to the electromagnetic field-strength tensor. Therefore, this effect can be safely neglected in the  $\phi$  model.

There is a somewhat more powerful constraint from SN1987a due to charge-current neutrino production. The mass-mixing of the reheaton with neutrinos leads to an effective four-Fermi operator, with

$$\epsilon_i^c \sim (m_\tau m_\nu)_i \left( \frac{\lambda Y_E^c v_{\text{us}} \mu_E M_L}{4 \pi m_S (M_4^2)_{\text{us}} (M_4)_i} \right)^2. \quad (4.16)$$

In the case of Majorana neutrino masses,  $\epsilon_i^c$  grows like  $\sqrt{i}$ , so that  $\sqrt{\sum_i (\epsilon_i^c)^2} \sim N$ . Once again taking into account the limit on  $T_{\text{RH}}$ , we have  $\sqrt{\sum_i (\epsilon_i^c)^2} \lesssim 10^{-24} N (M_L / \sqrt{4 \pi Y_E v})^4$ . The supernova bound is only  $\sim 10^{-5}$ , so that even for  $N \sim 10^{16}$ , the coupling is unconstrained for  $M_L$  near the weak scale.

Finally, limits on active-sterile neutrino oscillations can also bound  $\epsilon_i^c$ , both from cosmological measurements as well as active neutrino disappearance [131]. However, due to the Yukawa suppression of the neutrino mixing, the most relevant limits are those involving the tau neutrino, which are comparatively weak. Absent resonant mixing due to accidental degeneracies, which we expect to be atypical in our parameter space, the bounds from neutrino oscillations are negligible.

**Colliders** Models of  $N$ naturalness can provide collider signatures through both direct production of the reheaton as well as rare decays of SM particles. However, the smallness of the reheaton couplings, due to both large- $N$  suppression and  $T_{\text{RH}}$  constraints, precludes these signatures from being a generic feature of our models. In the  $\phi$  model, for example, rare Higgs decays proceed through  $\phi - h$  mixing. The dominant signature in this case is are invisible decays of the SM-like Higgs boson, with  $\text{BR}_{\text{inv}} \sim \theta_{\phi h}^2 \Delta N_{\text{eff}} / (1 + \Delta N_{\text{eff}}) \lesssim 10^{-12}$  after requiring sufficiently low  $T_{\text{RH}}$ . Even using optimistic estimates, future colliders such as TLEP or a 100 TeV machine (with  $10 \text{ ab}^{-1}$  of luminosity) will only produce  $\sim 10^6$  [132] or  $10^{10}$  [133, 134] Higgses, respectively, rendering such decays unobservable.

Direct production of  $\phi$  is similarly suppressed, since it must proceed through the same mixing angle. Even for  $m_\phi < m_h$ , in which case the production cross sections are somewhat larger, direct production of  $\phi$  will be unobservable. For example, a SM-like Higgs with a mass of 10 GeV gives a cross section only 2.5 times larger at TLEP and approximately 14 times larger at a 100 TeV  $p - p$  machine than a Higgs at 125 GeV. Nevertheless, if  $\phi$  is sufficiently light, there may be a variety of interesting signatures; see, *e.g.*, [135] for a study of current constraints which probe mixing angles down to  $\theta_{\phi h} \sim 10^{-5}$ . We leave a detailed study of detection prospects for  $m_\phi \lesssim 10$  GeV to future work, see *e.g.*, [136] for an analysis of a similar scenario.

In the  $L_4$  model, the new sectors and the reheaton are similarly difficult to observe; however, the vector-like leptons of our own sector may be accessible. As discussed above, the vector-like mass parameters should all be of order the weak scale. This implies they would likely be observable, both directly and through  $h \rightarrow \gamma \gamma$  and precision electroweak measurements. For a recent study of these bounds, see [137]. In particular, attempting to evade these constraints by raising the mass of the vector-like leptons will re-introduce tension with  $\Delta N_{\text{eff}}$ , as described in the Section 4.1.1.

**A Heavy Axion** An outstanding puzzle within the SM is the strong CP problem. If we have  $N$  copies of the SM, then naively they all have their own theta angles  $\theta_i$ . However, if the  $S_N$  symmetry is only softly broken by Higgs mass terms, then all of these angles would be equal. A shared axion would be able to set to zero all the  $\theta_i$ 's at the same time. The only difference between the version proposed here and the single sector story is that here there are  $N$

contributions to its mass from each  $\Lambda_{\text{QCD}}$ . The potential for the axion has three contributions

$$V(a) \ni \begin{cases} \frac{\Lambda_{\text{QCD},i}^6}{m_{H,i}^2} \left(\frac{a}{f_a} - \theta_i\right)^2 & \text{for } i < 0 \\ m_{\pi,i}^2 f_{\pi,i}^2 \left(\frac{a}{f_a} - \theta_i\right)^2 & \text{for } 0 \leq i < N_u \\ \Lambda_{\text{QCD},i}^4 \left(\frac{a}{f_a} - \theta_i\right)^2 & \text{for } i \geq N_u \end{cases}, \quad (4.17)$$

where  $\Lambda_{\text{QCD},i}$  is the QCD scale for the  $i^{\text{th}}$  sector,  $i < 0$  corresponds to sectors with  $\langle h \rangle H_i = 0$ , and  $N_u \sim 10^5$  is the sector with the smallest vev for which  $m_u > \Lambda_{\text{QCD}}$ . The contribution from the sectors with  $\langle h \rangle H_i = 0$  are due to higher dimensional operators from integrating out the Higgs doublet, the sectors with  $m_u < \Lambda_{\text{QCD}}$  yield the familiar contribution to the axion potential, and the final term is the result for pure QCD with no light quarks. Numerically, the first term can always be neglected, the second term dominates as long as  $N < N_u$ , and only the third term is relevant for  $N \gg N_u$ .

In order to estimate how much heavier this state will be as compared to the standard case, we have calculated Eq. (4.17) numerically including the one-loop running of  $\Lambda_{\text{QCD}}$ . For the first two sums in Eq. (4.17), we used chiral perturbation theory to calculate the contribution to the axion mass. For the last sum, we normalized it such that it is equal to the chiral perturbation theory result when  $m_u = \Lambda_{\text{QCD}}$ . A numerical fit to the axion mass gives approximately

$$\frac{m_a(N)}{m_a(1)} \simeq \begin{cases} 4 \times 10^3 \left(\frac{N}{10^4}\right)^1 & \text{for } N < N_u \\ 2 \times 10^{14} \left(\frac{N}{10^{16}}\right)^{0.9} & \text{for } N \gg N_u \end{cases}. \quad (4.18)$$

It is critical that the soft-breaking of the  $S_N$  symmetry by the different Higgs vevs does not lead to any issues via higher dimensional operators. For example, one class of operators that leads to a change in  $\theta_i$  between the sectors are

$$\mathcal{O}_{\Delta\theta_{\text{QCD}}} \sim Y_u H_i Q_i u_i^c \frac{|H^i|^2}{\Lambda_G^2}. \quad (4.19)$$

Because the different sectors have different Higgs vevs, a chiral rotation shows that the theta angles all differ by  $\sim |H_i|^2/\Lambda_G^2$ . Plugging this into Eq. (4.17), solving for the axion vev, and requiring that our theta angle is smaller than  $10^{-10}$ , we find that  $N < 10^{10}$  if a shared axion is the solution to the strong CP problem. This approach requires the important assumption that whatever resolves the hierarchy problem between  $\Lambda_H$  and  $\Lambda_G$  does not introduce these operators or any other Higgs dependent phases.

## Discussion

It is interesting to compare  $N$ naturalness with other approaches. It bears a superficial resemblance to large extra dimensions, which add  $10^{32}$  degrees of freedom in the form of KK gravitons, as well as the scenario of Dvali [55] which invokes  $10^{32}$  copies of the SM. We discussed them in Section 3.1. In each of these cases,  $M_{\text{pl}}$  is renormalized down to the TeV scale. Of course this predicts (as yet unseen) new particles accessible to the LHC [58]. By contrast,  $N$ naturalness solves the hierarchy problem with cosmological dynamics; the weak scale is parametrically removed from the cutoff, and so it does not demand new physics to be accessible at colliders.  $N$ naturalness has some features in common with low-energy SUSY as well. Both models invoke a softly broken symmetry: SUSY is broken by soft terms, and the  $S_N$  symmetry is broken by varying Higgs masses. Also in both cases, the most obvious implementations of the idea are experimentally excluded. If SUSY is directly broken in the MSSM sector, we

have the famous difficulties with charge and color breaking; in the case of  $N$ naturalness, direct reheating of all  $N$  sectors is grossly excluded by  $N_{\text{eff}}$ . Thus in both cases we need to have “mediators.” SUSY must be dominantly broken in another sector and have its effects mediated to the MSSM. Similarly, reheating must be dominantly communicated to the reheaton, which subsequently dumps its energy density into the other sectors. Finally, both models have additional scales that are not, on the face of it, tied to the physics responsible for naturalness. In SUSY there is a “ $\mu$  problem” in that the vector-like Higgsino mass must be comparable to the soft scalar masses, while in  $N$ naturalness the reheaton mass must be close to the bottom of the spectrum of Higgs masses. While in both cases there are simple pictures for how this can come about, these coincidences do not emerge automatically. Moving beyond purely field theoretic mechanisms, there is the proposal of the relaxion [118], discussed in the next Section, which invokes an extremely long period of inflation coupled with axionic dynamics to relax to a low weak scale. While both the relaxion and  $N$ naturalness mechanisms are cosmological, the physical mechanism of the relaxation, associated with the huge number of  $e$ -foldings of inflation, is *in principle* unobservable given our current accelerating Universe, much like the vast regions of the multiverse outside our cosmological horizon are imperceptible. By contrast, the cosmological dynamics associated with reheaton decay in  $N$ naturalness are sharply imprinted on the particle number abundance in all the sectors. They are not only in principle observable but, as we have stressed (at least for a small number of sectors “close” to ours), are detectable in practice within our Universe. We note that there is no obstacle to augmenting  $N$ naturalness with an anthropic solution to the cosmological constant problem (discussed in Section 3.4). The presence of extra sectors exponentially increases the number of available vacua. For example we could add to the SM a sector with  $m$  vacua and end up with  $m^N$ . Already  $N \simeq 10^4$  with two vacua per sector is more than enough to scan the cosmological constant without relying on string theory landscapes. When solving the entire hierarchy problem with  $N \simeq 10^{16}$ , the vacua utilized to scan the cosmological constant can even be the two minima of the Higgs potential; this requires a high cutoff so that the second minimum is below  $\Lambda_H$  and the difference in the potential energy of the two minima is  $\mathcal{O}(\Lambda_G)$ . To conclude, we would like to comment on the nature of the signals of  $N$ naturalness. For concreteness, three models that make  $N$ naturalness cosmologically viable were presented. However, it is easy to imagine a broader class of theories that realizes the same mechanism. We can relax the assumption that the Higgs masses are uniformly spaced (or even pulled from a uniform distribution) or that all the new sectors are exact copies of the SM. It is also possible to construct different models of reheating, with new physics near the weak scale to modify the UV behavior of the theory. Nonetheless our sector can not be special in any way. There will always be a large number of other sectors with massless particles and with matter and gauge contents similar to ours, leading to the following signatures:

- We expect extra radiation to be observable at future CMB experiments.
- The neutrinos in the closest  $m_H^2 < 0$  sectors are slightly heavier and slightly less abundant than ours. This implies  $\mathcal{O}(1)$  changes in neutrino cosmology, which will start to be probed at this level in the next generation of CMB experiments [138].
- If the strong CP problem is solved by an axion, its mass will be much larger than the standard prediction.
- If  $N \lesssim 10^4$  as motivated by grand unification, supersymmetry or new natural dynamics should appear beneath 10 TeV.

The natural parameter space is being probed now, and soon we may know if the  $N$ naturalness paradigm explains how the hierarchy problem has been solved by nature.

### 4.1.2 The Relaxion

The original relaxion solution [118] can be summarized by this potential valid up to a cut-off  $M$

$$V = (-M^2 + g\phi) |H|^2 + V_\phi(g\phi) + \frac{\phi}{f} \tilde{G}_{\mu\nu}^a G^{\mu\nu a}, \quad (4.20)$$

$$V_\phi(g\phi) = g^2 \phi^2 + gM^2 \phi + \dots, \quad (4.21)$$

accompanied by an exponentially large number of  $e$ -folds of low scale inflation ( $H_I \sim \Lambda_{\text{QCD}}$ , where  $H_I$  is the Hubble parameter during inflation). All terms in the potential proportional to  $g$  break the shift symmetry  $\phi \rightarrow \phi + c$ , so it is technically natural to take  $g \ll M$ , since in the limit  $g \rightarrow 0$  this symmetry is restored.

If we imagine that the relaxion field  $\phi$  starts from  $\phi \gtrsim M^2/g$ , during inflation it is going to slowly roll down its potential until it arrives at a field value where the Higgs mass crosses zero. When  $\phi > M^2/g$ ,  $m_h^2 > 0$ ,  $\langle h \rangle = 0$  and the potential is just a tadpole  $g\phi$ .

If we are at  $T \sim H_I \lesssim \Lambda_{\text{QCD}}$  this point is special from the relaxion point of view. It is where the barriers of size  $f_\pi^2 m_\pi^2$  generated by  $\frac{\phi}{f} \tilde{G}_{\mu\nu}^a G^{\mu\nu a}$ , start to appear, since they are proportional to the Higgs vev,  $m_\pi \propto m_u + m_d \propto v$ .

If inflation is still ongoing (i.e. the relaxion kinetic energy is negligible), the rolling of  $\phi$  is going to stop when the slope of

$$\frac{\phi}{f} \tilde{G}_{\mu\nu}^a G^{\mu\nu a} \sim f_\pi^2 m_\pi^2 \cos \frac{\phi}{f} \quad (4.22)$$

equals the slope of the other part of the potential  $gM^2\phi$ . This happens at

$$g \approx \frac{f_\pi^2 m_\pi^2}{f M^2} \approx 10^{-21} \text{ GeV} \left( \frac{10^9 \text{ GeV}}{f} \right) \left( \frac{10 \text{ TeV}}{M} \right)^2. \quad (4.23)$$

The value of  $f$  is chosen to respect current bounds on axion interactions and we have taken a low value of the cut-off  $M$ . Following our EFT discussion, it is technically natural to take  $g$  so small, since it is breaking the shift symmetry of  $\phi$ . However the value of  $g$  implies trans-Planckian field excursions

$$\Delta\phi \gtrsim M^2/g \gg M_{\text{Pl}} \quad (4.24)$$

that in our EFT formulation are allowed, but are usually problematic when gravity is taken into account [53, 115–117, 139, 140]. As mentioned above the solution also requires an exponentially large number of  $e$ -folds

$$N = \int dt H_I = \int d\phi \frac{H_I}{\dot{\phi}} \approx \Delta\phi \frac{H_I}{\dot{\phi}} \approx \Delta\phi \frac{H_I^2}{V'} \approx \frac{H_I^2}{g^2}. \quad (4.25)$$

The other conditions on the inflationary sector are

$$H_I > M^2/M_{\text{Pl}}, \quad (4.26)$$

to inflate throughout the rolling of  $\phi$ , and

$$H_I \lesssim \Lambda_{\text{QCD}}, \quad (4.27)$$

to have wiggles when the Higgs mass crosses zero and finally

$$H_I^3 \lesssim V', \quad (4.28)$$

so that classical rolling  $\phi_c \simeq V'/H_I$  dominates over quantum brownian motion  $\phi_Q \simeq H_I^2$ . Let us try to attach some numbers to these requirements, we can take  $f \gtrsim 10^8$  GeV from cooling of SN1987A [141] and  $M \gtrsim 10$  TeV from explaining at least the little hierarchy problem, this gives

$$\begin{aligned} g &\lesssim \frac{f_\pi^2 m_\pi^2}{f M^2} \simeq 10^{-21} \text{ GeV}, \\ \Delta\phi &\gtrsim 10^{10} M_{\text{Pl}}, \\ N &\gtrsim \frac{H_I^2}{g^2} \simeq 10^{36}. \end{aligned} \quad (4.29)$$

These numbers are all technically natural, but pretty extreme. Subsequent efforts were able to dispose of super-Planckian field excursions and loosen the requirements of the inflationary sector, introducing additional fields in the model [142–148]. We should also keep in mind that one has to add also an appropriate reheating sector that does not spoil the mechanism.

Note also that we have not solved the strong CP problem. In this model  $\theta \sim \mathcal{O}(1)$ . If we want to solve it without new fields,  $g$  needs to be smaller by a factor of  $\theta \sim 10^{-10}$  [118]. Alternatively we can include in the theory a second strongly interacting gauge group, under which new vector-like leptons getting an  $\mathcal{O}(1)$  fraction of their mass from the Higgs are charged. we discuss this in Section 4.2.3.

The mechanism at the core of the relaxion was proposed by Abbott to explain the value of the cosmological constant [149]. The first relaxion paper has had the merit to creatively apply this idea to  $m_h$ , although it must be pointed out that many of the ideas that have later taken root in the literature (for instance using  $\text{Tr}[G\tilde{G}]$  as a trigger or looking for dynamics that can explain  $m_h$  in the multiverse) were already presents in Dvali's first attempts in the early '00s [150–152] that we discuss in Section 4.7. Having said this, without the relaxion, many of us, including myself would not have started thinking about the problem in these terms and I think that it deserves its success. As is always the case in science, today much progress has been made and we know how to use similar ideas without the extreme requirements (or complex model building) that the relaxion demands.

## 4.2 Weak Scale Triggers

Traditional solutions to the hierarchy problem, discussed in the previous Chapter, aim at making  $m_h^2 = 0$  special, be it in the context of supersymmetry (where the chiral symmetry of fermion superpartners protects scalar masses), or theories of the Higgs as a pseudo-goldstone boson in either their four-dimensional or AdS avatars (where approximate shift symmetries play this role).

In this Chapter (and in anthropic solutions discussed in the previous one) we take a slightly different perspective. In the fundamental theory of particle interactions there is nothing special about  $m_h^2 = 0$ ; there is no difference in the number of degrees of freedom for massless versus massive spin zero particles, nor any obvious difference in the number of symmetries when  $m_h^2 = 0$ . However  $m_h^2 = 0$  is a special point for the evolution of the Universe.

To understand how this is possible we can take a step back and ask a more general QFT question, as we did in [153]: What varies in the SM (or a BSM theory), as we change the Higgs mass parameter  $m_h^2$ ? Obviously the spectrum of the Standard Model changes, and this is detected by the non-trivial  $m_h^2$  dependence of the two-point function propagators of the

gauge bosons, fermions and the Higgs. For instance the gauge-invariant electron two-point function,  $\bar{e}_\alpha(x)W(x,y)e_\alpha(y)$ , where  $W(x,y)$  is an appropriate Wilson line, depends on the distance between the two spacetime points  $(x-y)$  and certainly does strongly depend on  $m_h^2$ .

But we can also ask if there is any gauge invariant local operators  $\mathcal{O}(x)$ , whose vacuum expectation value is sensitive to  $m_h^2$ . We can probe  $\langle\mathcal{O}\rangle$  by coupling  $\mathcal{O}$ , parametrically weakly, to some scalar  $\phi$  via the coupling  $\xi\phi\mathcal{O}$ , and looking at the effective action induced for  $\phi$ . At tree-level, obviously  $\mathcal{O}_h = |H|^2$  depends on  $m_h^2$ . But of course, once loop corrections are taken into account,  $\langle\mathcal{O}_h\rangle$  is not calculable in the SM, which is one of the aspects of the hierarchy problem. We can simply look at the tadpole diagram, from  $\xi\phi|H|^2$  which induces  $\xi\phi\Lambda_H^2$  where  $\Lambda_H$  is the cutoff for the Higgs sector. This is completely insensitive to  $m_h^2$ , and indeed  $\langle|H|^2\rangle$  is essentially independent of the magnitude or sign of  $m_h^2$ . Continuing this line of thought leads to a more invariant characterization of “tuning” associated with solutions of the hierarchy problem. Recall that the hierarchy problem is sharply posed in theories that allow the Higgs mass squared to be calculable, rather than taken as an input parameter. A closely related characterization is to find a theory in which  $\langle|H|^2\rangle$  is calculable. In supersymmetric theories,  $\langle|H|^2\rangle \sim m_{\text{SUSY}}^2$  ( $m_{\text{SUSY}}$  is the soft supersymmetry breaking mass) while in composite Higgs models,  $\langle|H|^2\rangle \sim f_\pi^2$  ( $f_\pi$  is the decay constant of the composite meson/pion). From this perspective, the ‘degree of tuning’ becomes a well defined ratio  $r \sim m_h^2/\langle|H|^2\rangle$ , and in all known theories where both  $m_h^2$  and  $\langle|H|^2\rangle$  are calculable, making  $r$  tiny requires the usual fine-tuning of parameters in the ultra-violet (UV) theory.

The cosmological solutions to the hierarchy problem that we discuss in this Chapter follow a different line of attack: they use operators  $\mathcal{O}$  that are sensitive to, or *triggered by*, scalar  $m^2$  parameters to induce an early Universe event which explains the currently observed value of  $m_h^2$ . In this Section we give a general overview of these *Trigger Operators*. These objects have been utilized throughout the young history of cosmological selection of the weak scale (as early as [151]), but their general role and importance for phenomenology was first pointed out in [153].

The reason why it is interesting to focus on these objects is twofold:

1. First of all, one *trigger* can be used in many ways to solve the hierarchy problem, both in the context of cosmological selection of the weak scale and possibly also in completely different contexts. Therefore identifying one trigger corresponds to identify new or old physics which is generically related to the problem.
2. Secondly, we are looking for operators sensitive to the Higgs vev. In practice this means light ( $m \lesssim v$ ) new physics coupled to the Higgs. Therefore identifying triggers is equivalent to identifying promising signals of these new explanations for the value of  $m_h^2$ . In most cases these triggers give the first experimental sign that cosmological selection of the weak scale is at work.

This whole Chapter is an illustration of the first point, while we discuss the second one in Section 4.8. However, to get there, we first have to answer: what is a *weak scale trigger* exactly?

We consider operators whose vacuum expectation value is calculable and sensitive to  $m_h^2$ , i.e.  $d\log\langle\mathcal{O}\rangle/d\log m_h^2 \sim O(1)$ . In the SM itself there is essentially a unique option— $\mathcal{O}_G = (\text{Tr}[G\tilde{G}])$ . Another simple possibility for  $\mathcal{O}$  presents itself in a two-Higgs doublet extension of the Standard Model, with Higgses  $H_1, H_2$ . With the crucial imposition of a  $Z_4$  symmetry under which the product

$$(H_1H_2) \rightarrow -(H_1H_2), \tag{4.30}$$

the operator  $\mathcal{O}_H = H_1H_2$  is triggered by  $m_{1,2}^2$ . We dub this the “type-0” Two-Higgs Doublet Model (2HDM).



A third option consists in adding new fermions charged under a new confining gauge group, with Yukawa couplings to the Higgs. If an  $\mathcal{O}(1)$  fraction of their mass comes from the Higgs vev, the  $\theta$ -term of the new gauge group,  $\text{Tr}[F\widetilde{F}]$ , can act as a trigger.

To the best of my knowledge this completes the list of viable triggers. The list becomes much longer if we consider “imperfect” triggers, i.e. operators that are sensitive to the Higgs vev if they are part of a theory with a small enough cutoff.

All gauge invariant operators in the SM fall into this category, with a cutoff  $\Lambda_H \lesssim 4\pi v$ . From my point of view, it is fair not to consider these as triggers, for a simple practical reason. At energies below  $4\pi v$  there is no hierarchy problem and no need to solve it. There are, however, other options that cannot be discarded so lightheartedly. These corresponds to all the approximate symmetries of the SM. For instance we could consider the operator

$$\mathcal{O}_F = \frac{(Qu^c)(Qd^c)}{M^2}. \quad (4.31)$$

At two-loops it gets a cutoff-sensitive contribution to its vev, but it is suppressed by the small product  $y_u y_d$ . So in practice  $\mathcal{O}_F$  could be used to solve the little hierarchy problem. However at  $\Lambda_H$  we need to introduce a second Higgs doublet to protect the vev of  $\mathcal{O}_F$  from even higher energy contributions. In reality, this is a special case of the  $H_1 H_2$  trigger with a subset of a PQ symmetry protecting the vev. Interestingly, also  $\text{Tr}[W\widetilde{W}]$ , if we add  $B + L$  violation to the SM, might end up being a special case of the  $H_1 H_2$  trigger, as discussed in Section 4.2.4.

I have tried to find other options for about one year, at the moment without success. However, it might be possible to find other trigger operators by looking for symmetries that can protect their vev. It is not so trivial to find them, mostly because in the SM the symmetry options are limited and leave a single viable operator:  $\text{Tr}[G\widetilde{G}]$ . Extending the SM opens up a larger pool of possible symmetries, but it is not at all trivial to still accommodate new physics with the required properties after LEP, the Tevatron and the LHC.

In the next Subsections we discuss the properties and phenomenology of the weak scale triggers that we identified and comment on  $\text{Tr}[W\widetilde{W}]$ . We do not yet have a theorem, but it is fair to say that targeting  $\text{Tr}[G\widetilde{G}]$ ,  $H_1 H_2$  and  $\text{Tr}[F\widetilde{F}]$  should be nearly enough to say the final word on this class of solutions to the hierarchy problem.

### 4.2.1 The SM Trigger $\text{Tr}[G\widetilde{G}]$

As with the example of the operator  $|H|^2$  discussed above, almost all gauge invariant local operators in the SM have UV sensitive expectation values and are thus independent of  $m_h^2$ . Consider for example a Yukawa coupling,  $\mathcal{O}_q = qhu^c$ . If we add to the Lagrangian  $\xi_q \phi \mathcal{O}_q$  to probe its vev, at two-loops we generate the tadpole in Fig. 4.6  $\sim \frac{\xi_q y_q}{(16\pi^2)^2} \phi \Lambda^4$ , proportional to the cutoff  $\Lambda$ . The reason is that every gauge invariant local operator already appears in the SM effective Lagrangian and we can close the loops. Said more invariantly, there are no global symmetries carried by relevant or marginal operators  $\mathcal{O}$  in the SM, that are not broken by the presence of  $\mathcal{O}$  in the effective Lagrangian. Thus if we have  $\xi \phi \mathcal{O}$  in the Lagrangian,  $\phi$  is not charged under any symmetries. So nothing forbids  $\xi \phi \Lambda^n$  in the effective action. We can consider operators that are charged under the accidental baryon and lepton number global symmetries of the Standard Model; now these expectation values are not UV sensitive, but the global symmetries ensure that the expectation values for these operators are equal to zero, again independent of the value of  $m_h^2$ . We can also imagine that  $\phi$  has a shift symmetry  $\phi \rightarrow \phi + c$ , or equivalently, ask that  $\mathcal{O} = \partial_\mu V^\mu$  is a total derivative. Then,  $\phi \mathcal{O} = \phi \partial_\mu V^\mu = -(\partial_\mu \phi) V^\mu$ . Again the expectation value of  $\mathcal{O}$  is indeed UV insensitive, but at the same time  $\langle \mathcal{O} \rangle = 0$  independently of  $m_h^2$ .

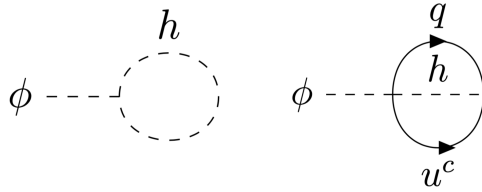


Figure 4.6: Almost all gauge invariant local operators  $\mathcal{O}$  in the SM have UV sensitive expectation values that are thus independent of  $m_h^2$ . We can probe their vevs by adding to the Lagrangian the parametrically weak interaction  $\phi\mathcal{O}$  and look at the effective action for  $\phi$ . If we add, for example,  $\phi|H|^2$  or  $\phi QHu^c$  we can always close the loops in this Figure and obtain a tadpole for  $\phi$  proportional to the cutoff. This happens because there are no global symmetries carried by  $\mathcal{O}$ , that are not already broken by the presence of  $\mathcal{O}$  in the SM effective Lagrangian.

There is one famous loophole to this argument, associated with the operator  $\text{Tr}[G\tilde{G}]$  (where the trace is over  $SU(3)$  indexes), which is the total derivative of a non-gauge invariant current,  $\text{Tr}[G\tilde{G}] = \partial_\mu K^\mu$ , and can be turned on instanton backgrounds which break the shift symmetry non-perturbatively. Of course  $\text{Tr}[G\tilde{G}]$  is parity odd, but  $\langle \text{Tr}[G\tilde{G}] \rangle$  can be non-zero with a  $\theta$  term. In pure QCD, we have  $\langle \text{Tr}[G\tilde{G}] \rangle \sim \theta \Lambda_{\text{QCD}}^4$ . With light quarks, we can rotate

$$\frac{\alpha_s}{8\pi}(\theta + \xi\phi)\text{Tr}[G\tilde{G}] \quad (4.32)$$

into the quark mass matrix with an anomalous chiral rotation and use chiral perturbation theory to get the effective potential

$$V_{G\phi} = -m_\pi^2 f_\pi^2 \sqrt{1 - \frac{4m_u m_d}{(m_u + m_d)^2} \sin^2\left(\xi\phi + \frac{\theta}{2}\right)} \simeq \frac{\Lambda^4(\langle h \rangle)}{2} (\xi\phi + \theta)^2 + \dots, \quad (4.33)$$

where the potential is switched on at the QCD phase transition by chiral symmetry breaking

$$\Lambda^4(\langle h \rangle) = m_\pi^2 f_\pi^2 \frac{m_u m_d}{(m_u + m_d)^2}. \quad (4.34)$$

Following the same reasoning as for other operators we can conclude that

$$\langle \text{Tr}[G\tilde{G}] \rangle \simeq \theta \Lambda^4(\langle h \rangle) \simeq \theta(m_u + m_d) \Lambda_{\text{QCD}}^3 \quad (4.35)$$

This is suppressed by  $\theta$  but is triggered by the weak scale through  $(m_u + m_d)$  and  $\Lambda_{\text{QCD}}$ . This triggering of  $\text{Tr}[G\tilde{G}]$  is used in the cosmological dynamics of relaxion models discussed in the previous Section [118] and in many of the models discussed in later Sections. To my knowledge the only model that exploits the connection between  $\theta$  and  $\langle h \rangle$  to explain both quantities at once is ours [154, 155]. In other cases, including the relaxion, this is seen as a hindrance (i.e. explaining  $\langle h \rangle$ , generically ruins  $\theta$ ).

From this discussion it is not yet manifest just how non-trivial it is that  $\langle \text{Tr}[G\tilde{G}] \rangle$  is sensitive to the Higgs vev. The potential in Eq. (4.33) is generated by the interference between  $U(1)_A$  breaking from instanton effects and that from quark masses.

The first non-trivial condition that is realized is that the SM breaks  $U(1)_A$  in the right way to interfere with the instantons. If we think of one instanton as an effective vertex, we need to attach one leg for each particle charged under  $SU(3)$  and  $U(1)_A$ , so each quark, both right-handed and left-handed comes out of this vertex. We can then close all these legs and interfere with this vertex by putting an insertion of each quark mass. This is the famous statement (that

can be easily derived using spurionic arguments [156]) that the potential for  $\theta$  is proportional to the determinant of the quark mass matrix.

The second non-trivial condition is that either 1) the explicit breaking of  $U(1)_A$  needed to interfere with the instanton is sensitive to  $\langle h \rangle$  or 2) the scale at which  $g_s$  becomes strong is sensitive to  $\langle h \rangle$ . In the SM both are satisfied. The first is satisfied in a rather non-trivial way. To interfere with the instanton we are using the SM Yukawas

$$QH u^c, QH^\dagger d^c, \dots \quad (4.36)$$

The vertex is dominated by  $H$  at its vev only because the instanton amplitude contains a factor

$$\int dE e^{-\frac{1}{g_s(E)^2}} \times \dots, \quad (4.37)$$

so the calculation is dominated by energies in the loops  $E \simeq \Lambda_{\text{QCD}} < v$ , and pairing Higgses from different mass insertions to give a UV sensitive loop gives an exponentially suppressed contribution compared to the one proportional to  $\langle h \rangle$ .

The third, and possibly most interesting, condition is that the scale at which instanton effects become important is not much bigger than  $\langle h \rangle$  (in this case, as we have just seen, it is actually smaller). In this way changing  $\langle h \rangle$  by  $\mathcal{O}(1)$  also changes  $V_{G\phi}$  by  $\mathcal{O}(1)$ . This is crucial to have a good trigger, i.e. an operator that can select the observed  $\langle h \rangle$ . All operators in the SM are in principle sensitive to  $\langle h \rangle$ , but numerically the weak scale is insignificant if the cutoff is large, for instance  $\langle |H|^2 \rangle \simeq v^2 + \Lambda_H^2$ . This quantity can be used to select  $v$  only in extremely tuned situations, where a relative change of  $\mathcal{O}(v^2/\Lambda_H^2) \ll 1$  in the potential of some scalar, leads to a dramatic change in the history of the Universe.

Incidentally anthropic arguments rely precisely on the coincidence  $\Lambda_{\text{QCD}} \simeq v$ . In a different universe, where this is not true,  $v$  might have little or no impact on chemistry.

To conclude, I take quite seriously the fact that  $\langle \text{Tr}[G\tilde{G}] \rangle$  is sensitive both to  $\langle h \rangle$  and to  $\theta$ . Either we are in front of a triple coincidence or the SM is telling us something.

## 4.2.2 The $H_1 H_2$ Trigger in the Type-0 2HDM

We now consider a two-Higgs doublet extension of the Standard Model, with Higgs scalars  $H_1, H_2$ . Here the operator  $\mathcal{O}_H = H_1 H_2$  is a good candidate to act as a trigger<sup>4</sup>. We want  $(H_1 H_2)$  to be charged under a discrete symmetry which we can probe by coupling to some  $\phi$  with  $\xi \phi H_1 H_2$ . The simplest choice is a symmetry under which  $\phi \rightarrow -\phi$  and  $(H_1 H_2) \rightarrow -(H_1 H_2)$ . This is part of the  $Z_4$  symmetry

$$H_1 \rightarrow ie^{i\alpha} H_1, \quad H_2 \rightarrow ie^{-i\alpha} H_2, \quad \phi \rightarrow -\phi \quad (4.38)$$

with  $\alpha$  in  $U(1)_Y$ . The  $Z_4$  symmetry acts also on quark and lepton bilinears and we have  $2^3$  possible charge assignments:  $\pm ie^{-i\alpha}$  for  $Qu^c, Qd^c, Le^c$ . The case where a single Higgs couples to the quarks and leptons will be phenomenologically safest, so we will focus on that in the following. This fixes the fermion charge assignments, giving the  $Z_4$  symmetry

$$\begin{aligned} H_1 &\rightarrow +ie^{i\alpha} H_1, & H_2 &\rightarrow +ie^{-i\alpha} H_2, & (H_1 H_2) &\rightarrow -(H_1 H_2), \\ (Qu^c) &\rightarrow -ie^{i\alpha} (Qu^c), & (Qd^c) &\rightarrow +ie^{-i\alpha} (Qd^c), & (Le^c) &\rightarrow +ie^{-i\alpha} (Le^c). \end{aligned} \quad (4.39)$$

---

<sup>4</sup>This operator was already considered in the context of the relaxion in [142] and in a different capacity related to fine-tuning in [150].

The renormalizable  $H_{1,2}$  potential invariant under this symmetry is

$$\begin{aligned}
V &= V_{H_1 H_2} + V_Y, \\
V_{H_1 H_2} &= m_1^2 |H_1|^2 + m_2^2 |H_2|^2 + \frac{\lambda_1}{2} |H_1|^4 + \frac{\lambda_2}{2} |H_2|^4 \\
&\quad + \lambda_3 |H_1|^2 |H_2|^2 + \lambda_4 |H_1 H_2|^2 + \left( \frac{\lambda_5}{2} (H_1 H_2)^2 + \text{h.c.} \right), \\
V_Y &= Y_u q H_2 u^c + Y_d q H_2^\dagger d^c + Y_e l H_2^\dagger e^c.
\end{aligned} \tag{4.40}$$

Note the absence of the  $B\mu$ -term,  $B\mu H_1 H_2$  and of the two quartics  $\lambda_{6,7} |H_{1,2}|^2 (H_1 H_2)$ , all forbidden by the  $Z_4$  symmetry. Note also the  $\lambda_5 (H_1 H_2)^2$  term which is allowed. Without this term, the potential would have an accidental Peccei-Quinn (PQ) symmetry and would yield a weak scale axion.

It is very important that  $B\mu = \lambda_{6,7} = 0$ , otherwise we would have  $m_{1,2}^2$ -independent contributions to the vev of our trigger operator from Fig. 4.8, as for instance

$$\mu^2 \equiv \langle H_1 H_2 \rangle \sim \xi \phi B\mu \log \frac{\Lambda^2}{|m_H^2|}. \tag{4.41}$$

where for simplicity we have taken the Higgs masses to a common value  $m_H^2$ . On the contrary, if  $B\mu = \lambda_{6,7} = 0$ , then  $\mu^2(m_1^2, m_2^2)$  is a UV-insensitive, calculable function of  $m_1^2, m_2^2$  for which the weak scale is a trigger. This is a consequence of the  $U(1)$  PQ symmetry of the potential in Eq. (4.40).  $H_1 H_2$  has charge 1 under this symmetry. The only explicit breaking of the PQ is by the quartic  $\lambda_5 (H_1 H_2)^2$ , for which  $\lambda_5$  has charge  $-2$ , and so no analytic expression in the couplings can give something of charge 1. This is shown schematically in Fig. 4.8.

Let us now see what is the value of  $\mu^2$  as a function of  $m_1^2$  and  $m_2^2$ . At tree level  $\mu^2 = 0$  unless both  $m_1^2$  and  $m_2^2$  are negative. If they are both negative, we have

$$\mu^2 = \langle H_1 \rangle \langle H_2 \rangle \sim \sqrt{\frac{|m_1^2| |m_2^2|}{\lambda_1 \lambda_2}} \tag{4.42}$$

where we have ignored all cross quartic couplings. For simplicity we will call  $\mu^2 \sim \sqrt{|m_1^2| |m_2^2|}$  for  $\lambda_{1,2}$  not too tiny. We will keep this characterization even including cross quartics. In this case  $m_{1,2}^2$  should be interpreted as  $(m_{1,2}^{\text{eff}})^2$  which include the cross quartics contributions. So, at tree level, we have the possible  $\mu^2$  shown in the left panel of Fig. 4.7.

The picture is a little more interesting taking QCD chiral symmetry breaking into account. In the following  $\Lambda_{\text{QCD}}$  is the QCD scale with all quark masses below  $\Lambda_{\text{QCD}}$ . If  $m_{1,2}^2 > 0$ , then we do not break  $SU(2) \times U(1)$  above the QCD scale. Since all the  $SU(2) \times U(1)$  invariants of charge  $-1$  under the  $Z_4$  involve  $H_1$ , in the low energy theory after integrating out  $H_{1,2}$ , there can be no linear terms in  $\phi$ . So we have to have one or both of  $m_{1,2}^2 < 0$ .

Consider first  $m_1^2 > 0$  and  $m_2^2 < 0$ . For  $|m_2^2| \gg m_1^2$  we can first integrate out  $H_2$ . In the effective theory containing the neutral and charged components of  $H_1 = (h_1^0, h_1^+)^T$  and  $\phi$ ,  $SU(2) \times U(1)$  is broken, but a  $Z_2$  subgroup of the  $Z_4$ ,

$$\begin{aligned}
H_1 &\rightarrow -H_1, & H_2 &\rightarrow H_2, & \phi &\rightarrow -\phi, \\
(Qu^c) &\rightarrow (Qu^c), & (Qd^c) &\rightarrow (Qd^c), & (Le^c) &\rightarrow (Le^c).
\end{aligned} \tag{4.43}$$

is preserved. This symmetry is still not broken also after integrating out  $(h_1^0, h_1^+)$ , so again in the low energy theory there are no linear terms in  $\phi$ .

Instead for  $m_1^2 \gg |m_2^2|$ , after integrating out  $H_1$ , we still have  $SU(2) \times U(1)$  but there is no operator of charge  $-1$  under the  $Z_4$  (again since all these involve  $H_1$ ). So again, no linear term in  $\phi$  is generated. Thus, if  $m_1^2 > 0$ , for any  $m_2^2$ , we have  $\mu^2 = 0$ .

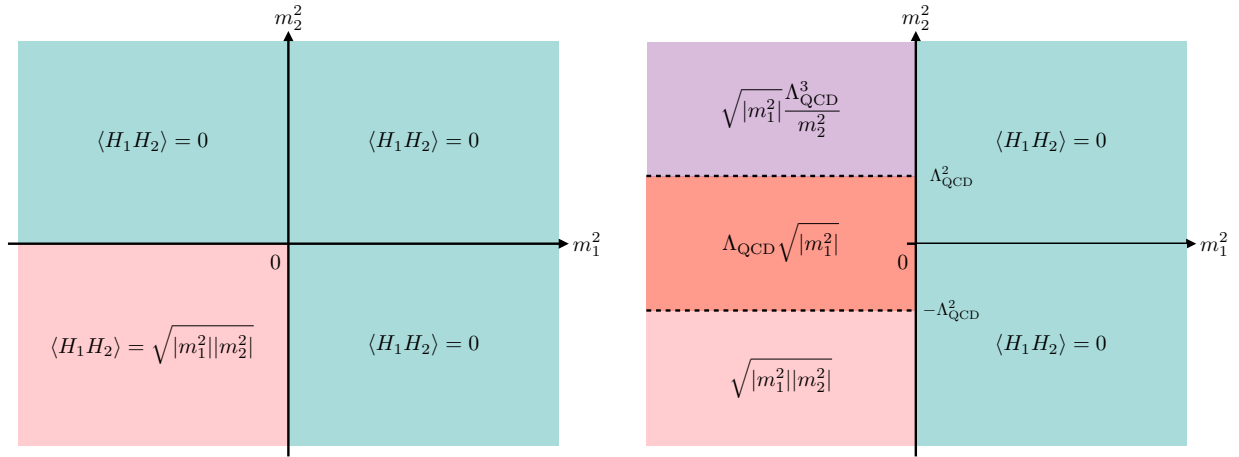


Figure 4.7: In the type-0 2HDM (Eq. (4.40)),  $\langle H_1 H_2 \rangle$  is a UV-insensitive, calculable function of the masses of the two Higgses:  $m_1^2, m_2^2$ . In the left panel we show its classical value while in the right one we include quantum effects.  $m_1^2, m_2^2$  in the Figure are effective masses that include contributions from cross quartic couplings.  $\Lambda_{\text{QCD}}$  is the QCD scale with all quark masses below  $\Lambda_{\text{QCD}}$ .

Now consider  $m_1^2 < 0$ . If  $m_2^2 < 0$ , we have  $\mu^2 \sim \sqrt{|m_1^2|} \max[\sqrt{|m_2^2|}, \Lambda_{\text{QCD}}]$ . If  $m_2^2 > 0$  and  $m_2^2 \gg m_1^2, \Lambda_{\text{QCD}}^2$ , we first integrate out  $H_2$  obtaining

$$\frac{\xi}{m_2^2} \phi H_1^* Q u^c + \dots \quad (4.44)$$

Hence after chiral symmetry breaking, we have  $\mu^2 \sim \frac{\sqrt{|m_1^2|} \Lambda_{\text{QCD}}^3}{m_2^2}$ . If  $|m_2^2| \ll m_1^2$ , we can first integrate out  $H_1$  giving

$$\xi \phi \sqrt{|m_1^2|} h_2^0 + \dots \quad (4.45)$$

Then if  $m_2^2 \gg \Lambda_{\text{QCD}}^2$  we get the same result as before:  $\mu^2 \sim \frac{\sqrt{|m_1^2|} \Lambda_{\text{QCD}}^3}{m_2^2}$ . If instead  $|m_2^2| \ll \Lambda_{\text{QCD}}^2$ , the quartic term dominates and the  $H_2$  VEV is just set by  $\Lambda_{\text{QCD}}$  from the potential

$$V(h_2^0) \simeq y_t \Lambda_{\text{QCD}}^3 h_2^0 + \lambda (h_2^0)^4, \quad (4.46)$$

so we have  $\langle h_2^0 \rangle \sim \frac{\Lambda_{\text{QCD}}}{\lambda^{1/3}} \sim \Lambda_{\text{QCD}}$  for a not too tiny quartic  $\lambda$ . This discussion is summarized in the right panel of Fig. 4.7. We have seen that in a 2HDM with a  $Z_4$  symmetry—what we have called the type-0 2HDM— $\mathcal{O}_H = H_1 H_2$  is a good weak scale trigger. We defer to Section 4.1 an explicit construction that uses  $\mathcal{O}_H$  to tie the cosmological constant to the value of the Higgs mass. In the next Section we explore the collider constraints on the type-0 2HDM.

In this Section we have worked in the limit  $B\mu = \lambda_{6,7} = 0$ . It is clear from the previous discussion that any  $B\mu \ll \mu_S^2$  and  $\lambda_{6,7} \ll \mu_S^2/M_*^2$  do not affect our conclusions or the phenomenology of the type-0 2HDM. However if we take  $B\mu$  and  $\lambda_{6,7}$  to be exactly zero, the model has a  $Z_2$  symmetry under which  $H_1 \rightarrow -H_1$ . To avoid a domain wall problem in the early Universe, we need to introduce a tiny breaking of this symmetry,  $B\mu \gtrsim v^4/M_{\text{Pl}}^2$ .

In our Universe, just below the critical temperature of the EW phase transition, domains of size  $\sim 1/v$  with different signs of the  $H_1$  vev are formed inside any Hubble volume. The walls separating these domains have an energy per unit area  $\sigma \simeq v^3$ . If locally the walls have curvature  $1/R$  they will try to flatten due to the tension  $\sigma$  that acts as an effective pressure

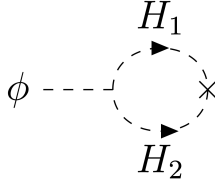


Figure 4.8: In a 2HDM with a  $Z_4$  symmetry (Eq.s (4.38) and (4.40)) the  $H_1 H_2$  vev is a UV-insensitive, calculable function of the two Higgs masses. This can be seen by adding to the Lagrangian the parametrically weak interaction  $\phi H_1 H_2$ . We can only close the loop in this Figure and generate a  $\phi$  tadpole independent of  $\langle H_1 H_2 \rangle$  with an insertion of  $B\mu, \lambda_6$  or  $\lambda_7$  which break the  $Z_4$  symmetry and are thus absent from our 2HDM potential in Eq. (4.40).

$p_T \simeq \sigma/R$ . Parametrically we can consider two extreme regimes: no coupling between the wall and the SM thermal bath or reflection of every SM particle by the wall.

In absence of interactions with the SM bath, the walls expand at the speed of light until we have one domain per Hubble patch. After this initial expansion the energy density in domain walls is  $\rho_W \simeq v^3 H$ , redshifting as  $1/a^2$ . At a temperature  $T_D \simeq v(v/M_{\text{Pl}})^{1/2} \simeq \text{keV}$  the walls dominate the energy density of the Universe. Interactions with the SM thermal bath slow down the expansion of the walls. If we ignore small couplings and assume that every SM particle is reflected with unit probability, we have a pressure  $p_F \simeq v_W T^4$  that slows down the expansion of the wall. Here  $v_W$  is the velocity of the wall. Balancing  $p_F$  with  $p_T$  we obtain a steady state solution with  $v_W \simeq v^{3/2}/(M_{\text{Pl}} H^{1/2})$  and  $R \simeq v^{3/2}/(M_{\text{Pl}} H^{3/2})$ . In this regime, the energy density of domain walls redshifts as  $1/a^3$ , but the initial energy density after one Hubble time at the phase transition is larger than that in the absence of friction. In the end we obtain the same temperature of domain walls domination as before ( $T_D \simeq v(v/M_{\text{Pl}})^{1/2} \simeq \text{keV}$ ). Note that both with and without friction the walls make up a negligibly small fraction of the energy density of the Universe during BBN.

In conclusion to avoid domain walls domination we need to introduce an energy difference between the two vacua  $\pm v_1$ , for example by turning on  $B\mu H_1 H_2$  in the Lagrangian. If we ask that the acceleration provided by this term  $B\mu/v$  is larger than Hubble at the time of domination  $H(T_D) \simeq v^3/M_{\text{Pl}}^2$ , we obtain  $B\mu \gtrsim v^4/M_{\text{Pl}}^2$ . It is easy to show that the wall subsequently collapse in approximately on Hubble time  $\sim 1/H(T_D)$ .

### 4.2.3 Vector-Like Leptons and the $\text{Tr}[F\tilde{F}]$ Trigger

If we go beyond the SM there is a simple way to generalize the success of  $\text{Tr}[G\tilde{G}]$ . Consider a new strong group that confines below  $v$  and new fermions charged under it.

We consider the new fermions  $(\ell, n)$  and their conjugates  $(\ell^c, n^c)$ .  $\ell$  and  $n$  carry the same SM charges as the lepton doublet  $L$  and right handed neutrino  $N$ , respectively. They are in the fundamental representation of the new gauge group.  $(\ell^c, n^c)$  are in the conjugate representations of their equivalents without superscript. Importantly, one can choose the charges of  $\ell, \ell^c, n, n^c$  such that a global  $U(1)_A$  is anomalous with respect to the new strong group.

At this point we can in principle repeat the same discussion as for  $\text{Tr}[G\tilde{G}]$  essentially unchanged, modulo a few phenomenological complications. First of all we have to include in the theory vector-like masses for the new fermions (or at least for  $\ell, \ell^c$ )

$$\mathcal{L} \supset -m_\ell \ell \ell^c - m_n n n^c - y_\ell h n^c - y_c \ell^c h^\dagger n \quad (4.47)$$

with  $m_\ell \gtrsim v$  to comply with current constraints on Higgs couplings and direct searches. If we

again couple a probe scalar to our candidate trigger

$$\xi\phi\text{Tr}[F\widetilde{F}], \quad (4.48)$$

we can see immediately that the vector-like masses contribute to its potential because if we want an anomaly, a chiral rotation must shift also  $\ell\ell^c$  and  $nn^c$  in the same way as the Yukawas. There is now a tension between experimental constraints that want the vector-like masses to be as large as possible, and the mechanism that requires sensitivity to  $\langle h \rangle$ . The best case scenario for us is that of a light neutral lepton, which is less severely constrained. We can therefore consider the parametrically simple case  $m_L \gg f_{\pi'} \gg m_N$ , where  $m_{N,L}$  are the physical masses of the charged/neutral fermions. In this case the tension is easy to spell out. If we integrate out  $\ell, \ell^c$  a simple estimate gives

$$V(\phi) \sim 4\pi f_{\pi'}^3 m_N \quad (4.49)$$

with  $m_N$  the physical mass of the lightest neutral fermion. The three contributions to  $m_N$  are  $yy_c\langle h \rangle^2/m_L$  at tree-level,  $(yy_c/16\pi^2)m_L \log \Lambda_{\text{UV}}/m_L$  from integrating out the charged fermions at one loop and  $yy_c f_{\pi'}^2/m_L$  from the new strong dynamics. If we want the first contribution to dominate we need

$$f_{\pi'} \lesssim \langle h \rangle, \quad m_L \lesssim \frac{4\pi\langle h \rangle}{\sqrt{\log \Lambda_{\text{UV}}/m_L}}. \quad (4.50)$$

Furthermore,  $m_N$  should be lighter than the confinement scale, otherwise the  $\phi$  potential is insensitive to it. The additional constraint is

$$f_{\pi'} \gtrsim \frac{yy_c\langle h \rangle^2}{4\pi m_L}. \quad (4.51)$$

These requirements make these new particles interesting for HL-LHC. A dedicated study on LHC data shows that  $\text{Tr}[F\widetilde{F}]$  is still viable experimentally as a trigger [157].

#### 4.2.4 A Possible Fourth Option?

The success of  $\text{Tr}[G\widetilde{G}]$  motivates us to try  $\text{Tr}[W\widetilde{W}]$  as a trigger. After all, neutrino masses break  $L$  and in principle we can hope to generate a potential for

$$\xi\phi\text{Tr}[W\widetilde{W}], \quad (4.52)$$

from  $SU(2)_L$  instantons that break  $B+L$ . Unfortunately it is not quite that simple. First of all, neutrino masses don't have the right quantum numbers to interfere with  $SU(2)_L$  instantons. We can think of the latter as an effective vertex with nine quark doublets and three lepton doublets coming out.

In a GUT, the natural candidate to interfere with them would be

$$\mathcal{O}_{B+L} = \frac{QQQL}{M_{\text{GUT}}^2}. \quad (4.53)$$

three insertions of  $\mathcal{O}_{B+L}$  can generate a potential for  $\phi$ . However, this potential is insensitive to  $\langle h \rangle$ . In the SM  $g_W$  grows in the UV, therefore the instanton amplitude that contains the factor

$$\int dE e^{-1/g_W^2(E)} \times \dots \quad (4.54)$$

is dominated by the largest scale in the theory  $\Lambda_{\text{UV}}$ . Taking Eq. (4.53), parametrically we get

$$V_\phi \sim \Lambda_{\text{UV}}^4 \left( \frac{\Lambda_{\text{UV}}}{M_{\text{GUT}}} \right)^3 f(\xi\phi). \quad (4.55)$$

To make use of  $\text{Tr}[W\widetilde{W}]$  to select the Higgs mass we have therefore two options: 1) we find an operator that can interfere with the  $SU(2)_L$  instantons which is sensitive to  $\langle h \rangle$  2) we make  $SU(2)_L$  confine at a scale that depends on  $\langle h \rangle$ .

Note that the first condition by itself is not enough, unless the operator that interferes with the instanton is a trigger. Let us clarify this by an example. Take

$$\mathcal{O}'_{\mathcal{B}+\mathcal{L}} = \frac{QQQL}{M_{\text{GUT}}^2} \frac{|H|^2}{M_{\text{GUT}}^2}. \quad (4.56)$$

This gives

$$V_\phi \sim \Lambda_{\text{UV}}^4 \left( \frac{\Lambda_{\text{UV}}}{M_{\text{GUT}}} \right)^6 f(\xi\phi), \quad (4.57)$$

still independent of  $\langle h \rangle$ . This might seem surprising since the equivalent of  $\mathcal{O}'_{\mathcal{B}+\mathcal{L}}$  for  $\text{Tr}[G\widetilde{G}]$  are Yukawa couplings ( $QH_u^c$ ) which are not triggers and have vevs sensitive to  $\Lambda_{\text{UV}}$ . The important difference is that  $g_s$  runs strong at a scale  $\Lambda_{\text{QCD}} < v$ , so large loop momenta are exponentially suppressed, while we have to include them for  $\text{Tr}[W\widetilde{W}]$ . To make the first option work we would need something like

$$\mathcal{O}''_{\mathcal{B}+\mathcal{L}} = \frac{QQQL}{M_{\text{GUT}}^2} \frac{H_1 H_2}{M_{\text{GUT}}^2}, \quad (4.58)$$

with no  $B\mu$ -term in the Lagrangian and the same phenomenology described in Sections 4.2.2 and 4.3 for  $H_1 H_2$ . However one might wonder why doing all this work, if in the end the actual trigger is in practice  $H_1 H_2$ . The answer might be phenomenological, since to discover the  $\text{Tr}[W\widetilde{W}]$  we would have to look for an interesting  $SU(2)_L$  axion.

The second option requires adding new  $SU(2)_L$  charged states with an  $\mathcal{O}(1)$  fraction of their mass coming from  $v$  and it must thoroughly vetted phenomenologically.

## 4.3 Collider Phenomenology of the $H_1 H_2$ Trigger: the type-0 2HDM

### 4.3.1 Masses and Couplings

In the previous Section we have described the conditions that make  $H_1 H_2$  a good weak scale trigger. We need to impose a  $Z_4$  symmetry which sets to zero  $B\mu, \lambda_6$  and  $\lambda_7$ . This gives the potential in Eq. (4.40). We also choose the  $Z_4$  charge assignment which allows only  $H_2$  to couple to the quarks and leptons:

$$V_Y = Y_u Q H_2 u^c + Y_d Q H_2^\dagger d^c + Y_e L H_2^\dagger e^c. \quad (4.59)$$

As we show in the following, even in this case it is not possible to decouple collider signatures. Many of the facts about Higgs couplings in this Section are well-known in the 2HDM literature, but we repeat them to be self-contained. For reviews we refer the reader to [158–160].

Hermiticity makes the potential in Eq. (4.40) CP-conserving. The only coupling that can have a phase is  $\lambda_5$ , but the rephasing  $H_1 \rightarrow H_1 e^{-i\arg(\lambda_5)/2}$  has no effect on the other terms in



the Lagrangian, so there is no mass mixing between CP-even and CP-odd states. The masses of the Higgs bosons in  $H_{1,2}$  are

$$\begin{aligned} m_A^2 &= -v^2 \lambda_5, \\ m_{H^\pm}^2 &= -v^2 \frac{\lambda_5 + \lambda_4}{2} \\ m_{h,H}^2 &= \frac{1}{2} \left( \lambda_1 v_1^2 + \lambda_2 v_2^2 \pm \sqrt{(\lambda_2 v_2^2 - \lambda_1 v_1^2)^2 + 4v_1^2 v_2^2 \lambda_{345}^2} \right). \end{aligned} \quad (4.60)$$

For convenience we have defined  $\lambda_{345} \equiv \lambda_3 + \lambda_4 + \lambda_5$ . This parameter sets the strength of the mixing between the two CP-even Higgses. Limits of enhanced symmetry include: 1) when  $\lambda_5 = 0$  a PQ symmetry acting on  $H_1 H_2$  is only spontaneously broken and  $A$  becomes a massless Goldstone boson, 2) when  $\lambda_4 = \lambda_5$  the potential acquires a  $SU(2)$  custodial symmetry under which  $\mathcal{H} = (H^+, iA, H^-)$  transforms as a triplet, hence  $m_A = m_{H^\pm}$ .

Measurements of Higgs couplings and low energy flavor observables require  $v_1 \lesssim v_2$ , as shown in Fig. 4.9. In this limit the SM-like Higgs  $h$  is heavier than its CP-even partner  $H$ . At leading order in  $v_1/v$  we have

$$\begin{aligned} m_h^2 &\simeq \lambda_2 v^2 \\ m_H^2 &\simeq v_1^2 \left( \lambda_1 - \frac{\lambda_{345}^2}{\lambda_2} \right). \end{aligned} \quad (4.61)$$

Eq.s (4.128) and (4.129) are interesting from a phenomenological perspective, as they imply that the new Higgses all have masses comparable to  $v$  or smaller. This is not surprising since we set to zero  $B\mu$ , the only other scale in the potential. Before discussing laboratory constraints on these new particles it is useful to take a look at their couplings to the SM at leading order in  $v_1/v$  (a more general approach to the decoupling limit was discussed in [158]). The charged and CP-odd Higgses have couplings to a pair of fermions suppressed by the small  $H_1$  vev

$$g_{H^+tb} \simeq g_{htt}^{\text{SM}} \frac{v_1}{v}, \quad g_{H^-tb^c} \simeq g_{hbb}^{\text{SM}} \frac{v_1}{v}, \quad g_{A\psi\psi} \simeq \pm g_{h\psi\psi}^{\text{SM}} \frac{v_1}{v}, \quad (4.62)$$

and no tree-level couplings to two SM gauge bosons,  $g_{H^\pm W^\mp Z} \simeq 0$ ,  $g_{H^\pm W^\mp \gamma} \simeq 0$ ,  $g_{AVV} \simeq 0$ . The coupling structure of the CP-even Higgs is slightly more complex. Its couplings also vanish in the small  $v_1/v$  limit, but there is a second relevant parameter,  $\lambda_{345}$ . If we tune its value we can take either a fermiophobic or a bosophobic limit,

$$g_{H\psi\psi} \simeq -g_{h\psi\psi}^{\text{SM}} \frac{\lambda_{345} v_1}{\lambda_2 v}, \quad g_{HVV} \simeq g_{hVV}^{\text{SM}} \frac{|\lambda_2 - \lambda_{345}| v_1}{\lambda_2 v}. \quad (4.63)$$

$\lambda_{345}$  also controls the coupling between the SM Higgs and a pair of new Higgses

$$\lambda_{hHH} \simeq \lambda_{345} v, \quad \lambda_{hAA} \simeq (\lambda_{345} - 2\lambda_5) v, \quad (4.64)$$

thus determining the decay width  $h \rightarrow HH$ . From Eq.s (4.62) and (4.63) it is clear that the new states can not be easily decoupled. Decreasing  $v_1$  reduces all couplings with a single new Higgs in the vertex, but makes  $H$  lighter. Taking  $\lambda_{345} \ll \lambda_2$  suppresses  $H$  couplings to fermions, but maximizes those to gauge bosons. If we tune  $\lambda_{345} \simeq \lambda_2$  we reduce couplings to gauge bosons, but those to fermions are unsuppressed. Phenomenologically we find that small  $\lambda_{345}$  is harder to detect, as shown in Fig. 4.9, but even in this limit  $H$  is within reach of future colliders. Notice that we need at least  $\lambda_5$  to be non-zero if we want  $A$  and  $H^\pm$  to be massive. In this case  $\lambda_{345} = 0$  does not give any extra symmetry, as can be seen for instance by inspecting one-loop RGEs [160].

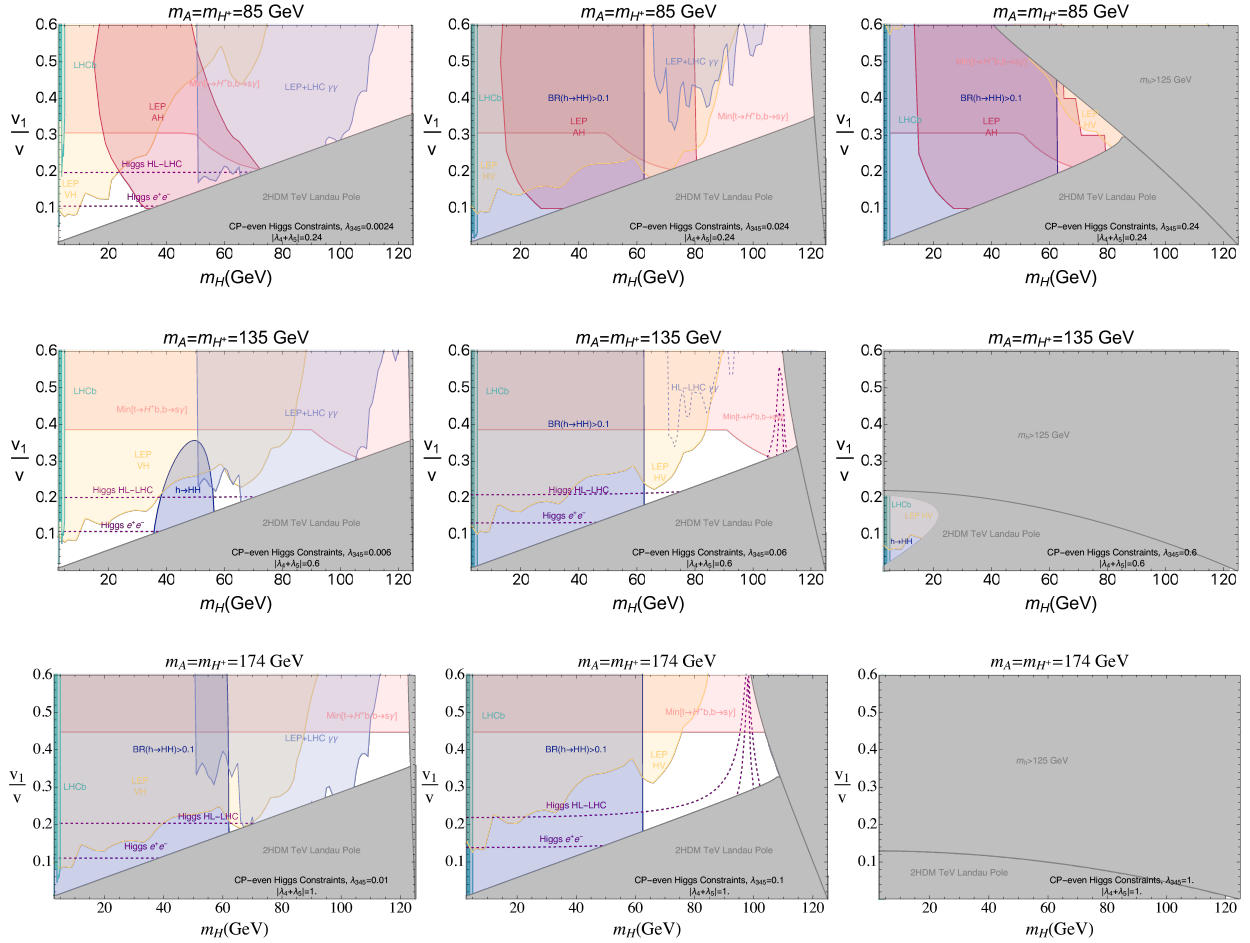


Figure 4.9: Experimental Constraints on the CP-even Higgs  $H$  for  $m_{H^\pm} = m_A$  and different values of  $\lambda_{345}$ . From top to bottom we increase  $m_{H^\pm}$ . From left to right we move from 1% tuning ( $\lambda_{345} = 0.01|\lambda_4 + \lambda_5|$ ) to natural values of the quartics ( $\lambda_{345} = |\lambda_4 + \lambda_5|$ ). In red we show the bound from  $e^+e^- \rightarrow Z \rightarrow AH$  at LEP [168] and in yellow from  $HZ$  associated production [168] followed by decays to fermions. In light blue we display the current sensitivity of  $H \rightarrow \gamma\gamma$  at LEP and the LHC [169–171] and a projection for the HL-LHC obtained rescaling [171]. In light green we show bounds from searches for  $B \rightarrow K^{(*)}H \rightarrow K^{(*)}\mu\mu$  at LHCb [172, 173]. Indirect constraints from Higgs coupling measurements (purple and blue) are discussed in Section 4.3.2. The pink shaded area shows the strongest bound point-by-point between searches for flavor changing processes, mainly  $b \rightarrow s\gamma$  [174, 175], and LHC searches for  $t \rightarrow H^+b$  [176–179]. Theoretical constraints (in gray) from low energy Landau poles and the SM Higgs mass are summarized at the beginning of Section 4.3.2.

Pair production of the new states is completely fixed, insensitive to  $v_1$  and other unknown parameters of the model. We do not list here  $HHV$ - and  $HHVV$ -type couplings, but they are  $\mathcal{O}(g)$  and  $\mathcal{O}(g^2)$ , respectively, for all three new Higgses. They can be found for instance in [159].

Now we have all the ingredients to establish if this model is still consistent with experimental constraints. The prime candidate for discovery is the CP-even Higgs, due to its relatively small mass. In the following we will see that most of the viable parameter space has already been explored by LEP and the LHC. All cross sections computed for our analysis were obtained from Madgraph 5 [161], while branching ratios and the electroweak oblique parameters [162–164] were computed with 2HDMC 1.8 [165, 166]. We draw Feynman diagrams using TikZ-Feynman [167].

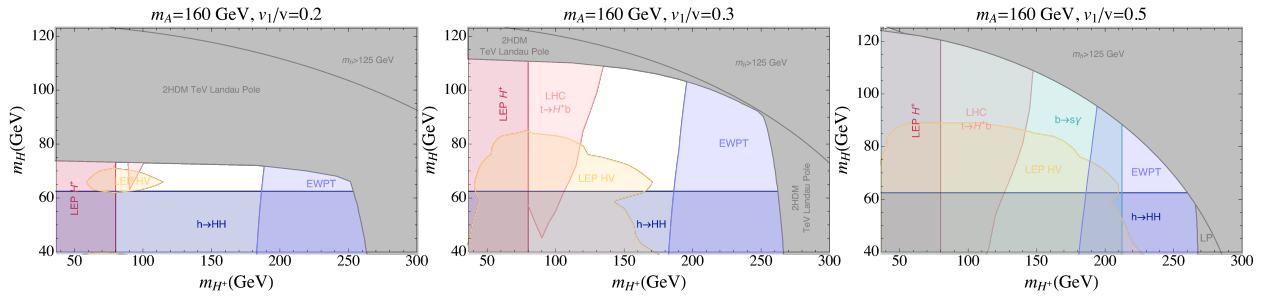


Figure 4.10: Experimental Constraints on the type-0 2HDM in the  $m_{H^\pm} - m_H$  plane (masses of the charged and new CP-even Higgses). The three panels correspond to three different choices for the vev of the new Higgs doublet  $v_1 = \langle H_1^0 \rangle = (0.2, 0.3, 0.5)v$ . The mass of the new CP-Odd Higgs  $m_A$  is fixed to 160 GeV. In all three cases we allow a 10% tuning of quartics, i.e. we take  $\lambda_3 + \lambda_4 + \lambda_5 = 0.1|\lambda_4 + \lambda_5| = 0.2(m_{H^\pm}/v)^2$ . In red we show the bound from  $H^\pm$  pair production at LEP [180, 181] and in yellow from  $HZ$  associated production and decays to fermions [168]. In light blue we display the bound from ElectroWeak Precision Tests [182] on the  $S$ ,  $T$  and  $U$  oblique parameters [163, 164]. In light green we show bounds from searches for  $B \rightarrow X_s \gamma$  [174, 175]. Indirect constraints from Higgs coupling measurements set an upper bound on  $\text{BR}(h \rightarrow HH)$  (in blue). The impact of LHC searches for  $t \rightarrow H^\pm b$  is shown in pink [176–179]. Theoretical constraints (in gray) from low energy Landau poles and the SM Higgs mass are summarized at the beginning of Section 4.3.2. At high masses there is no solution for the quartics which gives  $m_h = 125$  GeV.

### 4.3.2 Experimental Constraints

In this Section we discuss current constraints and future probes of the new Higgs doublet, which are summarized in Figs 4.10 and 4.9. The parameter  $\lambda_{345}$  is central to our discussion. It determines the maximum viable  $m_H$  from Eq. (4.128) and it sets  $H$  couplings to SM fermions and bosons in Eq. (4.63). Lower bounds on  $m_{H^\pm}^2 \sim -(\lambda_4 + \lambda_5)v^2$  and  $m_A = -\lambda_5 v^2$  determine a natural lower bound on  $\lambda_{345} = \lambda_3 + \lambda_4 + \lambda_5$ . In each panel of Figs 4.10 and 4.9 we take  $\lambda_{345}$  proportional to  $m_{H^\pm}^2$ . This explains the non-trivial dependence of  $H$  phenomenology on  $m_{H^\pm}$  in Fig. 4.10. In Fig. 4.9 we consider three different scenarios:  $\lambda_{345} = (0.01, 0.1, 1)(2m_{H^\pm}^2/v^2)$ , corresponding to three levels of tuning: 1%, 10% and no tuning. Tuning  $\lambda_{345}$  small decreases  $H$  couplings to fermions. This typically increases the allowed parameter space as shown in Fig. 4.9, but does not allow to decouple  $H$  and can lead to  $H \rightarrow \gamma\gamma$  become the dominant decay channel.

There are areas of our parameter space that are theoretically inaccessible. These are shown in gray in Figs 4.10 and 4.9. At large  $m_H$  and  $\lambda_{345}$  there is no real solution for  $\lambda_{1,2}$  that gives the observed SM Higgs mass. This happens when the argument of the square root in Eq. (4.128) becomes negative. The second set of theoretical constraints arises from running of the quartics. At large  $m_H$  and small  $v_1$ ,  $\lambda_1$  becomes large and one can get low energy Landau poles from  $d\lambda_1/dt \simeq (3/4\pi^2)\lambda_1^2$ . A similar situation occurs from the running of  $\lambda_{4,5}$  when  $m_A$  and/or  $m_{H^\pm}$  become large, as shown in Fig. 4.10. The remaining constraints in Figs 4.10 and 4.9 are discussed in the next two Subsections, starting with direct searches.

#### Direct Searches

**Charged Higgs** LEP-II gives a lower bound on the charged Higgs mass from  $H^+H^-$  pair production [180]:  $m_{H^\pm} \gtrsim 80$  GeV. This is shown in red in Fig. 4.10. The constraint on  $m_{H^\pm}$  comes from a combination of  $\tau\nu$  and  $cs$  final states and assumes the absence of  $H^\pm \rightarrow W^\pm H$  decays. In the presence of a light neutral Higgs  $m_H = 12$  GeV the bound is slightly relaxed to

$m_{H^\pm} \gtrsim 73$  GeV [180]. Note that the direct searches at LEP were performed for  $m_{H^\pm} > 38$  GeV. Masses below 39.6 GeV are excluded by measurements of the  $Z$  boson width [181] which receives a contribution from the charged Higgs [183]. The LHC is mostly sensitive to  $H^\pm$  production via top decays. Just like the  $Z$ , the top has a small width from electroweak interactions  $\Gamma_t \simeq \text{GeV}$ , so the branching ratio  $t \rightarrow H^+b$  can be sizeable given that it is proportional to the top Yukawa coupling. We find that LHC searches for  $t \rightarrow H^+b$  with  $H^+ \rightarrow \tau^+\nu_\tau$  and  $H^+ \rightarrow c\bar{s}$  [176–179] are sensitive to  $\text{BR}(t \rightarrow H^+b)$  down to a few percent. The bound is shown in pink in Figs 4.10 and 4.9. When the mass difference between  $H^\pm$  and  $A$  becomes  $\mathcal{O}(m_W)$ , also the decays  $H^\pm \rightarrow W^\pm A$  become relevant [184], but we do not consider this parameter space in our analysis since it is disfavored by bounds on  $h \rightarrow AA$  and Electroweak precision measurements. For larger  $m_{H^\pm}$ , when top decays are not kinematically allowed, direct searches for  $H^\pm$ , that typically target  $pp \rightarrow \bar{t}bH^+$  and decays to  $tb$  and  $\tau\nu$ , are not yet sensitive to our parameter space [176, 185–192]. To conclude this brief overview of the charged Higgs, it is interesting to notice that a CMS search for stau pair production [193] has a sensitivity comparable to LHC searches targeting  $H^+$  single production. The latter can be decoupled by making  $v_1$  small, while pair production rates are fixed by gauge invariance. In the CMS search the staus decay to  $\tau$ 's plus a light neutralino ( $m_\chi = \text{GeV}$ ). The analysis is thus sensitive to  $pp \rightarrow H^+H^- \rightarrow \tau^-\tau^+\nu_\tau\bar{\nu}_\tau$ . Naively superimposing the cross section limit from this search with  $H^+H^-$  VBF production gives a bound  $m_{H^\pm} \gtrsim 150$  GeV. The DY pair production cross section is too small and does not give a constraint. This shows that the LHC can already set a (almost) model-independent bound on  $H^\pm$  and warrants a more detailed analysis.

**CP Even Higgs** LEP searches target mainly associated production  $e^+e^- \rightarrow HZ$ , which is controlled by the coupling  $g_{HVV}$  in Eq. (4.63). The most sensitive channel is  $H \rightarrow \bar{b}b$  for  $m_H > 2m_b$  [168], but even below this threshold LEP retains a comparable cross section sensitivity (down to  $2m_\mu$ ) by targeting different decays [194]. The strongest constraint above  $2m_b$  is set by the combined searches for  $HZ$  production by the four LEP experiments [168]. This is shown in yellow in Figs 4.10 and 4.9. The bound has a non-trivial dependence on  $\lambda_{345}$ . When  $\lambda_{345} \ll \lambda_2$  the decays to SM fermions targeted by LEP are suppressed, but  $HZ$  production is enhanced. In this limit our new CP even Higgs is fermiophobic and searches for  $e^+e^- \rightarrow HZ \rightarrow \gamma\gamma Z$  become relevant. The LEP bound [169] dominates the light blue shaded area in Fig. 4.9 for  $m_H \lesssim 65$  GeV. When  $\lambda_{345} \simeq \lambda_2$ , the coupling to the  $Z$  is as small as it can be:  $g_{HVV} \simeq \mathcal{O}(v_1^3/v^3)$ , but the decay to  $\bar{b}b$  is enhanced compared to the limit  $\lambda_{345} \ll \lambda_2$ .

To conclude the discussion of LEP constraints, it is interesting to notice that if we compare the model-independent VBF cross-section  $e^+e^- \rightarrow HH\nu_e\nu_e$  with LEP pair production constraints [168] we find sensitivity in the mass range  $10 \text{ GeV} \lesssim m_H \lesssim 25 \text{ GeV}$ . This is a bound that relies only on the electroweak doublet nature of  $H_1$ . It applies to a Higgs decaying mostly to  $\bar{b}b$ . LEP searches for  $HH$  are optimized for CP-violating couplings, but the signal topology is not appreciably affected by the CP properties of the couplings [168]. However this is a rough estimate of the actual constraint (given also that the search is not designed for VBF production) and it would be interesting to perform a dedicated collider study.

The main LHC constraints on  $H$  arise from measurements of Higgs couplings, discussed in the next Section, and direct searches for  $H \rightarrow \gamma\gamma$  [170, 171]. As noted above, when  $\lambda_{345} \ll \lambda_2$  the CP-even Higgs couplings to fermions are suppressed and its BR to  $\gamma\gamma$  becomes  $\mathcal{O}(1)$ . The LHC bounds on  $H \rightarrow \gamma\gamma$  is shown in light blue in Fig. 4.9.

Other direct searches for SM and BSM Higgses,  $H \rightarrow \gamma\gamma$  [170, 171, 195–206],  $H \rightarrow \tau^+\tau^-$  [207–220],  $H \rightarrow \mu^+\mu^-$  [221–227],  $H \rightarrow \bar{b}b$  [228–237],  $H \rightarrow Z\gamma$  [238],  $H \rightarrow W^+W^-$ ,  $ZZ$  [239–253] and  $H \rightarrow ZA$  [254–257], give weaker constraints than the indirect probes discussed in the next Section and shown in Fig. 4.9.

At lower masses,  $0.3 \text{ GeV} \lesssim m_H \lesssim 5 \text{ GeV}$ , we have constraints from LHCb searches for rare  $B$  meson decays [172], from the CHARM beam dump experiment [135, 258] and excess cooling of

SN1987A [136,259]. For  $\lambda_{345} \gtrsim 10^{-2}$  both these constraints and the LHC bound on  $\Gamma(h \rightarrow HH)$ , discussed in the next Section, exclude the whole mass range. At lower values of  $\lambda_{345}$  all the probes of a low mass Higgs, which are mainly sensitive to the coupling to fermions  $g_{H\psi\psi} \sim \lambda_{345}/\lambda_2$ , loose sensitivity. However proposals for future beam dump experiments [260–262], the HL-LHC projections for LHCb [263] and proposed long-lived particle experiments [263–266] can cover most of the viable parameter space down to the lowest masses that we consider:  $m_H \simeq 300$  MeV.

**CP Odd Higgs** In the mass range  $0.3 \text{ GeV} \lesssim m_A \lesssim 5 \text{ GeV}$ ,  $A$  is excluded by LHCb searches for  $B \rightarrow K^{(*)}\mu\mu$  [172] and by the CHARM beam dump experiment [135,258]. The only exception are two mass windows ( $[2.95, 3.18]$  GeV and  $[3.59, 3.77]$  GeV) vetoed from the LHCb analysis to suppress the backgrounds from  $J/\psi$  and  $\psi'$  production. Furthermore,  $A$  can be lighter than  $m_h/2$  only if  $H$  is heavier than  $m_h/2$  due to the indirect constraint on  $\Gamma(h \rightarrow AA)$  and  $\Gamma(h \rightarrow HH)$  discussed in the next Section. For  $m_A < 145$  GeV direct searches for  $e^+e^- \rightarrow H_1H_2$  at LEP [168] exclude a large fraction of our parameter space due to the large  $AH$  production cross section at the  $Z$  pole,

$$g_{ZAH} \simeq -\frac{g}{2c_{\theta_W}}(p_A + p_H). \quad (4.65)$$

This is shown in red in Fig. 4.9. We do not show this constraint in Fig. 4.10 since it completely overlaps with other bounds. LHC searches for BSM and SM Higgses, listed for the CP even Higgs, do not add new constraints to our parameter space. The only exception are LHC searches for  $pp \rightarrow A \rightarrow ZH$  and  $pp \rightarrow A \rightarrow Zh$  [267–271]. For  $m_A \gtrsim 220$  GeV the LHC is already sensitive to an interesting range of our parameter space [271]. Most of this region is already excluded by the presence of low energy Landau poles, but a more detailed experimental study would be interesting.

Finally we can consider a light axion-like  $A$ , with  $m_A \ll v$ . However to be consistent with experiment this possibility requires  $v_1 \ll \Lambda_{\text{QCD}}$ , to suppress the couplings of  $A$  to the SM. This forces also  $H$  to be light, at odds with LHC bounds on  $\text{BR}(h \rightarrow HH)$  discussed in the next Section.

## Indirect Constraints

Measurements of low energy flavor changing processes, such as  $B \rightarrow X_s\gamma$  and  $B \rightarrow \tau\nu$ , are powerful probes of our charged Higgs [272,273]. In both cases the charged Higgs contributes at the same order as the leading SM diagram, given by a  $W$  boson exchange. If we include other well-measured processes sensitive to the charged Higgs ( $B \rightarrow K^*\gamma$ ,  $B_s \rightarrow \mu^+\mu^-$ ,  $D_s \rightarrow \tau\nu$ ,  $B \rightarrow K^{(*)}l^+l^-$ ,  $R_D$ ,  $R_{D^*}$  and  $B_s \rightarrow \phi\mu^+\mu^-$ ) [175], we find the bound in light green in Fig. 4.10 and in pink in Fig. 4.9.

The second set of indirect constraints that we need to consider arises from LHC measurements of SM Higgs couplings. At small  $v_1$  and fixed masses they read

$$\frac{g_{hVV} - g_{hVV}^{\text{SM}}}{g_{hVV}^{\text{SM}}} \simeq -\frac{v_1^2}{2v^2} \left(1 - \frac{\lambda_{345}v^2}{m_h^2 - m_H^2}\right)^2, \quad \frac{g_{h\psi\psi} - g_{h\psi\psi}^{\text{SM}}}{g_{h\psi\psi}^{\text{SM}}} \simeq -\frac{v_1^2}{2v^2} \left(1 - \frac{\lambda_{345}v^4}{(m_h^2 - m_H^2)^2}\right) \quad (4.66)$$

so  $v_1 \lesssim v$  insures that couplings to both vector bosons and fermions are consistent with experiment. As  $m_H$  approaches the SM Higgs mass at fixed  $\lambda_{345}$ , the sensitivity to  $v_1/v$  increases. We also have regions where  $\lambda_{345}v^2 \simeq m_h^2 - m_H^2$  and most sensitivity is lost. In Fig. 4.9 we show in purple projections for the HL-LHC and a future lepton collider at  $1\sigma$ . We take projected sensitivities from Table 1 in [274]<sup>5</sup>. To represent future lepton colliders we use ILC with unpo-

<sup>5</sup>This choice is conservative as it allows the presence of additional new physics that modifies Higgs couplings. In our model alone, we could have used a more constrained fit with two universal coupling modifiers for fermions and bosons and a free width to new particles.

larized beams and  $\sqrt{s} = 250$  GeV. Current bounds from the LHC [275, 276] are not shown in the Figure. They give the bound  $v_1/v \lesssim 0.45 \div 0.55$  and completely overlap with other constraints. The only exception are new decay modes of the SM Higgs. The new CP-even Higgs  $H$  is lighter than the SM Higgs. So for small enough  $m_H$  we also have to consider the new decay width  $\Gamma(h \rightarrow HH)$ . Direct searches for decays to four SM particles via two intermediate states,  $h \rightarrow HH \rightarrow 4\text{SM}$  [277–282], are less constraining than the indirect bound set by the dilution of SM branching ratios. LHC measurements of Higgs couplings give an upper bound on  $\lambda_{345}$  if  $m_H < m_h/2$ , from Eq. (4.64). If we consider the latest ATLAS combination of Higgs couplings measurements [276], we have a global signal strength  $\mu = 1.06 \pm 0.07$ . From CMS [275] we have  $\mu = 1.02_{-0.06}^{+0.07}$ . A very rough combination, assuming uncorrelated Gaussian errors, gives a  $2\sigma$  error  $\delta\mu_{95\%} \simeq 0.1$ . This implies  $\text{BR}(h \rightarrow HH) \lesssim 0.1$  at  $2\sigma$  and hence  $\lambda_{345} \lesssim 10^{-2}$ . If we restrict ourselves to the Yukawa couplings in Eq. (4.59) there is not much that we can do to relax this constraint. For example, increasing  $g_{hbb}$  to compensate for the new decay mode decreases  $g_{hVV}$ , as shown in Eq. (4.66). In more generality, barring detailed constructions that exploit flat directions in Higgs couplings constraints, we need  $\lambda_{345} = \mathcal{O}(10^{-2})$  for  $m_H < m_h/2$ , given our current knowledge of Higgs couplings. This is shown in Fig. 4.9. When we tune  $\lambda_{345}$  to be small we have no constraint, while in the more natural parameter space  $m_H < m_h/2$  is excluded. Note that if we take  $\lambda_{345}$  small the same reasoning leads to  $m_A > m_h/2$ , since  $\lambda_{hAA} \simeq (\lambda_{345} - 2\lambda_5)v$ .

To conclude, ElectroWeak Precision Tests [182], mainly the  $S$ ,  $T$  and  $U$  oblique parameters [163, 164] constrain mostly the mass difference between  $A$  and  $H^\pm$  that breaks the custodial symmetry. The bound is displayed in light blue in Fig. 4.10. A more detailed analytical discussion of oblique parameters, custodial symmetry and CP in 2HDMs can be found in [283, 284].

## 4.4 Crunching Dilaton

In the previous Section we have discussed in detail one generic feature of most models of cosmological naturalness, the existence of weak scale triggers. It is now time to put our triggers to work and discuss explicit models of cosmological selection of the weak scale. The example discussed in this Section is atypical, in the sense that it uses an imperfect trigger:  $|H|^2$ .

In this Section we review the ideas first presented in [285]. We introduce a model where the dilaton of a TeV-scale extra-dimension crunches all the patches of the Multiverse with the “wrong” Higgs mass squared. By crunching we mean that in all these patches a scalar field quickly rolls to a deep minimum where the cosmological constant is large and negative, say  $\Lambda_{\text{CC}} \simeq -M_{\text{GUT}}^4$ , independently of the positions in their potential of the other moduli that form the landscape.

### The Basic Concept

We assume a landscape of Higgs mass and cosmological constant values with a cutoff at the scale  $\Lambda$ :

$$V_H(H) = -m_{H,i}^2 |H|^2 + \lambda(|H|^2)^2 \quad (4.67)$$

where a typical  $m_{H,i}^2$  is  $\mathcal{O}(\Lambda^2)$ . We remain agnostic as to how this landscape is generated and populated. We introduce dynamics which can support the expansion of the universe only when the Higgs VEV,  $h \equiv \langle H^0 \rangle$ , is in a finite range,

$$H_I \lesssim h_{\text{min}} \lesssim h \leq h_{\text{crit}} \simeq \mathcal{O}(1 \text{ TeV}), \quad (4.68)$$

and cause an immediate crunch for other values. In the above equation  $H_I$  is Hubble during inflation. Such dynamics excludes all positive and large negative mass terms for the Higgs,

and only values of the VEV below the weak scale survive inflation. The mechanism is not sensitive to the minimal value  $h_{\min}$ , which can be generated in many ways briefly discussed in the Cosmological Constraints Section below.

The dynamics needed to achieve this is based on the mixing of the Higgs with a spontaneously broken CFT—or a bulk Higgs in the AdS picture with the Higgs potential, Eq. (4.73), on the UV brane. The CFT is spontaneously broken via the Goldberger-Wise (GW) mechanism, with the GW minimum for the dilaton  $\langle\chi\rangle = \chi_{GW}$  at a value of the potential above  $\Lambda^4$  and the scale of inflation  $M_I^4 \simeq M_{\text{Pl}}^2 H_I^2$ , so that the total vacuum energy in this minimum is always negative, even during the slow-roll regime of inflation. Any patch in which the dilaton has reached this minimum crunches. The heart of our mechanism is the generation of a second minimum for the dilaton by the bulk Higgs VEV, for which the vacuum energy is subdominant to the inflaton vacuum energy; any patch in this second minimum then goes through inflation without crunching. This minimum only exists for a finite range of small Higgs VEVs, set by the parameters of the bulk Higgs. Therefore, only this range of VEVs survive after inflation and until today. These small values are not typical in the landscape, thus generating a hierarchy and an apparent naturalness problem. We assume that one of the usual mechanisms (such as scanning in the multiverse plus anthropic selection) ensures a small positive CC in the shallower metastable minimum, while it cannot overcome the large negative energy of the true minimum.

## RS model

We use the 5D warped description [82] of the CFT with the Higgs field in the bulk of AdS space

$$ds^2 = \left(\frac{R}{z}\right)^2 (\eta_{\mu\nu} dx^\mu dx^\nu - dz^2). \quad (4.69)$$

Here  $R = 1/k$  is the AdS curvature and the location of the UV brane, while  $R'$  is the location of the IR brane, with  $\chi = 1/R'$  identified with the dilaton/radion field [84, 286, 287]. Note that the dilaton defined this way is not canonically normalized—its kinetic term is

$$\frac{3(N^2 - 1)}{4\pi^2} (\partial_\mu \chi)^2, \quad (4.70)$$

where  $N$  is the number of colors in the dual CFT picture, related to the 5D parameters by  $N^2 - 1 = 16\pi^2 (M_* R)^3$ , where  $M_*$  is the 5D Planck scale.

The Goldberger-Wise (GW) stabilization field [85] gives rise to the usual GW potential for the dilaton [84] that we parametrize as

$$V_{\text{GW}}(\chi) = -\lambda\chi^4 + \lambda_{\text{GW}} \frac{\chi^{4+\delta}}{k^\delta}. \quad (4.71)$$

We imagine that the GW minimum is at large negative values of the potential, such that the negative CC generated when  $\chi$  is at this minimum is larger than any other scale in the theory and leads to a rapid cosmic crunch. The  $\chi^4$  term is scale-invariant and in the RS framework can be understood as the effect of some mistuning of the tension of the IR brane and the bulk CC. The  $\chi^{4+\delta}$  term is the effect of the small explicit breaking<sup>6</sup> of scale invariance by an operator with anomalous dimension  $\delta$  in the 4D CFT. In the RS picture it is generated by the GW scalar bulk mass.

The novel pieces of the effective potential (valid below the warped-down local cutoff  $\Lambda_{IR}$ ) necessary for generating the Higgs-dependent second minimum are

$$V_{H\chi}(\chi, H) = \lambda_2 |H|^2 \frac{\chi^{2+\alpha}}{k^\alpha} - \lambda_{H\epsilon} |H|^2 \frac{\chi^{2+\alpha+\epsilon}}{k^{\alpha+\epsilon}} - \lambda_4 |H|^4 \frac{\chi^{2\alpha}}{k^{2\alpha}}, \quad (4.72)$$

---

<sup>6</sup>The dilaton is a non-compact Goldstone boson, thereby evading the type of generic problems a shift symmetric relaxation field poses [288].

and we assume that the couplings  $\lambda$ ,  $\lambda_{\text{GW}}$ ,  $\lambda_2$ ,  $\lambda_{H\epsilon}$ , and  $\lambda_4$  are all positive. These additional terms can be easily generated from interactions localized on the IR brane. We assume that the Higgs field is sourced on the UV brane where the usual  $\chi$ -independent part of the potential

$$V_H(H) = -m_{H,i}^2 |H|^2 + \lambda(|H|^2)^2 \quad (4.73)$$

arises from. We assume that the dynamics responsible for populating the landscape are localized on the UV brane and thus it is the coefficients of the UV Higgs potential that are being scanned. The scanning of the quartic changes our results only by  $\mathcal{O}(1)$  factors and so we focus only on the scanning of the Higgs mass. Due to our assumption of a UV localized landscape the bulk parameters are not being scanned. It would be interesting to consider the effect of scanning the bulk parameters as well, which we leave for future work. For simplicity we also assume that dimensionless couplings on the UV brane are not scanned, so we can straightforwardly apply Weinberg's argument to anthropically select a small CC in our Universe. This can be realized for example in a "friendly landscape" construction [105].

If the bulk mass of the Higgs is  $m_b^2$  (in units of  $R$ ) the Higgs VEV profile along the extra dimension will be of the form

$$H(z) = \frac{H_+}{\sqrt{R}} \left(\frac{z}{R}\right)^{2+\sqrt{4+m_b^2}} + \frac{H_-}{\sqrt{R}} \left(\frac{z}{R}\right)^{2-\sqrt{4+m_b^2}}, \quad (4.74)$$

with  $H_+ + H_- = |H|$  the UV brane VEV. Assuming to leading order a Neumann boundary condition on the IR brane we find  $H_+/H_- = \frac{2+\Delta}{2-\Delta} \left(\frac{R}{R'}\right)^{2\Delta}$ , where  $\Delta = \sqrt{4+m_b^2}$ . Solving for  $H_{\pm}$  we find the expression of the bulk Higgs field on the IR brane to be given by

$$H_{\text{IR}} = H_{\text{UV}} \left(\frac{R'}{R}\right)^{2-\Delta} \frac{2-\Delta}{2+\Delta}. \quad (4.75)$$

Introducing  $\alpha \equiv 2\Delta - 2$  we find that the IR brane value of the Higgs VEV will scale as

$$H_{\text{IR}} \propto H_{\text{UV}} \chi^{\frac{\alpha}{2}-1}. \quad (4.76)$$

We take  $\alpha$  to be small and positive, so  $m_b^2 \simeq -3$ . In accordance with Eq. (4.74) this implies a Higgs field approximately linear in  $z$ . Let us now consider the effect of an IR brane-localized Higgs quartic self-coupling  $\mathcal{L}_{\text{IR}} = \sqrt{g}\lambda_4 |H|^4|_{z=R'}$ . Using the AdS metric and the usual identification  $\chi = 1/R'$  we find that this term will give rise to a potential term

$$\lambda_4 |H_{\text{UV}}|^4 \chi^{2\alpha}. \quad (4.77)$$

Similarly, an IR-localized Higgs mass term will produce the  $|H|^2 \chi^{2+\alpha}$  term. If we also introduce localized terms that include the GW scalar  $\Phi \sim z^\epsilon$ , or any other field with an approximately marginal dimension, we obtain a modified quadratic term of the form  $|H|^2 \chi^{2+\alpha+\epsilon}$ , completing the terms outlined in Eq. (4.72).

**CFT interpretation** The detailed CFT interpretation of this mechanism is a spontaneously broken conformal sector, stabilized by the VEV of a marginal operator  $\mathcal{O}_{\text{GW}}$ , as in the standard GW stabilization of the dilaton. The "techni-quarks" of the CFT sector are charged under the EW gauge group and can form an  $SU(2)$  doublet operator  $\mathcal{O}_H$  of dimension  $3 + \alpha/2$  which couples linearly to a fundamental Higgs, i.e.  $\mathcal{O}_H^\dagger H$ . If we also assume the presence of a marginal operator needed for GW stabilization  $\mathcal{O}_\epsilon$  of dimension  $4 + \epsilon$ , which may or may not be the same operator as  $\mathcal{O}_{\text{GW}}$ , the deformations in the UV action are given by

$$\tilde{\lambda}_H \mathcal{O}_H^\dagger H + \tilde{\lambda}_\epsilon \mathcal{O}_\epsilon. \quad (4.78)$$

Expanding the effective potential for these terms in the IR, we reproduce the potential of Eq. (4.72). In essence, the fundamental Higgs acts as an additional stabilizing force on the CFT, generating a second stable minimum for the dilaton.



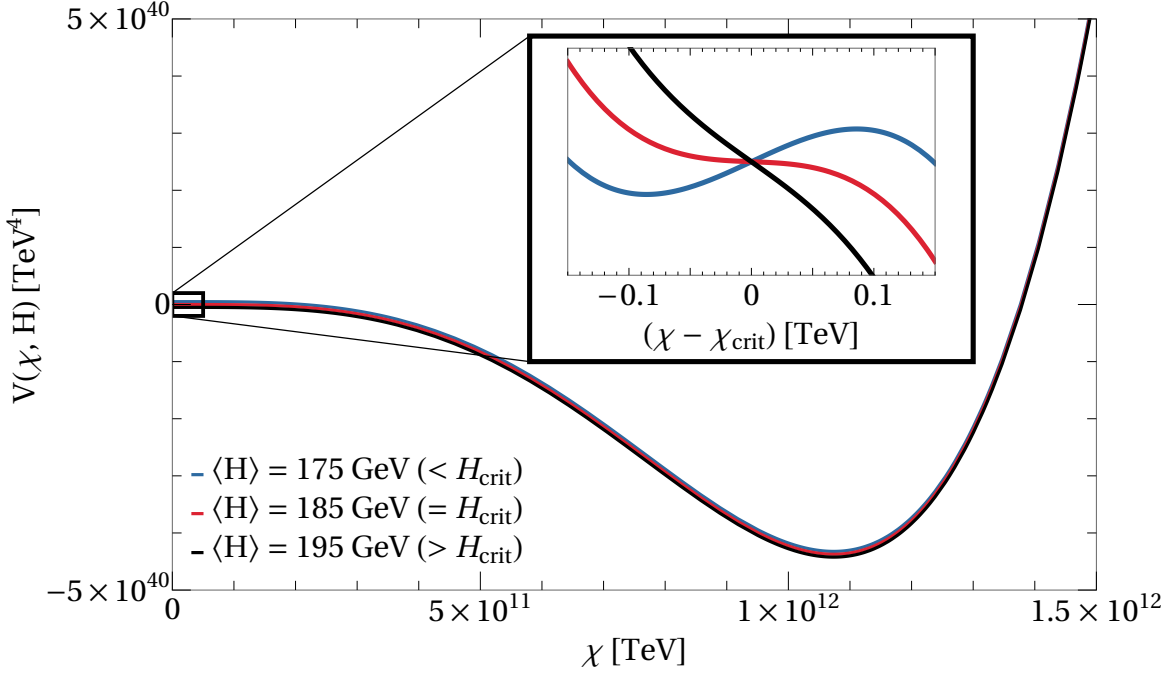


Figure 4.11: The dilaton potential  $V(\chi, H) = V_{\text{GW}}(\chi) + V_{H\chi}(\chi, H)$  for three different values of the Higgs VEV  $\langle h \rangle$ , using  $k = 10^8$  TeV,  $\lambda_{\text{GW}} = 1.2 \times 10^{-5}$ ,  $\lambda = 1.1\lambda_{\text{GW}}$ ,  $\lambda_2 = 0.005$ ,  $\lambda_{H,\epsilon} = 0.018$ ,  $\lambda_4 = 3$ ,  $\delta = 0.01$ ,  $\alpha = 0.05$ , and  $\epsilon = 0.1$ . The true vacuum is depicted in the main figure while the second minimum is visible in the inset; note the potentials are shifted so that the inflection point  $\chi_{\text{crit}}$  lies at the origin.

### Dynamics of the dilaton-Higgs potential

Let us now investigate the dynamics resulting from the Higgs-dilaton potential  $V(\chi, H) = V_{\text{GW}}(\chi) + V_{H\chi}(\chi, H) + V_H(H)$ , where  $V_{\text{GW}}$  and  $V_{H\chi}$  are given in Eqs. (4.71)–(4.72) and  $V_H$  is the UV brane-localized SM Higgs potential in Eq. (4.73). To ensure that the Higgs mass is still dominated by  $V_H$  we take the exponent  $\alpha$  in Eq. (4.72) to be positive and not too large, implying  $m_b^2 \simeq -3$  (and hence a Higgs field linear in  $z$ ). We also take  $V_{\text{GW}}$  to be subdominant to  $V_{H\chi}$  at small values of  $\chi$ , around the  $V_{H\chi}$  minimum.

For a finite range of Higgs values the  $\chi$  potential admits two minima, one generated by  $V_{\text{GW}}$  and the other by  $V_{H\chi}$ . Above the critical value of the Higgs VEV  $h_{\text{crit}}$  the latter disappears, leaving only the GW minimum (see Fig. 4.14). The minimum also disappears when the Higgs VEV is zero. The Higgs VEV in our part of the universe must be smaller than  $h_{\text{crit}}$ , or the dilaton would have rolled down to the GW minimum, resulting in a crunch. Hence, there is no tuning associated with the Higgs VEV.

If we neglect  $V_{\text{GW}}$  at small  $\chi$ ,  $h_{\text{crit}}$  can be computed by finding the value of  $h$  for which  $\partial_\chi V_{H\chi}$  has only one zero:

$$h_{\text{crit}} = k \left( \frac{\lambda_2}{\lambda_{H\epsilon}} \frac{4 - \alpha^2}{(2 + \epsilon)^2 - \alpha^2} \right)^{\frac{1-\alpha/2}{\epsilon}} \sqrt{\frac{\lambda_2}{\lambda_4} \frac{\epsilon(2 + \alpha)}{2\alpha(2 - \alpha + \epsilon)}}. \quad (4.79)$$

For  $h \lesssim h_{\text{crit}}$ , we can also estimate the second minimum of the  $\chi$  potential as

$$\chi_{\text{min}} \simeq \left( \frac{h^2}{k^\alpha} \frac{2\alpha\lambda_4}{(2 + \alpha)\lambda_2} \right)^{\frac{1}{2-\alpha}} \quad (4.80)$$

neglecting the  $\lambda_{H\epsilon}$  term, which is suppressed at the minimum by  $(\chi_{\text{min}}/k)^\epsilon$  relative to  $\lambda_2$ . For small  $\epsilon$  a mild hierarchy between couplings  $\lambda_2 \lesssim \lambda_{H\epsilon}$  can generate a large hierarchy of scales  $h_{\text{crit}}, \chi_{\text{min}} \ll k$ .

$\chi_{\min}$  sets the size of the extra dimension, hence determining the mass scale of new states potentially observable at colliders. The little hierarchy problem is reflected in the need to impose a mild hierarchy  $h/\chi_{\min} \lesssim 0.1$ . This implies a hierarchy of couplings  $\lambda_2, \lambda_{H\epsilon} < 10^{-2}\alpha\lambda_4$ . The resulting tuning (along with the NDA for these couplings) is discussed in detail at the end of this Subsection.

The most interesting consequence of this little hierarchy is the prediction of a light dilaton. Its mass for small  $\epsilon$ ,  $\alpha$  and  $\delta$  is

$$m_\chi \simeq m_h \sqrt{\frac{h}{\chi_{\min}} \frac{\pi \sin \theta}{\sqrt{6}N} - \frac{8\pi^2(\lambda - \lambda_{\text{GW}})}{N^2} \frac{\chi_{\min}^2}{m_h^2}}, \quad (4.81)$$

where

$$\sin \theta \sim \frac{(\lambda_2 - \lambda_{H\epsilon}) h \chi_{\min}}{N m_h^2} \quad (4.82)$$

parametrizes the dilaton mixing with the Higgs.

As stated above, the previous analysis is valid only if the GW potential is subleading to  $V_{\chi H}$  around  $\chi_{\text{crit}}$ , leading to an upper bound  $\lambda \sim \lambda_{\text{GW}} \lesssim \lambda_2^2/\lambda_4$ . If  $V_{\text{GW}}$  dominates over  $V_{\chi H}$  at  $\chi_{\text{crit}}$ , it washes out the metastable minimum.

We have seen that the phenomenologically successful models require small values of the couplings  $\lambda_2$ ,  $\lambda$  and  $\lambda_{\text{GW}}$ , which in turn will necessitate some tuning in the theory. Here we explain the underlying reasons and quantify the amount of tuning needed to achieve these small values of the couplings. We can easily understand the main reason behind the need for small couplings. First, there is an upper limit on the brane-localized Higgs quartic  $\lambda_4 \lesssim 3$  imposed by requiring that a Landau pole does not appear before we hit at least a few KK modes. The value of  $\chi$  at the metastable minimum sets the masses of KK modes for the bulk electroweak gauge bosons, which would appear as  $W'$  and  $Z'$ -type states. To avoid the LHC bounds [289, 290] on these  $W'$ ,  $Z'$  states we need  $\chi$  to be larger than 1 TeV. However, as we have seen Eq. (7) then leads to  $\lambda_4/\lambda_2 \gtrsim 10^2$ , and hence  $\lambda_2 \lesssim 10^{-2}$ . Finally, we must ensure that the GW part of the potential does not overwhelm the metastable minimum, by simply imposing the condition that at  $\chi \sim 1$  TeV the GW potential is smaller than the minimum value of the Higgs dependent part in Eq. (5). This yields  $\lambda, \lambda_{\text{GW}} \lesssim 10^{-5}$ . These values are quite a bit smaller than one would expect from simple NDA in a warped extra dimension. For example, consider the NDA for the coupling  $\lambda_2$ . This is the coefficient of an IR brane-localized mass term for the bulk Higgs scalar of the form

$$\int d^4x \sqrt{g^{\text{ind}}} \tilde{\lambda}_2 |H|^2|_{z=R'}, \quad (4.83)$$

where  $H$  is the dimension 3/2 bulk scalar field and  $\tilde{\lambda}_2$  is a dimension one coupling. Consider the contribution of a brane-localized loop of gauge fields to  $\tilde{\lambda}_2$ ; it is a quadratically divergent 4D loop giving the simple NDA estimate  $\tilde{\lambda}_2 \sim \frac{\Lambda_{\text{UV}}^2}{16\pi^2} g_5^2$ , where  $\Lambda_{\text{UV}}$  is the unwarped global cutoff and  $g_5$  is the bulk gauge coupling. To obtain the NDA value of the  $\lambda_2$  coupling we need to include the  $(R/R')^4$  factor from  $\sqrt{g}$ , use the scaling (4.76) for the expression of the Higgs field on the IR brane, define the local cutoff  $\Lambda_{\text{IR}} = \Lambda_{\text{UV}} \frac{R}{R'}$ , and assume  $g_5^2 \sim R$ . This will lead to the NDA estimate of  $\lambda_2$ :

$$\lambda_2 \sim \frac{1}{16\pi^2} \frac{\Lambda_{\text{IR}}^2}{\chi^2} \quad (4.84)$$

Note that  $\lambda_2$  will also get a contribution from bulk loops. However, since the brane term dominates the NDA, we restrict ourselves to that. Similarly, the NDA estimate for the GW quartic  $\lambda$  has been presented in [291] and is given by  $\lambda \sim \frac{1}{16\pi^2} \frac{\Lambda_{\text{IR}}^4}{\chi^4}$ . We can see that in order to minimize the tuning we should lower the local cutoff scale such that  $\Lambda_{\text{IR}} \lesssim \chi$ . In this case the

natural value for  $\lambda_2$  will be approximately  $\sim 10^{-2}$  as needed. Depending on the actual value of  $\Lambda_{\text{IR}} \lesssim \chi$  there may be some tuning still left in the the GW potential. For example, if  $\Lambda_{\text{IR}} \sim \chi$  we get a tuning of around a percent corresponding to the usual little hierarchy problem. If the Higgs VEV was a factor of  $\sim 10$  larger the NDA value for  $\lambda$  would have been sufficiently small since  $\chi$  could also have increased.

Whether one can achieve  $\Lambda_{\text{IR}}/\chi \lesssim 1$  depends on the particular UV completion of the theory. In a generic RS model, we expect  $\Lambda_{\text{IR}}$  to be the local warped down 5D cutoff, given by the lower of the gravitational or gauge cutoffs, where  $\Lambda_{\text{gravity}}^3 \sim 24\pi^3 M_*^3$  and  $\Lambda_{\text{gauge}} \sim 24\pi^3/g_5^2$ . Either way one expects  $\Lambda_{\text{IR}} > \chi$ . However, this is an upper bound on the cutoff, and one can of course always lower it by introducing additional new physics. For example, in a supersymmetric version of the RS model, the divergent contributions to the couplings vanish when SUSY is unbroken, and therefore  $\Lambda_{\text{IR}}$  will be set by the SUSY breaking scale on or near the IR brane. In this setting one may impose that the bulk is supersymmetric, while SUSY is broken on the UV brane (and also spontaneously broken on the IR brane to allow the generation of the dilaton quartic  $\chi^4$ ). This would be along the lines of [292], and imply that the fields in the bulk have light superpartners. While a complete discussion of such a setup is beyond the scope of this work, we outline a simple scenario without tuning. A high SUSY breaking scale on the UV brane ensures that all sfermions are ultra-heavy. The structure of SUSY breaking on the UV brane keeps the electroweak gauginos and Higgsinos light, of order a few hundred GeV, as in split SUSY models. In this case the IR brane cutoff relevant for  $\lambda$  would be lowered to the gaugino mass scale and  $\lambda \simeq 10^{-5}$  would be fully natural.

Finally it is useful to consider also the bounds on  $N$ . Requiring that the 5D gravitational theory is not strongly coupled (i.e. the 5D AdS scalar curvature  $20/R^2$  is smaller than the 5D cutoff  $\Lambda_{\text{gravity}}^3 \sim 24\pi^3 M_*^3$ ) yields  $N \gtrsim 3$ . Assuming that the gravitational KK modes have approximately the same  $1/N$  suppression as the weak gauge KK modes, and using the matching of weak gauge couplings, we get an upper bound  $N \lesssim 40$ .

## Phenomenological Consequences

While we are dealing with a warped 5D model, the essence of our mechanism for a light Higgs is completely different from a vanilla holographic composite Higgs model. Our theory does not have top partners, light or heavy; they play no role in the stabilization of the Higgs hierarchy. There are no KK gluons either. There have to be KK electroweak gauge bosons, since the Higgs propagates in the bulk, but they do not have to be light and also play no role in stabilizing the hierarchy. The Higgs gets a large fraction of its potential on the UV brane, and can be thought of as a mixture of elementary and composite states.

The most salient phenomenological feature of our model is the existence of a light dilaton, as shown in Eq. (4.81). Due to its mixing with the Higgs it inherits all SM Higgs couplings suppressed by the mixing angle  $\theta$ . In addition to these, the dilaton has direct couplings to the SM fields. Since the SM fermions are assumed to be localized on the UV brane and the dilaton is localized predominantly on the IR brane their direct couplings are negligible. In contrast, electroweak gauge bosons propagate in the bulk and their direct coupling to the dilaton is given by [287, 293]

$$\frac{\chi}{2\chi_{\text{min}} \log \frac{R'}{R}} (F_{\mu\nu}^2 + Z_{\mu\nu}^2 + 2W_{\mu\nu}^2). \quad (4.85)$$

The direct couplings to the  $Z, W$  mass terms are a small correction to those obtained from the mixing with the Higgs, and their effects can be neglected.

From Eqs. (4.81) and (4.82) we have an upper bound on the dilaton mass

$$m_\chi \lesssim m_h \sqrt{\frac{h}{\chi_{\text{min}}} \frac{\pi \sin \theta}{\sqrt{6}N}} \sim h \sqrt{\frac{\pi(\lambda_2 - \lambda_{H\epsilon})}{\sqrt{6}N^2}}. \quad (4.86)$$

As explained in the previous Subsection we require  $\lambda_2, \lambda_{H\epsilon} \lesssim 10^{-2}$  and  $N \gtrsim 3$ , which leads to an upper bound  $m_\chi \lesssim 10$  GeV.

There is also a lower bound determined by the contribution from  $V_{\text{GW}}$ . Given that we need  $\lambda_{\text{GW}} \lesssim \lambda$  to have a second minimum at large values of  $\chi$ , the  $V_{\text{GW}}$  contribution to the dilaton mass is always negative at the metastable minimum. Therefore, if we do not tune the two terms in Eq. (4.81),  $m_\chi^2 > 0$  implies

$$m_\chi \gtrsim 2\pi \frac{\chi_{\min}}{N} \sqrt{2(\lambda - \lambda_{\text{GW}})}. \quad (4.87)$$

Numerically  $\chi_{\min} \simeq \text{TeV}$ ,  $N \lesssim 40$  and  $\lambda, \lambda_{\text{GW}} \gtrsim 10^{-6}$ ; as explained in the previous Subsection. Hence, we expect a lower bound of  $\mathcal{O}(100)$  MeV.

In summary, we have a dilaton with mass  $0.1 \text{ GeV} \lesssim m_\chi \lesssim 10 \text{ GeV}$  and couplings to fermions proportional to  $\sin \theta \sim m_\chi^2/m_h^2$ . The direct coupling to photons in Eq. (4.85) plays an important role in its phenomenology, giving an  $\mathcal{O}(1)$  correction to its branching ratios.

To explore the properties of this dilaton and the experimental constraints on it, we randomly generated  $10^5$  points in the parameter space, fixing the parameters  $k = 10^{11}$  GeV,  $\delta = 0.01$ ,  $N = 3$  and  $\alpha = 0.05$ , while uniformly sampling the other parameters from the ranges  $\lambda_{\text{GW}} \in (0.5, 1.5) \times 10^{-5}$ ,  $\lambda_2 \in (0.5, 1.5) \times 10^{-2}$ ,  $\lambda_{H\epsilon} \in (2, 4) \cdot \lambda_2$ ,  $\lambda_4 \in (2, 3)$ , and  $\epsilon \in (0.03, 0.1)$ . We also took  $\lambda = 1.1 \lambda_{\text{GW}}$  and set the Higgs VEV  $\langle h \rangle \simeq 174$  GeV. The parameter values chosen here reflect the little hierarchy  $h_{\text{crit}}/\chi_{\min} \lesssim 0.1$  and  $V_{\text{GW}} \lesssim V_{H\chi}$  at  $\chi_{\min}$ .  $k$  could be taken larger than  $10^{11}$  GeV if desired, up to the Planck scale; in this case one can just as easily find satisfactory points in the parameter space, without substantially affecting our results. To probe lower dilaton masses, we performed a similar analysis of  $5 \times 10^4$  points, choosing  $N = 8$ ,  $\alpha = 0.1$ ,  $\lambda_{\text{GW}} = 2 \times 10^{-6}$ ,  $\lambda_2 \in (0.5, 1) \times 10^{-2}$ , and  $\epsilon \in (0.05, 0.1)$ , while keeping the other parameters the same. Points were excluded from our analysis if they failed to satisfy the following criteria: the metastable vacuum must exist and be located at  $\chi_{\min} > 1$  TeV;  $h_{\text{crit}} \leq 2$  TeV so the Higgs VEV is natural; the metastable vacuum reproduces the SM values of the Higgs mass and VEV and corresponds to a stable local minimum of the 2 dimensional potential; and the  $O(4)$  bounce action  $S_4$  between the two potential minima is at least  $\mathcal{O}(200)$  so that tunnelling is suppressed.

The bounce action (see [294]) was computed by numerically solving the Euclidean equation of motion, using the shooting method to satisfy the boundary conditions. In practice,  $S_4$  was at least  $\mathcal{O}(10^4)$  for points satisfying the other three criteria.

The results of the two scans are plotted in Fig. 4.12. We indicate the relevant experimental bounds from rare  $B$  meson decays [172,295], adapted from [296,297]. The region in the  $m_\chi - \sin \theta$  plane populated by the two scans can be understood from Eq. (4.81): the points approximately fall on the curve  $m_\chi \sim \sqrt{\sin \theta}$ , with upper (lower) bounds determined by the values of  $\lambda_{2,H\epsilon}$  ( $\lambda, \lambda_{\text{GW}}$ ). The lightest KK Higgs and KK EW gauge bosons lie around 3–4 TeV and 2.5–3.5 TeV respectively<sup>7</sup>, the precise number depending on the value of  $\chi_{\min}$  for each point. There are two regions in the parameter space free of bounds around 0.5–1.5 GeV and 5–7 GeV, as illustrated in Fig. 4.12 along with expected future experimental sensitivities [168, 194, 262–266, 297–302].

Finally, in Fig. 4.13 we plot the dilaton coupling to photons  $1/\Lambda_{\gamma\gamma}$  for each point in our scans, alongside current and projected experimental bounds adapted from [303–305]. These bounds provide constraints on the model that are independent of  $\sin \theta$ . We normalize the coupling such that the dilaton-photon interaction term is  $\frac{1}{4\Lambda_{\gamma\gamma}} \tilde{\chi} F_{\mu\nu}^2$ , with  $\tilde{\chi}$  the canonically normalized dilaton. The region of parameter space populated by our model evades the existing experimental bounds [306–308]; projections for future sensitivities [303, 309–311] are also presented in Fig. 4.13. A combination of beam dump experiments and a future lepton collider can cover all our viable parameter space.

<sup>7</sup>Note that the LHC bounds on the KK W and Z are not significantly reduced by moving the gluons and

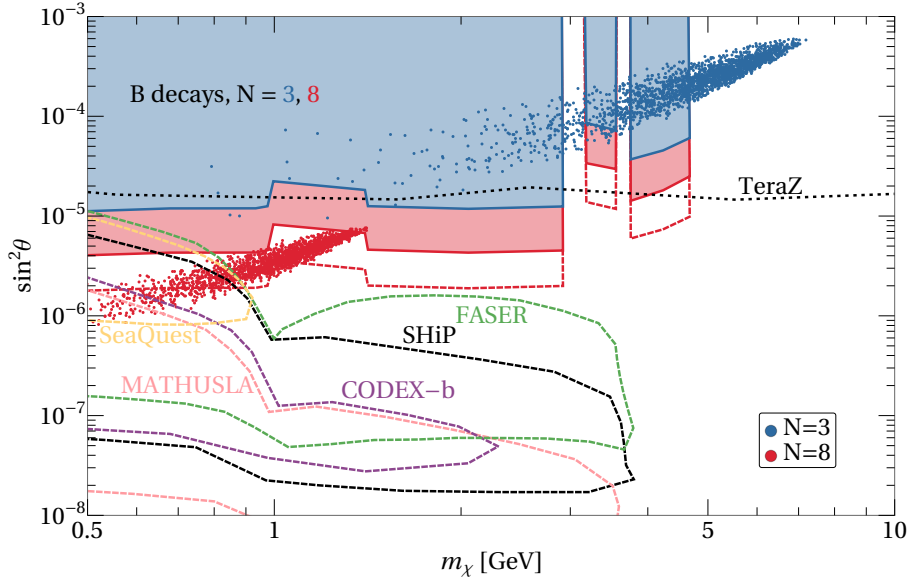


Figure 4.12: The dilaton mass  $m_\chi$  and its mixing angle with the Higgs  $\sin^2\theta$  for randomly sampled points from our model. The blue and red points use different parameter ranges, detailed in the body of the text. We show current bounds from  $B$  meson decays at LHCb [172, 295] (blue and red shaded regions), adapted from [296, 297]. We estimate updated  $B$  decay bounds for  $N = 8$  following Run 3 of the LHC (dotted red line), assuming an integrated luminosity of  $15 \text{ fb}^{-1}$  [299]. We also include projections (using  $N = 8$ ) for bounds from searches for hidden light particles, at the beamdump experiments SHiP [262] and SeaQuest [298, 299], as well as the collider experiments MATHUSLA [265, 266], CODEX-b [263, 301], and FASER [264, 300] (dashed lines). Finally, we include a projection for  $Z \rightarrow Z^*\chi$  at the FCCee running on the  $Z$  pole (Tera- $Z$ ) [297] (dotted black line), rescaled from the corresponding LEP limits [168, 194].

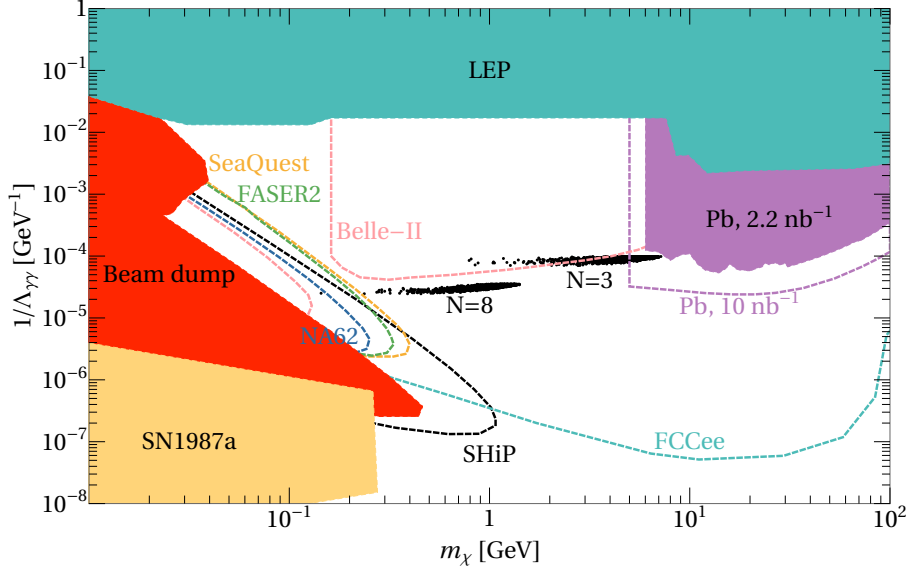


Figure 4.13: The dilaton coupling to photons  $1/\Lambda_{\gamma\gamma}$  for randomly sampled points from our model. We include points from both of our two choices of parameter ranges. We show bounds, adapted from [303], from searches at LEP for  $e^+e^- \rightarrow \gamma\chi \rightarrow 3\gamma$  [306, 307] (turquoise), beam dump experiments [312] (red), supernova SN1987a [313, 314] (orange), and  $\gamma\gamma \rightarrow \chi \rightarrow \gamma\gamma$  in lead ion collisions at the LHC with  $2.2 \text{ nb}^{-1}$  of data [308] (purple). We also include projected bounds for an FCCee search for  $e^+e^- \rightarrow \gamma\chi \rightarrow 3\gamma$  [303, 309], lead ion collisions with  $10 \text{ nb}^{-1}$  of data [310, 311], Belle-II, FASER2, NA62, SeaQuest, and SHiP (dashed lines) [304, 305].

## Cosmological Constraints

First, we require that the energy density in the true vacuum is indeed always negative—i.e.  $\lambda\chi_{GW}^4 > M_I^4$ , which results in  $k \gtrsim 17M_I$  for  $\lambda \simeq 10^{-5}$ . In addition, if we assume that the cosmological constant problem is solved via a standard anthropic mechanism, we need to require that the highest possible CC in the landscape is below  $\sim \lambda\chi_{GW}^4$ , so that all patches reaching the true minimum of the GW potential crunch. This condition may naturally arise for an  $\mathcal{O}(\Lambda)$  SUSY breaking scale on the UV brane.

A second important requirement is that quantum diffusion never dominates over classical evolution of the dilaton. This prevents patches with the wrong value of  $h$  to enter a phase of eternal inflation. We want to ensure that for a Higgs VEV large enough or small enough such that the dilaton potential has only one minimum with a negative CC, the dilaton does indeed roll to that minimum during inflation and does not get stuck in an eternally inflating phase. For large Higgs VEVs, the second derivative of the dilaton potential is always at least of  $\mathcal{O}(v^2 \simeq (174 \text{ GeV})^2)$  (see Eq. (4.72)), so classical rolling dominates over quantum diffusion, as we already imposed that the Hubble scale is less than the electroweak scale.

The case of a small or vanishing Higgs VEV could potentially be more problematic. Once the Higgs VEV is zero, the  $\chi$  potential is a pure  $\chi^4$  term even for very small values of  $\chi$ , leading to a very small second derivative near the origin. Hence for any choice of the Hubble scale during inflation there are regions which support eternal inflation. This can be avoided by a simple modification of the model following the ideas of [315, 316], which was also used in [317]. We include an additional term  $\lambda_\gamma\chi^\gamma\hat{\Lambda}^{4-\gamma}$  in the  $\chi$  potential, corresponding to explicit breaking of scale invariance at the scale  $\hat{\Lambda} \ll k$ . This term does not change our analysis for

---

quarks onto the UV brane, due to the tail of the KK gauge wave functions only being logarithmically suppressed on the UV brane.

$\chi \gg \chi_*$ , defined as the scale where the effective quartic coupling blows up, i.e.  $\chi_* \sim \tilde{\Lambda} \lambda_\gamma^{\frac{1}{4-\gamma}}$ . However for  $\chi \lesssim \chi_*$  the potential is dominated by the explicit breaking term, which signals that for  $\chi \lesssim \chi_*$  the description in terms of a dilaton breaks down. In that region we expect the effective potential to be dominated by the mass scale  $\chi_*$ , and effectively behave as if a negative mass term of order  $\chi_*^2$  was generated. Such an explicit breaking term can be generated by any relevant operator which has a negligible coupling in the UV and grows to be  $\mathcal{O}(1)$  in the IR. One such realization could be to have the SM QCD (or a BSM QCD-like gauge theory) in the bulk.

The RG evolution of the gauge coupling for the additional group in the bulk, assuming the presence of a UV and IR brane [293, 315] is given by:

$$\frac{1}{g^2(Q, \chi)} = \frac{\log \frac{k}{\chi}}{kg_5^2} - \frac{b_{\text{UV}}}{8\pi^2} \log \frac{k}{Q} - \frac{b_{\text{IR}}}{8\pi^2} \log \frac{\chi}{Q} + \tau \quad (4.88)$$

where  $Q$  is the running scale and the dependence on  $\chi$  is introduced due to the finite size of the extra dimension.  $\tau = \tau_{\text{UV}} + \tau_{\text{IR}}$  contains the brane-localized kinetic terms and  $b_{\text{UV,IR}}$  are the 4D  $\beta$ -functions on the two branes. Note that Eq. (4.88) is valid only for  $Q < \chi$ . From Eq. (4.88) we get the  $\chi$  dependence of the dynamical scale of the bulk gauge group

$$\begin{aligned} \tilde{\Lambda}(\chi) &= \left( k^{b_{\text{UV}}} \chi^{b_{\text{IR}}} e^{-8\pi^2 \tau} \left( \frac{\chi}{k} \right)^{-b_{\text{CFT}}} \right)^{\frac{1}{b_{\text{UV}} + b_{\text{IR}}}} \\ &= \Lambda_0 \left( \frac{\chi}{\chi_{\text{min}}} \right)^n. \end{aligned} \quad (4.89)$$

For our benchmark point of  $\chi_{\text{min}} \simeq 1$  TeV and  $\langle H \rangle = 0$ , QCD in the bulk gives  $\tilde{\Lambda}(\chi_{\text{min}}) \sim \Lambda_{\text{QCD}} \sim 100$  MeV. The lower bound on  $n$  is  $n \gtrsim 0.1$ , which results in  $\chi_* \sim 10\text{--}100$  MeV  $\sim \Lambda_{\text{QCD}}$ .

For our benchmark point of  $\chi_{\text{min}} \simeq 1$  TeV and  $\langle H \rangle = 0$ , bulk QCD gives  $\tilde{\Lambda} \sim \chi_* \sim \Lambda_{\text{QCD}}$ .

While for  $\chi > \chi_*$  the additional  $\lambda_\gamma \chi^\gamma \tilde{\Lambda}^{4-\gamma}$  term generated from the bulk QCD is negligible, for  $\chi \lesssim \chi_*$  the potential is dominated by the explicit breaking term, which signals that for  $\chi \lesssim \chi_*$  the description in terms of a dilaton breaks down. In that region we expect the effective potential to be dominated by the mass scale  $\chi_*$ , and effectively behave as if a negative mass term of order  $\chi_*^2$  was generated.

To avoid eternal inflation we have to take the highest Hubble constant in the landscape to be just below  $\chi_*$ . Assuming that the corresponding cutoff also sets the scale of the CC landscape, we find that  $\Lambda < \sqrt{\chi_* M_{\text{Pl}}} \lesssim 10^5$  TeV for SM QCD in the bulk; with a different gauge group, the cutoff can be taken all the way to  $10^7$  TeV. This addition also generates a minimal value for the Higgs VEV  $h_{\text{min}}$  below which the universe will crunch. This will occur when the corresponding  $\chi_{\text{min}}$  is of order  $\chi_*$ , and so  $h_{\text{min}} \sim 0.1\chi_*$ . Note that including QCD in the bulk also has an impact on the light dilaton phenomenology whose study we leave to future work.

## 4.5 Sliding Naturalness

In the previous Section we have discussed a possible implementation of the general idea that patches of the Multiverse with the “wrong” Higgs mass rapidly crunch. The model predicted a quite unique phenomenology in the realm of extra-dimensional theories for the Higgs mass. There is also a simpler implementation of this general idea that does not rely on extra-dimensions and does not predict any new physics with gauge couplings to the SM around a TeV. Interestingly, this second implementation can potentially solve the strong-CP problem at the same time. We first introduced the idea in [154] and then further elaborated on it in [155]. This proposal has the following qualities:

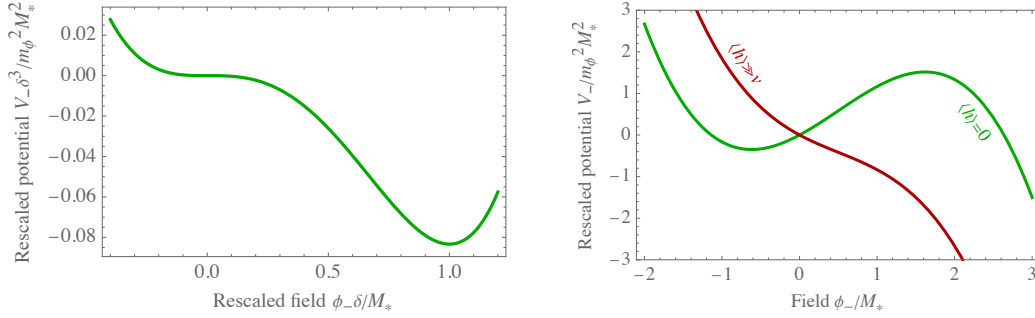


Figure 4.14: Example potential  $V_-(\phi_-)$  with two widely separated minima. The right panel zooms in close to the safe local minimum at  $\phi \sim M_*$ . This is destabilised if the Higgs acquires a large vev (red line). Note the different rescaling in the two panels for both the field and the potential.

1. It is entirely described by a simple polynomial potential for two weakly-coupled light scalars.
2. It does not make any assumption on what can explain current CMB observations, in particular it is compatible with one’s favorite mechanism (and scale) for inflation, but also with de Sitter swampland conjectures.
3. It can explain a small value of the Higgs vev  $v \simeq 246$  GeV, even if the Higgs is coupled at  $\mathcal{O}(1)$  with particles at  $M_{\text{Pl}}$ .
4. It is not affected by problems of measure in the landscape<sup>8</sup>.

### 4.5.1 Basic Idea

At low energy the theory includes a new scalar  $\phi_-$  with an approximate shift symmetry. The  $\phi_-$  potential has two widely separated minima. The deepest minimum of the potential has energy density of  $\mathcal{O}(-M^2 M_*^2)$  with  $M$  the largest mass scale in the theory and  $M_* = M/g_* \sim M$  a vev associated to it. This energy density is  $\mathcal{O}(1)$  larger than the largest cosmological constant in the landscape. Universes where  $\phi_-$  rolls to this minimum rapidly crunch. The shallow “safe” minimum of  $\phi_-$  has energy density  $\mathcal{O}(m_{\phi_-}^2 M_*^2)$ , with  $m_{\phi_-} \ll M$ . In this minimum the CC can be scanned finely around zero. Its observed value today can, for instance, be selected by Weinberg’s anthropic argument [318]. The  $\phi_-$  potential is schematically depicted in the left panel of Fig. 4.14.

A small value for the Higgs vev,  $\langle h \rangle \ll M_*$ , is selected by a  $\langle h \rangle$ -dependent tadpole in the  $\phi_-$  potential. This tadpole destabilizes the safe metastable minimum when the Higgs vev is larger than  $v$ . The tadpole is generated by a coupling of  $\phi_-$  to an operator  $\mathcal{O}_T$

$$V_{H\phi} = -a\phi_- \mathcal{O}_T + \text{h.c.} \quad (4.90)$$

<sup>8</sup>If the landscape is populated via eternal inflation there will be a measure problem if one is interested in understanding what values of fundamental parameters are more likely in the Multiverse. However this does not affect the validity of the mechanism, since we are not asking probabilistic questions in the Multiverse. We instead have a theory where all unwanted patches are either always empty or always crunch. So we never need to know if the unwanted patches are more or less likely (occupy a smaller or larger volume in the Multiverse) than the one that we observe.



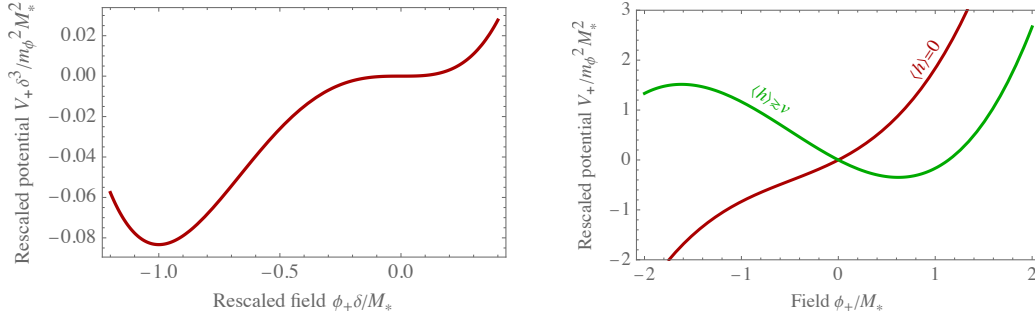


Figure 4.15: Example potential  $V_+(\phi_+)$ , that selects a nonzero Higgs vev. The right panel zooms in close to the safe local minimum at  $\phi_+ \sim M_*$ , present only if the Higgs acquires a sufficiently large vev (green line).

whose vev is a monotonic function of  $\langle h \rangle$ . When  $\langle h \rangle \gg v$  the tadpole in Eq. (4.90) dominates the  $\phi_-$  potential around  $M_*$  and destroys the safe minimum (see Fig. 4.14), so all universes with large and negative Higgs mass squared rapidly crunch. The small number that separates the weak scale from the cutoff  $M_*$  is  $m_\phi$ , i.e. universes where the tadpole dominates near the metastable minimum of  $\phi_-$ ,

$$\frac{a\langle \mathcal{O}_T \rangle}{m_\phi^2 M_*} \gg 1, \quad (4.91)$$

are those which crunch fast. The separation between  $m_{\phi_-}$  and  $M_*$  is technically natural, because  $\phi_-$  is part of a very weakly coupled sector that can naturally be approximately scale-invariant or supersymmetric, without any measurable trace of scale invariance or supersymmetry in the SM.

The basic “crunching” setup is conceptually the same as [285, 319], but, as we will see in more detail in the following, there are two important differences: 1) differently from [285] in our case inflation can happen at a very high scale and possibly be eternal. Crunching of patches where  $\langle h \rangle \gg v$  occurs after reheating at temperatures below  $v$ , independently of the details of inflation. 2) In [285] the SM becomes approximately scale invariant already above a few TeV. In [319] new physics that protects the Higgs mass must appear at a few TeVs. Here and in [154] the symmetries protecting the  $\phi_-$  potential can be invisible in the SM sector.

We have seen that  $\phi_-$  stabilizes a hierarchy between the Higgs vev and the cutoff, but we can still have universes with vanishing Higgs vev. Universes with small (or vanishing) Higgs vevs are destabilized by an additional scalar  $\phi_+$  coupled to  $\mathcal{O}_T$  in the same way as  $\phi_-$ . The main difference is that  $\phi_+$  does not have a safe metastable minimum when  $\langle h \rangle = 0$ . This minimum is generated only if  $\langle h \rangle \gtrsim v$ . Then, as shown in Fig. 4.15, the universe rapidly crunches unless the Higgs acquires a sufficiently large vev. The mechanism with both scalars  $\phi_\pm$  selects a *small* and *non-zero* Higgs vev.

In Fig. 4.16 we show the allowed parameter space for  $m_{\phi_+} = m_{\phi_-}$  and  $\mathcal{O}_T = H_1 H_2$ , which we discuss in more detail in Section 4.5.3. The Figure shows that cutoffs as large as  $\sim M_{\text{Pl}}$  can be explained by the mechanism. For cutoffs of  $\mathcal{O}(M_{\text{GUT}})$  coherent oscillations of the new scalars can be the DM of our Universe. The crunching time of Universes without the shallow minimum is approximately  $1/m_{\phi_\pm}$ . This gives an upper bound on the  $\phi_+$  mass:  $m_{\phi_+} \lesssim H(v) \simeq 10^{-4}$  eV. For heavier  $\phi_+$  also universes with the observed Higgs vev rapidly crunch, because crunching would occur before the effect of the Higgs vev in our universe is felt by  $\phi_+$ .

Note also that the lifetime of our “safe” metastable minimum is much longer than the

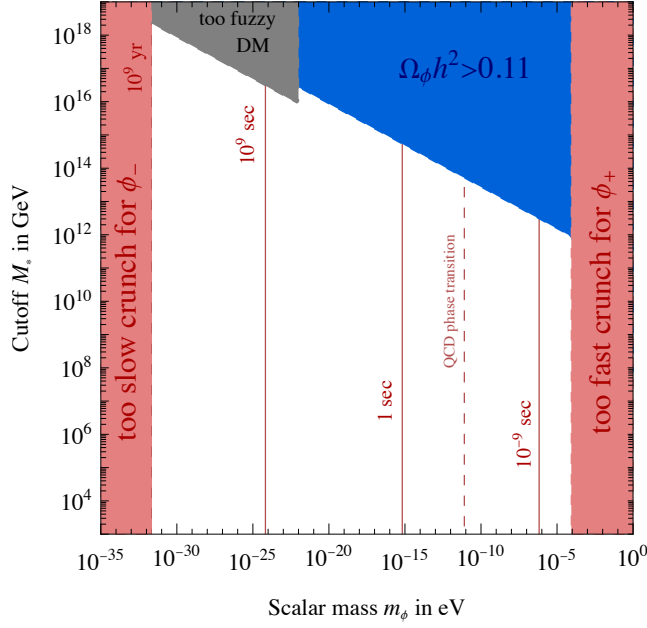


Figure 4.16: Parameter space of the mechanism, assuming the same mass for both scalars. The red lines denote the maximal crunching time of patches with the “wrong” value of the weak scale. Red-shaded regions are excluded either because the crunching time is cosmologically long or because crunching would occur before the Electroweak phase transition. In the blue region oscillations of the scalars produce too much dark matter, at its boundary the cosmological DM abundance is reproduced. In the gray region the DM mass is larger than astrophysical lower bounds [320].

age of our universe. The tunneling rate is  $\Gamma/V \lesssim M_*^4 e^{-8\pi^2 M_*^2/m_{\phi_{\pm}}^2}$ . If we take for instance  $M_* \simeq 10^{14}$  GeV and  $m_{\phi_+} = m_{\phi_-} = 10^{-11}$  eV, a point in our Fig. 4.16 where we also reproduce the observed DM relic density, we obtain a tunneling action  $S > 8\pi^2 M_*^2/m_{\phi_{\pm}}^2 \sim 10^{69}$ . Lowering  $M_*$  all the way to a TeV and raising  $m_{\phi}$  to  $H(\Lambda_{\text{QCD}})$  does not change the conclusion that our minimum is orders of magnitude more long-lived than the current age of the Universe.

## 4.5.2 Scalar Potential and Selection of the Weak Scale

To make the previous discussion more explicit, we consider the scalar potential

$$V_{\phi_-} = m_{\phi_-}^2 M_*^2 \left( \frac{\phi_-}{M_*} + \frac{\phi_-^2}{2M_*^2} - \frac{\phi_-^3}{3M_*^3} + \frac{\delta}{4} \frac{\phi_-^4}{M_*^4} \right) + \dots \quad (4.92)$$

and imagine that the quartic coupling is small ( $\delta \ll 1$ ). We have set to one possible numerical coefficients of the  $\phi_-$  monomials, but our discussion applies also to more general choices.  $V_-$  has a low-energy minimum at  $\phi_- \sim M_*$ , where  $|V_-| \sim m_{\phi_-}^2 M_*^2 \ll M^2 M_*^2$  and a deep stable minimum at  $\phi_- \sim M_*/\delta$  where  $-V_- \sim m_{\phi_-}^2 M_*^2/\delta^3 \gtrsim M^2 M_*^2$ . The potential is shown in the left panel of Fig. 4.14.

This potential can naturally arise from simple supersymmetric models. We can consider for instance the superpotential

$$W_{\phi_-} = L\Phi_- + \mu\Phi_-^2 + \lambda\Phi_-^3, \quad (4.93)$$

and the SUSY breaking term

$$V_B = \epsilon\mu\phi_-^3. \quad (4.94)$$

In absence of SUSY breaking, the potential from  $W_{\phi_-}$  can have two widely separated minima in field space. One is at  $\phi_- \sim L/\mu$  the other at  $\phi_- \sim \mu/\lambda$ , both have zero vacuum energy. The SUSY breaking term can split the two minima by a large amount without making the construction unnatural. In particular, for  $L = m_{\phi_-} M_*$ ,  $\mu = m_{\phi_-}$ ,  $\epsilon = m_{\phi_-}/M_*$  and  $\lambda = \sqrt{\delta}\epsilon \ll \epsilon$  we recover  $V_{\phi_-}$  shifted by an unimportant overall CC of  $\mathcal{O}(m_{\phi_-}^2 M_*^2)$ .

This supersymmetric UV completion shows that more general choices than Eq. (4.92) are natural and lead to the structure with a deep and a shallow minimum that we are interested in. In particular we do not need to consider the form in Eq. (4.92) that is suggestive of the potential for a pseudo-Goldstone boson. We could take mass, cubic and tadpole at different scales. We could also consider, as we did in [154], a  $\mathbb{Z}_2$ -symmetric potential, protected by approximate scale invariance, where the deep minimum comes from a negative quartic coupling, eventually stabilized by non-renormalizable operators at large field values. For simplicity we use Eq. (4.92) in the rest of this Section, which is manifestly natural if  $(m_{\phi_-}/M_*)^2 \lesssim \delta$ . The second scalar that we introduced,  $\phi_+$ , can have the same potential as  $\phi_-$ , but a different sign for the cubic term

$$V_{\phi_+} = m_{\phi_+}^2 M_*^2 \left( \frac{\phi_+}{M_*} + \frac{\phi_+^2}{2M_*^2} + \frac{\phi_+^3}{3M_*^3} + \frac{\delta \phi_+^4}{4M_*^4} \right) + \dots \quad (4.95)$$

In this case the metastable minimum is not present. We only have the deep minimum at  $\phi_+ \sim M_*/\delta$ . The potential is shown in the left panel of Fig. 4.15. Clearly other possibilities are viable, but to simplify the discussion we consider the same structure for the potentials of  $\phi_{\pm}$ . In principle the vev  $M_*$  and the parameter  $\delta$  can be different for the two scalars, as we discussed in [154]. When appropriate we will comment on the impact of this possibility on phenomenology. The last aspect that we need to specify is the coupling of  $\phi_{\pm}$  to the SM. In this work we will mainly consider

$$V_{\phi_+ H} + V_{\phi_- H} = -\kappa H_1 H_2 (m_{\phi_+} \phi_+ + m_{\phi_-} \phi_-) + \text{h.c.}, \quad (4.96)$$

where  $H_1$  is a new Higgs doublet present in addition to the SM-like Higgs  $H_2$  and  $\kappa \leq 1$ . For  $H_1 H_2$  to be a good “trigger”, i.e. select the weak scale, we need to impose an approximate  $\mathbb{Z}_2$  on the Two Higgs Doublet Model (2HDM) potential. We discuss this in Section 4.5.4. Finally, we could consider cross-couplings between  $\phi_+$  and  $\phi_-$ . For  $\kappa \ll 1$  it is technically natural to take them to be negligibly small. Therefore, for simplicity in this work we set them to zero, although we expect that our mechanism is effective also in the presence of cross-couplings, provided that the potential has the structure with two minima that realizes our crunching mechanism.

The mechanism can be realized also for a trigger operator  $\mathcal{O}_T$  purely within the SM, as we did in [154]. In the following we discuss

$$V_{\phi_+ G} + V_{\phi_- G} = -\frac{\alpha_s}{8\pi} \left( \frac{\phi_+}{F_+} + \frac{\phi_-}{F_-} \right) \text{Tr}[G\tilde{G}], \quad (4.97)$$

expanding on the results in [154]. We discuss the coupling to  $\text{Tr}[G\tilde{G}]$  in Section 4.5.5, while in the following we consider the potential<sup>9</sup>:

$$\begin{aligned} V &= V_{\phi_+} + V_{\phi_-} + V_{H\phi_+} + V_{H\phi_-} = m_{\phi_+}^2 M_* \phi_+ + m_{\phi_-}^2 M_* \phi_- + \frac{m_{\phi_+}^2}{2} \phi_+^2 + \frac{m_{\phi_-}^2}{2} \phi_-^2 \\ &+ \frac{m_{\phi_+}^2}{3M_*} \phi_+^3 - \frac{m_{\phi_-}^2}{3M_*} \phi_-^3 + \delta \frac{m_{\phi_+}^2}{4M_*^2} \phi_+^4 + \delta \frac{m_{\phi_-}^2}{4M_*^2} \phi_-^4 - \kappa (m_{\phi_+} \phi_+ + m_{\phi_-} \phi_-) (H_1 H_2 + \text{h.c.}), \end{aligned} \quad (4.98)$$

<sup>9</sup>For those more used to a relaxion-like parametrization of the potential:  $gM^2\phi + g^2\phi^2 + \dots$ , we note that  $g = m_{\phi}$ ,  $M_* = M^2/m_{\phi}$ .

where we recall that  $\delta \ll 1$ . The potential is technically natural for  $\kappa \lesssim 4\pi$ ,  $\delta \gtrsim \max[\kappa^6(v^4/m_{H,\min}^4), m_\phi^2/M_*^2]$  where  $m_{H,\min}$  is the smallest Higgs mass in the landscape. If  $m_{H,\min} \simeq 0$  the IR divergence is cutoff by  $m_{\phi_\pm}$ . Notice that as long as these conditions are verified, large mixed couplings are not generated by loops, at least if the parameters of the two scalars are not too different. Furthermore we will see that the values of  $\kappa$  that give the observed dark matter relic density in the form of coherent oscillations of  $\phi_\pm$  are  $\kappa \lesssim 10^{-5}$ , making induced cross couplings completely negligible. Therefore, for simplicity we can set the mixed couplings to zero, as mentioned above, to keep the analytic treatment tractable. Notice however that  $\mathcal{O}(1)$  cross couplings do not necessarily spoil our mechanism, provided that at large field values they do not lift the deep minimum of  $V$ .

The global minimum of  $V$  is at  $\phi_\pm \sim \mp M_*/\delta$ , where the potential is  $V \sim -(m_{\phi_+}^2 + m_{\phi_-}^2)M_*^2/\delta^3$ . Since the universes where the scalars are at this minimum must crunch, this is also the value of the maximal CC allowed in the landscape for our mechanism to work. For  $\delta \lesssim ((m_{\phi_+}^2 + m_{\phi_-}^2)/M_*^2)^{1/3}$  this is  $\sim M_*^4$  or larger, i.e. at the cutoff of the EFT.

The potential in Eq. (4.133) has one metastable local minimum (where neither  $\phi_+$  nor  $\phi_-$  are at their global minimum) only for

$$\mu_S^2 \lesssim \langle H_1 H_2 \rangle \lesssim \mu_B^2, \quad (4.99)$$

where

$$\mu_S^2 \simeq \frac{m_{\phi_+} M_*}{\kappa}, \quad \mu_B^2 \simeq \frac{m_{\phi_-} M_*}{\kappa}. \quad (4.100)$$

This result can be more easily understood by considering independently the potentials for the two scalars.  $V_{\phi_-}$  is depicted in the left panel of Fig. 4.14 and it has two cosmologically long-lived minima. If  $\phi_-$  rolls to the deepest minimum the universe rapidly crunches. The coupling to the Higgs  $V_{H\phi_-}$  induces a tadpole that destroys the metastable minimum at  $\phi_- \sim M_*$  if  $\langle H_1 H_2 \rangle \gtrsim \mu_B^2$  (right panel of Fig 4.14), giving the second equality in (4.100).  $V_{\phi_+}$  is depicted in the left panel of Fig. 4.15 and it has one cosmologically long-lived minimum. If  $\phi_+$  rolls to the minimum the universe rapidly crunches. The coupling to the Higgs  $V_{H\phi_+}$  induces a tadpole that generates a metastable minimum at  $\phi_+ \sim M_*$  only if  $\langle H_1 H_2 \rangle \gtrsim \mu_S^2$  (right panel of Fig 4.14). This gives the first equality in (4.100). Only universes where this metastable minimum exists both for  $\phi_\pm$  can live for cosmologically long times. These are universe where  $\mu_S^2 < \langle H_1 H_2 \rangle < \mu_B^2$ .

Given our choice of trigger operator we are really selecting the vev of  $H_1 H_2$ . This is sufficient to select the weak scale (i.e. the vev of the SM-like Higgs) under the conditions described in Section 4.5.4. As shown in that Section, if we want to select the weak scale we need parametrically  $\langle H_1 H_2 \rangle \simeq v^2$  which implies

$$m_{\phi_\pm} \simeq \frac{\kappa v^2}{M_*}. \quad (4.101)$$

At the local minimum, if it exists, the potential is thus of order  $V \simeq \kappa^2 v^4$  and the  $\phi$ -only potential  $V_{\phi_+} + V_{\phi_-}$  is comparable to the Higgs-induced potential  $V_{H\phi_+} + V_{H\phi_-}$ . We imagine that the CC problem at the local minimum is solved by tuning in the landscape plus Weinberg's argument.

### 4.5.3 Cosmology

In this Section we describe the cosmology of the model. The initial reheating temperature does not affect our main results. For concreteness, we take all universes to be reheated at

$T \simeq M_*$ . We imagine that the scalars can be in any position on their potential after reheating. In Section 4.5.3 we show that  $\phi_{\pm}$  are good DM candidates. In Section 4.5.3 we show that the crunching time for universes with the “wrong” Higgs vev is dominated by the local part of the potential ( $|\phi_{\pm}| \lesssim M_*$ ) and is at most  $t_c \sim \max[1/m_{\phi_+}, 1/m_{\phi_-}]$ .

## Dark Matter

As in the previous Section, we focus on the coupling to  $H_1 H_2$  in Eq. (4.96). Similar results for the coupling to gluons are discussed in [154] and Section 4.5.5.

The scalars  $\phi_{\pm}$  are stable over cosmological timescales<sup>10</sup>

$$\Gamma_{\phi} \simeq \Gamma(\phi \rightarrow \gamma\gamma) \simeq \frac{G_F \alpha^2 m_{\phi}^5}{9\sqrt{2}\pi^3 m_h^2} \left(\frac{\kappa}{\lambda}\right)^2 \simeq \frac{1}{10^{17} \times (13 \times 10^9 \text{ years})} \left(\frac{m_{\phi}}{\text{eV}}\right)^5 \left(\frac{\kappa}{\lambda}\right)^2, \quad (4.102)$$

and their coherent oscillations can constitute the DM of the Universe. To compute the relic density, we note that  $\phi_{\pm}$  get a “kick” at the Electroweak (EW) phase transition, when  $T \simeq v$ , and acquire an energy density in the form of a misalignment from their minimum. To be more explicit let us consider a single scalar with potential

$$V = V_{\phi} + V_{H\phi} = m_{\phi}^2 M_*^2 \left( \frac{\phi}{M_*} + \frac{\phi^2}{2M_*^2} - \frac{\phi^3}{3M_*^3} + \delta \frac{\phi^4}{4M_*^4} \right) - (\kappa m_{\phi} \phi H_1 H_2 + \text{h.c.}) \quad (4.103)$$

Before the EW phase transition, under the conditions discussed in Section 4.5.4 that are necessary to select the weak scale,  $\langle H_1 H_2 \rangle = 0$ , so at early times we can focus on  $V_{\phi}$ . Our universe survived for cosmologically long times, so initially  $|\phi| \lesssim M_*$ . Universes with different initial conditions eventually see  $\phi$  roll to its deep minimum and crunch independently of the value of  $\langle h \rangle$ . Early on, as long as  $m_{\phi} \lesssim H(T)$ ,  $\phi$  is stuck with an initial misalignment from the minimum  $\phi_I$  and an energy density given by  $V_{\phi} \simeq m_{\phi}^2 \phi_I^2 \lesssim m_{\phi}^2 M_*^2$ . When  $m_{\phi} \gtrsim H(T)$  it starts to oscillate around its metastable minimum  $\phi_{\min} \simeq M_*$ , and its energy density starts to redshift like cold DM. This can occur either before ( $m_{\phi} \gtrsim H(v) \simeq 10^{-5} \text{ eV}$ ) or after ( $m_{\phi} \lesssim H(v)$ ) the EW phase transition. We can call  $\phi_{\text{EW}}$  the average amplitude of the field at the EW phase transition. This is given by  $\phi_{\text{EW}} = \phi_I$  if  $m_{\phi} \lesssim H(v)$  and  $\phi_{\text{EW}} = \phi_I (a(T_{\text{osc}})/a(v))^{3/2}$  if  $m_{\phi} \gtrsim H(v)$ , where  $a(T)$  is the scale factor of our universe and  $T_{\text{osc}}$  the temperature at which  $\phi$  starts to oscillate. In both cases  $|\phi_{\text{EW}}| \lesssim M_*$ .

At the EW phase transition the average position of  $\phi$  in its potential is  $\bar{\phi} \simeq M_* + \phi_{\text{EW}} \simeq M_*$  and  $V_{H\phi}$  starts contributing to the  $\phi$  potential

$$\Delta V = V_{H\phi} \simeq \kappa m_{\phi} M_* \langle H_1 H_2 \rangle_{\text{us}} \simeq \kappa m_{\phi} M_* v^2, \quad (4.104)$$

where  $\langle H_1 H_2 \rangle_{\text{us}}$  is the operator vev in our universe. If our universe is close to one of the boundaries of the “safe” region for the Higgs vev, i.e.  $\langle H_1 H_2 \rangle_{\text{us}} \simeq \mu_S^2$  or  $\langle H_1 H_2 \rangle_{\text{us}} \simeq \mu_B^2$ , then  $\Delta V \simeq V_{\phi}(M_*)$  and the minimum of  $\phi$  is shifted from its initial position,

$$\Delta\phi_{\min} \simeq M_*. \quad (4.105)$$

This contributes another factor of  $M_*$  to  $\phi$ ’s initial misalignment. Generically we expect to be in the situation  $\langle H_1 H_2 \rangle_{\text{us}} \simeq \mu_B^2$ , given the distribution of mass squared parameters in a typical landscape (i.e. since we need to tune to make  $\langle H_1 H_2 \rangle$  small, larger values are generically preferred). Therefore in the following we imagine that  $\langle H_1 H_2 \rangle_{\text{us}} \simeq \mu_B^2$  when  $\langle h \rangle \simeq v$  and take Eq. (4.105) as a good parametric estimate of the misalignment of  $\phi_-$  at the EW phase transition. If  $M_*$  and  $\kappa$  are the same for both scalars,  $\phi_+$  gives at most a comparable contribution to the

<sup>10</sup>Here  $\lambda$  is an  $\mathcal{O}(1)$  combination of quartics in the 2HDM Higgs sector.

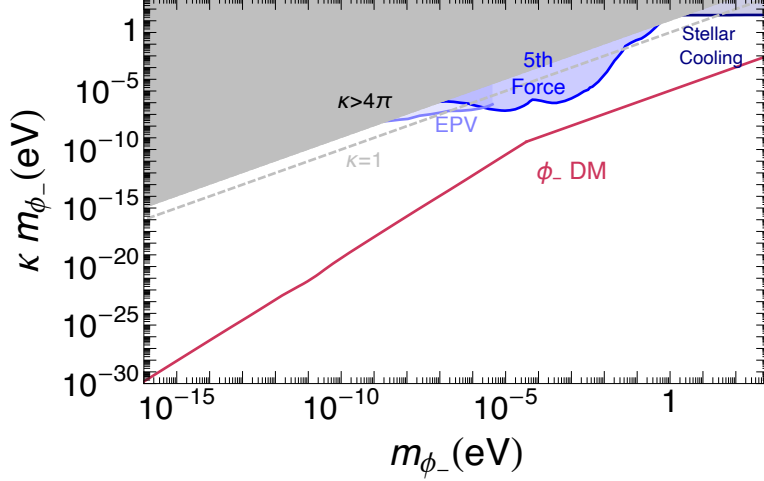


Figure 4.17: Laboratory and astrophysical constraints on a scalar coupled to the Higgs boson via the trilinear interaction  $\kappa m_{\phi_-} \phi_- |H|^2$ . The bounds include tests of the equivalence principle [321–323], tests of the Newtonian and Casimir potentials (5th force) [324–332] and stellar cooling constraints [333]. The red solid line shows the target given by  $\phi_-$  reproducing the observed dark matter relic density. Above the gray dashed line  $\kappa > 1$ . In the gray shaded region  $\kappa > 4\pi$ , making the scalar potential unnatural. The constraint from AURIGA [334] is not shown because the mass range explored is too narrow to be visible on this scale. The bound does not touch our DM parameter space. Bounds on this coupling and future probes, spanning a larger mass range, can be found in [296, 335].

DM relic density, and only if it starts oscillating and redshifting as cold DM after the EW phase transition. Since we are interested in a first estimate of the relic density, we neglect the  $\phi_+$  relic density and continue with our single scalar description, which captures the relevant parametrics.

The kick at the EW phase transition gives the dominant contribution to the relic density if  $m_\phi \gtrsim H(v)$ , since the initial misalignment (that can be at most  $\mathcal{O}(M_*)$ ) has already partially redshifted away. If  $m_\phi \lesssim H(v)$ , ignoring the initial misalignment still gives parametrically the correct result, since it can give at most an  $\mathcal{O}(1)$  correction on top of the EW-induced misalignment. Therefore modulo  $\mathcal{O}(1)$  factors, we get

$$\rho_{\phi_-}(T \simeq v) \simeq m_\phi^2 M_*^2 \gtrsim \rho_{\phi_+}(T \simeq v). \quad (4.106)$$

From Eq. (4.101) we know that to select the weak scale we need  $m_\phi^2 M_*^2 \simeq \kappa^2 v^4$ , so the relic density is entirely specified by giving the coupling  $\kappa$  of the scalars to the SM, and their mass  $m_\phi$ , which determines the moment in time when they start to oscillate and redshift as cold DM ( $m_\phi \simeq H(T_{\text{osc}})$ ). We are in the same situation described in [153, 154]. Light scalars coupled to trigger operators offer universal targets to DM searches. We now give an estimate of the target. The relic density today is

$$\frac{\rho_{\phi_-} + \rho_{\phi_+}}{\rho_{\text{DM}}} \simeq \frac{\rho_{\phi_-}}{\rho_{\text{DM}}} \simeq m_\phi^2 M_*^2 \frac{s_0}{\rho_{\text{DM}}^0 \min[s(v), s(T_{\text{osc}})]}. \quad (4.107)$$

To highlight the phenomenological significance of this result we can use Eq. (4.101):  $m_\phi^2 M_*^2 \simeq \kappa^2 v^4$  and rewrite our expression in terms of the effective trilinear coupling of  $\phi_-$  with the Higgs that determines the strength of  $\phi_-$  interactions with the SM:

$$\mathcal{L} \supset -b_- \phi_- H_1 H_2 + \text{h.c.} \simeq -b_- \phi_- |H|^2 + \dots, \quad b_- \simeq \kappa m_{\phi_-}. \quad (4.108)$$

Here for simplicity we have taken the limit of a small coupling of  $H_1$  to SM fermions (i.e.  $\lambda_3 + \lambda_4 + \lambda_5 \ll \lambda_2$  with  $\lambda_i$ 's defined in Eq. (4.121); generalizing introduces additional  $\mathcal{O}(1)$  factors that do not qualitatively affect our discussion). In conclusion

$$\frac{\rho_\phi}{\rho_{\text{DM}}} = \frac{b_-^2 v^4}{m_{\phi_-}^2 \rho_{\text{DM}}^0 \min[s(v), s(T_{\text{osc}})]} \simeq \begin{cases} \frac{b_-^2 v}{m_{\phi_-}^2 T_{\text{eq}}} & m_{\phi_-} \geq H(v) \\ \frac{b_-^2 v^4}{m_{\phi_-}^{7/2} M_{\text{Pl}}^{3/2} T_{\text{eq}}} & m_{\phi_-} < H(v) \end{cases} \quad (4.109)$$

where  $T_{\text{eq}} \simeq \text{eV}$  is the temperature of matter-radiation equality, and we have a target for ultralight DM searches:

$$b_{\text{DM}} \simeq m_{\phi_-} \sqrt{\frac{T_{\text{eq}}}{v}} \min \left[ 1, \frac{m_{\phi_-}^{3/2} M_{\text{Pl}}^{3/2}}{v^3} \right]. \quad (4.110)$$

For any given mass only one value of the coupling to the SM  $b_{\text{DM}}$  gives the observed relic density. In Figure 4.17 we show this ultralight DM target and current constraints on our parameter space. The bounds include tests of the equivalence principle [321–323], tests of the Newtonian and Casimir potentials (5th force) [324–332] and stellar cooling [333].

Future probes of  $\phi_-$  dark matter, including torsion balance experiments [336], atom interferometry [337], optical/optical clock comparisons and nuclear/optical clock comparisons [338], resonant mass detectors (DUAL and SiDUAL [339]) and gravitational-wave detectors [340, 341] are orders of magnitude too weak to probe our parameter space. Current constraints on 5th forces that are more than twenty years old are relatively close to motivated parameter space in the range  $10^{-5} \text{ eV} \lesssim m_{\phi_-} \lesssim 10^{-3} \text{ eV}$  and we hope that this study will motivate future efforts towards improving their sensitivity.

Modulo factors related to the multiplicity of scalars, the prediction for the relic density is exactly the same as in [153] and similar considerations can be made in relaxion models [342]. This is one manifestation of the universality of this prediction. Light scalars that can select the weak scale, generically get the biggest contribution to their relic density from a SM phase transition. If the Universe is reheated above the relevant phase transition, their relic density today depends only on their mass and coupling to the SM.

## Crunching dynamics

In this Section we consider the dynamics of  $\phi_\pm$  crunching in detail and calculate the crunching time. We follow the evolution of the Universe after inflation, starting from a SM reheating temperature of the order of the cutoff,  $T \sim M_*$ . If the reheating temperature is lower than this, similar considerations are possible.

We want to solve the classical equations of motion in an expanding universe

$$\ddot{\phi} + 3H\dot{\phi} + \frac{\partial V}{\partial \phi} = 0, \quad (4.111)$$

for both  $\phi_+$  and  $\phi_-$ , assuming that initially  $\dot{\phi}_\pm(t_0) = 0$ ,  $T \simeq M_*$ . Since the two scalars are approximately decoupled ( $\kappa \lesssim 10^{-5}$  to get the observed DM relic density) we can solve Eq. (4.111) separately for  $\phi_+$  and  $\phi_-$ . As in the DM case we can consider a single scalar  $\phi$ , solve its equations of motion and then see how the solution applies to  $\phi_+$  and  $\phi_-$ .

In principle there are four relevant regimes (that if needed can be glued together). They correspond to the position of  $\phi$  (near the local minimum or as far as it can be, see Fig. 4.18) and to whether  $H(T)$  is dominated by the  $\phi_\pm$  vacuum energy or SM radiation. If  $\phi_\pm$  vacuum energy dominates the expansion of the universe the patch is in a state of  $\phi_\pm$ -driven inflation

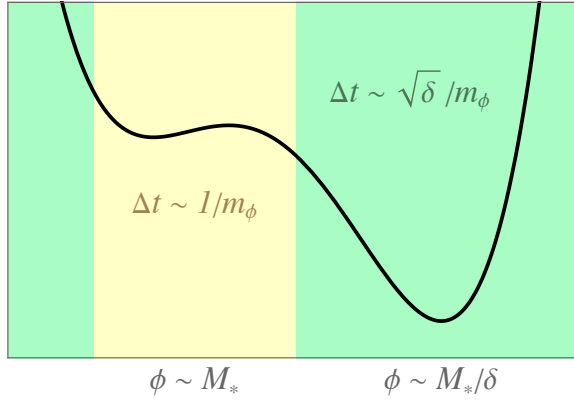


Figure 4.18: Schematic view of the structure of the potential including the time to cross the local (global) region around (far from) the metastable minimum. Scalars that roll to the deep minimum and lead to a crunching universe take most of the time to cross the local region ( $\sqrt{\delta} \ll 1$ ).

until the rolling of the scalars makes it crunch. These patches do not reheat<sup>11</sup>, because of the feeble  $\phi_{\pm}$  interactions. As a consequence, independently on the rolling time, these patches are basically empty, excluded by the standard anthropic arguments on the possibility of complex structures. In summary only two cases are actually relevant:

1.  $H(T) \simeq T^2/M_{\text{Pl}}$ ,  $\phi(t_0) \simeq M_*$
2.  $H(T) \simeq T^2/M_{\text{Pl}}$ ,  $\phi(t_0) \simeq M_*/\delta$ .

First consider patches that start with the fields  $\phi_{\pm}$ , denoted generically by  $\phi$ , at the scale of the local minimum of the potential, i.e.  $\phi \sim M_*$ . Since at this scale  $V \sim m_{\phi}^2 M_*^2 \ll M^2 M_*^2$ , the patch is initially radiation-dominated and the evolution of the scalars is given by

$$\ddot{\phi} + \frac{3}{2t}\dot{\phi} + \frac{\partial V}{\partial \phi} = 0. \quad (4.112)$$

In universes destined to crunch and in the local region  $|\phi| \lesssim M_*$ , we can approximate  $V$  with a tadpole (either the Higgs induced one for  $\phi_-$  or the one in  $V_{\phi_+}$  for  $\phi_+$ ), so  $\frac{\partial V}{\partial \phi} \simeq \text{const.}$  and we can solve Eq. (4.112) exactly. We find that  $\phi_{\pm}$  cross a region of  $\mathcal{O}(M_*)$  in a time

$$\begin{aligned} \Delta t_-(M_*) &= \frac{\sqrt{5}}{2\sqrt{\kappa(m_{\phi_-}/M_*)}\mu_H}, \quad \mu_H^2 \equiv \langle H_1 H_2 \rangle, \\ \Delta t_+(M_*) &= \frac{\sqrt{5}}{2m_{\phi_+}}, \end{aligned} \quad (4.113)$$

respectively. The longest crossing time for universes with  $\langle h \rangle \gtrsim v$  is obtained for  $\langle H_1 H_2 \rangle \simeq \mu_B^2$ , i.e. when the Higgs-induced tadpole has the smallest slope that can still destroy the local minimum for  $\phi_-$ . This happens for  $\Delta t_-(M_*) \simeq 1/m_{\phi_-}$ .

To make sure that this calculation is consistent we need to check that in a time  $\Delta t_{\pm}$  the temperature has not dropped enough from the initial value to take the universe to a new phase of inflation. We have

$$\Delta t_{\pm} = - \int_{M_*}^{T_{\pm}} \frac{dT}{H(T)T} \rightarrow T_{\pm}^4 = \frac{M_*^4}{(2H(M_*)\Delta t_{\pm} + 1)^2}. \quad (4.114)$$

<sup>11</sup>More precisely, as described in [343], while the scalar slides down its potential a subdominant thermal bath is formed, due to the tiny interaction with the SM photons. When the vacuum energy crosses zero and crunching starts, both the kinetic energy of  $\phi$  and the thermal bath rapidly blue-shift until the big crunch.



Comparing with  $V_{\phi_{\pm}} \simeq m_{\phi_{\pm}} M_*^2$  we get that we do not enter a phase of inflation if

$$\frac{H(M_*)}{M_*} \lesssim 1, \quad (4.115)$$

which is satisfied for sub-Planckian  $M_*$ . Now, let us instead assume that the patch starts from a value of the scalar fields at the global scale, i.e.  $\phi \sim M_*/\delta$  and  $V \sim m_{\phi}^2 M_*^4/\delta^3$ . If  $\delta^3 \lesssim m_{\phi}^2/M_*^2$  the scalar potential dominates with respect to the thermal bath and the patch is in a state of  $\phi$ -driven inflation until the rolling of the scalars makes it crunch. As explained above these universes are empty.

In the opposite regime  $\delta^3 \gtrsim m_{\phi}^2/M_*^2$  the patch starts as radiation-dominated. After a time  $\Delta t_s \lesssim \sqrt{\delta}/m_{\phi}$  Hubble friction becomes negligible<sup>12</sup>. This can be estimated for instance by showing that when  $H(T) \simeq m_{\phi}/\sqrt{\delta}$ ,  $\phi$  is slow rolling over a range  $\Delta\phi \simeq M_*/\delta$  in one Hubble time. When Hubble friction is negligible we can solve Eq. (4.111) in its simpler form

$$\ddot{\phi} + \frac{\partial V}{\partial \phi} \simeq 0. \quad (4.116)$$

We obtain that  $\phi$  crosses the ‘‘global’’ region  $\Delta\phi \simeq M_*/\delta$ , in a time  $\Delta t_g \simeq \sqrt{\delta}/m_{\phi}$ . Therefore the longest time that  $\phi$  can spend in this region of the potential, obtained combining the two times (the time in which  $\phi$  can be stuck due to Hubble friction and the time needed to cross the region),  $\Delta t_g + \Delta t_s \simeq \sqrt{\delta}/m_{\phi}$ , is much shorter than the one required to cross the region around the local minimum:  $\Delta t_{\pm} \lesssim 1/m_{\phi}$ .

In summary, as shown in Fig. 4.18, the longest time that it can take a universe with the wrong Higgs vev to crunch is parametrically

$$\Delta t_c^{\max} \simeq \max[1/m_{\phi_+}, 1/m_{\phi_-}], \quad (4.117)$$

dominated by patches where  $\phi_{\pm}$  are initially in the region where their local minimum can be generated  $|\phi_{\pm}| \lesssim M_*$ .

Finally, notice that: 1) If  $\Delta t_g$  is consistently smaller than a Hubble time, the global region is crossed in a time  $\Delta t_g$  and the crunching time is dominated by the time to cross the local region, as discussed above. In the opposite case, instead, the temperature drops until  $T^4 \sim M_{\text{Pl}}^2 m_{\phi}^2/\delta$ . This can be smaller than  $V$  itself, signalling the onset of a stage of  $\phi$ -driven inflation, which would give an empty patch till crunching. 2) a patch starting from sufficiently far away from the local minimum could be doomed to crunch anyway, independently on the value of the Higgs vev, since the kinetic energy of  $\phi$  when Hubble friction becomes negligible, which for  $\phi$  initially at  $M_*/\delta$  is given by

$$\dot{\phi}^2 \simeq \frac{m_{\phi}^2 M_*^2}{\delta^3}, \quad (4.118)$$

can be sufficient to overtake the local maximum and access the unstable region of the potential. Nevertheless, the crunching time of these patches is at most the one given in Eq. (4.117), so our mechanism is effective as long as  $t_c \sim 1/m_{\phi}$  is short enough.

In conclusion some patches might crunch or enter a phase of  $\phi$ -driven inflation, leading to an empty universe, even if they have the observed Higgs vev. However all patches with the wrong Higgs vev rapidly crunch or enter a phase of  $\phi$ -driven inflation, in a time bounded by (4.117), making our mechanism an effective way to select the weak scale.

<sup>12</sup>Hubble friction can be negligible from the beginning for low cutoffs, i.e. if  $H(M_*) \simeq M_*/M_{\text{Pl}} \lesssim m_{\phi}/\sqrt{\delta}$ .

## Parameter space

Our parameter space is summarized in Fig. 4.16. The scalar mass  $m_\phi$  is bounded from below by the requirement that the crunching time must be shorter than the cosmological scale, say  $10^9$  yr, otherwise patches with heavy Higgs, or without EW symmetry breaking, are too long-lived. Imposing a shorter maximum crunching time a more stringent limit is obtained, as shown in Fig. 4.16. On the other hand,  $m_\phi$  is bounded from above by the requirement that the crunching time for  $\phi_+$  must be longer than  $1/H$  at the EW phase transition, so that the Higgs vev has the possibility to stop the rolling of  $\phi_+$  in due time. Finally, the cutoff  $M_*$  is bounded from above by the requirement that scalar oscillations do not overclose the Universe. If  $M_* \gtrsim 10^{12}$  GeV, they can reproduce the observed DM relic density. If this is the case, the scalars must however be heavier than  $\approx 10^{-22}$  eV, because of limits on fuzzy DM [320].

### 4.5.4 The $H_1H_2$ trigger

The essence of our mechanism is the generation of a Higgs-dependent tadpole for two scalars  $\phi_\pm$ . When the Higgs vev is larger than a certain threshold,  $\langle h \rangle \gtrsim \bar{\mu}_S$ , this tadpole generates a “safe” minimum for  $\phi_+$ . When it gets even larger,  $\langle h \rangle \gtrsim \bar{\mu}_B \gtrsim \bar{\mu}_S$ , it destabilizes a minimum for  $\phi_-$ . As discussed in Section 4.5.3, only universes with the Higgs vev in the range  $\bar{\mu}_S \lesssim \langle h \rangle \lesssim \bar{\mu}_B$ , do not rapidly crunch. So far we have mainly considered one operator that can generate this Higgs-dependent tadpole

$$\mathcal{O}_T = H_1H_2, \quad \mathcal{L} \supset -\kappa H_1H_2(m_{\phi_+}\phi_+ + m_{\phi_-}\phi_-) + \text{h.c.} \quad (4.119)$$

This type of operator is a *trigger* in the definition of [153]. When the Higgs vev (and thus the operator vev) crosses certain upper or lower bounds, a cosmological event is triggered via the coupling to the new scalar(s). In our case the event is a rapid crunch of the universe.

In this Section we discuss the dependence of  $\langle H_1H_2 \rangle$  on the vev of the SM Higgs in more detail. In particular we show how bounding the vev of  $H_1H_2$  selects a value for  $\langle h \rangle$  if the Two Higgs Doublet Model (2HDM) has a  $\mathbb{Z}_2$  symmetry:  $H_1H_2 \rightarrow -H_1H_2$ . This singles out a very specific kind of 2HDM potential that leads to characteristic signals at the LHC. We find interesting that discovering new fundamental scalars at the LHC, without new symmetries protecting their masses, is traditionally considered as a “death sentence” for naturalness. On the contrary, our study and the work in [153] show that this can be the first manifestation of naturalness of the Higgs mass.

We consider the most general  $\mathbb{Z}_2$  symmetric 2HDM potential [153]

$$H_1H_2 \rightarrow -H_1H_2, \quad V_{H_1H_2} \rightarrow V_{H_1H_2}, \quad (4.120)$$

where

$$\begin{aligned} V_{H_1H_2} = & \frac{m_1^2}{2}|H_1|^2 + \frac{m_2^2}{2}|H_2|^2 + \frac{\lambda_1}{2}|H_1|^4 + \frac{\lambda_2}{2}|H_2|^4 \\ & + \lambda_3|H_1|^2|H_2|^2 + \lambda_4|H_1H_2|^2 + \left( \frac{\lambda_5}{2}(H_1H_2)^2 + \text{h.c.} \right). \end{aligned} \quad (4.121)$$

This potential does not contain odd spurions that can generate contributions to  $\mu_H^2 = \langle H_1H_2 \rangle$  sensitive to the cutoff. If the  $\mathbb{Z}_2$  is exact we have  $\mu_H^2 = 0$ . Coupling  $H_1H_2$  to  $\phi_\pm$ , as in Eq. (4.119), does not break the  $\mathbb{Z}_2$  symmetry if  $\phi_\pm \rightarrow -\phi_\pm$ . Furthermore it leaves  $\mu_H^2$  and all 2HDM phenomenology approximately unaltered, since the couplings between the new scalars and the 2HDM are minuscule  $m_\phi \lesssim v^2/M_*$ , as discussed in Section 4.5.3. Therefore, in the study of  $\mu_H^2$  we can ignore the coupling to  $\phi_\pm$  and only (4.121) matters.

The vevs of  $H_{1,2}$  and the QCD condensate break the  $\mathbb{Z}_2$  and generate  $\mu_H^2 \neq 0$ . To compute the value of  $\mu_H^2$  we need to assign  $\mathbb{Z}_2$  charges to the quarks and leptons. We choose

$$H_2 \rightarrow -H_2, \quad (qu^c) \rightarrow -(qu^c), \quad (qd^c) \rightarrow -(qd^c), \quad (le^c) \rightarrow -(le^c), \quad (4.122)$$

so that one of the two Higgs doublets is inert and the only Yukawa couplings in the model are

$$V_Y = Y_u q H_2 u^c + Y_d q H_2^\dagger d^c + Y_e l H_2^\dagger e^c + \text{h.c.} . \quad (4.123)$$

This is the safest choice phenomenologically. It was shown in [153] that this charge assignment is still viable experimentally, but it will be decisively probed by HL-LHC.

The model defined by Eq.s (4.121) and (4.123) has a UV-insensitive and calculable vev  $\mu_H^2$ , shown in Fig. 4.19.  $\mu_H^2$  gives a tadpole to  $\phi_\pm$  and so the mechanism is really selecting

$$\mu_S^2 \lesssim \langle H_1 H_2 \rangle \lesssim \mu_B^2, \quad (4.124)$$

which is not the vev of the SM Higgs:  $\langle h \rangle \simeq \sqrt{|m_2^2|}$ . In principle  $\mu_H^2$  can be close to  $v^2$  also for universes with very different EW-symmetry breaking compared to ours, for instance  $m_1^2 \sim -v^4/M_*^2$ ,  $m_2^2 \sim -M_*^2$  still gives  $\mu_H^2(T=0) \simeq v^2$ . However our selection mechanism takes place at  $T \neq 0$ . In practice we never need to worry about these patches provided that  $\phi_+$  is heavy enough to roll to its stable minimum before  $H_1 H_2$  gets a vev in these universes. In our universe  $\mu_H^2 \neq 0$  already at the EW phase transition, while in these patches it is zero until much later:  $T^2 \lesssim v^4/M_*^2$ .

There is one additional subtlety to consider. QCD can generate a vev for  $H_1 H_2$  even for  $m_2^2 \geq 0$  (see the right panel of Fig. 4.19): at the QCD phase transition quark bilinears condensate. This gives an effective tadpole for  $H_2$ , via (4.123). As a consequence,  $\mu_H^2$  can be close to  $v^2$  also for another class of universes with very different EW-symmetry breaking compared to ours, for instance  $m_1^2 \sim -v^4/\Lambda_{\text{QCD}}^2$ ,  $m_2^2 \simeq 0$  still gives  $\mu_H^2(T=0) \simeq v^2$ . For concreteness here and in the following we assume that dimensionless couplings do not scan in the landscape.  $\Lambda_{\text{QCD}}$  is still different from universe to universe due to the different SM Higgs vevs, but this does not affect our discussion, so we do not show explicitly this dependence here and in the following.

As in the previous case, these unwanted patches rapidly crunch if  $\phi_+$  is heavy enough to roll to its stable minimum before the QCD phase transition. Indeed, as shown in the left panel of Fig. 4.19, before the QCD phase transition  $\mu_H^2$  can be nonzero only if both  $m_{1,2}^2 < 0$  and larger, in absolute size, than the positive thermal contribution. These considerations favour a relative heavy  $\phi_+$ , close to the boundary of its allowed region  $m_{\phi_+} \lesssim H(v) \simeq 10^{-4}$  eV.

There are other possibilities to solve the problem raised by these unwanted patches (both those with  $m_2^2 > 0$  and those with small  $m_1^2$  or  $m_2^2$ ). We can consider low cutoffs  $M_* \lesssim v^2/\Lambda_{\text{QCD}}$ , so that these patches are not present in the Multiverse or supplement the mechanism with the anthropic considerations in [153].

The model that we just described has an accidental symmetry, as noted in [153]. The Lagrangian is actually  $\mathbb{Z}_4$ -symmetric

$$H_1 \rightarrow iH_1 \quad H_2 \rightarrow iH_2 \quad (qu^c) \rightarrow -i(qu^c) \quad (qd^c) \rightarrow i(qd^c) \quad (le^c) \rightarrow i(le^c), \quad (4.125)$$

this creates a potential cosmological problem. After EW symmetry breaking a  $\mathbb{Z}_2$  subgroup of the  $\mathbb{Z}_4$  survives

$$H_1 \rightarrow -H_1. \quad (4.126)$$

This  $\mathbb{Z}_2$  subgroup can be obtained from the  $\mathbb{Z}_4$  after a global hypercharge rotation. As a consequence the model has a domain-wall problem, i.e. domain walls between regions with  $\pm v_1$

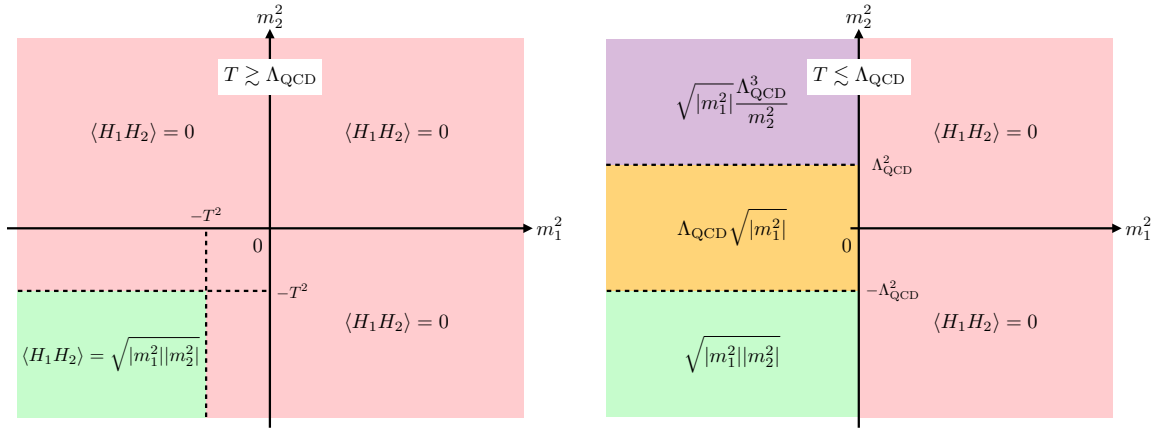


Figure 4.19: Vacuum expectation value of  $H_1H_2$  in the model of Eq.s (4.121) and (4.123) as a function of the two Higgs masses. We show the vev before (left) and after (right) the QCD phase transition.  $m_{1,2}$  are effective masses with the dimensions of vevs that contain contributions from  $\mathcal{O}(1)$  quartic couplings.  $\Lambda_{\text{QCD}}$  is a function of the Higgs vevs and varies within the purple and yellow boxes. We have approximated thermal corrections to  $m_{1,2}^2$  with  $T^2$  to improve readability. Note that in the light red regions the vev is not exactly zero, because of a small effective  $B\mu$  term induced by the  $\phi_{\pm}$  vevs. However this effect is too small to affect our conclusions. It only gets rid of dangerous domain walls, as discussed in the main body of the text.

are generated at the EW phase transition and they come to dominate the energy density of our Universe at  $T \simeq v(v/M_{\text{Pl}})^{1/2} \simeq \text{keV}$ . We can solve the problem via a tiny breaking of the  $\mathbb{Z}_4$  that does not alter any of our conclusions. If the 2HDM potential contains a  $B\mu$ -term of size

$$V_{H_1H_2} \supset -B\mu H_1H_2 + \text{h.c.} \quad B\mu \simeq \frac{v^4}{M_{\text{Pl}}^2}. \quad (4.127)$$

This insures that the domain walls annihilate at  $T \simeq \text{keV}$ . At larger temperatures they constitute a negligibly small fraction of the total energy density [153]. This  $B\mu$  term breaks also our original  $\mathbb{Z}_2$ , but it is numerically negligible in our analysis. In a large fraction of our parameter space, shown in Fig. 4.16, the misalignment of  $\phi_{\pm}$  at the EW phase transition automatically generates a large enough  $B\mu$ , and we do not need Eq. (4.127).

As noted in [153] the phenomenology of this  $\mathbb{Z}_2$  symmetric “type-0” 2HDM is very interesting. Since we effectively set to zero any scale in the potential besides the two masses ( $B\mu \simeq \frac{v^4}{M_{\text{Pl}}^2} \ll v^2$ ), the new Higgs states contained in  $H_1$  are close to the weak scale. If we adopt the usual notation for charged, scalar and pseudo-scalar Higgses we have

$$\begin{aligned} m_A^2 &= -v^2\lambda_5, \\ m_{H^{\pm}}^2 &= -v^2\frac{\lambda_5 + \lambda_4}{2} \\ m_{h,H}^2 &= \frac{1}{2} \left( \lambda_1 v_1^2 + \lambda_2 v_2^2 \pm \sqrt{(\lambda_2 v_2^2 - \lambda_1 v_1^2)^2 + 4v_1^2 v_2^2 \lambda_{345}^2} \right) \end{aligned} \quad (4.128)$$

and to avoid TeV-scale Landau poles we need all quartics to be  $\lesssim 2$  around the weak scale [153]. Therefore we have a sharp target for searches at the LHC and HL-LHC, which is made even sharper if we notice two well-known facts: 1) There are couplings between the SM and two new Higgses proportional to the  $SU(2)_L$  gauge coupling, which are fixed by gauge invariance. 2) Couplings with a single new Higgs, that are proportional to  $v_1$ , can not be made arbitrarily small.

Both points are quite interesting for the LHC: 1) a CMS search for staus in a  $\tau^+\tau^- + \text{MET}$  final state, is sensitive to pair production of  $H^+H^-$  [193]. If recasted it can potentially extend LEP's bound on the  $H^\pm$  mass to about 150 GeV [153]. 2) At small  $v_1$  the new scalar Higgs becomes light

$$m_H^2 = v_1^2 \left( \lambda_1 - \frac{\lambda_{345}^2}{\lambda_2} \right) + \mathcal{O}(v_1^4/v^4). \quad (4.129)$$

So when trying to decouple  $H_1$  we rapidly run into stringent constraints from LEP, B-factories and beam-dump experiments. Quantitatively this means that Higgs coupling deviations in this model will be visible at HL-LHC. A more complete summary of signals and constraints can be found in [153].

To conclude this section it is worth to point out that the  $\mathbb{Z}_2$  symmetry is not mandatory. However disposing of it forces two coincidences of scale to make  $\mu_H^2$  sensitive to the SM Higgs vev.

To show this we can write a left-right symmetric model which is approximately invariant under  $H_1 \leftrightarrow H_2$  as in [142, 151]. If  $B\mu \lesssim 16\pi^2 v^2$  and  $\lambda_{6,7} \lesssim 16\pi^2 v^2/M_*^2$ ,  $\mu_H^2$  is dominated by the tree-level contributions from the vevs. Furthermore, the exchange symmetry forces  $|m_{1,2}^2| \simeq v^2$  when  $\mu_H^2 \simeq v^2$ , just what we want to select the weak scale from  $H_1 H_2$ . Nonetheless, to make this model compatible with present LHC constraints we need both  $||m_1^2| - |m_2^2|| \gtrsim v^2$  and  $B\mu \gtrsim v^2$ . As we have just shown, to make  $H_1 H_2$  a good trigger we have upper bounds of the same order on both quantities: 1) we do not want loop corrections to  $\mu_H^2$  to dominate on the vevs, hence  $B\mu \lesssim 16\pi^2 v^2$ , 2) we can not take the two masses too far apart, since breaking too much the exchange symmetry can lead to  $\langle H_1 H_2 \rangle \simeq B\mu \frac{|m_1^2|}{|m_2^2|}$ , which can be close to the weak scale even when  $m_2^2 \simeq -m_1^2 \simeq M_*^2$ . In summary we need both  $||m_1^2| - |m_2^2||$  and  $B\mu$  to be of  $\mathcal{O}(v^2)$ . So this is still an interesting possibility to consider, but it is not as simple as imposing the  $\mathbb{Z}_2$  symmetry.

### 4.5.5 The Standard Model Trigger

We now consider the SM trigger, expanding the discussion of [154]. We take  $\phi_\pm$  to have an axion-like coupling to gluons

$$V_{G\phi} = -\frac{1}{32\pi^2} \left( \frac{\phi_+}{F_+} + \frac{\phi_-}{F_-} + \theta \right) \text{Tr}[G\tilde{G}]. \quad (4.130)$$

As we discussed in Section 4.5.5, for  $m_{u,d} \lesssim 4\pi f_\pi$ , if we rotate  $\phi_\pm$  in the quark mass matrix and match to the chiral Lagrangian at low energy, Eq. (4.130) gives

$$V_{G\phi} = -m_\pi^2 f_\pi^2 \sqrt{1 - \frac{4m_u m_d}{(m_u + m_d)^2} \sin^2 \left( \frac{\phi_+}{2F_+} + \frac{\phi_-}{2F_-} + \frac{\theta}{2} \right)} \simeq \frac{\Lambda^4(\langle h \rangle)}{2} \left( \frac{\phi_+}{F_+} + \frac{\phi_-}{F_-} + \theta \right)^2, \quad (4.131)$$

where the potential is switched on at the QCD phase transition by chiral symmetry breaking

$$\Lambda^4(\langle h \rangle) = m_\pi^2 f_\pi^2 \frac{m_u m_d}{(m_u + m_d)^2}. \quad (4.132)$$

We stress that its size is a monotonic function of the Higgs vev even in the regime  $m_{u,d} \gtrsim 4\pi f_\pi$ , although the functional form of  $\Lambda(\langle h \rangle)$  becomes different. For the moment, we assume that the vacuum angle  $\theta$  (which includes the quark-mass phases) is fixed and small because of some UV-mechanism that solves the strong-CP problem. Later, in Section 4.5.5 we will relax this assumption and show that the mechanism can actually also solve the strong-CP problem by itself in a novel way [154], if the  $\theta$  angle instead scans in the landscape.

We consider a scalar potential with the same form as in Section 4.5.2:

$$V_{\pm}(\phi_{\pm}) = m_{\pm}^2 M_{\pm}^2 \left( \frac{\phi_{\pm}}{M_{\pm}} + \frac{\phi_{\pm}^2}{2M_{\pm}^2} \pm \frac{\phi_{\pm}^3}{3M_{\pm}^3} + \frac{\delta}{4} \frac{\phi_{\pm}^4}{M_{\pm}^4} \right) + \dots \quad (4.133)$$

with the total potential being  $V = V_+ + V_- + V_{G\phi}$ . Notice that (4.131) does not impose constraints on the naturalness of  $V_{\pm}$ . Therefore,  $M_{\pm}$  are not related to the Higgs cutoff, which can be arbitrarily large. We take  $M_{\pm}/F_{\pm} \ll 1$  so that in the local region of the potential  $V_{G\phi}$  is dominated by the quadratic term in the second equality of Eq. (4.131). As we will see in the following this is required by current measurements of the QCD  $\theta$ -angle.

We assume  $m_+ \lesssim H(\Lambda_{\text{QCD}})$ , so that when  $\phi_+$  starts to move, from the local region  $\phi_+ \sim M_+$  (otherwise the patch crunches anyway), the potential (4.131) is already switched on. Then, the  $\phi_+$  potential is locally stabilized only if  $\langle h \rangle > \mu_S$ , with

$$\Lambda_S^4 \equiv \Lambda^4(\langle \mu_S \rangle) \simeq m_+^2 F_+^2. \quad (4.134)$$

This can be understood as follows: in absence of  $V_{G\phi}$ ,  $\phi_+$  does not have a metastable minimum in the local region  $|\phi_+| \lesssim M_+$ . In this region  $V_{G\phi}$  is given approximately by the quadratic term in the second equality of Eq. (4.131). The only monomial that can generate a minimum is the  $\phi_+^2$  term in  $V_{G\phi}$ . The minimum is generated only if this term (with positive sign) dominates within  $|\phi_+| \lesssim M_+$ .

In general we may not have  $\mu_S \simeq v$ , so in this section we give formulas valid also for  $\mu_S < v$ , which is enough to select successfully the weak scale. For instance, in this case the size of local stable region around the metastable minimum is increased from  $M_+$ , at  $\mu_S = v$ , to <sup>13</sup>

$$\widetilde{M}_+ \simeq \frac{\Lambda_{\text{QCD}}^4}{\Lambda_S^4} M_+. \quad (4.135)$$

The physical mass of the scalar is

$$m_{\phi_+}^2 \simeq \frac{\Lambda_{\text{QCD}}^4}{F_+^2} \simeq \frac{\Lambda_{\text{QCD}}^4}{\Lambda_S^4} m_+^2. \quad (4.136)$$

The above arguments show how we get a lower bound on the weak scale. An upper bound is generated as long as the  $\phi_-$  potential in (4.131) is dominated by the tadpole, i.e.  $M_-/F_- \lesssim \widetilde{M}_+/F_+ + \theta$ . In this case, the safe local minimum exists as long as  $\langle h \rangle < \mu_B$ , with

$$\Lambda_B^4 \equiv \Lambda^4(\langle \mu_B \rangle) \simeq \frac{m_-^2 M_- F_-}{\theta + \widetilde{M}_+/F_+}. \quad (4.137)$$

If both  $\phi_+$  and  $\phi_-$  exist in Nature, the only patches that do not crunch are those with  $\mu_S < \langle h \rangle < \mu_B$ . Given that, typically, large Higgs masses are favoured in the landscape, we have  $v \approx \mu_B$ , so that  $\Lambda_B \approx \Lambda_{\text{QCD}}$ . The physical scalar mass is  $m_{\phi_-} \simeq m_-$ . This could be smaller or bigger than  $m_+$  and  $H(\Lambda_{\text{QCD}})$ . Accordingly, during  $\phi_-$  dynamics the other scalar  $\phi_+$  could be still frozen by Hubble friction or not. We have replaced the unknown  $\phi_+$  misalignment at the time when  $\phi_-$  starts to move, with its typical value  $\widetilde{M}_+$ , i.e. the size of the local stability region close to the safe metastable minimum of  $\phi_+$ . Notice that  $\phi_+$  moves by an amount  $\sim \widetilde{M}_+$  after the QCD phase transition, so even patches for which the denominator in (4.137) is initially

---

<sup>13</sup>This formula is valid if the instability is generated by a cubic term, as in (4.133). If, instead, the instability is generated by a quartic coupling, like in the example potential of [154], we find  $\widetilde{M}_+ \simeq M_+ \Lambda_{\text{QCD}}^2 / \Lambda_S^2$ .

tuned to be small can survive until today only if  $\langle h \rangle \lesssim \mu_B$ , since the denominator will effectively be detuned when  $\phi_+$  starts to move. The  $\theta$ -angle today is

$$\theta_0 \simeq \theta + \frac{\widetilde{M}_+}{F_+} + \frac{M_-}{F_-} \simeq \theta + \frac{\widetilde{M}_+}{F_+}. \quad (4.138)$$

We had already assumed  $\theta \lesssim 10^{-10}$  from an unspecified UV solution to the strong CP problem (for instance of the Nelson-Barr type [344, 345]), we further require  $\widetilde{M}_+/F_+ \lesssim \theta_{\text{exp}} \simeq 10^{-10}$ .

Notice that along the flat direction of (4.131),  $F_- \phi_+ = -F_+ \phi_- - \theta F_+ F_-$ , the potential is not sensitive to the Higgs vev. However, with our assumptions (and at fixed  $\theta$ ), generically the flat direction does not intersect the local stability region  $\phi_{\pm} \sim M_{\pm}$  and hence it does not pose a threat to the mechanism.

### Solving also the strong-CP problem

So far we have assumed that the  $\theta$  angle is set to be small by some unspecified mechanism operating at a high energy scale ( $E \gg \sqrt{m_{\phi_{\pm}} M_{\pm}}$ ). We now show that the usual Peccei-Quinn solution is not compatible with the mechanism. Let us assume that an axion  $a$  is present, heavier than  $\phi_{\pm}$ , so that (4.131) is modified to

$$V_{G\phi a} \simeq \frac{\Lambda^4(\langle h \rangle)}{2} \left( \frac{\phi_+}{F_+} + \frac{\phi_-}{F_-} + \frac{a}{f} \right)^2, \quad (4.139)$$

having used the shift-symmetry of  $a$  to absorb the UV  $\theta$  angle. Then, the first scalar that starts rolling is the axion itself, which rapidly relaxes the whole  $\langle h \rangle$ -dependent potential to 0; this is continuously readjusted to 0 even subsequently, during the slower motion of  $\phi_{\pm}$ . As a consequence,  $\phi_{\pm}$  would not be sensitive to the Higgs vev. Notice that some small Peccei-Quinn breaking potential for the axion, coming from the UV, would not help, being independent on the Higgs vev.

However, if the  $\theta$ -angle is also scanned in the landscape (for instance because of the presence of a scalar coupled to  $G\widetilde{G}$  and lighter than  $\phi_{\pm}$ ), then *our mechanism itself solves the strong-CP problem in a novel way*, in addition to the Higgs hierarchy problem [154]. This occurs because the  $\phi_+$  metastable minimum is generated only if  $\theta$  is small enough that the minimum of (4.131) lies within the local region  $\phi \sim M_+$ , where the destabilizing cubic term of  $V_+$  does not dominate. Otherwise the patch crunches, in the same way as the ones with a “wrong” value of the Higgs vev. A small  $\theta$  is selected by this requirement:

$$\frac{\widetilde{M}_+}{F_+} \gtrsim \theta. \quad (4.140)$$

The only patches that do not crunch are those with  $\mu_S \lesssim \langle h \rangle \lesssim \mu_B$  and  $\theta_0 \ll 1$ . This novel solution to the strong-CP problem has its own phenomenological features that distinguish it clearly from the axion one, as discussed in [154] and summarized in the next subsection. Additionally, the same dynamics selects a small and nonzero Higgs vev.

Before discussing the phenomenology, we point out a subtlety that arises once  $\theta$  scans in the landscape. In this case, there certainly exist patches with tuned values of  $\theta$  such that the flat direction of (4.131) crosses the local stability region  $\phi_{\pm} \sim M_{\pm}$  and therefore becomes relevant. Recall that along the flat direction the potential is not sensitive to the Higgs vev. On the one hand, it is possible to show that the potential along this direction is locally stabilized by the quadratic terms of (4.133), as long as  $\Lambda_B \gtrsim \Lambda_S$ . On the other hand, this “tuned” local minimum keeps being present in the potential even for large values of  $\Lambda(\langle h \rangle) \gg \Lambda_{\text{QCD}}$ , threatening the successful selection of  $\langle h \rangle \lesssim v$ : as just mentioned along the flat direction the potential is locally

stable to start with, along the orthogonal direction it is made stable by the large contribution of (4.131). However, our mechanism is still successful because these metastable patches with  $\Lambda(\langle h \rangle) \gg \Lambda_{\text{QCD}}$  are *doubly tuned*. First, in order for the flat direction to cross the local stability region,  $\theta$  needs to be tuned by an amount

$$\epsilon_\theta \sim \frac{M_-/F_-}{\widetilde{M}_+/F_+} \ll 1 \quad (4.141)$$

as compared to stable patches with  $\Lambda(\langle h \rangle) \sim \Lambda_{\text{QCD}}$ . Second, given that the flat direction is essentially parallel to  $\phi_- \sim \text{const.}$ , the barrier along it is  $\Delta V_\parallel \sim m_-^2 M_-^2$ . Then, for these “bad” patches to be metastable, the initial value of  $\phi_+$  needs to be tuned to lie within a tiny region of size  $\Delta\phi_+$  such that  $\Delta V_\perp \lesssim \Delta V_\parallel$ , otherwise the combined evolution of  $\phi_\pm$ , which explores the phase-space energetically allowed, would probe the instability. This gives an additional tuning  $\epsilon_{\phi_+} \sim \Delta\phi_+/\widetilde{M}_+$ , with:

$$\frac{\Lambda(\langle h \rangle)^4 \Delta\phi_+^2}{F_+^2} \sim m_-^2 M_-^2, \quad (4.142)$$

yielding

$$\epsilon_{\phi_+} \sim \sqrt{\frac{M_-/F_-}{\widetilde{M}_+/F_+} \frac{\Lambda_B^2}{\Lambda(\langle h \rangle)^2}} \ll 1. \quad (4.143)$$

The combined tuning  $\epsilon_\theta \epsilon_{\phi_+}$  can be made arbitrarily small by taking  $M_-/F_- \ll \widetilde{M}_+/F_+$ , so to compensate any reasonable a priori preference for large values of  $\Lambda(\langle h \rangle)$  in the landscape, thus making the doubly tuned patches irrelevant, being arbitrarily rare or absent altogether<sup>14</sup>.

### Smoking-gun phenomenological pattern

The cosmology of the  $\widetilde{m}$  model is basically the same as for the  $H_1 H_2$  trigger, with the role of the electroweak phase transition replaced by the QCD one. In particular, the scalar  $\phi_+$  needs to be lighter than  $H(\Lambda_{\text{QCD}})$ , or the universe would crunch independently of  $\langle h \rangle$  before the Higgs-dependent potential is switched on.

Both scalars can constitute the totality of dark matter in the Universe, yielding a DM phenomenology cross-correlated with EDM experiments, as studied in detail in [154] for  $\phi_+$ . Let us start from this scalar. At the QCD phase transition it gets a kick of order  $\widetilde{M}_+$ , which dominates its oscillations. Then, its energy density when it starts oscillating after the QCD transition is  $\rho_+ \sim m_{\phi_+}^2 \widetilde{M}_+^2 \sim \theta_0^2 \Lambda_{\text{QCD}}^4$ , giving the relic density today

$$\frac{\rho_{\phi_+}}{\rho_{\text{DM}}} \simeq \frac{\theta_0^2 \Lambda_{\text{QCD}}^4}{T_{\text{eq}} M_{\text{Pl}}^{3/2} m_{\phi_+}^{3/2}} \simeq \left( \frac{\theta_0}{10^{-10}} \right)^2 \left( \frac{10^{-19} \text{ eV}}{m_{\phi_+}} \right)^{3/2}. \quad (4.144)$$

Therefore, its relic density is  $\simeq \theta_0^2$  times smaller than the one of a Peccei-Quinn axion with the same mass, avoiding overclosure constraints on light axions. Also  $\phi_-$  can be the dark matter of the Universe, if light enough. Analogously to  $\phi_+$ , its energy density at the onset of its oscillations is  $\rho_- \sim m_-^2 M_-^2 \sim (M_-/F_-) \theta_0 \Lambda_{\text{QCD}}^4 \lesssim \theta_0^2 \Lambda_{\text{QCD}}^4$ , smaller than the one for  $\phi_+$ . However, it can give the correct relic density if lighter than  $\phi_+$ :

$$\frac{\rho_{\phi_-}}{\rho_{\text{DM}}} \simeq \frac{\theta_0 \Lambda_{\text{QCD}}^4 M_-/F_-}{T_{\text{eq}} M_{\text{Pl}}^{3/2} m_{\phi_-}^{3/2}} \simeq \left( \frac{\theta_0}{10^{-10}} \right) \left( \frac{M_-/F_-}{10^{-10}} \right) \left( \frac{10^{-19} \text{ eV}}{m_{\phi_-}} \right)^{3/2}. \quad (4.145)$$

<sup>14</sup>This latter possibility happens in case the tuned initial values of  $\theta$  or  $\phi_+$  are forbidden by additional interactions in the UV, for instance non-minimal couplings to gravity during inflation.



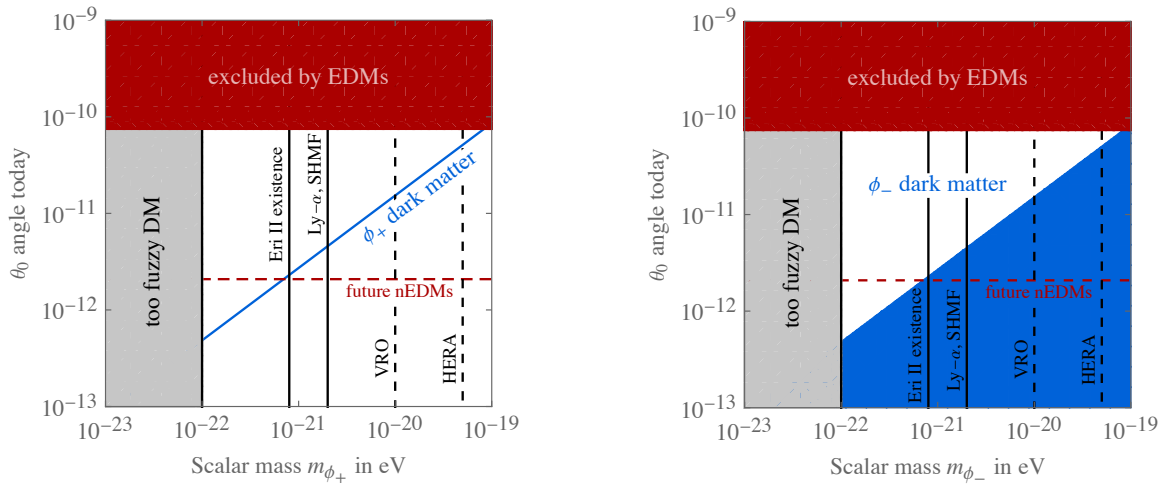


Figure 4.20: Parameter space for which  $\phi_+$  (left panel) or  $\phi_-$  (right panel) constitute the totality of DM of the Universe, as function of their mass and the  $\theta$ -angle today. The DM relic density is reproduced along the blue line (left panel) or white region (right panel). The red shaded region (dashed line) shows bounds [14] (future prospects [346–348]) from hadronic EDM searches. New ideas involving molecular compounds could further improve future sensitivities [349–353]. We also plot in black constraints on fuzzy DM from Lyman- $\alpha$  forest [354–359], measurements of the subhalo mass function [360] and the Eridanus II dwarf galaxy [361] (similar to the constraints from other dwarf galaxies [362,363]). We shade the area where multiple observations disfavor the corresponding DM mass hypotheses [320]. The dashed lines denotes the potential sensitivity from future observations in 21 cm cosmology (HERA) [364] and by the Vera Rubin Observatory [365].

Summarizing, the scalar  $\phi_+$  is an axion of mass  $m_{\phi_+} \lesssim 10^{-11}$  eV which lies on the QCD line  $m_{\phi_+} \simeq \Lambda_{\text{QCD}}^2/F_+$ , as it can be seen by combining (4.134) and (4.136). Instead,  $\phi_-$  is an ALP with a mass comparable to or larger than a QCD axion with the same couplings, as it can be seen from (4.137) and  $M_-/F_- \lesssim \theta_0$ .

Notice that  $\phi_{\pm}$  do not give rise to black hole superradiance in the region  $m_{\phi_{\pm}} \sim 10^{-12}$  eV because of the self-coupling in Eq. (4.133) [366]. If either of them is observed in this region, this would then constitute a first characteristic trait that distinguishes our scalars from the Peccei-Quinn axion.

However, the best phenomenological prospects occur if they are lighter and constitute the dark matter of the Universe, as shown in Figure 4.20. Their relic density is strongly correlated with the value of the  $\theta$  angle today. This is a 1-to-1 correspondence for  $\phi_+$ , while for  $\phi_-$  there is an additional parameter  $M_-/F_-$ . However this ratio has the upper bound  $M_-/F_- \lesssim \theta_0$ . As a consequence, limits on fuzzy DM imply  $\theta_0 \gtrsim 10^{-12}$ , observable at future EDM experiments [346–348]: if either  $\phi_+$  or  $\phi_-$  is dark matter, we predict sizeable EDMs. A joint observation of  $\theta_0$  in the near future and a measurement of the DM mass would allow to test the smoking-gun relations in Eq. (4.144) or (4.145). A combination of future EDM measurements and fuzzy DM probes [320, 354–365] can fully test the hypothesis of  $\phi_{\pm}$  DM, as shown in Fig. 4.20.

## 4.5.6 Conclusions

The two main discoveries of the LHC so far have been: the Higgs boson and the unnaturality of its mass. In this work we have presented a novel mechanism that explains this unnaturality by means of cosmological selection: the multiverse is populated by patches with different values of the Higgs mass; the ones where the EW scale is too small or too large crunch in a short time, the other ones, with the observed (unnaturally small) value of the EW scale survive and expand cosmologically, resulting in an universe as the one that we observe. In [154] we called this scenario *Sliding Naturalness*, since the crunching is due to two light scalars sliding down their potential.

The phenomenology of our proposals depends strongly on the trigger operator that connects the two scalars to the SM. For the  $H_1 H_2$  trigger, as discussed in detail in [153] and summarized in Section 4.5.4, the most favourable prospects for detection come from the observation of the type-0 2HDM at colliders, with the high-luminosity LHC probing completely this possibility. For the SM trigger  $G\tilde{G}$ , the mechanism yields ALP phenomenology. However, a remarkable feature of our scenario [154] is that in this case it also solves automatically the strong-CP problem, in a novel way, different from the usual Peccei-Quinn mechanism, as described in Section 4.5.5.

In both cases, the oscillations of the two scalars can constitute the totality of dark matter in the Universe (see Section 4.5.3). In the case of the SM trigger, this possibility additionally implies a large value of the QCD angle  $\theta \gtrsim 10^{-12}$ , observable in the near future, and strongly correlated to the DM mass, the latter in the fuzzy-DM range (see Figure 4.20).

There are a number of important features that single out our mechanism as compared to other existing proposals in the literature. First, an important distinction between models of cosmological naturalness arises from how they influence inflation. In some cases the Hubble rate during inflation is required to be smaller than  $m_h$  and an exponentially large number of  $e$ -folds might be needed. This clearly requires additional model building that the reader is screened from, but which might considerably complicate the model or introduce tuning. Our mechanism, instead, factorizes from the sector responsible for inflation. Second, the model can have large cutoffs (comparable to  $M_{\text{Pl}}$ ) for both the CC and Higgs mass and at low energy only predicts two extremely weakly coupled scalars with a simple potential. Finally, as argued

in [154], Sliding Naturalness is compatible with modern swampland conjectures and does not suffer from ambiguities connected to eternal inflation.<sup>15</sup>

We cannot know if the unnaturalness of the Higgs mass discovered by the LHC will ultimately be explained by cosmological dynamics. However, the progress of the last years gives us a plausible alternative to traditional solutions to the problem or to accepting tuning. This framework can be tested experimentally in the next decade. In this context, the novel mechanism that we propose is, in our opinion, a particularly attractive solution, in view of its simplicity, and compatibility with simple realizations of other sectors of the theory.

## 4.6 Triggered Landscapes

We now present a vacuum selection mechanism in the context of an explicit construction of the landscape, where the weak scale as a trigger is crucially needed to find a vacuum with tiny enough cosmological constant. We first introduced it in [153] We imagine there is a “UV landscape” containing moderately many vacua, not enough to find vacua with our small Cosmological Constant (CC). The UV landscape scans the CC and the Higgs mass(es) without scanning dimensionless couplings [105].

We also imagine a separate “IR landscape”, with  $n_\phi$  ultra-light, weakly coupled scalars  $\phi_i$ , each with a (spontaneously broken)  $Z_2$  discrete symmetry, potentially giving a factor of  $2^{n_\phi}$  more vacua. The  $\phi_i$  also couple to a trigger operator  $\mathcal{O}_T$ . If  $\langle \mathcal{O}_T \rangle$  is too small, the  $2^{n_\phi}$  vacua of the  $\phi_i$  sector are all degenerate and they don’t help with making smaller vacuum energies possible. If  $\langle \mathcal{O}_T \rangle$  is too big, the symmetry is broken so badly that only one vacuum remains for each  $\phi_i$ , and there is again no way to find small vacuum energy. The only way to find small vacuum energy is to tune Higgs vacuum expectation values so that  $\mu_S^{\Delta_T} < \langle \mathcal{O}_T \rangle < \mu_B^{\Delta_T}$ . Thus using the weak scale as a trigger allows us to tie solutions to the cosmological constant and hierarchy problems.

Our low-energy effective theory, contains in addition to the SM or the type-0 2HDM, a “IR landscape” consisting of  $n_\phi$  scalars  $\phi_i$ . In first approximation the scalars are uncoupled, and each have a  $Z_2$  discrete symmetry, described by the potential:

$$V_{N\phi} = \sum_{i=1}^{n_\phi} \frac{\epsilon_i^2}{4} (\phi_i^2 - M_{*,i}^2)^2. \quad (4.146)$$

In absence of new symmetries or dynamics below  $M_*$ , we take the  $\phi_i$  vevs  $M_{*,i}$  to be the fundamental scale of the theory  $\mathcal{O}(M_*)$ .  $\epsilon_i$  is an order parameter that quantifies the breaking of the shift symmetry on  $\phi_i$ , such that  $m_{\phi_i} \sim \epsilon_i M_{*,i} \ll M_*$  is technically natural. We assume that the cosmological constant and the Higgs mass(es) squared are scanned uniformly in a “UV landscape”, which has  $N_{UV}$  vacua, with  $N_{UV}$  too small to find a vacuum with small enough CC. The smallest CC in the UV landscape is  $\simeq M_*^4/N_{UV}$ . In vacua where Higgs mass(es) squared are  $\sim v^2$  the minimal CC is larger and we call this value of the CC  $\Lambda_*$ .

We now imagine that each of the  $\phi_i$  also couples to our weak scale trigger operator  $\mathcal{O}_T$ ,

$$V_{N\phi T} = \sum_{i=1}^{n_\phi} \frac{\kappa_i \epsilon_i M_{*,i}^{3-\Delta_T}}{\sqrt{n_\phi}} \phi_i \mathcal{O}_T + \text{h.c.} \quad (4.147)$$

Here  $\kappa_i$  parametrizes an additional weak coupling, breaking the  $(Z_2)^{n_\phi}$  symmetry down to a single diagonal  $Z_2$ . Note that gravity loops also couple the different sectors, but the coupling

---

<sup>15</sup>More precisely, our mechanism is compatible with eternal inflation (but does not require it, as long as the landscape is populated by some mechanism), and at the same time it does not suffer from the so-called measure problem, since the relevant dynamics that selects the Higgs mass takes place after reheating, at the EW or QCD phase transition.

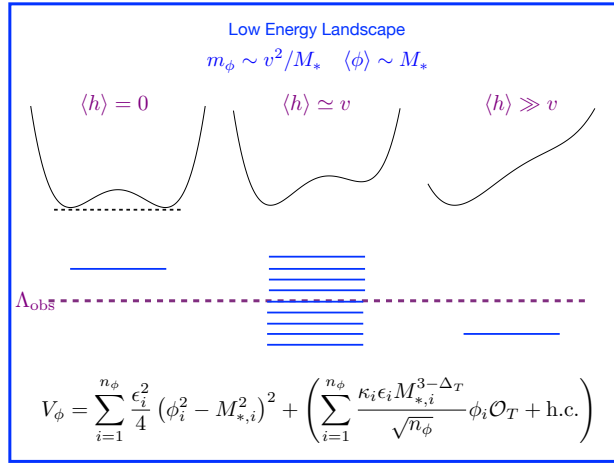


Figure 4.21: The landscape contains a UV sector and an IR sector (in this Figure). The high energy sector is generated by fields of mass close to the cutoff  $m_\Phi \sim M_*$  and does not have enough vacua to scan the CC down to  $\Lambda_{\text{obs}} \simeq \text{meV}^4$ , but can scan the Higgs mass(es)  $m_H^2$  down to the weak scale. The low energy sector is generated by fields of mass  $m_\phi \sim v^2/M_*$  and has a number of non-degenerate minima dependent on the Higgs vev. When  $\langle h \rangle \simeq v$  we can scan the CC down to its observed value.

to gravity doesn't break the  $(Z_2)^{n_\phi}$  discrete symmetry that we have when  $\kappa \rightarrow 0$ , (and at any rate, induces parametrically minuscule cross-quartics of order  $\epsilon_i^2 \epsilon_j^2 \phi_i^2 \phi_j^2$ ). The structure of our IR landscape is depicted in Fig. 4.21 while their role in scanning the CC is sketched in Fig. 4.22. The interaction in Eq. (4.147) makes the number of minima in the landscape sensitive to the value of  $\langle \mathcal{O}_T \rangle$ . If<sup>16</sup>

$$\langle \mathcal{O}_T \rangle \gtrsim \frac{\epsilon}{\kappa} \sqrt{n_\phi} M_*^{\Delta_T} \equiv \mu_B^{\Delta_T}, \quad (4.148)$$

some minima are lost, as shown in Fig. 4.21, which makes it impossible for the CC to have the observed value.

If  $\langle \mathcal{O}_T \rangle$  is too small

$$\langle \mathcal{O}_T \rangle \lesssim \frac{\sqrt{n_\phi}}{\epsilon \kappa} \frac{\Lambda_*}{M_*^4} M_*^{\Delta_T} \equiv \mu_S^{\Delta_T} \quad (4.149)$$

the degeneracy between the minima of Eq. (4.146) is not lifted enough to scan the CC down to  $(\text{meV})^4$ . This defines the two scales  $\mu_S$  and  $\mu_B$ . To see how these two opposite pressures on the vev of  $\langle \mathcal{O}_T \rangle$  select the weak scale we need to specify the field content of  $\mathcal{O}_T$ . In the two following Sections we discuss  $\mathcal{O}_T = G\tilde{G}$  and  $\mathcal{O}_T = H_1 H_2$ .

### 4.6.1 SM Trigger of the Landscape

The simplest trigger  $\mathcal{O}_T$  is already present in the SM. It is given by the familiar  $G\tilde{G}$  operator that we now couple to the  $n_\phi$  scalars in the low energy landscape,

$$V_{N\phi G} = \frac{1}{32\pi^2} \sum_{i=1}^{n_\phi} \left( \frac{\phi_i}{f_i} + \theta \right) G\tilde{G}, \quad G\tilde{G} \equiv \epsilon^{\mu\nu\rho\sigma} \sum_a G_{\mu\nu}^a G_{\rho\sigma}^a. \quad (4.150)$$

<sup>16</sup>For simplicity we have dropped the subscript  $i$ , assuming that all  $\epsilon_i$ ,  $\kappa_i$  and  $M_{*,i}$  are close to a common value.

Values of the Cosmological Constant in the Landscape

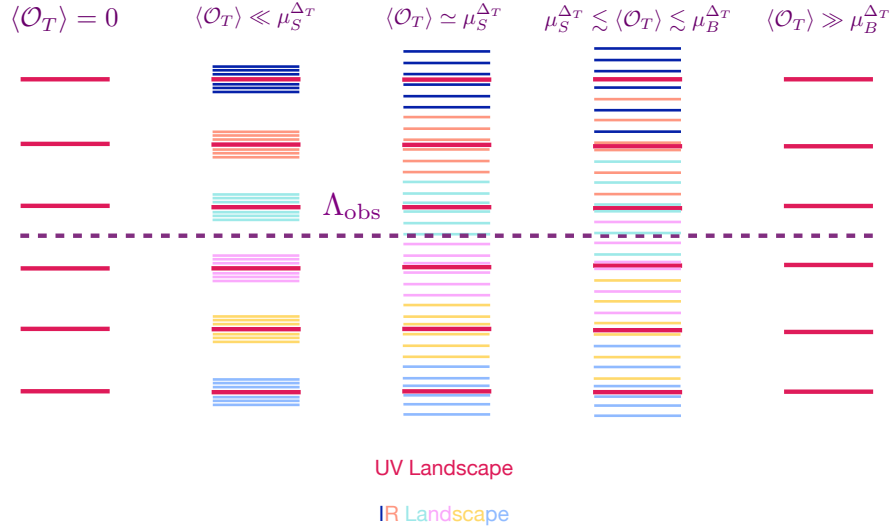


Figure 4.22: Values of the Cosmological Constant in our two-sectors landscape. When  $\langle \mathcal{O}_T \rangle = 0$  the UV landscape does not have enough minima to scan the CC from  $M_*^4$  down to  $\Lambda_{\text{obs}} \simeq \text{meV}^4$ . The minimal value of the CC in the landscape is  $M_*^4/N_{\text{UV}} \gg \text{meV}^4$ . When  $\langle \mathcal{O}_T \rangle \neq 0$  the degeneracy in the vacua of the low energy landscape in Fig. 4.21 is broken and if  $\mu_S^{\Delta_T} \lesssim \langle \mathcal{O}_T \rangle \lesssim \mu_B^{\Delta_T}$  we can harness the full potential of its  $2^{n_\phi}$  vacua and scan the CC down to  $\text{meV}^4$ . If  $\langle \mathcal{O}_T \rangle \gg \mu_B^{\Delta_T}$  the low energy landscape loses all its minima but one and the minimal CC in the landscape is again  $M_*^4/N_{\text{UV}} \gg \text{meV}^4$ .

Here we only briefly discuss how to use this trigger in the context of our landscapes. We give more details in the next Section for the  $H_1 H_2$  trigger.

In the notation of the previous section we have

$$\mathcal{O}_T = G\tilde{G}, \quad \frac{1}{f_i} = \frac{32\pi^2 \kappa_i \epsilon_i}{\sqrt{n_\phi} M_{*,i}}. \quad (4.151)$$

We imagine that one of the usual mechanisms solves the strong CP problem, leaving at low energy a residual  $\theta$  angle smaller than  $10^{-10}$ . We also impose  $\langle \phi_i \rangle / f_i \lesssim 10^{-10} / n_\phi$  to avoid re-introducing the problem. To study the effect of  $V_{N\phi G}$  in Eq. (4.150) we can move  $\phi_i$  into the quark mass matrix with an anomalous chiral rotation and use chiral perturbation theory to get

$$V_{N\phi G} \simeq \begin{cases} f_\pi^2(\langle h \rangle) m_\pi^2(\langle h \rangle) \left( \sum_i \frac{\phi_i}{f_i} + \theta \right)^2 + \dots, & \langle h \rangle \lesssim \frac{\Lambda_{\text{QCD}}(\langle h \rangle)}{y_u}, \\ \Lambda_{\text{QCD}}^4(\langle h \rangle) \left( \sum_i \frac{\phi_i}{f_i} + \theta \right)^2 + \dots, & \langle h \rangle \gtrsim \frac{\Lambda_{\text{QCD}}(\langle h \rangle)}{y_u}. \end{cases} \quad (4.152)$$

In the previous equation we have introduced  $\Lambda_{\text{QCD}}(v_*)$ , which is the chiral condensate with quark masses proportional to the vev  $v_*$ . Similarly  $f_\pi^2(v_*)$  and  $m_\pi^2(v_*)$  are the values of these parameters with EW symmetry breaking at the scale  $v_*$ . Note that the dependence on  $v_*$  saturates when  $\Lambda_{\text{QCD}}(v_*) \geq v_*$  and QCD itself becomes the main source of EW symmetry breaking.

The potential in Eq. (4.152) makes the number of minima in the landscape sensitive to the value of the Higgs vev  $\langle h \rangle$ . When  $\langle h \rangle$  is too large some minima are lost, when it is too small the minima of Eq. (4.146) remain almost degenerate. To see why minima are lost when  $\langle h \rangle$  is

large consider the limit  $\Lambda_{\text{QCD}}^4 M_*/f \gg \epsilon^2 M_*^4$ , where Eq. (4.152) dominates over the potential in (4.146). Then at the minimum Eq. (4.152) is effectively fixing  $\sum_i(\phi_i/f_i) = -\theta$ . We can implement this condition as a Lagrange multiplier

$$\mathcal{L} = \lambda \left( \sum_i \frac{\phi_i}{f_i} + \theta \right) - V_{N\phi}. \quad (4.153)$$

From the point of view of this Lagrangian fixing  $\sum_i(\phi_i/f_i) = -\theta$  corresponds to  $\lambda/f_i \gg \partial V_{N\phi}/\partial\phi_i$ , so when we try to solve the cubic equation

$$f_i \frac{\partial V_{N\phi}}{\partial\phi_i} = f_i \epsilon_i^2 \phi_i (\phi_i^2 - M_{*,i}^2) = \lambda, \quad (4.154)$$

we are guaranteed to find at most one solution. This would be true also if  $V_{N\phi}$  was a periodic potential. This discussion shows that in the limit of large  $\langle h \rangle$  all minima in the low energy landscape (but one) are lost.

In summary we have an upper and a lower bound on  $\langle h \rangle$  that depend on the mass of the scalars in the landscape and on  $\Lambda_*$  (the smallest CC in the UV landscape). If we imagine that both opposing ‘‘pressures’’ are saturated at the same value of  $\langle h \rangle$ , then in the multiverse this is the only value consistent with Weinberg’s anthropic argument. We have measured this value to be the weak scale  $v$ , so the mass scale in the low energy landscape and the residual CC must be:

$$m_\phi \simeq \frac{f_\pi m_\pi}{\min[f, \sqrt{f M_*/\theta}]}, \quad \Lambda_* \simeq \left( N_2 f_\pi m_\pi \sqrt{\frac{\theta M_*}{f}} \right)^2 \lesssim (100 \text{ keV})^4 \left( \frac{\theta}{10^{-10}} \right), \quad (4.155)$$

where  $m_\pi$  and  $f_\pi$  are those observed in our universe. In Eq. (4.155) the value of  $m_\phi$  determines whether minima are lost or not, so it depends on the term that dominates the QCD potential of the new scalars. This can either be the linear one if  $\theta > M_*/f_i$  or the quadratic one in the opposite limit. On the contrary  $\Lambda_*$  is sensitive only to the linear term, since  $\Lambda_{\text{QCD}}^4 \theta \phi/f$  provides the only difference between the value of the potential at the two minima  $\phi \simeq \pm M_*$ . This shows that we cannot have an axion lighter than the  $\phi_i$ ’s and the strong CP problem has to be solved at higher energies.

There is a priori no reason why the two pressures on  $\langle h \rangle$  are saturated at the same scale, given that they arise from two distinct physical requirements ( $V_{N\phi G} \lesssim V_{N\phi}$  and  $\Lambda_* \simeq V_{N\phi G}^{\min}$ ). In general we expect a range around the weak scale,  $\mu_S \lesssim \langle h \rangle \lesssim \mu_B$ , to be viable. We further expand on this point in the next Section.

## 4.6.2 Type-0 2HDM Triggering of the Landscape

We now consider the case where the triggering operator is  $\mathcal{O}_T = \mathcal{O}_H = H_1 H_2$ , so that we have

$$V^{(I)} = \sum_{i=1}^{n_\phi} \left[ \frac{\epsilon^2}{4} (\phi_i^2 - M_*^2)^2 + \frac{\epsilon \kappa}{\sqrt{n_\phi}} M_* \phi_i H_1 H_2 \right] + V_H^{(I)}. \quad (4.156)$$

For simplicity we have dropped the subscript  $i$ , assuming that all  $\epsilon_i$ ,  $\kappa_i$  and  $M_{*,i}$  are close to a common value. The Higgs potential reads

$$\begin{aligned} V_H^{(I)} &= (m_1^2)^{(I)} |H_1|^2 + (m_2^2)^{(I)} |H_2|^2 + \Lambda^{(I)} + \\ &+ \frac{\lambda_1}{2} |H_1|^4 + \frac{\lambda_2}{2} |H_2|^4 + \lambda_3 |H_1|^2 |H_2|^2 + \lambda_4 |H_1 H_2|^2 + \left( \frac{\lambda_5}{2} (H_1 H_2)^2 + \text{h.c.} \right) \\ &+ Y_u q H_2 u^c + Y_d q H_2^\dagger d^c + Y_e l H_2^\dagger e^c. \end{aligned} \quad (4.157)$$

Here  $I = 1, \dots, N_{\text{UV}}$  labels vacua in the UV landscape. We imagine that  $\Lambda^{(I)}, (m_{1,2}^2)^{(I)}$  are uniformly distributed between  $(-M_*^4, M_*^4), (-\Lambda_H^2, \Lambda_H^2)$  where  $\Lambda_H$  is the Higgs cutoff. Of course the simplest choice is to assume  $\Lambda_H^2 \sim M_*^2$ , but it is possible to have  $\Lambda_H^2 \ll M_*^2$  and on occasion we will consider  $\Lambda_H$  much smaller than  $M_*$ .

The first term in Eq. (4.156) has a large  $(Z_2)^{n_\phi}$  discrete symmetry. The couplings  $\phi_i H_1 H_2$  break it down to a single diagonal  $Z_2$  under which all  $\phi_i$ 's are odd and  $H_1 H_2$  is odd. The small parameter  $\epsilon$  is a measure of the small breaking of the shift symmetry  $\phi_i \rightarrow \phi_i + c_i$ , while  $\kappa$  is a further weak coupling of  $\phi_i$  to  $H_1 H_2$ , which breaks  $(Z_2)^{n_\phi}$  down to the diagonal  $Z_2$ . By spurion analysis we should also include

$$\Delta V_{ij} \sim \sum_{i,j} \epsilon^2 \kappa^2 \phi_i \phi_j M_*^2 \quad (4.158)$$

in the potential for  $\phi$ , which is logarithmically induced by a one-loop diagram. Now, suppose we are in a region of the big landscape where the operator  $(H_1 H_2)$  is *not* triggered, i.e.  $\mu^2 \equiv \langle H_1 H_2 \rangle = 0$ , say with  $m_{1,2}^2 > 0$  and close to the cutoff  $\Lambda_H^2$ . From the UV landscape, we have a distribution of vacua with CC splittings of order  $\Delta\Lambda_{\text{UV}} \simeq M_*^4/N_{\text{UV}}$ . When  $\kappa = 0$ , each of these vacua is  $2^{n_\phi}$  degenerate, as in the first column of Fig. 4.22. Turning on  $\kappa$ , from  $\Delta V_{ij}$  in Eq. (4.158) we get CC splittings of order  $\epsilon^2 \kappa^2 M_*^4$ . If this splitting was much bigger than  $\Delta\Lambda_{\text{UV}} \simeq M_*^4/N_{\text{UV}}$ , we would already finely scan the CC. So, we assume that  $\kappa$  is small enough so this splitting is much smaller than the splitting in the UV landscape,

$$\epsilon^2 \kappa^2 M_*^4 \ll \frac{M_*^4}{N_{\text{UV}}}. \quad (4.159)$$

Note that if we tune down the Higgs masses squared to  $m_1^2$  and  $m_2^2$ , the CC splitting in the UV landscape increases as

$$\Delta\Lambda_{\text{UV}}(m_1^2, m_2^2) \sim \frac{M_*^4}{N_{\text{UV}}} \frac{\Lambda_H^2}{|m_1^2|} \frac{\Lambda_H^2}{|m_2^2|}, \quad (4.160)$$

so if the condition in Eq. (4.159) is satisfied, then obviously the loop-induced  $\epsilon^2 \kappa^2 M_*^4$  splitting gets even smaller relative to  $\Delta\Lambda_{\text{UV}}$ . Thus we must have  $\mu^2 = \langle H_1 H_2 \rangle \neq 0$  in order to be able to find a vacuum with the CC much smaller than  $\Delta\Lambda_{\text{UV}} \simeq M_*^4/N_{\text{UV}}$ .

Now let's look at the region in the landscape with  $m_{1,2}^2 < 0$ , and look at tree-level where  $\mu^2 = \sqrt{|m_1^2||m_2^2|}$ . If  $\mu^2$  is too big, we tilt the  $\phi_i$  potentials so much as to lose one of the vacua, as shown in Fig. 4.21. This happens for  $\mu^2 \gtrsim \mu_B^2$  where  $\mu_B^2$  is determined from

$$\epsilon^2 M_*^4 \sim \kappa \epsilon M_*^2 \mu_B^2 \rightarrow \mu_B^2 \sim \frac{\epsilon}{\kappa} M_*^2. \quad (4.161)$$

When  $\mu$  drops below  $\mu_B$ , we want the splittings in the  $N_{\text{IR}} = 2^{n_\phi}$  vacua, now of order  $\epsilon \kappa \mu_B^2 M_*^2 \simeq \kappa^2 \mu_B^4$ , to be much larger than

$$\Delta\Lambda_{\text{UV}}(m_1^2, m_2^2) \sim \frac{M_*^4}{N_{\text{UV}}} \frac{\Lambda_H^4}{|m_1^2 m_2^2|} \sim \frac{M_*^4}{N_{\text{UV}}} \frac{\Lambda_H^4}{\mu_B^4}. \quad (4.162)$$

So we should have

$$\kappa^2 \gg \frac{M_*^4}{N_{\text{UV}}} \frac{\Lambda_H^4}{\mu_B^8}. \quad (4.163)$$

Putting Eq.s (4.159) and (4.163) together, we have

$$\frac{\Lambda_H^2 M_*^2}{N_{\text{UV}}^{1/2} \mu_B^4} \ll \kappa \ll \frac{M_*}{\mu_B} \frac{1}{N_{\text{UV}}^{1/4}}. \quad (4.164)$$

This forces  $N_{\text{UV}} \gg (\Lambda_H^2 M_* / \mu_B^3)^4$ . So for  $\mu_B^2 \simeq v^2$ , suppose we take the simplest possibility where  $\Lambda_H \sim M_* \sim M_{\text{Pl}}$ . Then, the above inequality tells us that  $N_{\text{UV}} \gg 10^{180}$ . In this case, our mechanism is clearly irrelevant. There would be more than enough vacua in the UV landscape to simply tune down one Higgs and the CC. For our mechanism to be relevant, we would like to have  $N_{\text{UV}} \ll (M_*^4 / \Lambda_{\text{obs}})(\Lambda_H^2 / v^2) \simeq 10^{120} \Lambda_H^2 / v^2$ . Thus we must have

$$\frac{\Lambda_H^8 M_*^4}{v^{12}} \ll 10^{120} \frac{\Lambda_H^2}{v^2}, \quad (4.165)$$

and we get an upper bound on the Higgs cutoff:  $\Lambda_H \ll 10^{12}$  GeV. Note that since  $N_{\text{UV}} \gg (\Lambda_H^2 M_* / \mu_B^3)^4$ , and  $\kappa \ll \frac{M_*}{\mu_B} \frac{1}{N_{\text{UV}}^{1/4}}$ , we have also an upper bound on the coupling of the new scalars to the Higgses

$$\kappa \ll \frac{\mu_B^2}{\Lambda_H^2} \sim \frac{v^2}{\Lambda_H^2}. \quad (4.166)$$

With these conditions,  $\Lambda_H \ll 10^{12}$  GeV and  $\kappa \ll v^2 / \Lambda_H^2$ , satisfied, our mechanism works. For instance if we take  $\Lambda_H \simeq 10^6$  GeV,  $M_* \simeq M_{\text{GUT}} \simeq 10^{16}$  GeV,  $\kappa \simeq 10^{-5}$ ,  $\epsilon \simeq 10^{-30}$ ,  $N_{\text{UV}} \simeq 10^{77}$ , we have  $\mu_S \simeq 100$  GeV,  $\mu_B \simeq 6$  TeV and the smallest CC in the UV landscape corresponds to an Hubble size of  $\mathcal{O}(10R_\odot)$ . With this choice of parameters we have  $n_\phi \simeq 120$  light scalars with mass  $m_\phi \simeq 10^{-5}$  eV in the IR landscape which scan the CC down to its observed value. In the next Section we discuss  $\phi_i$  dark matter, but let us mention here two cosmological constraints necessary for our mechanism to work. First, we must have  $H_{\text{inf}} \ll M_*$  during inflation. This ensures that the fluctuations of the  $\phi_i$  during inflation are small, so that after inflation, our Hubble patch has the  $\phi_i$ s in the basin of attraction of one of the  $N_{\text{IR}} = 2^{n_\phi}$  minima. Obviously the condition  $H_{\text{inf}} \ll M_*$  is trivially satisfied for  $M_* \sim M_{\text{Pl}}$ . We also want the  $\phi_i$ s to be massive enough to actually oscillate and reach their minima. Minimally we should have  $m_{\phi_i} \gg H_{\text{today}}$ . Putting  $m_\phi \sim \epsilon M_* \sim \kappa \mu_B^2 / M_*$ , we have that  $\kappa v^2 / M_* \gg H_{\text{today}}$  which gives a lower bound on  $\kappa$ .

$$\frac{v^2 M_*}{M_{\text{Pl}}^3} \ll \kappa \ll \frac{v^2}{\Lambda_H^2}. \quad (4.167)$$

The resulting condition on  $\Lambda_H$ ,  $\Lambda_H^2 M_* \ll M_{\text{Pl}}^3$ , is trivially satisfied once  $\Lambda_H \leq M_* \leq M_{\text{Pl}}$ . Indeed,  $m_\phi \simeq H_{\text{today}}$  is the limit in which  $\Delta \Lambda_{\text{UV}} < H_{\text{today}}^2 M_*^2 \leq H_{\text{today}}^2 M_{\text{Pl}}^2 \sim \Lambda_{\text{obs}}$  and the maximum scan of  $\phi$  is smaller than the observed CC and thus our mechanism would be irrelevant.

As we keep dropping  $\mu$ , at some point the splitting  $\epsilon \kappa \mu^2 M_*^2 \sim \kappa^2 \mu^2 \mu_B^2$  will eventually become smaller than  $\Delta \Lambda_{\text{UV}}$ . This happens for  $\mu = \mu_S$ , where  $\mu_S$  is defined by

$$\kappa^2 \mu_S^2 \mu_B^2 \sim \frac{M_*^4}{N_{\text{UV}}} \frac{\Lambda_H^4}{\mu_S^4}, \quad (4.168)$$

which determines  $\mu_S$  as

$$\mu_S \sim \frac{M_*^{2/3} \Lambda_H^{2/3}}{\mu_B^{1/3}} \frac{1}{N_{\text{UV}}^{1/6} \kappa^{1/3}}. \quad (4.169)$$

Below  $\mu \sim \mu_S$ , the extra scanning of  $N_{\text{IR}} = 2^{n_\phi}$  vacua cannot bring the smallest CC down, and the minimum CC shoots back up to  $M_*^4 / N_{\text{UV}}$ . A schematic plot of the smallest CC in the landscape, as a function of  $\mu^2$ , is shown in Fig. 7. As we have seen, only for  $\mu_S^2 \lesssim \mu^2 \lesssim \mu_B^2$  can the power of the extra  $2^{n_\phi}$  vacua be harnessed to exponentially suppress the CC's we can get from the landscape.



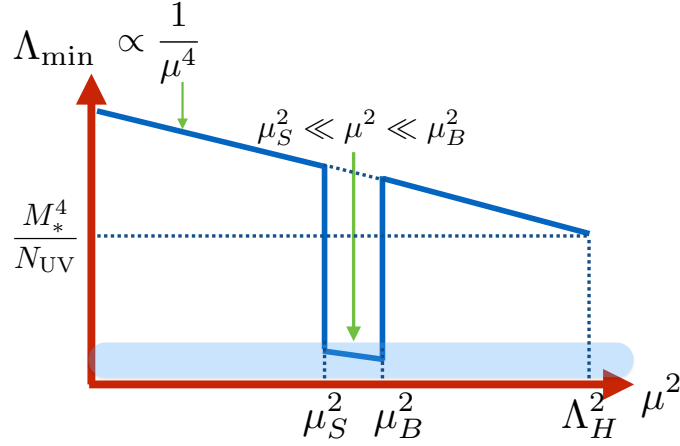


Figure 4.23: The smallest CC in the landscape as a function of  $\mu^2 \equiv \langle H_1 H_2 \rangle$ . In the light blue area the CC is smaller than its observed value, while for  $\mu^2 > \mu_B^2$  or  $\mu_S < \mu_S^2$  it is much larger,  $M_*^4/N_{UV} \gg \text{meV}^4$ .

We can perform a similar analysis for the case where  $m_1^2 < 0$  and  $m_2^2 > 0$ , in which  $\mu^2 \sim \sqrt{|m_1^2|} \Lambda_{\text{QCD}}^3/m_2^2$ . Here keeping  $\mu^2 < \mu_S^2$  is easy since  $\mu^2$  is naturally tiny ( $\simeq \Lambda_{\text{QCD}}^3/\Lambda_H$ ). Instead the constraint is in making  $\mu$  big enough for the splitting  $\kappa^2 \mu^2 \mu_B^2$  to be bigger than  $\Delta\Lambda_{UV}$ . Clearly  $\Delta\Lambda_{UV}(\mu)$  is minimized when  $m_1^2 \sim -\Lambda_H^2$ . Then  $\mu^2 \sim \Lambda_H \Lambda_{\text{QCD}}^3/m_2^2$  and we obtain

$$\Delta\Lambda_{UV}(-\Lambda_H^2, m_2^2) \sim \frac{M_*^4}{N_{UV}} \frac{\Lambda_H^2}{m_2^2} \sim \frac{M_*^4}{N_{UV}} \frac{\mu^2 \Lambda_H}{\Lambda_{\text{QCD}}^3}. \quad (4.170)$$

To scan the CC to its observed value, we need the splittings in the IR landscape to be larger than  $\Delta\Lambda_{UV}$ . Then we must have

$$\kappa^2 \mu^2 \mu_B^2 \gg \frac{M_*^4}{N_{UV}} \frac{\mu^2 \Lambda_H}{\Lambda_{\text{QCD}}^3}, \quad (4.171)$$

which gives a lower bound on  $\mu_B^2$ ,

$$\mu_B^2 \gg \frac{1}{N_{UV} \kappa^2} \frac{M_*^4 \Lambda_H}{\Lambda_{\text{QCD}}^3}. \quad (4.172)$$

If this happens we can also find small CC vacua in this part of the landscape. But note that we can never find a vacuum that looks like our world here. While the W/Z bosons are massive, near the cutoff  $\Lambda_H$ , the fermions are massless in the effective field theory beneath  $\Lambda_H$ . If we integrate out  $H_2$ , the 4 fermi operators  $(qq^c)(ee^c)/m_2^2$  are generated and leptons also get minuscule masses  $\sim \Lambda_{\text{QCD}}^3/m_2^2 \sim \mu^2/\Lambda_H$  after chiral symmetry breaking. But if we suppose the parameters of the model are such as to have  $\mu^2 \lesssim \mu_B^2 \lesssim v^2$ , the lepton masses are suppressed by at least by a factor of  $v/\Lambda_H$  compared to our world. In this situation for atoms to form, the temperature of the universe must drop by a factor of  $v/\Lambda_H$  further relative to our universe, meaning that the CC must be further smaller by a factor of  $(\frac{v}{\Lambda_H})^4$  before atoms can form. It could easily be that  $N_{\text{IR}} = 2^{n_\phi}$  is not large enough to realize this possibility. Thus while finding vacua with tiny CC suppressed by  $1/N_{\text{IR}} = 2^{-n_\phi}$  is possible with  $m_1^2 \sim -\Lambda_H^2$ , forcing  $m_2^2 > 0$  to be tuned small, these worlds look nothing like ours. It is only possible to get a world that looks like ours with  $m_1^2 < 0$  and  $m_2^2 < 0$ . As we have seen in our discussion of the phenomenology of this model, since the weak scale is set by the largest of the Higgs VEVs, this forces the existence of new light charged and neutral Higgs states which we cannot decouple or tune away.

## 4.7 Statistical Selection in the Multiverse

The very first attempts at explaining the Higgs mass cosmologically were made, to the best of my knowledge, in [150–152]. The idea was to create a Multiverse with an exponential accumulation of vacua near  $m_h^2 = 0$ . The basic mechanism can be described as follows. We have our usual 4-form

$$F_4 = dA_3, \quad (4.173)$$

introduced in Section 3.4, where we have used a shorthand for Eq. (3.62) employing the definition of the exterior derivative. The theory contains the terms relevant for the mechanism

$$S \supset \int d^4x \sqrt{-g} \left( -\frac{F_4^2}{48} + M_{\text{Pl}}^2 \left( -1 + \frac{F_4^2}{M_{\text{Pl}}^2} \right) h^2 \right) + q(h) \int d^3\xi A_{\mu\nu\rho} \frac{\partial x^\mu}{\partial \xi^a} \frac{\partial x^\nu}{\partial \xi^b} \frac{\partial x^\rho}{\partial \xi^c} \epsilon^{abc}. \quad (4.174)$$

The nucleation of bubbles can proceed as in Section 3.4, following the Brown-Teitelboim idea. The crucial difference is that

$$q(h) = \frac{h^N}{M_{\text{Pl}}^{N-2}}, \quad (4.175)$$

this can be enforced via a discrete symmetry [151, 152]. After every nucleation, the brane charge decreases. If  $N > 2$ ,

$$\frac{\Delta \langle h \rangle^2}{\langle h \rangle^2} \propto \langle h \rangle^{N-2}, \quad (4.176)$$

the vast majority of vacua have  $\langle h \rangle$  close to zero. We have illustrated the idea for a scalar, but it can be generalized to an  $SU(2)_L$  doublet. To populate these vacua, through nucleation of branes (which is an exponentially slow semiclassical process) eternal inflation is needed. This introduces the problem of measuring how likely a certain vacuum is. Even if we have a theory with exponentially more vacua at  $\langle h \rangle \simeq 0$  compared to large values of the vev, we still can not compute how likely these vacua are in the Multiverse, due to the well-known measure problem of eternal inflation [367]. This is a common problem of models that aim to explain  $m_h$  using “statistical” arguments, i.e. by populating a special landscape where small  $m_h^2$  is more likely. Other interesting examples include [368–370]. They most rely on the fact that regions at the top of the potential, i.e. with larger positive vacuum energy, inflate more, presumably becoming more likely in the Multiverse. However, they run into the problem of measure just described.

## 4.8 General Aspects of Cosmological Naturalness

In the previous Sections we have described a number of creative ideas that trace the origin of the weak scale to early times in the history of the Universe and more are present in the literature [118, 119, 151–154, 285, 319, 368–372]. Taken at face value these ideas seem widely different, selecting the weak scale by unrelated mechanisms and predicting different phenomenology. In this Section we identify the basic structure common to these proposals and find that a large subset of these ideas have common ingredients which often lead to similar low-energy predictions.

Cosmological explanations of the weak scale have the schematic structure shown in Fig. 4.24. Early in the history of the universe (left panel) we have a landscape of values for  $m_h^2$  and a symmetric sector weakly coupled to the SM. In the symmetric sector a large hierarchy of scales is technically natural and it is not destabilized by the small coupling to the SM. The sector is

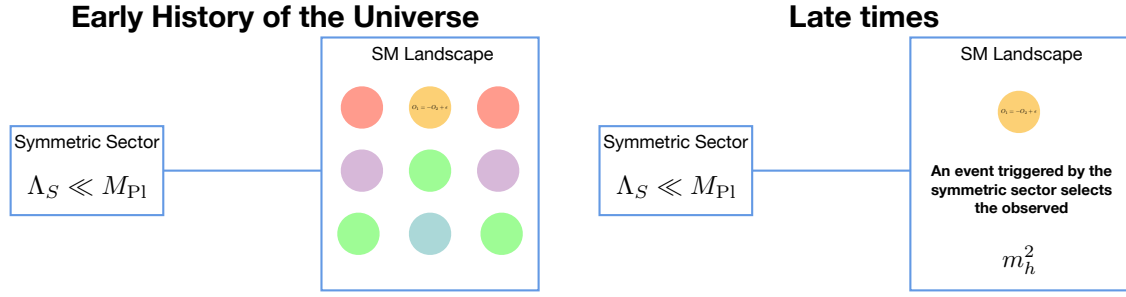


Figure 4.24: Models of cosmological selection of the weak scale. A symmetric sector, where a large hierarchy of scales is technically natural, is weakly coupled to a landscape of values of  $m_h^2$ . The SM landscape contains tuned values of  $m_h^2$  including the observed one and is populated early in the history of the Universe. At a later time a cosmological event selects the observed value of  $m_h^2$  through the coupling to the symmetric sector. Different selection mechanisms are shown in Fig. 4.25.

*symmetric* in the sense that its approximate symmetries naturally stabilize a large hierarchy of scales. At late times, a cosmological event triggered by the Higgs vev and the coupling between SM and symmetric sector selects the observed value of the weak scale (right panel of Fig. 4.24).

The landscape of vacua can be realized in the form of causally disconnected patches of the Universe forming a Multiverse [101, 367, 373], possibly populated during inflation. It is easy to always approximately decouple the landscape to the point of making detection prospects of the multitude of vacua almost non-existent. However it is useful to keep in mind that the more standard string theory (or field theory [105, 374]) landscape is not the only option. The landscape can also be entirely contained in our patch of the Universe, either in the form of a scanning field coupled to the Higgs, as is the case for the Relaxion [118], or of feebly interacting copies of the Standard Model, as was proposed in Nnaturalness [119].

We identify three broad categories for the selection mechanism in Fig. 4.25: 1) *Anthropic Selection* [104, 375–377]. Observers can arise only if  $\langle h \rangle \simeq v$ . 2) *Statistical Selection* [151, 152, 368–370]. Given some measure, the Multiverse is dominated by patches where  $\langle h \rangle \simeq v$ . 3) *Dynamical Selection* [118, 119, 153, 154, 285, 319, 371, 372]. Only non-empty<sup>17</sup> patches where  $\langle h \rangle \simeq v$  live for cosmologically long times.

Anthropic and statistical selection do not require new observable physics coupled to the SM. The mechanism that populates the landscape and generate its structure can take place at unobservably high energies or be due to non-dynamical fields with extremely feeble couplings to the SM [151, 152, 370, 372].

Dynamical selection occurs when at early times we have a “standard” landscape, with no preference for small  $\langle h \rangle$ , but at late times only universes with  $\langle h \rangle \simeq v$  exist and are not empty. The distinction between this class of ideas and anthropic selection might seem blurred. However there are one conceptual difference and one (more important) practical difference. The conceptual difference is that dynamical selection mechanisms do not require the absence of observers from other patches of the Multiverse. The “wrong” values of the Higgs vev are matter and/or radiation dominated for a very short time compared to the age of the observable

<sup>17</sup>The simplest definition of an empty a patch is given by a universe where a positive CC always dominates the energy density. However for our purposes it is sufficient that, as explained below, observers can only exist for a sufficiently short time. We can consider empty also patches where the CC is positive and larger than a certain threshold  $\Lambda > \Lambda_{\min}$ . In these patches we can have a period of radiation and/or matter domination that lasts at most  $\sim M_{Pl}/\sqrt{\Lambda_{\min}}$ . For an empty patch this time has to be much shorter compared to the age of our universe. In most models this time is much shorter than typical particle physics scales ( $\ll 1/v$ ).

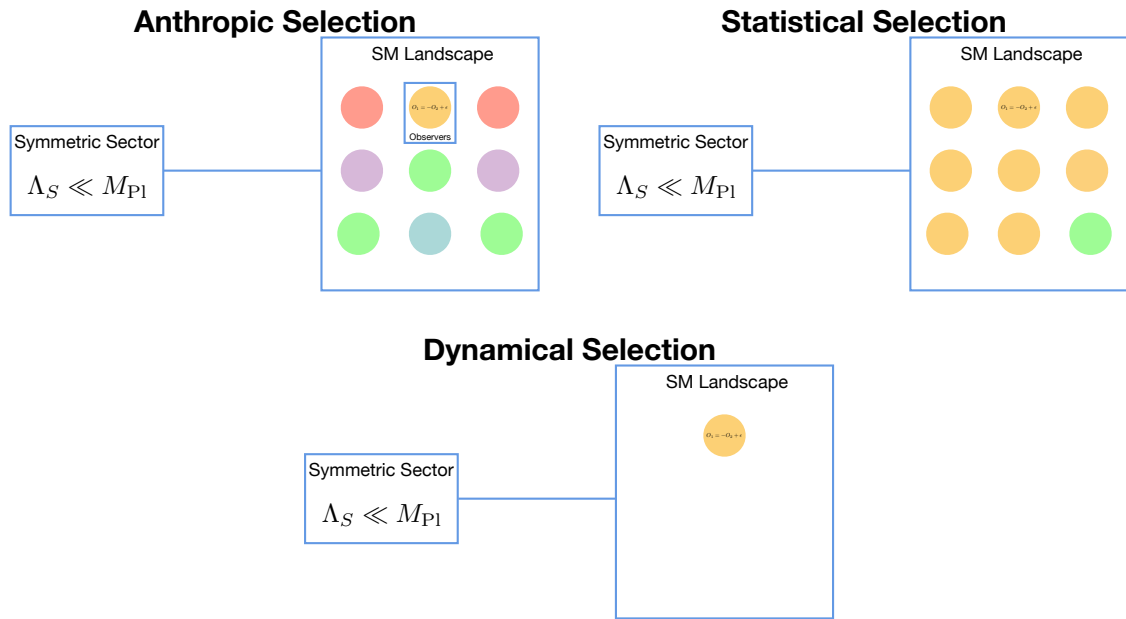


Figure 4.25: Models of cosmological selection of the weak scale. Anthropic selection (upper left panel), Statistical selection (upper right panel) and Dynamical selection (lower panel) are distinguished by the structure of the landscape at late times. In the anthropic case the landscape contains all values of  $m_h^2$  with no preference for  $\langle h \rangle \simeq v$ . In the statistical case  $\langle h \rangle \simeq v$  dominates Multiverse according to some measure, but also all other values are present. In the dynamical case only universes with  $\langle h \rangle \simeq v$  are cosmologically long-lived and non-empty.

Universe (often even compared to particle physics scales). During this time, an observer whose typical timescales are  $1/M \ll 1/v$  can possibly exist, but it does not change the statement that the only way to have a universe even remotely resembling our own is to have  $\langle h \rangle \simeq v$ . The practical difference is that dynamical selection requires new physics coupled to the Higgs and can be detected in the near future. From now on we focus on this class of models that does not suffer from measure problems and has the best chance of being tested experimentally. Our idea belongs to this category.

Having said this, it is clear that what we have called dynamical solutions have anthropic elements. First of all, most of them, including our proposal, rely on Weinberg’s argument to explain the CC. Secondly, the existence of a macroscopic, long-lived and non-empty universe *is* Weinberg’s argument. We have already argued that dynamical solutions, unlike anthropic ones, do not require the absence of observers from other universes, but we can see how this conceptual point can be the starting point of endless debates. However we find that the distinction between these two classes of ideas has practical value in light of the important phenomenological distinctions that we now discuss.

In existing “dynamical” models the selection mechanism is composed of two ingredients: 1) one or more new scalars or pseudo-scalars with masses inversely proportional to the cutoff of the Higgs sector and 2) an operator whose vev is a monotonic function of the Higgs vev. These operators are coupled to the new scalar(s) and were collectively identified as *triggers* in [153]. When the Higgs vev (and thus the operator vev) crosses certain upper or lower bounds, a cosmological event is triggered via the coupling to the new scalar(s).

In the next two Subsections we show why we expect new particles with masses inversely proportional to the cutoff and how the choice of trigger operator determines the phenomenology

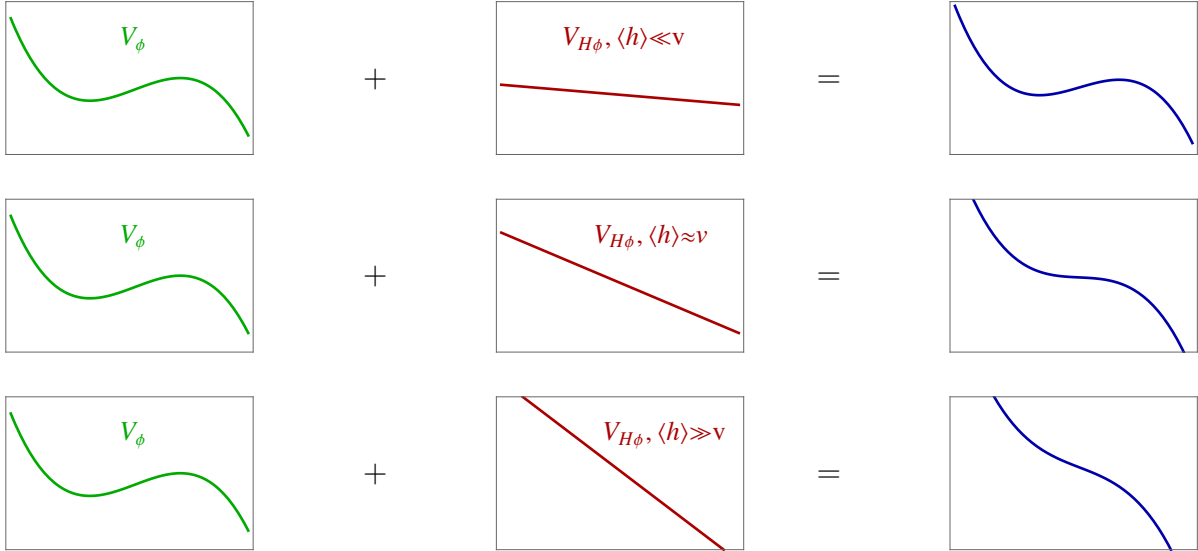


Figure 4.26: Schematic structure of how the Higgs-dependent potential  $V_{H\phi}$  can affect the scalar potential  $V_\phi$  to trigger a qualitative change when  $\langle h \rangle \simeq v$ .

of dynamical selection. Our considerations apply to the majority of these models, but exceptions to the power counting arguments in the next Section exist, either because the weak scale is not selected by comparing two different terms in the potential of a new scalar, but rather directly its mass to that of SM particles [119] or because it occurs via a non-dynamical field [372].

### 4.8.1 Cosmological Naturalness Power Counting

The presence of new light scalars  $\phi$ , in many of the models that dynamically select the weak scale in the early history of the Universe, can be understood from a simple parametric argument. Neglecting  $\mathcal{O}(1)$  factors we can write any term in the  $\phi$  potential as

$$V_\phi \supset m_\phi^2 M_*^2 \left( \frac{\phi}{M_*} \right)^m. \quad (4.177)$$

Here and in the following, we restore units of  $\hbar$  [378] to infer the correct parametrics. However, for simplicity, we keep giving formulas in natural units  $\hbar = 1$ . If  $\hbar \neq 1$  masses and scalar fields/vevs have different dimensions and we will be careful about this distinction. In our formulas  $M_*$  is a cutoff scale (with the same dimensions as  $\phi$ ), whereas  $m_\phi$  is a mass. Dimensionally, mass = coupling  $\times$  scale.

We can now include an interaction between  $\phi$  and the Higgs boson. We denote the cutoff scale of the Higgs sector by  $\Lambda_H$  and by  $\tilde{v} \leq v$  possible light SM or BSM scales, not depending explicitly on the Higgs vev  $\langle h \rangle$ . Then, integrating out the SM *at tree-level* we have

$$V_{\langle H \rangle \phi} \simeq \mu^2 M_*^2 \left( \frac{\phi}{M_*} \right)^n \frac{\tilde{v}^{2q-j} \langle h \rangle^j}{\Lambda_H^{2q}}, \quad (4.178)$$

with  $q \geq 1$  and  $j > 0$ . Examples of couplings of  $\phi$  to the SM present in the literature include: 1)  $\phi \text{Tr}[G\tilde{G}]$  [118, 151, 152, 154, 368], giving

$$\tilde{v}^{2q-j} \langle h \rangle^j \simeq f_\pi^3 \langle h \rangle \quad (4.179)$$

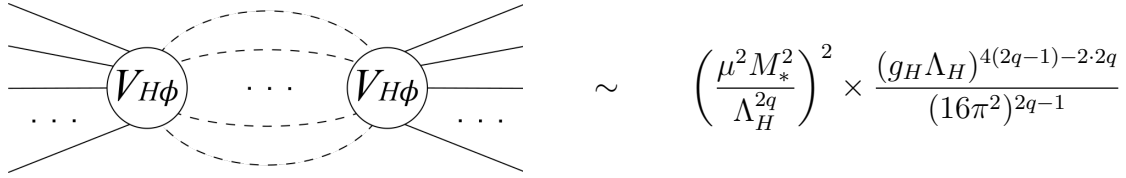


Figure 4.27: Schematic diagram giving loop corrections to the potential  $V_\phi$  from two insertions of  $V_{H\phi}$ . The scalar  $\phi$  is denoted by a continuous line, the  $2q$  Higgs propagators by dashed lines.

for QCD (note that  $f_\pi$  depends on  $\langle h \rangle$ ). A similar result holds for BSM gauge groups whose quarks get part of their mass from the Higgs. 2)  $\phi^n H_1 H_2$  [153]:

$$\tilde{v}^{2q-j} \langle h \rangle^j = \frac{\sin 2\beta}{2} \langle h \rangle^2 \quad (4.180)$$

and 3)  $\phi^n |H|^2$  [285, 319, 369]:  $\tilde{v}^{2q-j} \langle h \rangle^j = \langle h \rangle^2$ .

To select the weak scale, we need the Higgs-induced part of the potential  $V_{\langle H \rangle \phi}$  to be comparable to the Higgs-independent part  $V_\phi$  when  $\langle h \rangle \simeq v$ , as sketched in Fig. 4.26. Alternatively, if the mechanism involves, for instance, stopping a slow-rolling scalar, we want the first derivatives with respect to  $\phi$  to be comparable [118]. With our parametrization of the potential these two conditions lead parametrically to the same result

$$\frac{m_\phi^2}{\mu^2} \simeq \frac{\tilde{v}^{2q-j} v^j}{\Lambda_H^{2q}} \lesssim \frac{v^{2q}}{\Lambda_H^{2q}}. \quad (4.181)$$

This shows that the separation between the weak scale and the Higgs cutoff is given by an approximate symmetry on  $\phi$  that protects its mass and potential. Furthermore, it gives a smoking-gun signature for these models. If we measure the  $\phi$  mass, its coupling to the SM  $\mu$  and the Higgs cutoff  $\Lambda_H$ , we can test Eq. (4.181).

We can go even further and obtain an upper bound on  $m_\phi$  that depends only on the cutoff scales  $M_*$ ,  $\Lambda_H$ , by noticing that  $\mu^2$  has two upper bounds. One is determined by experiment, since  $\mu^2$  sets the strength of  $\phi$  interactions with the SM. The other one comes from quantum corrections, since integrating out the SM beyond tree-level can generate contributions to  $V_\phi$ , but to select the weak scale  $V_\phi$  cannot be too large (i.e. it has to be comparable to the tree-level Higgs-induced potential  $V_{\langle H \rangle \phi}$  when  $\langle h \rangle \simeq v$ ). We now use these constraints to derive upper bounds on  $m_\phi$  for three different types of couplings of  $\phi$  to the SM.

The simplest example is given by the  $\phi |H|^2$  coupling. Let us first consider the impact of quantum corrections on  $\mu$ . In this case the leading contribution to  $V_\phi$  is from a single insertion of  $V_{H\phi}$ ,

$$V_{H\phi} = \mu^2 M_* \phi \frac{|H|^2}{\Lambda_H^2}. \quad (4.182)$$

By closing the Higgs loop we see that (barring fine-tuning)  $m_\phi^2 \gtrsim g_H^2 \mu^2 / 16\pi^2$ , with  $g_H$  being a coupling in the Higgs sector. This takes into account that Higgs loop integrals are cut off by a mass scale  $g_H \Lambda_H$  (and not a vev  $\Lambda_H$ ). Eq. (4.181) supplemented by this condition on  $\mu$  shows that a cosmological selection mechanism with the trilinear coupling  $\phi |H|^2$  can solve only the little hierarchy problem

$$g_H \mu \lesssim 4\pi m_\phi \rightarrow g_H \Lambda_H \lesssim 4\pi v. \quad (4.183)$$

To get the bound on  $m_\phi$  we may use the fact that  $\mu$  has an experimental bound  $\mu < \mu_{\text{exp}}(m_\phi; M_*, \Lambda_H)$ , so that (4.181) gives:  $m_\phi \lesssim \mu_{\text{exp}}$ . We do not give the explicit value of  $\mu_{\text{exp}}$  since it depends strongly on  $m_\phi$ . In Fig. 4.17 we plot it in terms of  $\kappa \equiv \mu^2 M_*/(\Lambda_H^2 m_\phi)$  for  $m_\phi \lesssim \text{eV}$ .

Instead, if the leading contribution to  $V_\phi$  arises from two (or more) insertions of  $V_{H\phi}$  (for instance in the  $\phi H_1 H_2$  case) we have

$$\frac{g_H^{4q-4}}{(16\pi^2)^{2q-1}} \frac{\mu^4 M_*^4}{\Lambda_H^4} \lesssim m_\phi^2 M_*^2, \quad (4.184)$$

as shown in Fig. 4.27, assuming for simplicity  $j = 2q$ , so that extra light scales  $\tilde{v}$  are absent. If we put this together with Eq. (4.181) we obtain

$$m_\phi \lesssim \frac{g_H^2 \Lambda_H^2}{4\pi M_*} \left( \frac{4\pi v}{g_H \Lambda_H} \right)^{2q} \lesssim \frac{4\pi v^2}{M_*}, \quad (4.185)$$

where the last inequality is valid in the  $\phi H_1 H_2$  case, i.e.  $2q = 2$ . We can raise the cutoff all the way to  $M_{\text{Pl}}$ , predicting very light scalars with  $m_\phi \lesssim v^2/M_*$ .

As our last example, we consider the coupling  $(\phi/M_*)\text{Tr}[G\tilde{G}]$ . With this choice, quantum corrections do not give us any information on  $m_\phi$  beyond Eq. (4.181). In this case experiment is more useful. Stringent bounds on axion couplings allow us to conclude

$$m_\phi^2 \lesssim \mu_{\text{exp}}^2 \frac{v f_\pi^3}{\Lambda_H^4} \simeq (0.1 \text{ eV})^2 \left( \frac{10^8 \text{ GeV}}{M_*} \right)^2 \quad (4.186)$$

for QCD. A similar discussion holds for  $(\phi/M_*)\text{Tr}[F\tilde{F}]$  with a new non-abelian gauge group whose charged fermions have a  $\langle h \rangle$ -dependent mass [118].

These three examples make more precise the intuition from Eq. (4.181). The separation between the Higgs vev and the cutoff is made stable by a symmetry protecting  $m_\phi$ . They also provide a second type of inequalities that can be used to test these mechanisms: the bigger the cutoff  $M_*$  of the  $\phi$  sector the lighter we expect the new scalars to be. Note that Eq. (4.181) on its own, in the  $\phi\text{Tr}[G\tilde{G}]$  case, does not give an experimentally interesting relation between  $m_\phi$  and  $\Lambda_H$ , because  $\mu$  depends on  $\Lambda_H$  in a way that cancels it from the equation.

To conclude we remark that one can couple  $\phi$  to the SM more weakly than what naturalness or experiment require, making it even lighter. The dilaton in [285],  $m_\chi \simeq \text{MeV} - \text{GeV}$ , saturates our upper bound for the cutoff  $M_* \simeq \Lambda_H \simeq \text{few TeV}$ . On the contrary, the scalar in [319] is much lighter  $m_\phi \lesssim v^4/M_{\text{Pl}}^3$  even if the same  $|H|^2$  trigger was used and the cutoff is of a similar order. The relation in Eq. (4.181) between the  $\phi$  mass and the coupling to the SM remains valid. This gives an interesting target to laboratory searches, as we discuss in Section 4.5.3 in the context of dark matter.

## 4.8.2 Trigger Operators and Low Energy Predictions

The second generic prediction of mechanisms selecting the weak scale dynamically is old or new physics with relatively small mass  $m \lesssim 4\pi m_h$  coupled at  $\mathcal{O}(1)$  to the Higgs. This is what we have called the trigger, i.e. the local operator whose vev depends on  $\langle h \rangle$ . We have already seen in the previous Section that three examples exist in the literature:  $\phi\text{Tr}[G\tilde{G}]$ ,  $\phi H_1 H_2$ ,  $\phi\text{Tr}[F\tilde{F}]$ , where  $G$  is the QCD field strength and  $F$  the field strength of a BSM gauge group. In the previous Section we have also discussed  $\phi|H|^2$ , but as noted also in Section 4.2 this is an imperfect trigger that can barely explain the little hierarchy problem.

Clearly the choice of trigger is central to the phenomenology of the model. From the point of view of experiment, models of cosmological naturalness can be conveniently classified based on

their trigger. For example, theories with a  $\phi\text{Tr}[G\widetilde{G}]$  coupling predict axion-like phenomenology at low energy, while theories with  $\phi H_1 H_2$ , Equivalence-Principle-violating light scalars and a new Higgs doublet.

In the SM we essentially have only one possible category of operators that can act as a trigger, given by divergences of non-gauge invariant currents:  $\text{Tr}[G\widetilde{G}]$  and  $\text{Tr}[W\widetilde{W}]$ . In this case QCD and EW interactions are the physics coupled to the Higgs, characterized by mass scales comparable or smaller than  $m_h$ . However purely within the SM the weak  $\theta$ -angle is not observable [379]. The difficulties associated to using  $\text{Tr}[W\widetilde{W}]$  as a trigger beyond the SM are discussed in Section 4.2.4.

Constructing BSM triggers requires introducing new physics coupled to the Higgs. For instance we can have a second Higgs doublet and the operator  $\mathcal{O}_T = H_1 H_2$  [142, 150, 153] or a new confining gauge group whose fermions have a Yukawa coupling to the Higgs [118] with trigger operator  $\mathcal{O}_T = \text{Tr}[F\widetilde{F}]$ . In general if we introduce in the BSM theory masses much larger than  $m_h$  the vev of the trigger operators will be proportional to those scales rather than  $v$ , just from dimensional analysis. This is one of the familiar incarnations of the hierarchy problem, i.e. dimensional analysis works.

Other examples of triggers that might work in extensions of the SM are  $\text{Tr}[W\widetilde{W}]$  or higher dimensional operators breaking baryon and/or lepton number. Both options require adding to the SM new baryon and/or lepton number breaking sensitive to the Higgs vev. To assess the feasibility of these ideas a phenomenological study comparable in scope to the one performed in [153] for  $H_1 H_2$  is needed.

The difficulty in finding BSM “trigger” operators  $\mathcal{O}_T$  lies in the requirement that  $\langle\mathcal{O}_T\rangle$  must be sensitive to the Higgs vev. In general we need new particles coupled at  $\mathcal{O}(1)$  to the Higgs whose typical mass scales are at most comparable to the weak scale. Beyond the SM it is extremely challenging to find new physics with these characteristics not already excluded by the LHC. Currently viable models, as the type-0 2HDM proposed in [153], which leads to the operator in (4.96), are on the verge of being discovered or excluded. A similar phenomenological analysis has been performed for  $\text{Tr}[F\widetilde{F}]$  in [157].

In practice only a limited number of trigger operators is viable and each trigger can be used in many different ways to select the Higgs mass. For example  $\text{Tr}[G\widetilde{G}]$  is used in [118, 151, 152, 154, 368]. So each trigger identifies phenomenology that is generically associated to Higgs naturalness, independently of a specific construction.

This feature is generic to a large class of models that select the observed value of the weak scale in the early history of the Universe: only a few choices of couplings to the SM are possible. This leads to unified expectations for their phenomenology and the concrete possibility of testing in the near future the concept of cosmological naturalness for the Higgs mass.



# Chapter 5

## Conclusion

It was the best of times, it was  
the worst of times

---

*Charles Dickens*

The questions surrounding the Higgs boson mass have driven most of the research in particle physics in the last decades. Experiments at LEP and at the LHC have neither discovered the symmetries that we expected [29, 30, 63–66, 68, 380–383] nor those that initially we did not expect [384, 385], leaving the value of the Higgs mass as puzzling as ever.

This situation has led some to question the problem rather than its proposed solutions. However, the problem is more concrete and interesting today than it ever was. It is more concrete because we have discovered the Higgs boson, measured its mass and established that it is a fundamental scalar<sup>1</sup>. The results from LEP were already pointing to a naturalness problem, but before the LHC we did not know what caused electroweak symmetry breaking in the Standard Model.

The problem is now more interesting because its most elegant solutions can not be realized in their simplest form and it is unclear whether we should abandon them entirely and radically change our outlook on the weak scale or accept some amount of tuning as a fundamental aspect of physics. Either way we will learn something new about Nature.

Possibly the most fascinating aspect of this question is that even ignoring it amounts to making important assumptions about physics at high energies. The Higgs boson mass is not calculable in the Standard Model, it is a measured parameter of the effective theory, so we could say that in our current description of Nature there is no problem and forget the whole issue.

However this leaves open only two possibilities: 1) The Higgs mass is not calculable at any energy 2) There is no mass scale beyond the Standard Model sufficiently strongly coupled to the Higgs to generate a fine-tuning problem. The first option, even if seemingly harmless, strongly constrains fundamental physics at high energies, to the point that we do not know a theory of quantum gravity that realizes it. The second one has interesting implications for model building and the description of other aspects of fundamental physics (dark matter, gauge coupling unification, ...) [94–96], and it forces us to think about theories of gravity with no new scales [47–51] whose consistency is still unclear [90–93] or to even more speculative generalizations of 2D theories [52].

At the moment the (theoretically) most conservative attitude is to assume that supersymmetry (or anything else that makes the Higgs mass calculable) exists below the scale of quantum gravity. For concreteness we can imagine that string theory describes gravity at high energies

---

<sup>1</sup>At least up to a factor of ten in energy above its mass

and supersymmetry is broken somewhere below the string scale. In this case, at the theory level the naturalness problem of the Higgs mass squared can be stated sharply, already at tree-level and without any ambiguity. The Higgs mass is a calculable function of supersymmetric parameters that in principle we can measure independently. If two or more measured contributions to the Higgs mass are much larger in absolute value than its central value we want to understand why. It is not guaranteed that the explanation will manifest itself at low energy, it might be related to the distribution of supersymmetry breaking parameters in a Multiverse or to the constraints imposed on their values by quantum gravity. However, even in these cases, thinking about the problem can shed light on fundamental aspects of physics.

We have been looking for symmetric (or dynamical) explanations for the Higgs mass for more than 40 years and we have not yet found any obvious sign that they are realized in Nature. This has generated a “little” hierarchy problem [34, 46]. We have established a hierarchy between the Higgs mass  $m_h$  and the scale at which new sources of flavor and CP violation can appear in Nature. This considerably complicates extending the SM to accommodate a symmetry or new dynamics that can protect the Higgs mass. The problem is further complicated by the null direct searches at LEP and the LHC.

Faced with these results we can take a different perspective and consider seriously the existence of a landscape for  $m_h^2$ . If we accept the existence of a vast landscape of vacua (for instance because of the cosmological constant or just because of string theory), it is likely that  $m_h^2$  varies from vacuum to vacuum. Note that even if we extrapolate to the extreme the explanatory power of current swampland conjectures [117] and imagine that the measured Cosmological Constant (CC) can be understood from the internal consistency of string theory, we still expect the existence of a vast landscape of vacua.

Historically the existence of a landscape for  $m_h^2$  coincides with anthropic solutions to the electroweak hierarchy problem [104]. Recently a new class of ideas emerged that makes a very different use of the landscape [118, 119, 154, 285, 319, 372], with much better prospects for detection and little or no recourse to anthropic arguments. In these models a dynamical event is triggered by the Higgs vev during the early history of the Universe. This event selects the value of  $m_h^2$  that we observe today, leaving traces at low energy that can escape current searches, but are in principle detectable in the near future.

The newest implementations of this idea are simple, in particular [154] has the following qualities : 1) It is entirely described by a simple polynomial potential for two weakly-coupled light scalars 2) it does not make any assumption on what can explain current CMB observations, in particular it is compatible with one’s favorite mechanism (and scale) for inflation, but also with de Sitter swampland conjectures 3) it can explain a small value of the Higgs vev  $v \simeq 246$  GeV, even if the Higgs is coupled at  $\mathcal{O}(1)$  with particles at  $M_{\text{Pl}}$ , 4) it is not affected by problems of measure in the landscape<sup>2</sup>. 5) It makes definite experimental predictions that can be tested in the near future.

The main lesson that I have learned from [154] and many more ideas of cosmological selection for  $m_h$  that were discussed or referenced in this work are that we are still far from exploring experimentally all possible low energy traces of naturalness.

A second more technical, but equally interesting point is that  $m_h$  and the QCD  $\theta$ -angle might be more intimately related than previously thought. It was well known that the vev of  $\text{Tr}[G\tilde{G}]$  depends on both, but I find fascinating that this is the only SM operator sensitive to  $\langle h \rangle$  and that the explanations for this sensitivity are highly non-trivial. The series of apparent

---

<sup>2</sup>If the landscape is populated via eternal inflation there will be a measure problem if one is interested in understanding what values of fundamental parameters are more likely in the Multiverse. However this does not affect the validity of the mechanism, since we are not asking probabilistic questions in the Multiverse. We instead have a theory where all unwanted patches are either always empty or always crunch. So we never need to know if the unwanted patches are more or less likely (occupy a smaller or larger volume in the Multiverse) than the one that we observe.

coincidences that make it possible might be concealing something deep about Nature.

Many might find the restrictions imposed by  $m_h^2$  cosmological selection on the landscape not very palatable. However, they do not violate any real or imagined constraint imposed by string theory, so to them I say: experiment will decide. Our aesthetic sense has already failed us more than once, particularly spectacularly about  $m_h^2$  (for instance about supersymmetry at LEP). I think that this is the time to be humble and explore alternatives that might seem overly adventurous to our EFT intuition.

Paraphrasing Dickens only slightly: It is the best of times, it is the worst of times, it is the age of wisdom, it is the age of foolishness, it is the epoch of belief, it is the epoch of incredulity, it is the season of light, it is the season of darkness, it is the spring of hope, it is the winter of despair.



# Bibliography

- [1] **ATLAS** Collaboration, G. Aad *et al.*, “Observation of a new particle in the search for the Standard Model Higgs boson with the ATLAS detector at the LHC,” *Phys. Lett.* **B716** (2012) 1–29, [arXiv:1207.7214 \[hep-ex\]](#).
- [2] **CMS** Collaboration, S. Chatrchyan *et al.*, “Observation of a New Boson at a Mass of 125 GeV with the CMS Experiment at the LHC,” *Phys. Lett.* **B716** (2012) 30–61, [arXiv:1207.7235 \[hep-ex\]](#).
- [3] R. Rattazzi, “Bsm for millennials.” <https://www.ggi.infn.it/showevent.pl?id=382>.
- [4] J. Polchinski, “Effective field theory and the Fermi surface,” in *Theoretical Advanced Study Institute (TASI 92): From Black Holes and Strings to Particles*, pp. 0235–276. 6, 1992. [arXiv:hep-th/9210046](#).
- [5] A. V. Manohar, “Effective field theories,” *Lect. Notes Phys.* **479** (1997) 311–362, [arXiv:hep-ph/9606222](#).
- [6] S. Weinberg, “Feynman Rules for Any Spin. 2. Massless Particles,” *Phys. Rev.* **134** (1964) B882–B896.
- [7] S. Weinberg, “Photons and Gravitons in  $S$ -Matrix Theory: Derivation of Charge Conservation and Equality of Gravitational and Inertial Mass,” *Phys. Rev.* **135** (1964) B1049–B1056.
- [8] E. P. Wigner, *The collected works of Eugen Paul Wigner. Pt. A: The scientific papers. Vol. 3.* 1997.
- [9] B. Hall, *Lie Groups, Lie Algebras, and Representations: An Elementary Introduction.* 2015.
- [10] G. Altarelli, “Partons in Quantum Chromodynamics,” *Phys. Rept.* **81** (1982) 1.
- [11] T. D. Lee, “History of weak interactions,” in *Summer School on Quantitative Particle Physics*, pp. 733–759. 1992.
- [12] N. Cabibbo, “Unitary symmetry and leptonic decays,” *Phys. Rev. Lett.* **10** (Jun, 1963) 531–533. <https://link.aps.org/doi/10.1103/PhysRevLett.10.531>.
- [13] M. Kobayashi and T. Maskawa, “CP-Violation in the Renormalizable Theory of Weak Interaction,” *Progress of Theoretical Physics* **49** (02, 1973) 652–657, <https://academic.oup.com/ptp/article-pdf/49/2/652/5257692/49-2-652.pdf>. <https://doi.org/10.1143/PTP.49.652>.
- [14] **nEDM** Collaboration, C. Abel *et al.*, “Measurement of the permanent electric dipole moment of the neutron,” *Phys. Rev. Lett.* **124** (2020) no. 8, 081803, [arXiv:2001.11966 \[hep-ex\]](#).

- [15] **Particle Data Group** Collaboration, P. A. Zyla *et al.*, “Review of Particle Physics,” *PTEP* **2020** (2020) no. 8, 083C01.
- [16] F. Zwicky, “Die Rotverschiebung von extragalaktischen Nebeln,” *Helv. Phys. Acta* **6** (1933) 110–127.
- [17] R. H. Wechsler and J. L. Tinker, “The Connection between Galaxies and their Dark Matter Halos,” *Ann. Rev. Astron. Astrophys.* **56** (2018) 435–487, [arXiv:1804.03097](https://arxiv.org/abs/1804.03097) [astro-ph.GA].
- [18] A. D. Sakharov, “Violation of CP Invariance, C asymmetry, and baryon asymmetry of the universe,” *Pisma Zh. Eksp. Teor. Fiz.* **5** (1967) 32–35.
- [19] J. C. Zorn, G. E. Chamberlain, and V. W. Hughes, “Experimental limits for the electron-proton charge difference and for the charge of the neutron,” *Phys. Rev.* **129** (Mar, 1963) 2566–2576. <https://link.aps.org/doi/10.1103/PhysRev.129.2566>.
- [20] **SNO Collaboration** Collaboration, S. N. Ahmed, A. E. Anthony, E. W. Beier, A. Bellerive, S. D. Biller, J. Boger, M. G. Boulay, M. G. Bowler, T. J. Bowles, S. J. Brice, T. V. Bullard, Y. D. Chan, M. Chen, X. Chen, B. T. Cleveland, G. A. Cox, X. Dai, F. Dalnoki-Veress, P. J. Doe, R. S. Dosanjh, G. Doucas, M. R. Dragowsky, C. A. Duba, F. A. Duncan, M. Dunford, J. A. Dunmore, E. D. Earle, S. R. Elliott, H. C. Evans, G. T. Ewan, J. Farine, H. Fergani, F. Fleurot, J. A. Formaggio, M. M. Fowler, K. Frame, W. Frati, B. G. Fulsom, N. Gagnon, K. Graham, D. R. Grant, R. L. Hahn, J. C. Hall, A. L. Hallin, E. D. Hallman, A. S. Hamer, W. B. Handler, C. K. Hargrove, P. J. Harvey, R. Hazama, K. M. Heeger, W. J. Heintzelman, J. Heise, R. L. Helmer, R. J. Hemingway, A. Hime, M. A. Howe, P. Jagam, N. A. Jelley, J. R. Klein, M. S. Kos, A. V. Krumins, T. Kutter, C. C. M. Kyba, H. Labranche, R. Lange, J. Law, I. T. Lawson, K. T. Lesko, J. R. Leslie, I. Levine, S. Luoma, R. MacLellan, S. Majerus, H. B. Mak, J. Maneira, A. D. Marino, N. McCauley, A. B. McDonald, S. McGee, G. McGregor, C. Mifflin, K. K. S. Miknaitis, G. G. Miller, B. A. Moffat, C. W. Nally, M. S. Neubauer, B. G. Nickel, A. J. Noble, E. B. Norman, N. S. Oblath, C. E. Okada, R. W. Ollerhead, J. L. Orrell, S. M. Oser, C. Ouellet, S. J. M. Peeters, A. W. P. Poon, B. C. Robertson, R. G. H. Robertson, E. Rollin, S. S. E. Rosendahl, V. L. Rusu, M. H. Schwendener, O. Simard, J. J. Simpson, C. J. Sims, D. Sinclair, P. Skensved, M. W. E. Smith, N. Starinsky, R. G. Stokstad, L. C. Stonehill, R. Tafirout, Y. Takeuchi, G. Tešić, M. Thomson, M. Thorman, R. Van Berg, R. G. Van de Water, C. J. Virtue, B. L. Wall, D. Waller, C. E. Waltham, H. W. C. Tseung, D. L. Wark, N. West, J. B. Wilhelmy, J. F. Wilkerson, J. R. Wilson, P. Wittich, J. M. Wouters, M. Yeh, and K. Zuber, “Constraints on nucleon decay via invisible modes from the sudbury neutrino observatory,” *Phys. Rev. Lett.* **92** (Mar, 2004) 102004. <https://link.aps.org/doi/10.1103/PhysRevLett.92.102004>.
- [21] C. D. Froggatt and H. B. Nielsen, “Hierarchy of Quark Masses, Cabibbo Angles and CP Violation,” *Nucl. Phys. B* **147** (1979) 277–298.
- [22] M. Leurer, Y. Nir, and N. Seiberg, “Mass matrix models,” *Nucl. Phys. B* **398** (1993) 319–342, [arXiv:hep-ph/9212278](https://arxiv.org/abs/hep-ph/9212278).
- [23] M. Leurer, Y. Nir, and N. Seiberg, “Mass matrix models: The Sequel,” *Nucl. Phys. B* **420** (1994) 468–504, [arXiv:hep-ph/9310320](https://arxiv.org/abs/hep-ph/9310320).

- [24] **Supernova Search Team** Collaboration, A. G. Riess *et al.*, “Observational evidence from supernovae for an accelerating universe and a cosmological constant,” *Astron. J.* **116** (1998) 1009–1038, [arXiv:astro-ph/9805201](#) [astro-ph].
- [25] **Supernova Cosmology Project** Collaboration, S. Perlmutter *et al.*, “Measurements of  $\Omega$  and  $\Lambda$  from 42 high redshift supernovae,” *Astrophys. J.* **517** (1999) 565–586, [arXiv:astro-ph/9812133](#) [astro-ph].
- [26] P. Charalambous, S. Dubovsky, and M. M. Ivanov, “Hidden Symmetry of Vanishing Love Numbers,” *Phys. Rev. Lett.* **127** (2021) no. 10, 101101, [arXiv:2103.01234](#) [hep-th].
- [27] P. Charalambous, S. Dubovsky, and M. M. Ivanov, “On the Vanishing of Love Numbers for Kerr Black Holes,” *JHEP* **05** (2021) 038, [arXiv:2102.08917](#) [hep-th].
- [28] R. Rattazzi, “Bsm for millennials.” <https://www.ggi.infn.it/showevent.pl?id=382>.
- [29] G. 't Hooft, “Naturalness, chiral symmetry, and spontaneous chiral symmetry breaking,” *NATO Sci. Ser. B* **59** (1980) 135–157.
- [30] S. P. Martin, “A Supersymmetry primer,” [arXiv:hep-ph/9709356](#) [hep-ph]. [Adv. Ser. Direct. High Energy Phys.18,1(1998)].
- [31] J. Terning, *Modern supersymmetry: Dynamics and duality*. 2006.
- [32] J. Wess and J. Bagger, *Supersymmetry and supergravity*. Princeton University Press, Princeton, NJ, USA, 1992.
- [33] N. Seiberg, “Naturalness versus supersymmetric nonrenormalization theorems,” *Phys. Lett. B* **318** (1993) 469–475, [arXiv:hep-ph/9309335](#).
- [34] R. Barbieri and G. F. Giudice, “Upper Bounds on Supersymmetric Particle Masses,” *Nucl. Phys. B* **306** (1988) 63–76.
- [35] R. Kitano and Y. Nomura, “Supersymmetry, naturalness, and signatures at the LHC,” *Phys. Rev. D* **73** (2006) 095004, [arXiv:hep-ph/0602096](#).
- [36] G. Giudice and R. Rattazzi, “Living Dangerously with Low-Energy Supersymmetry,” *Nucl. Phys. B* **757** (2006) 19–46, [arXiv:hep-ph/0606105](#).
- [37] R. Rattazzi, V. S. Rychkov, E. Tonni, and A. Vichi, “Bounding scalar operator dimensions in 4D CFT,” *JHEP* **12** (2008) 031, [arXiv:0807.0004](#) [hep-th].
- [38] G. Marques Tavares, M. Schmaltz, and W. Skiba, “Higgs mass naturalness and scale invariance in the UV,” *Phys. Rev. D* **89** (2014) no. 1, 015009, [arXiv:1308.0025](#) [hep-ph].
- [39] **Super-Kamiokande** Collaboration, A. Takenaka *et al.*, “Search for proton decay via  $p \rightarrow e^+\pi^0$  and  $p \rightarrow \mu^+\pi^0$  with an enlarged fiducial volume in Super-Kamiokande I-IV,” *Phys. Rev. D* **102** (2020) no. 11, 112011, [arXiv:2010.16098](#) [hep-ex].
- [40] R. N. Mohapatra, “Neutron-Anti-Neutron Oscillation: Theory and Phenomenology,” *J. Phys. G* **36** (2009) 104006, [arXiv:0902.0834](#) [hep-ph].

- [41] **MEG** Collaboration, A. M. Baldini *et al.*, “Search for the lepton flavour violating decay  $\mu^+ \rightarrow e^+ \gamma$  with the full dataset of the MEG experiment,” *Eur. Phys. J. C* **76** (2016) no. 8, 434, arXiv:1605.05081 [hep-ex].
- [42] G. Isidori, Y. Nir, and G. Perez, “Flavor Physics Constraints for Physics Beyond the Standard Model,” *Ann. Rev. Nucl. Part. Sci.* **60** (2010) 355, arXiv:1002.0900 [hep-ph].
- [43] **CMS** Collaboration, A. M. Sirunyan *et al.*, “Combined measurements of Higgs boson couplings in proton–proton collisions at  $\sqrt{s} = 13$  TeV,” *Eur. Phys. J. C* **79** (2019) no. 5, 421, arXiv:1809.10733 [hep-ex].
- [44] **ATLAS** Collaboration, M. Aaboud *et al.*, “Observation of Higgs boson production in association with a top quark pair at the LHC with the ATLAS detector,” *Phys. Lett. B* **784** (2018) 173–191, arXiv:1806.00425 [hep-ex].
- [45] **ATLAS, CMS** Collaboration, G. Aad *et al.*, “Measurements of the Higgs boson production and decay rates and constraints on its couplings from a combined ATLAS and CMS analysis of the LHC pp collision data at  $\sqrt{s} = 7$  and 8 TeV,” *JHEP* **08** (2016) 045, arXiv:1606.02266 [hep-ex].
- [46] R. Barbieri and A. Strumia, “The ‘LEP paradox’,” in *4th Rencontres du Vietnam: Physics at Extreme Energies (Particle Physics and Astrophysics)*. 7, 2000. arXiv:hep-ph/0007265.
- [47] K. S. Stelle, “Renormalization of Higher Derivative Quantum Gravity,” *Phys. Rev. D* **16** (1977) 953–969.
- [48] A. Salvio and A. Strumia, “Agravity,” *JHEP* **06** (2014) 080, arXiv:1403.4226 [hep-ph].
- [49] G. F. Giudice, G. Isidori, A. Salvio, and A. Strumia, “Softened Gravity and the Extension of the Standard Model up to Infinite Energy,” *JHEP* **02** (2015) 137, arXiv:1412.2769 [hep-ph].
- [50] K. Kannike, G. Hütsi, L. Pizza, A. Racioppi, M. Raidal, A. Salvio, and A. Strumia, “Dynamically Induced Planck Scale and Inflation,” *JHEP* **05** (2015) 065, arXiv:1502.01334 [astro-ph.CO].
- [51] A. Salvio and A. Strumia, “Agravity up to infinite energy,” *Eur. Phys. J. C* **78** (2018) no. 2, 124, arXiv:1705.03896 [hep-th].
- [52] S. Dubovsky, V. Gorbenko, and M. Mirbabayi, “Natural Tuning: Towards A Proof of Concept,” *JHEP* **09** (2013) 045, arXiv:1305.6939 [hep-th].
- [53] H. Ooguri and C. Vafa, “On the Geometry of the String Landscape and the Swampland,” *Nucl. Phys. B* **766** (2007) 21–33, arXiv:hep-th/0605264.
- [54] M. M. Anber and J. F. Donoghue, “On the running of the gravitational constant,” *Phys. Rev. D* **85** (2012) 104016, arXiv:1111.2875 [hep-th].
- [55] G. Dvali, “Black Holes and Large N Species Solution to the Hierarchy Problem,” *Fortsch. Phys.* **58** (2010) 528–536, arXiv:0706.2050 [hep-th].
- [56] G. Dvali and M. Redi, “Black Hole Bound on the Number of Species and Quantum Gravity at LHC,” *Phys. Rev. D* **77** (2008) 045027, arXiv:0710.4344 [hep-th].



- [57] G. Dvali and G. R. Farrar, “Strong CP Problem with  $10^{32}$  Standard Model Copies,” *Phys. Rev. Lett.* **101** (2008) 011801, [arXiv:0712.3170 \[hep-th\]](#).
- [58] G. Dvali and M. Redi, “Phenomenology of  $10^{32}$  Dark Sectors,” *Phys. Rev.* **D80** (2009) 055001, [arXiv:0905.1709 \[hep-ph\]](#).
- [59] R. Rattazzi, “Cargese lectures on extra-dimensions,” in *Cargese School of Particle Physics and Cosmology: the Interface*, pp. 461–517. 8, 2003. [arXiv:hep-ph/0607055](#).
- [60] R. Contino, T. Kramer, M. Son, and R. Sundrum, “Warped/composite phenomenology simplified,” *JHEP* **05** (2007) 074, [arXiv:hep-ph/0612180 \[hep-ph\]](#).
- [61] L. Susskind, “Dynamics of Spontaneous Symmetry Breaking in the Weinberg-Salam Theory,” *Phys. Rev.* **D20** (1979) 2619–2625.
- [62] S. Weinberg, “Implications of Dynamical Symmetry Breaking,” *Phys. Rev.* **D13** (1976) 974–996. [Addendum: *Phys. Rev.* **D19**, 1277(1979)].
- [63] S. Dimopoulos and L. Susskind, “Mass Without Scalars,” *Nucl. Phys.* **B155** (1979) 237–252. [2,930(1979)].
- [64] H. Terazawa, K. Akama, and Y. Chikashige, “Unified Model of the Nambu-Jona-Lasinio Type for All Elementary Particle Forces,” *Phys. Rev. D* **15** (1977) 480.
- [65] D. B. Kaplan and H. Georgi, “SU(2) x U(1) Breaking by Vacuum Misalignment,” *Phys. Lett.* **136B** (1984) 183–186.
- [66] D. B. Kaplan, H. Georgi, and S. Dimopoulos, “Composite Higgs Scalars,” *Phys. Lett.* **136B** (1984) 187–190.
- [67] H. Georgi, D. B. Kaplan, and P. Galison, “Calculation of the Composite Higgs Mass,” *Phys. Lett.* **143B** (1984) 152–154.
- [68] M. J. Dugan, H. Georgi, and D. B. Kaplan, “Anatomy of a Composite Higgs Model,” *Nucl. Phys.* **B254** (1985) 299–326.
- [69] G. F. Giudice, C. Grojean, A. Pomarol, and R. Rattazzi, “The Strongly-Interacting Light Higgs,” *JHEP* **06** (2007) 045, [arXiv:hep-ph/0703164](#).
- [70] N. Arkani-Hamed, A. G. Cohen, and H. Georgi, “Electroweak symmetry breaking from dimensional deconstruction,” *Phys. Lett. B* **513** (2001) 232–240, [arXiv:hep-ph/0105239](#).
- [71] N. Arkani-Hamed, A. G. Cohen, T. Gregoire, and J. G. Wacker, “Phenomenology of electroweak symmetry breaking from theory space,” *JHEP* **08** (2002) 020, [arXiv:hep-ph/0202089](#).
- [72] N. Arkani-Hamed, A. G. Cohen, E. Katz, and A. E. Nelson, “The Littlest Higgs,” *JHEP* **07** (2002) 034, [arXiv:hep-ph/0206021](#).
- [73] G. Panico and A. Wulzer, *The Composite Nambu-Goldstone Higgs*, vol. 913. Springer, 2016. [arXiv:1506.01961 \[hep-ph\]](#).
- [74] F. Caracciolo, A. Parolini, and M. Serone, “UV Completions of Composite Higgs Models with Partial Compositeness,” *JHEP* **02** (2013) 066, [arXiv:1211.7290 \[hep-ph\]](#).

- [75] D. Marzocca, A. Parolini, and M. Serone, “Supersymmetry with a pNGB Higgs and Partial Compositeness,” *JHEP* **03** (2014) 099, arXiv:1312.5664 [hep-ph].
- [76] J. Barnard, T. Gherghetta, and T. S. Ray, “UV descriptions of composite Higgs models without elementary scalars,” *JHEP* **02** (2014) 002, arXiv:1311.6562 [hep-ph].
- [77] G. Ferretti and D. Karateev, “Fermionic UV completions of Composite Higgs models,” *JHEP* **03** (2014) 077, arXiv:1312.5330 [hep-ph].
- [78] G. Ferretti, “UV Completions of Partial Compositeness: The Case for a SU(4) Gauge Group,” *JHEP* **06** (2014) 142, arXiv:1404.7137 [hep-ph].
- [79] R. Contino, Y. Nomura, and A. Pomarol, “Higgs as a holographic pseudoGoldstone boson,” *Nucl. Phys.* **B671** (2003) 148–174, arXiv:hep-ph/0306259 [hep-ph].
- [80] K. Agashe, R. Contino, and A. Pomarol, “The Minimal composite Higgs model,” *Nucl. Phys.* **B719** (2005) 165–187, arXiv:hep-ph/0412089 [hep-ph].
- [81] R. Contino, “The Higgs as a Composite Nambu-Goldstone Boson,” in *Theoretical Advanced Study Institute in Elementary Particle Physics: Physics of the Large and the Small*, pp. 235–306. 2011. arXiv:1005.4269 [hep-ph].
- [82] L. Randall and R. Sundrum, “A Large mass hierarchy from a small extra dimension,” *Phys. Rev. Lett.* **83** (1999) 3370–3373, arXiv:hep-ph/9905221 [hep-ph].
- [83] L. Randall and R. Sundrum, “An Alternative to compactification,” *Phys. Rev. Lett.* **83** (1999) 4690–4693, arXiv:hep-th/9906064.
- [84] R. Rattazzi and A. Zaffaroni, “Comments on the holographic picture of the Randall-Sundrum model,” *JHEP* **04** (2001) 021, arXiv:hep-th/0012248 [hep-th].
- [85] W. D. Goldberger and M. B. Wise, “Modulus stabilization with bulk fields,” *Phys. Rev. Lett.* **83** (1999) 4922–4925, arXiv:hep-ph/9907447.
- [86] M. Drees, R. Godbole, and P. Roy, *Theory and phenomenology of sparticles: An account of four-dimensional N=1 supersymmetry in high energy physics*. 2004.
- [87] P. Fayet, “Supergauge Invariant Extension of the Higgs Mechanism and a Model for the electron and Its Neutrino,” *Nucl. Phys. B* **90** (1975) 104–124.
- [88] **ATLAS** Collaboration. <https://twiki.cern.ch/twiki/bin/view/AtlasPublic/SupersymmetryPublicResults>.
- [89] **CMS** Collaboration. <https://twiki.cern.ch/twiki/bin/view/CMSPublic/PhysicsResultsSUS>.
- [90] T. D. Lee and G. C. Wick, “Negative Metric and the Unitarity of the S Matrix,” *Nucl. Phys. B* **9** (1969) 209–243.
- [91] A. Salvio and A. Strumia, “Quantum mechanics of 4-derivative theories,” *Eur. Phys. J. C* **76** (2016) no. 4, 227, arXiv:1512.01237 [hep-th].
- [92] A. Strumia, “Interpretation of quantum mechanics with indefinite norm,” *MDPI Physics* **1** (2019) no. 1, 17–32, arXiv:1709.04925 [quant-ph].
- [93] C. Gross, A. Strumia, D. Teresi, and M. Zirilli, “Is negative kinetic energy metastable?,” *Phys. Rev. D* **103** (2021) no. 11, 115025, arXiv:2007.05541 [hep-th].

- [94] M. Farina, D. Pappadopulo, and A. Strumia, “A modified naturalness principle and its experimental tests,” *JHEP* **08** (2013) 022, [arXiv:1303.7244 \[hep-ph\]](#).
- [95] A. de Gouvea, D. Hernandez, and T. M. P. Tait, “Criteria for Natural Hierarchies,” *Phys. Rev. D* **89** (2014) no. 11, 115005, [arXiv:1402.2658 \[hep-ph\]](#).
- [96] T. Hambye, A. Strumia, and D. Teresi, “Super-cool Dark Matter,” *JHEP* **08** (2018) 188, [arXiv:1805.01473 \[hep-ph\]](#).
- [97] J. D. Brown and C. Teitelboim, “Neutralization of the Cosmological Constant by Membrane Creation,” *Nucl. Phys. B* **297** (1988) 787–836.
- [98] J. D. Brown and C. Teitelboim, “Dynamical Neutralization of the Cosmological Constant,” *Phys. Lett. B* **195** (1987) 177–182.
- [99] G. W. Gibbons and S. W. Hawking, “Action Integrals and Partition Functions in Quantum Gravity,” *Phys. Rev. D* **15** (1977) 2752–2756.
- [100] M. R. Douglas and S. Kachru, “Flux compactification,” *Rev. Mod. Phys.* **79** (2007) 733–796, [arXiv:hep-th/0610102](#).
- [101] R. Bousso and J. Polchinski, “Quantization of four form fluxes and dynamical neutralization of the cosmological constant,” *JHEP* **06** (2000) 006, [arXiv:hep-th/0004134 \[hep-th\]](#).
- [102] S. Weinberg, “Anthropic Bound on the Cosmological Constant,” *Phys. Rev. Lett.* **59** (1987) 2607.
- [103] N. Arkani-Hamed, S. Dimopoulos, and S. Kachru, “Predictive landscapes and new physics at a TeV,” [arXiv:hep-th/0501082](#).
- [104] V. Agrawal, S. M. Barr, J. F. Donoghue, and D. Seckel, “Viable range of the mass scale of the standard model,” *Phys. Rev.* **D57** (1998) 5480–5492, [arXiv:hep-ph/9707380 \[hep-ph\]](#).
- [105] N. Arkani-Hamed, S. Dimopoulos, and S. Kachru, “Predictive landscapes and new physics at a TeV,” [arXiv:hep-th/0501082 \[hep-th\]](#).
- [106] J. D. Barrow and F. J. Tipler, *The Anthropic Cosmological Principle*. Oxford U. Pr., Oxford, 1988.
- [107] N. Craig and S. Koren, “IR Dynamics from UV Divergences: UV/IR Mixing, NCFT, and the Hierarchy Problem,” [arXiv:1909.01365 \[hep-ph\]](#).
- [108] R. J. Szabo, “Quantum field theory on noncommutative spaces,” *Phys. Rept.* **378** (2003) 207–299, [arXiv:hep-th/0109162](#).
- [109] M. R. Douglas and N. A. Nekrasov, “Noncommutative field theory,” *Rev. Mod. Phys.* **73** (2001) 977–1029, [arXiv:hep-th/0106048](#).
- [110] T. Filk, “Divergencies in a field theory on quantum space,” *Phys. Lett. B* **376** (1996) 53–58.
- [111] S. Minwalla, M. Van Raamsdonk, and N. Seiberg, “Noncommutative perturbative dynamics,” *JHEP* **02** (2000) 020, [arXiv:hep-th/9912072](#).

- [112] J. Gomis and T. Mehen, “Space-time noncommutative field theories and unitarity,” *Nucl. Phys. B* **591** (2000) 265–276, [arXiv:hep-th/0005129](#).
- [113] N. Arkani-Hamed, L. Motl, A. Nicolis, and C. Vafa, “The String landscape, black holes and gravity as the weakest force,” *JHEP* **06** (2007) 060, [arXiv:hep-th/0601001](#).
- [114] B. Heidenreich, M. Reece, and T. Rudelius, “Sharpening the Weak Gravity Conjecture with Dimensional Reduction,” *JHEP* **02** (2016) 140, [arXiv:1509.06374 \[hep-th\]](#).
- [115] H. Ooguri, E. Palti, G. Shiu, and C. Vafa, “Distance and de Sitter Conjectures on the Swampland,” *Phys. Lett. B* **788** (2019) 180–184, [arXiv:1810.05506 \[hep-th\]](#).
- [116] S. K. Garg and C. Krishnan, “Bounds on Slow Roll and the de Sitter Swampland,” *JHEP* **11** (2019) 075, [arXiv:1807.05193 \[hep-th\]](#).
- [117] E. Palti, “The Swampland: Introduction and Review,” *Fortsch. Phys.* **67** (2019) no. 6, 1900037, [arXiv:1903.06239 \[hep-th\]](#).
- [118] P. W. Graham, D. E. Kaplan, and S. Rajendran, “Cosmological Relaxation of the Electroweak Scale,” *Phys. Rev. Lett.* **115** (2015) no. 22, 221801, [arXiv:1504.07551 \[hep-ph\]](#).
- [119] N. Arkani-Hamed, T. Cohen, R. T. D’Agnolo, A. Hook, H. D. Kim, and D. Pinner, “Solving the Hierarchy Problem at Reheating with a Large Number of Degrees of Freedom,” *Phys. Rev. Lett.* **117** (2016) no. 25, 251801, [arXiv:1607.06821 \[hep-ph\]](#).
- [120] L. J. Hall, K. Jedamzik, J. March-Russell, and S. M. West, “Freeze-In Production of FIMP Dark Matter,” *JHEP* **03** (2010) 080, [arXiv:0911.1120 \[hep-ph\]](#).
- [121] R. Cooke, M. Pettini, R. A. Jorgenson, M. T. Murphy, and C. C. Steidel, “Precision measures of the primordial abundance of deuterium,” *Astrophys. J.* **781** (2014) no. 1, 31, [arXiv:1308.3240 \[astro-ph.CO\]](#).
- [122] **Planck** Collaboration, P. A. R. Ade *et al.*, “Planck 2015 results. XIII. Cosmological parameters,” [arXiv:1502.01589 \[astro-ph.CO\]](#).
- [123] N. F. Bell, E. Pierpaoli, and K. Sigurdson, “Cosmological signatures of interacting neutrinos,” *Phys. Rev.* **D73** (2006) 063523, [arXiv:astro-ph/0511410 \[astro-ph\]](#).
- [124] Z. Hou, R. Keisler, L. Knox, M. Millea, and C. Reichardt, “How Massless Neutrinos Affect the Cosmic Microwave Background Damping Tail,” *Phys. Rev.* **D87** (2013) 083008, [arXiv:1104.2333 \[astro-ph.CO\]](#).
- [125] B. Follin, L. Knox, M. Millea, and Z. Pan, “First Detection of the Acoustic Oscillation Phase Shift Expected from the Cosmic Neutrino Background,” *Phys. Rev. Lett.* **115** (2015) no. 9, 091301, [arXiv:1503.07863 \[astro-ph.CO\]](#).
- [126] D. Baumann, D. Green, J. Meyers, and B. Wallisch, “Phases of New Physics in the CMB,” *JCAP* **1601** (2016) 007, [arXiv:1508.06342 \[astro-ph.CO\]](#).
- [127] S. Dodelson *et al.*, “Working Group Report: Dark Energy and CMB,” in *Community Summer Study 2013: Snowmass on the Mississippi (CSS2013) Minneapolis, MN, USA, July 29-August 6, 2013*. 2013. [arXiv:1309.5386 \[astro-ph.CO\]](#).
- [128] S. Davidson, B. Campbell, and D. C. Bailey, “Limits on particles of small electric charge,” *Phys. Rev.* **D43** (1991) 2314–2321.

- [129] S. Davidson, S. Hannestad, and G. Raffelt, “Updated bounds on millicharged particles,” *JHEP* **05** (2000) 003, [arXiv:hep-ph/0001179](#) [hep-ph].
- [130] G. Raffelt and D. Seckel, “Bounds on Exotic Particle Interactions from SN 1987a,” *Phys. Rev. Lett.* **60** (1988) 1793.
- [131] M. Cirelli, G. Marandella, A. Strumia, and F. Vissani, “Probing oscillations into sterile neutrinos with cosmology, astrophysics and experiments,” *Nucl. Phys.* **B708** (2005) 215–267, [arXiv:hep-ph/0403158](#) [hep-ph].
- [132] **TLEP Design Study Working Group** Collaboration, M. Bicer *et al.*, “First Look at the Physics Case of TLEP,” *JHEP* **01** (2014) 164, [arXiv:1308.6176](#) [hep-ex].
- [133] N. Arkani-Hamed, T. Han, M. Mangano, and L.-T. Wang, “Physics Opportunities of a 100 TeV Proton-Proton Collider,” [arXiv:1511.06495](#) [hep-ph].
- [134] T. Golling *et al.*, “Physics at a 100 TeV pp collider: beyond the Standard Model phenomena,” [arXiv:1606.00947](#) [hep-ph].
- [135] J. D. Clarke, R. Foot, and R. R. Volkas, “Phenomenology of a very light scalar (100 MeV  $\leq m_h \leq$  10 GeV) mixing with the SM Higgs,” *JHEP* **02** (2014) 123, [arXiv:1310.8042](#) [hep-ph].
- [136] G. Krnjaic, “Probing Light Thermal Dark-Matter With a Higgs Portal Mediator,” *Phys. Rev. D* **94** (2016) no. 7, 073009, [arXiv:1512.04119](#) [hep-ph].
- [137] W. Altmannshofer, M. Bauer, and M. Carena, “Exotic Leptons: Higgs, Flavor and Collider Phenomenology,” *JHEP* **01** (2014) 060, [arXiv:1308.1987](#) [hep-ph].
- [138] R. Allison, P. Caucal, E. Calabrese, J. Dunkley, and T. Louis, “Towards a cosmological neutrino mass detection,” *Phys. Rev.* **D92** (2015) no. 12, 123535, [arXiv:1509.07471](#) [astro-ph.CO].
- [139] A. Nicolis, “On Super-Planckian Fields at Sub-Planckian Energies,” *JHEP* **07** (2008) 023, [arXiv:0802.3923](#) [hep-th].
- [140] G. Obied, H. Ooguri, L. Spodyneiko, and C. Vafa, “De Sitter Space and the Swampland,” [arXiv:1806.08362](#) [hep-th].
- [141] G. G. Raffelt, “Astrophysical axion bounds,” *Lect. Notes Phys.* **741** (2008) 51–71, [arXiv:hep-ph/0611350](#).
- [142] J. R. Espinosa, C. Grojean, G. Panico, A. Pomarol, O. Pujolàs, and G. Servant, “Cosmological Higgs-Axion Interplay for a Naturally Small Electroweak Scale,” *Phys. Rev. Lett.* **115** (2015) no. 25, 251803, [arXiv:1506.09217](#) [hep-ph].
- [143] A. Hook and G. Marques-Tavares, “Relaxation from particle production,” *JHEP* **12** (2016) 101, [arXiv:1607.01786](#) [hep-ph].
- [144] E. Hardy, “Electroweak relaxation from finite temperature,” *JHEP* **11** (2015) 077, [arXiv:1507.07525](#) [hep-ph].
- [145] S. P. Patil and P. Schwaller, “Relaxing the Electroweak Scale: the Role of Broken dS Symmetry,” *JHEP* **02** (2016) 077, [arXiv:1507.08649](#) [hep-ph].

- [146] B. Batell, G. F. Giudice, and M. McCullough, “Natural Heavy Supersymmetry,” *JHEP* **12** (2015) 162, [arXiv:1509.00834 \[hep-ph\]](#).
- [147] J. L. Evans, T. Gherghetta, N. Nagata, and Z. Thomas, “Naturalizing Supersymmetry with a Two-Field Relaxion Mechanism,” *JHEP* **09** (2016) 150, [arXiv:1602.04812 \[hep-ph\]](#).
- [148] O. Matsedonskyi, “Mirror Cosmological Relaxation of the Electroweak Scale,” *JHEP* **01** (2016) 063, [arXiv:1509.03583 \[hep-ph\]](#).
- [149] L. F. Abbott, “A Mechanism for Reducing the Value of the Cosmological Constant,” *Phys. Lett.* **150B** (1985) 427–430.
- [150] G. R. Dvali and A. Vilenkin, “Field theory models for variable cosmological constant,” *Phys. Rev. D* **64** (2001) 063509, [arXiv:hep-th/0102142](#).
- [151] G. Dvali and A. Vilenkin, “Cosmic attractors and gauge hierarchy,” *Phys. Rev. D* **70** (2004) 063501, [arXiv:hep-th/0304043](#).
- [152] G. Dvali, “Large hierarchies from attractor vacua,” *Phys. Rev. D* **74** (2006) 025018, [arXiv:hep-th/0410286](#).
- [153] N. Arkani-Hamed, R. T. **D’Agnolo**, and H. D. Kim, “The Weak Scale as a Trigger,” [arXiv:2012.04652 \[hep-ph\]](#).
- [154] R. T. **D’Agnolo** and D. Teresi, “Sliding Naturalness,” [arXiv:2106.04591 \[hep-ph\]](#).
- [155] R. Tito D’Agnolo and D. Teresi, “Sliding Naturalness: Cosmological Selection of the Weak Scale,” [arXiv:2109.13249 \[hep-ph\]](#).
- [156] S. Weinberg, *The quantum theory of fields. Vol. 2: Modern applications*. Cambridge University Press, 8, 2013.
- [157] H. Beauchesne, E. Bertuzzo, and G. Grilli di Cortona, “Constraints on the relaxion mechanism with strongly interacting vector-fermions,” *JHEP* **08** (2017) 093, [arXiv:1705.06325 \[hep-ph\]](#).
- [158] J. F. Gunion and H. E. Haber, “The CP conserving two Higgs doublet model: The Approach to the decoupling limit,” *Phys. Rev. D* **67** (2003) 075019, [arXiv:hep-ph/0207010](#).
- [159] A. Djouadi, “The Anatomy of electro-weak symmetry breaking. II. The Higgs bosons in the minimal supersymmetric model,” *Phys. Rept.* **459** (2008) 1–241, [arXiv:hep-ph/0503173](#).
- [160] G. Branco, P. Ferreira, L. Lavoura, M. Rebelo, M. Sher, and J. P. Silva, “Theory and phenomenology of two-Higgs-doublet models,” *Phys. Rept.* **516** (2012) 1–102, [arXiv:1106.0034 \[hep-ph\]](#).
- [161] J. Alwall, R. Frederix, S. Frixione, V. Hirschi, F. Maltoni, O. Mattelaer, H. S. Shao, T. Stelzer, P. Torrielli, and M. Zaro, “The automated computation of tree-level and next-to-leading order differential cross sections, and their matching to parton shower simulations,” *JHEP* **07** (2014) 079, [arXiv:1405.0301 \[hep-ph\]](#).  
CERN-PH-TH-2014-064, CP3-14-18, LPN14-066, MCNET-14-09, ZU-TH-14-14.

- [162] W. Grimus, L. Lavoura, O. Og Reid, and P. Osland, “The Oblique parameters in multi-Higgs-doublet models,” *Nucl. Phys. B* **801** (2008) 81–96, [arXiv:0802.4353 \[hep-ph\]](#).
- [163] M. E. Peskin and T. Takeuchi, “Estimation of oblique electroweak corrections,” *Phys. Rev. D* **46** (1992) 381–409.
- [164] G. Altarelli and R. Barbieri, “Vacuum polarization effects of new physics on electroweak processes,” *Phys. Lett. B* **253** (1991) 161–167.
- [165] D. Eriksson, J. Rathsman, and O. Stal, “2HDMC: Two-Higgs-Doublet Model Calculator Physics and Manual,” *Comput. Phys. Commun.* **181** (2010) 189–205, [arXiv:0902.0851 \[hep-ph\]](#).
- [166] R. Harlander, M. Mühlleitner, J. Rathsman, M. Spira, and O. Stal, “Interim recommendations for the evaluation of Higgs production cross sections and branching ratios at the LHC in the Two-Higgs-Doublet Model,” [arXiv:1312.5571 \[hep-ph\]](#).
- [167] J. Ellis, “TikZ-Feynman: Feynman diagrams with TikZ,” *Comput. Phys. Commun.* **210** (2017) 103–123, [arXiv:1601.05437 \[hep-ph\]](#).
- [168] **ALEPH, DELPHI, L3, OPAL, LEP Working Group for Higgs Boson Searches** Collaboration, S. Schael *et al.*, “Search for neutral MSSM Higgs bosons at LEP,” *Eur. Phys. J. C* **47** (2006) 547–587, [arXiv:hep-ex/0602042](#).
- [169] P. Achard *et al.*, “Search for a higgs boson decaying into two photons at lep,” *Physics Letters B* **534** (2002) no. 1, 28 – 38.  
<http://www.sciencedirect.com/science/article/pii/S0370269302015721>.
- [170] **ATLAS** Collaboration, G. Aad *et al.*, “Search for Scalar Diphoton Resonances in the Mass Range 65 – 600 GeV with the ATLAS Detector in  $pp$  Collision Data at  $\sqrt{s} = 8$  TeV,” *Phys. Rev. Lett.* **113** (2014) no. 17, 171801, [arXiv:1407.6583 \[hep-ex\]](#).
- [171] **CMS** Collaboration, A. M. Sirunyan *et al.*, “Search for a standard model-like Higgs boson in the mass range between 70 and 110 GeV in the diphoton final state in proton-proton collisions at  $\sqrt{s} = 8$  and 13 TeV,” *Phys. Lett.* **B793** (2019) 320–347, [arXiv:1811.08459 \[hep-ex\]](#).
- [172] **LHCb** Collaboration, R. Aaij *et al.*, “Differential branching fraction and angular analysis of the  $B^+ \rightarrow K^+ \mu^+ \mu^-$  decay,” *JHEP* **02** (2013) 105, [arXiv:1209.4284 \[hep-ex\]](#).
- [173] **Belle** Collaboration, J.-T. Wei *et al.*, “Measurement of the Differential Branching Fraction and Forward-Backward Asymmetry for  $B \rightarrow K^{(*)} \ell^+ \ell^-$ ,” *Phys. Rev. Lett.* **103** (2009) 171801, [arXiv:0904.0770 \[hep-ex\]](#).
- [174] **HFLAV** Collaboration, Y. S. Amhis *et al.*, “Averages of  $b$ -hadron,  $c$ -hadron, and  $\tau$ -lepton properties as of 2018,” [arXiv:1909.12524 \[hep-ex\]](#).
- [175] A. Arbey, F. Mahmoudi, O. Stal, and T. Stefaniak, “Status of the Charged Higgs Boson in Two Higgs Doublet Models,” *Eur. Phys. J. C* **78** (2018) no. 3, 182, [arXiv:1706.07414 \[hep-ph\]](#).
- [176] **CMS** Collaboration, “Search for charged Higgs bosons with the  $H^\pm \rightarrow \tau^\pm \nu_\tau$  decay channel in the fully hadronic final state at  $\sqrt{s} = 13$  TeV,” CMS-PAS-HIG-16-031.

- [177] **CMS** Collaboration, “Search for a light charged Higgs boson in the  $H^\pm \rightarrow cs$  channel at 13 TeV,”. CMS-PAS-HIG-18-021.
- [178] **CMS** Collaboration, “Search for Charged Higgs boson to  $c\bar{b}$  in lepton+jets channel using top quark pair events,”. CMS-PAS-HIG-16-030.
- [179] **CMS** Collaboration, “Search for  $H^+$  to  $cs$ -bar decay,”. CMS-PAS-HIG-13-035.
- [180] **ALEPH, DELPHI, L3, OPAL, LEP** Collaboration, G. Abbiendi *et al.*, “Search for Charged Higgs bosons: Combined Results Using LEP Data,” *Eur. Phys. J.* **C73** (2013) 2463, arXiv:1301.6065 [hep-ex].
- [181] **ALEPH, DELPHI, L3, OPAL, LEP Electroweak Working Group, SLD Heavy Flavor Group** Collaboration, “A Combination of preliminary electroweak measurements and constraints on the standard model,” arXiv:hep-ex/0212036.
- [182] **ALEPH, DELPHI, L3, OPAL, SLD, LEP Electroweak Working Group, SLD Electroweak Group, SLD Heavy Flavour Group** Collaboration, S. Schael *et al.*, “Precision electroweak measurements on the  $Z$  resonance,” *Phys. Rept.* **427** (2006) 257–454, arXiv:hep-ex/0509008.
- [183] **DELPHI** Collaboration, J. Abdallah *et al.*, “Search for charged Higgs bosons at LEP in general two Higgs doublet models,” *Eur. Phys. J. C* **34** (2004) 399–418, arXiv:hep-ex/0404012.
- [184] **CMS** Collaboration, “Search for a light charged higgs boson decaying to a  $w$  boson and a  $cp$ -odd higgs boson in final states with  $e\mu\mu$  or  $\mu\mu\mu$  in proton-proton collisions at  $\sqrt{s} = 13$  TeV,” *Phys. Rev. Lett.* **123** (Sep, 2019) 131802. <https://link.aps.org/doi/10.1103/PhysRevLett.123.131802>.
- [185] **ATLAS** Collaboration, “Search for charged Higgs bosons decaying into a top-quark and a bottom-quark at  $\sqrt{s} = 13$  TeV with the ATLAS detector,”. ATLAS-CONF-2020-039.
- [186] **CMS** Collaboration, A. M. Sirunyan *et al.*, “Search for charged Higgs bosons decaying into a top and a bottom quark in the all-jet final state of pp collisions at  $\sqrt{s} = 13$  TeV,” arXiv:2001.07763 [hep-ex]. CMS-HIG-18-015, CERN-EP-2019-277.
- [187] **ATLAS** Collaboration, M. Aaboud *et al.*, “Search for charged Higgs bosons decaying into top and bottom quarks at  $\sqrt{s} = 13$  TeV with the ATLAS detector,” *JHEP* **11** (2018) 085, arXiv:1808.03599 [hep-ex]. CERN-EP-2018-168.
- [188] **CMS** Collaboration, “Search for a charged Higgs boson decaying into top and bottom quarks in proton-proton collisions at 13TeV in events with electrons or muons,”. CMS-PAS-HIG-18-004.
- [189] **CMS** Collaboration, “Search for charged Higgs bosons decaying into top and a bottom quark in the fully hadronic final state at 13 TeV,”. CMS-PAS-HIG-18-015.
- [190] **ATLAS** Collaboration, M. Aaboud *et al.*, “Search for charged Higgs bosons produced in association with a top quark and decaying via  $H^\pm \rightarrow \tau\nu$  using  $pp$  collision data recorded at  $\sqrt{s} = 13$  TeV by the ATLAS detector,” *Phys. Lett. B* **759** (2016) 555–574, arXiv:1603.09203 [hep-ex].
- [191] **CMS** Collaboration, “Search for charged Higgs bosons with the  $H^\pm \rightarrow \tau^\pm\nu_\tau$  decay channel in proton-proton collisions at  $\sqrt{s} = 13$  TeV,”. CMS-PAS-HIG-18-014.



- [192] **CMS** Collaboration, “Search for charged Higgs bosons with the  $H^+$  to tau nu decay channel in the fully hadronic final state at  $\sqrt{s} = 8$  TeV,”.
- [193] **CMS** Collaboration, A. M. Sirunyan *et al.*, “Search for direct pair production of supersymmetric partners to the  $\tau$  lepton in proton-proton collisions at  $\sqrt{s} = 13$  TeV,” *Eur. Phys. J. C* **80** (2020) no. 3, 189, [arXiv:1907.13179](#) [[hep-ex](#)].
- [194] **L3** Collaboration, M. Acciarri *et al.*, “Search for neutral Higgs boson production through the process  $e^+ e^- \rightarrow Z^* H_0$ ,” *Phys. Lett. B* **385** (1996) 454–470.
- [195] **ATLAS** Collaboration, “Search for resonances decaying to photon pairs in  $139 \text{ fb}^{-1}$  of  $pp$  collisions at  $\sqrt{s} = 13$  TeV with the ATLAS detector,”. ATLAS-CONF-2020-037.
- [196] **ATLAS** Collaboration, “Measurement of the properties of Higgs boson production at  $\sqrt{s}=13$  TeV in the  $H \rightarrow \gamma\gamma$  channel using  $139 \text{ fb}^{-1}$  of  $pp$  collision data with the ATLAS experiment,”. ATLAS-CONF-2020-026.
- [197] **CMS** Collaboration, “Measurements of Higgs boson properties in the diphoton decay channel at  $\sqrt{s} = 13$  TeV,”. CMS-PAS-HIG-19-015.
- [198] **ATLAS** Collaboration, M. Aaboud *et al.*, “Search for resonances in diphoton events at  $\sqrt{s}=13$  TeV with the ATLAS detector,” *JHEP* **09** (2016) 001, [arXiv:1606.03833](#) [[hep-ex](#)].
- [199] **CMS** Collaboration, “Search for an Higgs Like resonance in the diphoton mass spectra above 150 GeV with 8 TeV data,”. CMS-PAS-HIG-14-006.
- [200] **ATLAS** Collaboration, G. Aad *et al.*, “Search for a fermiophobic Higgs boson in the diphoton decay channel with the ATLAS detector,” *Eur. Phys. J. C* **72** (2012) 2157, [arXiv:1205.0701](#) [[hep-ex](#)].
- [201] **CMS** Collaboration, “Evidence for a new state decaying into two photons in the search for the standard model Higgs boson in  $pp$  collisions,”. CMS-PAS-HIG-12-015.
- [202] **CMS** Collaboration, “Search for new resonances in the diphoton final state in the mass range between 80 and 115 GeV in  $pp$  collisions at  $\sqrt{s} = 8$  TeV,”. CMS-PAS-HIG-14-037.
- [203] **CMS** Collaboration, “Search for new resonances in the diphoton final state in the mass range between 70 and 110 GeV in  $pp$  collisions at  $\sqrt{s} = 8$  and 13 TeV,”. CMS-PAS-HIG-17-013.
- [204] **ATLAS** Collaboration, M. Aaboud *et al.*, “Search for new phenomena in high-mass diphoton final states using  $37 \text{ fb}^{-1}$  of proton–proton collisions collected at  $\sqrt{s} = 13$  TeV with the ATLAS detector,” *Phys. Lett. B* **775** (2017) 105–125, [arXiv:1707.04147](#) [[hep-ex](#)].
- [205] A. Mariotti, D. Redigolo, F. Sala, and K. Tobioka, “New LHC bound on low-mass diphoton resonances,” *Phys. Lett. B* **783** (2018) 13–18, [arXiv:1710.01743](#) [[hep-ph](#)].
- [206] **CMS** Collaboration, V. Khachatryan *et al.*, “Search for diphoton resonances in the mass range from 150 to 850 GeV in  $pp$  collisions at  $\sqrt{s} = 8$  TeV,” *Phys. Lett. B* **750** (2015) 494–519, [arXiv:1506.02301](#) [[hep-ex](#)].
- [207] **CMS** Collaboration, “Measurement of Higgs boson production in the decay channel with a pair of  $\tau$  leptons,”. CMS-PAS-HIG-19-010.

- [208] **ATLAS** Collaboration, M. Aaboud *et al.*, “Search for additional heavy neutral Higgs heavy neutral Higgs and gauge bosons in the ditau final state produced in  $36 \text{ fb}^{-1}$  of pp collisions at  $\sqrt{s} = 13 \text{ TeV}$  with the ATLAS detector,” *JHEP* **01** (2018) 055, arXiv:1709.07242 [hep-ex].
- [209] **ATLAS** Collaboration, M. Aaboud *et al.*, “Search for Minimal Supersymmetric Standard Model Higgs bosons  $H/A$  and for a  $Z'$  boson in the  $\tau\tau$  final state produced in pp collisions at  $\sqrt{s} = 13 \text{ TeV}$  with the ATLAS Detector,” *Eur. Phys. J.* **C76** (2016) no. 11, 585, arXiv:1608.00890 [hep-ex].
- [210] **ATLAS** Collaboration, G. Aad *et al.*, “Search for neutral Higgs bosons of the minimal supersymmetric standard model in pp collisions at  $\sqrt{s} = 8 \text{ TeV}$  with the ATLAS detector,” *JHEP* **11** (2014) 056, arXiv:1409.6064 [hep-ex]. CERN-PH-EP-2014-210.
- [211] **CMS** Collaboration, A. M. Sirunyan *et al.*, “Search for additional neutral MSSM Higgs bosons in the  $\tau\tau$  final state in proton-proton collisions at  $\sqrt{s} = 13 \text{ TeV}$ ,” *JHEP* **09** (2018) 007, arXiv:1803.06553 [hep-ex].
- [212] **CMS** Collaboration, “Search for the Standard-Model Higgs boson decaying to tau pairs in proton-proton collisions at  $\sqrt{s} = 7$  and  $8 \text{ TeV}$ ,”. CMS-PAS-HIG-13-004.
- [213] **CMS** Collaboration, “Higgs to tau tau (MSSM),”. CMS-PAS-HIG-13-021.
- [214] **CMS** Collaboration, “Search for a neutral MSSM Higgs boson decaying into  $\tau\tau$  at  $13 \text{ TeV}$ ,”. CMS-PAS-HIG-16-006.
- [215] **CMS** Collaboration, “Search for a neutral MSSM Higgs boson decaying into  $\tau\tau$  with  $12.9 \text{ fb}^{-1}$  of data at  $\sqrt{s} = 13 \text{ TeV}$ ,”. CMS-PAS-HIG-16-037.
- [216] **CMS** Collaboration, “Search for a low-mass  $\tau^-\tau^+$  resonance in association with a bottom quark in proton-proton collisions at  $\sqrt{s} = 13 \text{ TeV}$ ,”. CMS-PAS-HIG-17-014.
- [217] **CMS** Collaboration, “Search for additional neutral MSSM Higgs bosons in the di-tau final state in pp collisions at  $\sqrt{s} = 13 \text{ TeV}$ ,”. CMS-PAS-HIG-17-020.
- [218] **CMS** Collaboration, “Measurement of Higgs boson production and decay to the  $\tau\tau$  final state,”. CMS-PAS-HIG-18-032.
- [219] **CMS** Collaboration, “Search for additional neutral Higgs bosons decaying to a pair of tau leptons in pp collisions at  $\sqrt{s} = 7$  and  $8 \text{ TeV}$ ,”. CMS-PAS-HIG-14-029.
- [220] **CMS** Collaboration, “Constraints on anomalous HVV couplings in the production of Higgs bosons decaying to tau lepton pairs,”. CMS-PAS-HIG-17-034.
- [221] **ATLAS** Collaboration, G. Aad *et al.*, “A search for the dimuon decay of the Standard Model Higgs boson with the ATLAS detector,” arXiv:2007.07830 [hep-ex].
- [222] **CMS** Collaboration, A. M. Sirunyan *et al.*, “Evidence for Higgs boson decay to a pair of muons,” arXiv:2009.04363 [hep-ex].
- [223] **ATLAS** Collaboration, M. Aaboud *et al.*, “Search for scalar resonances decaying into  $\mu^+\mu^-$  in events with and without  $b$ -tagged jets produced in proton-proton collisions at  $\sqrt{s} = 13 \text{ TeV}$  with the ATLAS detector,” *JHEP* **07** (2019) 117, arXiv:1901.08144 [hep-ex].

- [224] **CMS** Collaboration, “Search for neutral MSSM Higgs bosons decaying to  $\mu^+\mu^-$  in pp collisions at  $\sqrt{s} = 13$  TeV,”. CMS-PAS-HIG-18-010.
- [225] **CMS** Collaboration, “A Search for Beyond Standard Model Light Bosons Decaying into Muon Pairs,”. CMS-PAS-HIG-16-035.
- [226] **CMS** Collaboration, “Search for a light pseudo-scalar Higgs boson produced in association with bottom quarks in pp collisions at 8 TeV,”. CMS-PAS-HIG-15-009.
- [227] A. M. Sirunyan *et al.*, “Search for MSSM Higgs bosons decaying to  $\mu^+\mu^-$  in proton-proton collisions at  $\sqrt{s} = 13$  TeV, collaboration =,”.
- [228] **ATLAS** Collaboration, G. Aad *et al.*, “Measurements of  $WH$  and  $ZH$  production in the  $H \rightarrow b\bar{b}$  decay channel in  $pp$  collisions at 13 TeV with the ATLAS detector,” arXiv:2007.02873 [hep-ex].
- [229] **ATLAS** Collaboration, G. Aad *et al.*, “Measurement of the associated production of a Higgs boson decaying into  $b$ -quarks with a vector boson at high transverse momentum in  $pp$  collisions at  $\sqrt{s} = 13$  TeV with the ATLAS detector,” arXiv:2008.02508 [hep-ex].
- [230] **ATLAS** Collaboration, G. Aad *et al.*, “Search for Higgs boson production in association with a high-energy photon via vector-boson fusion with decay into bottom quark pairs at  $\sqrt{s}=13$  TeV with the ATLAS detector,” arXiv:2010.13651 [hep-ex].
- [231] **ATLAS** Collaboration, “Measurement of the Higgs boson decaying to  $b$ -quarks produced in association with a top-quark pair in  $pp$  collisions at  $\sqrt{s} = 13$  TeV with the ATLAS detector,”. ATLAS-CONF-2020-058.
- [232] **CMS** Collaboration, “Inclusive search for a highly boosted Higgs boson decaying to a bottom quark-antiquark pair at  $\sqrt{s} = 13$  TeV with  $137 \text{ fb}^{-1}$ ,”. CMS-PAS-HIG-19-003.
- [233] **CMS** Collaboration, “Search for nonresonant Higgs boson pair production in the 4 leptons plus 2 b jets final state in proton-proton collisions at  $\sqrt{s} = 13$  TeV,”. CMS-PAS-HIG-20-004.
- [234] **CMS** Collaboration, “Search for Higgs bosons produced in association with b quarks and decaying into a b-quark pair with 13 TeV data,”. CMS-PAS-HIG-16-018.
- [235] **CMS** Collaboration, “Higgs to bb in the VBF channel,”. CMS-PAS-HIG-13-011.
- [236] **ATLAS** Collaboration, G. Aad *et al.*, “Search for heavy neutral Higgs bosons produced in association with  $b$ -quarks and decaying to  $b$ -quarks at  $\sqrt{s} = 13$  TeV with the ATLAS detector,” arXiv:1907.02749 [hep-ex].
- [237] **CMS** Collaboration, “Search for a narrow heavy decaying to bottom quark pairs in the 13 TeV data sample,”. CMS-PAS-HIG-16-025.
- [238] **ATLAS** Collaboration, M. Aaboud *et al.*, “Searches for the  $Z\gamma$  decay mode of the Higgs boson and for new high-mass resonances in  $pp$  collisions at  $\sqrt{s} = 13$  TeV with the ATLAS detector,” *JHEP* **10** (2017) 112, arXiv:1708.00212 [hep-ex].
- [239] **ATLAS** Collaboration, “Measurement of the Higgs boson mass in the  $H \rightarrow ZZ^* \rightarrow 4\ell$  decay channel with  $\sqrt{s} = 13$  TeV  $pp$  collisions using the ATLAS detector at the LHC,”. ATLAS-CONF-2020-005.

- [240] **ATLAS** Collaboration, G. Aad *et al.*, “Higgs boson production cross-section measurements and their EFT interpretation in the  $4\ell$  decay channel at  $\sqrt{s} = 13$  TeV with the ATLAS detector,” *Eur. Phys. J. C* **80** (2020) no. 10, 957, arXiv:2004.03447 [hep-ex].
- [241] **ATLAS** Collaboration, “Observation of vector-boson-fusion production of Higgs bosons in the  $H \rightarrow WW^* \rightarrow e\nu\mu\nu$  decay channel in  $pp$  collisions at  $\sqrt{s} = 13$  TeV with the ATLAS detector,”. ATLAS-CONF-2020-045.
- [242] **ATLAS** Collaboration, “Constraints on Higgs boson properties using  $WW^*(\rightarrow e\nu\mu\nu) jj$  production in  $36.1\text{fb}^{-1}$  of  $\sqrt{s} = 13\text{TeV}$  pp collisions with the ATLAS detector,”. ATLAS-CONF-2020-055.
- [243] **CMS** Collaboration, “Constraints on anomalous Higgs boson couplings to vector bosons and fermions in production and decay in the  $H \rightarrow 4\ell$  channel,”. CMS-PAS-HIG-19-009.
- [244] **CMS** Collaboration, “Update on the search for the standard model Higgs boson in pp collisions at the LHC decaying to  $W + W$  in the fully leptonic final state,”. CMS-PAS-HIG-13-003.
- [245] **CMS** Collaboration, “Search for a new scalar resonance decaying to a pair of Z bosons in proton-proton collisions at  $\sqrt{s} = 13$  TeV,”. CMS-PAS-HIG-17-012.
- [246] **ATLAS** Collaboration, G. Aad *et al.*, “Search for a high-mass Higgs boson decaying to a  $W$  boson pair in  $pp$  collisions at  $\sqrt{s} = 8$  TeV with the ATLAS detector,” *JHEP* **01** (2016) 032, arXiv:1509.00389 [hep-ex].
- [247] **ATLAS** Collaboration, M. Aaboud *et al.*, “Search for heavy resonances decaying into  $WW$  in the  $e\nu\mu\nu$  final state in  $pp$  collisions at  $\sqrt{s} = 13$  TeV with the ATLAS detector,” *Eur. Phys. J.* **C78** (2018) no. 1, 24, arXiv:1710.01123 [hep-ex].
- [248] **ATLAS** Collaboration, M. Aaboud *et al.*, “Search for heavy  $ZZ$  resonances in the  $\ell^+\ell^-\ell^+\ell^-$  and  $\ell^+\ell^-\nu\bar{\nu}$  final states using proton-proton collisions at  $\sqrt{s} = 13$  TeV with the ATLAS detector,” *Eur. Phys. J.* **C78** (2018) no. 4, 293, arXiv:1712.06386 [hep-ex].
- [249] **ATLAS** Collaboration, M. Aaboud *et al.*, “Search for a heavy Higgs boson decaying into a  $Z$  boson and another heavy Higgs boson in the  $\ell\ell b\bar{b}$  final state in  $pp$  collisions at  $\sqrt{s} = 13$  TeV with the ATLAS detector,” *Phys. Lett.* **B783** (2018) 392–414, arXiv:1804.01126 [hep-ex].
- [250] **CMS** Collaboration, “Search for a standard model like Higgs boson in the decay channel  $H$  to  $ZZ$  to  $l+l-$  q qbar at CMS,”. CMS-PAS-HIG-12-024.
- [251] **CMS** Collaboration, “Search for a heavy Higgs boson in the  $H$  to  $ZZ$  to  $2l2\nu$  channel in pp collisions at  $\sqrt{s} = 7$  and  $8$  TeV,”. CMS-PAS-HIG-13-014.
- [252] **CMS** Collaboration, “Search for high mass Higgs to  $WW$  with fully leptonic decays using 2015 data,”. CMS-PAS-HIG-16-023.
- [253] **CMS** Collaboration, “Search for a heavy scalar boson decaying into a pair of Z bosons in the  $2\ell 2\nu$  final state,”. CMS-PAS-HIG-16-001.
- [254] **CMS** Collaboration, “Search for 2HDM neutral Higgs bosons through the  $H \rightarrow ZA \rightarrow \ell^+\ell^-\bar{b}b$  process in proton-proton collisions at  $\sqrt{s} = 13$  TeV,”. CMS-PAS-HIG-18-012.

- [255] **CMS** Collaboration, “Search for H/A decaying into Z+A/H, with Z to  $ll$  and A/H to fermion pair,”. CMS-PAS-HIG-15-001.
- [256] **CMS** Collaboration, “Search for a heavy Higgs boson decaying to a pair of W bosons in proton-proton collisions at  $\sqrt{s} = 13$  TeV,”. CMS-PAS-HIG-17-033.
- [257] **CMS** Collaboration, “Search for H to Z( $ll$ )+A( $bb$ ) with 2015 data,”. CMS-PAS-HIG-16-010.
- [258] F. Bergsma, J. Dorenbosch, J. Allaby, U. Amaldi, G. Barbiellini, C. Berger, W. Flegel, L. Lancieri, M. Metcalf, C. Nieuwenhuis, J. Panman, C. Santoni, K. Winter, I. Abt, J. A. and F.W. Busser, H. Daumann, P. Gall, T. Hebbeker, F. N. and P. Schutt, P. Stahelin, P. Gorbunov, E. Grigoriev, V. Kaftanov, V. Khovansky, A. Rosanov, A. Baroncelli, L. Barone, B. B. and C. Bosio, A. Capone, M. Diemoz, U. Dore, F. Ferroni, L. L. P. Monacelli, F. D. Notaristefani], P. Pistilli, R. Santacesaria, L. Tortora, and V. Valente, “Search for axion-like particle production in 400 gev proton-copper interactions,” *Physics Letters B* **157** (1985) no. 5, 458 – 462. <http://www.sciencedirect.com/science/article/pii/0370269385904009>.
- [259] N. Ishizuka and M. Yoshimura, “Axion and Dilaton Emissivity from Nascent Neutron Stars,” *Progress of Theoretical Physics* **84** (08, 1990) 233–250, <https://academic.oup.com/ptp/article-pdf/84/2/233/5402055/84-2-233.pdf>. <https://doi.org/10.1143/ptp/84.2.233>.
- [260] A. Berlin, S. Gori, P. Schuster, and N. Toro, “Dark Sectors at the Fermilab SeaQuest Experiment,” *Phys. Rev. D* **98** (2018) no. 3, 035011, arXiv:1804.00661 [hep-ph].
- [261] [https://indico.cern.ch/event/580599/contributions/2476110/attachments/1418854/2173371/TH\\_Lanfranchi.pdf](https://indico.cern.ch/event/580599/contributions/2476110/attachments/1418854/2173371/TH_Lanfranchi.pdf).
- [262] S. Alekhin *et al.*, “A facility to Search for Hidden Particles at the CERN SPS: the SHiP physics case,” *Rept. Prog. Phys.* **79** (2016) no. 12, 124201, arXiv:1504.04855 [hep-ph].
- [263] V. V. Gligorov, S. Knapen, M. Papucci, and D. J. Robinson, “Searching for Long-lived Particles: A Compact Detector for Exotics at LHCb,” *Phys. Rev. D* **97** (2018) no. 1, 015023, arXiv:1708.09395 [hep-ph].
- [264] J. L. Feng, I. Galon, F. Kling, and S. Trojanowski, “Dark Higgs bosons at the Forward Search Experiment,” *Phys. Rev. D* **97** (2018) no. 5, 055034, arXiv:1710.09387 [hep-ph].
- [265] J. A. Evans, “Detecting Hidden Particles with MATHUSLA,” *Phys. Rev. D* **97** (2018) no. 5, 055046, arXiv:1708.08503 [hep-ph].
- [266] J. P. Chou, D. Curtin, and H. Lubatti, “New Detectors to Explore the Lifetime Frontier,” *Phys. Lett. B* **767** (2017) 29–36, arXiv:1606.06298 [hep-ph].
- [267] **ATLAS** Collaboration, G. Aad *et al.*, “Search for a heavy Higgs boson decaying into a Z boson and another heavy Higgs boson in the  $llbb$  and  $llWW$  final states in  $pp$  collisions at  $\sqrt{s} = 13$  TeV with the ATLAS detector,” arXiv:2011.05639 [hep-ex].
- [268] **ATLAS** Collaboration, G. Aad *et al.*, “Search for a CP-odd Higgs boson decaying to Zh in  $pp$  collisions at  $\sqrt{s} = 8$  TeV with the ATLAS detector,” *Phys. Lett. B* **744** (2015) 163–183, arXiv:1502.04478 [hep-ex].

- [269] **CMS** Collaboration, “Search for extended Higgs sectors in the H to hh and A to Zh channels in  $\sqrt{s} = 8$  TeV pp collisions with multileptons and photons final states,” CMS-PAS-HIG-13-025.
- [270] **CMS** Collaboration, “Search for a pseudoscalar boson A decaying into a Z and an h boson in the llbb final state,” CMS-PAS-HIG-14-011.
- [271] **CMS** Collaboration, “Search for a heavy pseudoscalar boson decaying to a Z boson and a Higgs boson at  $\sqrt{s}=13$  TeV,” CMS-PAS-HIG-18-005.
- [272] R. Barbieri and G. Giudice, “b  $\rightarrow$  j s gamma decay and supersymmetry,” *Phys. Lett. B* **309** (1993) 86–90, [arXiv:hep-ph/9303270](#).
- [273] S. Gori, C. Grojean, A. Juste, and A. Paul, “Heavy Higgs Searches: Flavour Matters,” *JHEP* **01** (2018) 108, [arXiv:1710.03752 \[hep-ph\]](#).
- [274] J. De Blas, G. Durieux, C. Grojean, J. Gu, and A. Paul, “On the future of Higgs, electroweak and diboson measurements at lepton colliders,” *JHEP* **12** (2019) 117, [arXiv:1907.04311 \[hep-ph\]](#).
- [275] **CMS** Collaboration, “Combined Higgs boson production and decay measurements with up to 137 fb<sup>-1</sup> of proton-proton collision data at  $\sqrt{s} = 13$  TeV,” CMS-PAS-HIG-19-005.
- [276] **ATLAS** Collaboration, “A combination of measurements of Higgs boson production and decay using up to 139 fb<sup>-1</sup> of proton–proton collision data at  $\sqrt{s} = 13$  TeV collected with the ATLAS experiment,”.
- [277] **ATLAS** Collaboration, G. Aad *et al.*, “Search for Higgs boson decays into two new low-mass spin-0 particles in the 4b channel with the ATLAS detector using pp collisions at  $\sqrt{s} = 13$  TeV,” [arXiv:2005.12236 \[hep-ex\]](#).
- [278] **CMS** Collaboration, “Search for a low-mass dilepton resonance in Higgs boson decays to four-lepton final states at  $\sqrt{s} = 13$  TeV,” CMS-PAS-HIG-19-007.
- [279] **CMS** Collaboration, A. M. Sirunyan *et al.*, “Search for a light pseudoscalar Higgs boson in the boosted  $\mu\mu\tau\tau$  final state in proton-proton collisions at  $\sqrt{s} = 13$  TeV,” *JHEP* **08** (2020) 139, [arXiv:2005.08694 \[hep-ex\]](#).
- [280] **CMS** Collaboration, A. M. Sirunyan *et al.*, “Search for an exotic decay of the Higgs boson to a pair of light pseudoscalars in the final state with two b quarks and two  $\tau$  leptons in proton-proton collisions at  $\sqrt{s} = 13$  TeV,” *Phys. Lett. B* **785** (2018) 462, [arXiv:1805.10191 \[hep-ex\]](#).
- [281] **CMS** Collaboration, A. M. Sirunyan *et al.*, “Search for an exotic decay of the Higgs boson to a pair of light pseudoscalars in the final state of two muons and two  $\tau$  leptons in proton-proton collisions at  $\sqrt{s} = 13$  TeV,” *JHEP* **11** (2018) 018, [arXiv:1805.04865 \[hep-ex\]](#).
- [282] **ATLAS** Collaboration, M. Aaboud *et al.*, “Search for Higgs boson decays into a pair of light bosons in the  $bb\mu\mu$  final state in pp collision at  $\sqrt{s} = 13$  TeV with the ATLAS detector,” *Phys. Lett. B* **790** (2019) 1–21, [arXiv:1807.00539 \[hep-ex\]](#).
- [283] H. E. Haber and D. O’Neil, “Basis-independent methods for the two-Higgs-doublet model III: The CP-conserving limit, custodial symmetry, and the oblique parameters S, T, U,” *Phys. Rev. D* **83** (2011) 055017, [arXiv:1011.6188 \[hep-ph\]](#).

- [284] A. Pomarol and R. Vega, “Constraints on CP violation in the Higgs sector from the rho parameter,” *Nucl. Phys. B* **413** (1994) 3–15, [arXiv:hep-ph/9305272](#).
- [285] C. Csáki, R. T. **D’Agnolo**, M. Geller, and A. Ismail, “Crunching Dilaton, Hidden Naturalness,” *Phys. Rev. Lett.* **126** (2021) 091801, [arXiv:2007.14396](#) [hep-ph].
- [286] C. Csaki, M. Graesser, L. Randall, and J. Terning, “Cosmology of brane models with radion stabilization,” *Phys. Rev.* **D62** (2000) 045015, [arXiv:hep-ph/9911406](#) [hep-ph].
- [287] C. Csaki, M. L. Graesser, and G. D. Kribs, “Radion dynamics and electroweak physics,” *Phys. Rev.* **D63** (2001) 065002, [arXiv:hep-th/0008151](#) [hep-th].
- [288] R. S. Gupta, Z. Komargodski, G. Perez, and L. Ubaldi, “Is the Relaxion an Axion?,” *JHEP* **02** (2016) 166, [arXiv:1509.00047](#) [hep-ph].
- [289] **ATLAS** Collaboration, M. Aaboud *et al.*, “Combination of searches for heavy resonances decaying into bosonic and leptonic final states using 36 fb<sup>-1</sup> of proton-proton collision data at  $\sqrt{s} = 13$  TeV with the ATLAS detector,” *Phys. Rev. D* **98** (2018) no. 5, 052008, [arXiv:1808.02380](#) [hep-ex].
- [290] **CMS** Collaboration, A. M. Sirunyan *et al.*, “Combination of CMS searches for heavy resonances decaying to pairs of bosons or leptons,” *Phys. Lett. B* **798** (2019) 134952, [arXiv:1906.00057](#) [hep-ex].
- [291] B. Bellazzini, C. Csaki, J. Hubisz, J. Serra, and J. Terning, “A Higgslike Dilaton,” *Eur. Phys. J. C* **73** (2013) no. 2, 2333, [arXiv:1209.3299](#) [hep-ph].
- [292] R. Sundrum, “SUSY Splits, But Then Returns,” *JHEP* **01** (2011) 062, [arXiv:0909.5430](#) [hep-th].
- [293] C. Csaki, J. Hubisz, and S. J. Lee, “Radion phenomenology in realistic warped space models,” *Phys. Rev. D* **76** (2007) 125015, [arXiv:0705.3844](#) [hep-ph].
- [294] S. R. Coleman, “The Fate of the False Vacuum. 1. Semiclassical Theory,” *Phys. Rev. D* **15** (1977) 2929–2936. [Erratum: *Phys.Rev.D* 16, 1248 (1977)].
- [295] **LHCb** Collaboration, R. Aaij *et al.*, “Search for hidden-sector bosons in  $B^0 \rightarrow K^{*0} \mu^+ \mu^-$  decays,” *Phys. Rev. Lett.* **115** (2015) no. 16, 161802, [arXiv:1508.04094](#) [hep-ex].
- [296] T. Flacke, C. Frugiuele, E. Fuchs, R. S. Gupta, and G. Perez, “Phenomenology of relaxion-Higgs mixing,” *JHEP* **06** (2017) 050, [arXiv:1610.02025](#) [hep-ph].
- [297] C. Frugiuele, E. Fuchs, G. Perez, and M. Schlaffer, “Relaxion and light (pseudo)scalars at the HL-LHC and lepton colliders,” *JHEP* **10** (2018) 151, [arXiv:1807.10842](#) [hep-ph].
- [298] S. Gardner, R. Holt, and A. Tadepalli, “New Prospects in Fixed Target Searches for Dark Forces with the SeaQuest Experiment at Fermilab,” *Phys. Rev. D* **93** (2016) no. 11, 115015, [arXiv:1509.00050](#) [hep-ph].
- [299] J. Beacham *et al.*, “Physics Beyond Colliders at CERN: Beyond the Standard Model Working Group Report,” [arXiv:1901.09966](#) [hep-ex].
- [300] J. L. Feng, I. Galon, F. Kling, and S. Trojanowski, “ForwArD Search ExpeRiment at the LHC,” *Phys. Rev. D* **97** (2018) no. 3, 035001, [arXiv:1708.09389](#) [hep-ph].

- [301] J. A. Evans, S. Gori, and J. Shelton, “Looking for the WIMP Next Door,” *JHEP* **02** (2018) 100, arXiv:1712.03974 [hep-ph].
- [302] FCC Collaboration, A. Abada *et al.*, “FCC-ee: The Lepton Collider,” *Eur. Phys. J. ST* **228** (2019) no. 2, 261–623.
- [303] M. Bauer, M. Heiles, M. Neubert, and A. Thamm, “Axion-Like Particles at Future Colliders,” *Eur. Phys. J. C* **79** (2019) no. 1, 74, arXiv:1808.10323 [hep-ph].
- [304] D. Aloni, C. Fanelli, Y. Soreq, and M. Williams, “Photoproduction of Axionlike Particles,” *Phys. Rev. Lett.* **123** (2019) no. 7, 071801, arXiv:1903.03586 [hep-ph].
- [305] M. J. Dolan, T. Ferber, C. Hearty, F. Kahlhoefer, and K. Schmidt-Hoberg, “Revised constraints and Belle II sensitivity for visible and invisible axion-like particles,” *JHEP* **12** (2017) 094, arXiv:1709.00009 [hep-ph].
- [306] K. Mimasu and V. Sanz, “ALPs at Colliders,” *JHEP* **06** (2015) 173, arXiv:1409.4792 [hep-ph].
- [307] J. Jaeckel and M. Spannowsky, “Probing MeV to 90 GeV axion-like particles with LEP and LHC,” *Phys. Lett. B* **753** (2016) 482–487, arXiv:1509.00476 [hep-ph].
- [308] ATLAS Collaboration, G. Aad *et al.*, “Measurement of light-by-light scattering and search for axion-like particles with 2.2 nb<sup>-1</sup> of Pb+Pb data with the ATLAS detector,” arXiv:2008.05355 [hep-ex].
- [309] M. Bauer, M. Neubert, and A. Thamm, “Collider Probes of Axion-Like Particles,” *JHEP* **12** (2017) 044, arXiv:1708.00443 [hep-ph].
- [310] S. Knapen, T. Lin, H. K. Lou, and T. Melia, “Searching for Axionlike Particles with Ultraperipheral Heavy-Ion Collisions,” *Phys. Rev. Lett.* **118** (2017) no. 17, 171801, arXiv:1607.06083 [hep-ph].
- [311] S. Knapen, T. Lin, H. K. Lou, and T. Melia, “LHC limits on axion-like particles from heavy-ion collisions,” *CERN Proc.* **1** (2018) 65, arXiv:1709.07110 [hep-ph].
- [312] J. Bjorken, S. Ecklund, W. Nelson, A. Abashian, C. Church, B. Lu, L. Mo, T. Nunamaker, and P. Rassmann, “Search for Neutral Metastable Penetrating Particles Produced in the SLAC Beam Dump,” *Phys. Rev. D* **38** (1988) 3375.
- [313] A. Payez, C. Evoli, T. Fischer, M. Giannotti, A. Mirizzi, and A. Ringwald, “Revisiting the SN1987A gamma-ray limit on ultralight axion-like particles,” *JCAP* **02** (2015) 006, arXiv:1410.3747 [astro-ph.HE].
- [314] J. Jaeckel, P. Malta, and J. Redondo, “Decay photons from the axionlike particles burst of type II supernovae,” *Phys. Rev. D* **98** (2018) no. 5, 055032, arXiv:1702.02964 [hep-ph].
- [315] B. von Harling and G. Servant, “QCD-induced Electroweak Phase Transition,” *JHEP* **01** (2018) 159, arXiv:1711.11554 [hep-ph].
- [316] P. Baratella, A. Pomarol, and F. Rompineve, “The Supercooled Universe,” *JHEP* **03** (2019) 100, arXiv:1812.06996 [hep-ph].



- [317] I. M. Bloch, C. Csáki, M. Geller, and T. Volansky, “Crunching away the cosmological constant problem: dynamical selection of a small  $\Lambda$ ,” *JHEP* **12** (2020) 191, arXiv:1912.08840 [hep-ph].
- [318] S. Weinberg, “The Cosmological Constant Problem,” *Rev. Mod. Phys.* **61** (1989) 1–23.
- [319] A. Strumia and D. Teresi, “Relaxing the Higgs mass and its vacuum energy by living at the top of the potential,” *Phys. Rev. D* **101** (2020) no. 11, 115002, arXiv:2002.02463 [hep-ph].
- [320] L. Hui, J. P. Ostriker, S. Tremaine, and E. Witten, “Ultralight scalars as cosmological dark matter,” *Phys. Rev. D* **95** (2017) no. 4, 043541, arXiv:1610.08297 [astro-ph.CO].
- [321] G. L. Smith, C. D. Hoyle, J. H. Gundlach, E. G. Adelberger, B. R. Heckel, and H. E. Swanson, “Short range tests of the equivalence principle,” *Phys. Rev.* **D61** (2000) 022001.
- [322] S. Schlamminger, K. Y. Choi, T. A. Wagner, J. H. Gundlach, and E. G. Adelberger, “Test of the equivalence principle using a rotating torsion balance,” *Phys. Rev. Lett.* **100** (2008) 041101, arXiv:0712.0607 [gr-qc].
- [323] J. Bergé, P. Brax, G. Métris, M. Pernot-Borràs, P. Touboul, and J.-P. Uzan, “MICROSCOPE Mission: First Constraints on the Violation of the Weak Equivalence Principle by a Light Scalar Dilaton,” *Phys. Rev. Lett.* **120** (2018) no. 14, 141101, arXiv:1712.00483 [gr-qc].
- [324] R. Spero, J. K. Hoskins, R. Newman, J. Pellam, and J. Schultz, “Test of the Gravitational Inverse-Square Law at Laboratory Distances,” *Phys. Rev. Lett.* **44** (1980) 1645–1648.
- [325] J. K. Hoskins, R. D. Newman, R. Spero, and J. Schultz, “Experimental tests of the gravitational inverse square law for mass separations from 2-cm to 105-cm,” *Phys. Rev.* **D32** (1985) 3084–3095.
- [326] J. Chiaverini, S. J. Smullin, A. A. Geraci, D. M. Weld, and A. Kapitulnik, “New experimental constraints on nonNewtonian forces below 100 microns,” *Phys. Rev. Lett.* **90** (2003) 151101, arXiv:hep-ph/0209325 [hep-ph].
- [327] C. D. Hoyle, D. J. Kapner, B. R. Heckel, E. G. Adelberger, J. H. Gundlach, U. Schmidt, and H. E. Swanson, “Sub-millimeter tests of the gravitational inverse-square law,” *Phys. Rev.* **D70** (2004) 042004, arXiv:hep-ph/0405262 [hep-ph].
- [328] S. J. Smullin, A. A. Geraci, D. M. Weld, J. Chiaverini, S. P. Holmes, and A. Kapitulnik, “New constraints on Yukawa-type deviations from Newtonian gravity at 20 microns,” *Phys. Rev.* **D72** (2005) 122001, arXiv:hep-ph/0508204 [hep-ph]. [Erratum: *Phys. Rev.* **D72**, 129901(2005)].
- [329] D. J. Kapner, T. S. Cook, E. G. Adelberger, J. H. Gundlach, B. R. Heckel, C. D. Hoyle, and H. E. Swanson, “Tests of the gravitational inverse-square law below the dark-energy length scale,” *Phys. Rev. Lett.* **98** (2007) 021101, arXiv:hep-ph/0611184 [hep-ph].
- [330] M. Bordag, U. Mohideen, and V. M. Mostepanenko, “New developments in the Casimir effect,” *Phys. Rept.* **353** (2001) 1–205, arXiv:quant-ph/0106045 [quant-ph].

- [331] M. Bordag, G. L. Klimchitskaya, U. Mohideen, and V. M. Mostepanenko, “Advances in the Casimir effect,” *Int. Ser. Monogr. Phys.* **145** (2009) 1–768.
- [332] S. G. Turyshev and J. G. Williams, “Space-based tests of gravity with laser ranging,” *Int. J. Mod. Phys.* **D16** (2007) 2165–2179, [arXiv:gr-qc/0611095](#) [gr-qc].
- [333] E. Hardy and R. Lasenby, “Stellar cooling bounds on new light particles: plasma mixing effects,” *JHEP* **02** (2017) 033, [arXiv:1611.05852](#) [hep-ph].
- [334] A. Branca *et al.*, “Search for an Ultralight Scalar Dark Matter Candidate with the AURIGA Detector,” *Phys. Rev. Lett.* **118** (2017) no. 2, 021302, [arXiv:1607.07327](#) [hep-ex].
- [335] A. Banerjee, H. Kim, O. Matsedonskyi, G. Perez, and M. S. Safronova, “Probing the Relaxed Relaxion at the Luminosity and Precision Frontiers,” *JHEP* **07** (2020) 153, [arXiv:2004.02899](#) [hep-ph].
- [336] P. W. Graham, D. E. Kaplan, J. Mardon, S. Rajendran, and W. A. Terrano, “Dark Matter Direct Detection with Accelerometers,” *Phys. Rev.* **D93** (2016) no. 7, 075029, [arXiv:1512.06165](#) [hep-ph].
- [337] A. Arvanitaki, P. W. Graham, J. M. Hogan, S. Rajendran, and K. Van Tilburg, “Search for light scalar dark matter with atomic gravitational wave detectors,” *Phys. Rev. D* **97** (2018) no. 7, 075020, [arXiv:1606.04541](#) [hep-ph].
- [338] A. Arvanitaki, J. Huang, and K. Van Tilburg, “Searching for dilaton dark matter with atomic clocks,” *Phys. Rev. D* **91** (2015) no. 1, 015015, [arXiv:1405.2925](#) [hep-ph].
- [339] P. Leaci, A. Vinante, M. Bonaldi, P. Falferi, A. Pontin, G. A. Prodi, and J. P. Zendri, “Design of wideband acoustic detectors of gravitational waves equipped with displacement concentrators,” *Phys. Rev. D* **77** (2008) 062001.
- [340] H. Grote and Y. V. Stadnik, “Novel signatures of dark matter in laser-interferometric gravitational-wave detectors,” *Phys. Rev. Res.* **1** (2019) no. 3, 033187, [arXiv:1906.06193](#) [astro-ph.IM].
- [341] S. M. Vermeulen *et al.*, “Direct limits for scalar field dark matter from a gravitational-wave detector,” [arXiv:2103.03783](#) [gr-qc].
- [342] A. Banerjee, H. Kim, and G. Perez, “Coherent relaxion dark matter,” [arXiv:1810.01889](#) [hep-ph].
- [343] A. Strumia and D. Teresi, “Cosmological constant: relaxation vs multiverse,” *Phys. Lett. B* **797** (2019) 134901, [arXiv:1904.07876](#) [gr-qc].
- [344] A. E. Nelson, “Naturally Weak CP Violation,” *Phys. Lett. B* **136** (1984) 387–391.
- [345] S. M. Barr, “Solving the Strong CP Problem Without the Peccei-Quinn Symmetry,” *Phys. Rev. Lett.* **53** (1984) 329.
- [346] C. Abel *et al.*, “The n2EDM experiment at the Paul Scherrer Institute,” *EPJ Web Conf.* **219** (2019) 02002, [arXiv:1811.02340](#) [physics.ins-det].
- [347] nEDM experiment at Spallation Neutron Source. <http://www.nedm.caltech.edu/>, last accessed on 2021-05-28.

- [348] B. W. Filippone, “Worldwide Search for the Neutron EDM,” in *13th Conference on the Intersections of Particle and Nuclear Physics*. 10, 2018. arXiv:1810.03718 [nucl-ex].
- [349] N. R. Hutzler *et al.*, “Searches for new sources of CP violation using molecules as quantum sensors,” arXiv:2010.08709 [hep-ph].
- [350] D. E. Maison, L. V. Skripnikov, and V. V. Flambaum, “Theoretical study of  $^{173}\text{YbOH}$  to search for the nuclear magnetic quadrupole moment,” *Phys. Rev. A* **100** (Sep, 2019) 032514. <https://link.aps.org/doi/10.1103/PhysRevA.100.032514>.
- [351] Y. Hao, L. F. Pašteka, L. Visscher, P. Aggarwal, H. L. Bethlem, A. Boeschoten, A. Borschevsky, M. Denis, K. Esajas, S. Hoekstra, K. Jungmann, V. R. Marshall, T. B. Meijknecht, M. C. Mooij, R. G. E. Timmermans, A. Touwen, W. Ubachs, L. Willmann, Y. Yin, and A. Zapara, “High accuracy theoretical investigations of caf, srf, and baf and implications for laser-cooling,” *The Journal of Chemical Physics* **151** (2019) no. 3, 034302, <https://doi.org/10.1063/1.5098540>.  
<https://doi.org/10.1063/1.5098540>.
- [352] M. Bishof, R. H. Parker, K. G. Bailey, J. P. Greene, R. J. Holt, M. R. Kalita, W. Korsch, N. D. Lemke, Z.-T. Lu, P. Mueller, T. P. O’Connor, J. T. Singh, and M. R. Dietrich, “Improved limit on the  $^{225}\text{Ra}$  electric dipole moment,” *Phys. Rev. C* **94** (Aug, 2016) 025501. <https://link.aps.org/doi/10.1103/PhysRevC.94.025501>.
- [353] P. Yu and N. R. Hutzler, “Probing Fundamental Symmetries of Deformed Nuclei in Symmetric Top Molecules,” *Phys. Rev. Lett.* **126** (2021) no. 2, 023003, arXiv:2008.08803 [physics.atom-ph].
- [354] K.-H. Leong, H.-Y. Schive, U.-H. Zhang, and T. Chiueh, “Testing extreme-axion wave-like dark matter using the BOSS Lyman-alpha forest data,” *Mon. Not. Roy. Astron. Soc.* **484** (2019) no. 3, 4273–4286, arXiv:1810.05930 [astro-ph.CO].
- [355] V. Iršič, M. Viel, M. G. Haehnelt, J. S. Bolton, and G. D. Becker, “First constraints on fuzzy dark matter from Lyman- $\alpha$  forest data and hydrodynamical simulations,” *Phys. Rev. Lett.* **119** (2017) no. 3, 031302, arXiv:1703.04683 [astro-ph.CO].
- [356] T. Kobayashi, R. Murgia, A. De Simone, V. Iršič, and M. Viel, “Lyman- $\alpha$  constraints on ultralight scalar dark matter: Implications for the early and late universe,” *Phys. Rev. D* **96** (2017) no. 12, 123514, arXiv:1708.00015 [astro-ph.CO].
- [357] E. Armengaud, N. Palanque-Delabrouille, C. Yèche, D. J. Marsh, and J. Baur, “Constraining the mass of light bosonic dark matter using SDSS Lyman- $\alpha$  forest,” *Mon. Not. Roy. Astron. Soc.* **471** (2017) no. 4, 4606–4614, arXiv:1703.09126 [astro-ph.CO].
- [358] B. Bozek, D. J. Marsh, J. Silk, and R. F. Wyse, “Galaxy UV-luminosity function and reionization constraints on axion dark matter,” *Mon. Not. Roy. Astron. Soc.* **450** (2015) no. 1, 209–222, arXiv:1409.3544 [astro-ph.CO].
- [359] J. Zhang, J.-L. Kuo, H. Liu, Y.-L. S. Tsai, K. Cheung, and M.-C. Chu, “The Importance of Quantum Pressure of Fuzzy Dark Matter on Lyman-Alpha Forest,” *Astrophys. J.* **863** (2018) 73, arXiv:1708.04389 [astro-ph.CO].
- [360] K. Schutz, “Subhalo mass function and ultralight bosonic dark matter,” *Phys. Rev. D* **101** (2020) no. 12, 123026, arXiv:2001.05503 [astro-ph.CO].

- [361] D. J. E. Marsh and J. C. Niemeyer, “Strong Constraints on Fuzzy Dark Matter from Ultrafaint Dwarf Galaxy Eridanus II,” *Phys. Rev. Lett.* **123** (2019) no. 5, 051103, arXiv:1810.08543 [astro-ph.CO].
- [362] M. Safarzadeh and D. N. Spergel, “Ultra-light Dark Matter is Incompatible with the Milky Way’s Dwarf Satellites,” arXiv:1906.11848 [astro-ph.CO].
- [363] N. Bar, D. Blas, K. Blum, and S. Sibiryakov, “Galactic rotation curves versus ultralight dark matter: Implications of the soliton-host halo relation,” *Phys. Rev. D* **98** (2018) no. 8, 083027, arXiv:1805.00122 [astro-ph.CO].
- [364] J. B. Muñoz, C. Dvorkin, and F.-Y. Cyr-Racine, “Probing the Small-Scale Matter Power Spectrum with Large-Scale 21-cm Data,” *Phys. Rev. D* **101** (2020) no. 6, 063526, arXiv:1911.11144 [astro-ph.CO].
- [365] **LSST Dark Matter Group** Collaboration, A. Drlica-Wagner *et al.*, “Probing the Fundamental Nature of Dark Matter with the Large Synoptic Survey Telescope,” arXiv:1902.01055 [astro-ph.CO].
- [366] M. Baryakhtar, M. Galanis, R. Lasenby, and O. Simon, “Black hole superradiance of self-interacting scalar fields,” arXiv:2011.11646 [hep-ph].
- [367] S. Winitzki, *Eternal inflation*. 2008.
- [368] M. Geller, Y. Hochberg, and E. Kuflik, “Inflating to the Weak Scale,” *Phys. Rev. Lett.* **122** (2019) no. 19, 191802, arXiv:1809.07338 [hep-ph].
- [369] C. Cheung and P. Saraswat, “Mass Hierarchy and Vacuum Energy,” arXiv:1811.12390 [hep-ph].
- [370] G. F. Giudice, M. McCullough, and T. You, “Self-Organised Localisation,” arXiv:2105.08617 [hep-ph].
- [371] A. Arvanitaki, S. Dimopoulos, V. Gorbenko, J. Huang, and K. Van Tilburg, “A small weak scale from a small cosmological constant,” *JHEP* **05** (2017) 071, arXiv:1609.06320 [hep-ph].
- [372] G. F. Giudice, A. Kehagias, and A. Riotto, “The Selfish Higgs,” arXiv:1907.05370 [hep-ph].
- [373] B. Freivogel, “Making predictions in the multiverse,” *Class. Quant. Grav.* **28** (2011) 204007, arXiv:1105.0244 [hep-th].
- [374] P. Ghorbani, A. Strumia, and D. Teresi, “A landscape for the cosmological constant and the Higgs mass,” *JHEP* **01** (2020) 054, arXiv:1911.01441 [hep-th].
- [375] L. J. Hall, D. Pinner, and J. T. Ruderman, “The Weak Scale from BBN,” *JHEP* **12** (2014) 134, arXiv:1409.0551 [hep-ph].
- [376] G. D’Amico, A. Strumia, A. Urbano, and W. Xue, “Direct anthropic bound on the weak scale from supernovæ explosions,” *Phys. Rev. D* **100** (2019) no. 8, 083013, arXiv:1906.00986 [astro-ph.HE].
- [377] N. Arkani-Hamed and S. Dimopoulos, “Supersymmetric unification without low energy supersymmetry and signatures for fine-tuning at the LHC,” *JHEP* **06** (2005) 073, arXiv:hep-th/0405159.

- [378] H. Georgi, “Generalized dimensional analysis,” *Phys. Lett. B* **298** (1993) 187–189, [arXiv:hep-ph/9207278](#).
- [379] M. Shifman and A. Vainshtein, “(In)dependence of  $\Theta$  in the Higgs regime without axions,” *Mod. Phys. Lett. A* **32** (2017) no. 14, 1750084, [arXiv:1701.00467 \[hep-th\]](#).
- [380] S. Dimopoulos and H. Georgi, “Softly Broken Supersymmetry and SU(5),” *Nucl. Phys.* **B193** (1981) 150–162.
- [381] S. Dimopoulos, S. Raby, and F. Wilczek, “Supersymmetry and the Scale of Unification,” *Phys. Rev.* **D24** (1981) 1681–1683.
- [382] J. Bagger and J. Wess, “Supersymmetry and supergravity,”.
- [383] S. Weinberg, *The quantum theory of fields. Vol. 3: Supersymmetry*. Cambridge University Press, 6, 2013.
- [384] Z. Chacko, H.-S. Goh, and R. Harnik, “The Twin Higgs: Natural electroweak breaking from mirror symmetry,” *Phys. Rev. Lett.* **96** (2006) 231802, [arXiv:hep-ph/0506256 \[hep-ph\]](#).
- [385] G. Burdman, Z. Chacko, H.-S. Goh, and R. Harnik, “Folded supersymmetry and the LEP paradox,” *JHEP* **02** (2007) 009, [arXiv:hep-ph/0609152 \[hep-ph\]](#).